



Universität Hamburg
DER FORSCHUNG | DER LEHRE | DER BILDUNG

Wearable Haptic Technology for 3D Selection and Guidance

an der Universität Hamburg eingereichte Dissertation

vorgelegt von

Oscar Ariza

Human-Computer Interaction

Fachbereich Informatik

Fakultät für Mathematik, Informatik und Naturwissenschaften

2020

Erstgutachter: Prof. Dr. Frank Steinicke
Zweitgutachter: Dr. Anatole Lécuyer
Vorsitzender der Prüfungskommission: Prof. Dr. Timo Gerkmann
Stellvertretender Vorsitzender der Prüfungskommission: Prof. Dr. Matthias Rarey

Datum der Disputation: 19.03.2021

Dedicado a “*la cambia mundos*”

Abstract

The integration of wearable haptic technology in Virtual Environments (VEs) has enormous potential to improve user performance and accuracy while executing 3D selection and manipulation tasks, as well as providing proximity-based guidance during aiming and navigation tasks. However, the lack of haptic feedback has been commonly reported in VEs, combined with insufficient alternatives to incorporate feedback for tactile, kinesthetic, and other modalities in 3D user interfaces (3DUIs). Hence, there is a need to develop and evaluate novel haptic technology that circumvents these interaction problems and improves usability, reducing the performance gap between traditional interfaces and 3DUIs. This thesis's primary goal is to improve the usability and performance of basic 3D interaction tasks involving selection and guidance in VEs by integrating and evaluating wearable haptic technology and hand tracking.

First, we explore the use of proximity-based multimodal cues supporting **3D selection**, specifically, for motions involving ballistic and correction phases during common approaching movements of the human arm. We present multimodal combinations of tactile and audio-visual cues improving the performance or reducing errors during 3D object selections. Additionally, we show how feedback combinations could affect the user's selection movements and depth under-/overestimation.

Second, we present the use of **perceptual illusions** supported by the use of vibrotactile feedback to reproduce the elongated-arm illusion to enable the user to manipulate out-of-reach 3D objects while interacting in-place. Our results support the persistent illusion of body transfer after brief phases of automatic and synchronized visual-haptic stimulation instead of the traditional approach based on manual stimulation. Additionally, we present multimodal combinations of haptic feedback to create a plausible touch illusion. Our approach relies on combining different haptic feedback (i.e., kinesthetic, pseudo, and tactile) to convey sensations for contact, stiffness, and activation for 3DUIs.

Third, we explore vibrotactile technology supporting **3D navigation** tasks in VEs. We propose wireless and wearable devices attached to both hemispheres of the user's head with assistive vibrotactile cues for guidance, reducing the time used to turn and locate a target object. Moreover, we evaluate vibrotactile feedback embedded in shoe soles and handhelds for the sense of presence, user acceptance, and obstacle detection in VEs.

Additionally, besides the studies conducted, we developed and evaluated haptic technology. It features light-weight, unencumbering, and versatile form factors compatible with natural interaction and hand-tracking technologies. We append all the designs, specifications, embedded code, firmware, and resources to enable practitioners to replicate the conducted experiments.

Zusammenfassung

Die Integration tragbarer haptischer Technologien in virtuelle Umgebungen (Virtual Environments, VEs) bietet ein enormes Potenzial (i) zur Verbesserung der Benutzerleistung und -genauigkeit bei der Ausführung von 3D-Auswahl- und Manipulationsaufgaben sowie (ii) zur Bereitstellung einer auf Nähe basierenden Orientierungshilfe bei Ziel- und Navigationsaufgaben. Nichtsdestotrotz wird in VEs nur selten mit haptischem Feedback gearbeitet, was unter anderem auf unzureichende Optionen zur Einbeziehung von taktilen, kinästhetischen und anderen Modalitäten in 3D-Benutzeroberflächen (3D UIs) zurückzuführen ist. Aus diesem Grund besteht ein Bedarf nach neuartigen haptischen Technologien, welche diese Interaktionsprobleme umgehen und die Benutzerfreundlichkeit verbessern, wodurch die Leistungslücke zwischen herkömmlichen Schnittstellen und 3D UIs verringert wird. Das Hauptziel dieser Arbeit besteht darin, grundlegende 3D-Interaktionsaufgaben wie die Selektion und Führung in VEs in Bezug auf Benutzerfreundlichkeit und Durchsatz zu verbessern, indem tragbare haptische Technologien und Hand-Tracking integriert und evaluiert werden.

Zunächst untersuchen wir die Verwendung von Nähe-basierten multimodalen Hinweisen, welche die 3D-Selektion unterstützen. Insbesondere fokussieren wir uns auf typische Armbewegungen bei der Annäherung an Zielobjekte, welche ballistische und korrigierende Phasen beinhalten. Wir präsentieren multimodale Kombinationen von taktilen und audiovisuellen Hinweisen, die die Leistung verbessern oder Fehler bei der Auswahl von 3D-Objekten reduzieren. Zusätzlich zeigen wir, wie Feedback-Kombinationen die Selektionsbewegungen des Benutzers und die Unter- / Überschätzung der Distanz beeinflussen können.

Anschließend stellen wir durch vibrotaktilen Feedback unterstützte Wahrnehmungsillusionen vor, mit deren Hilfe der Eindruck eines verlängerten Arms reproduziert werden kann. Auf diese Weise kann der Benutzer nicht erreichbare 3D-Objekte manipulieren, während er an Ort und Stelle interagiert. Unsere Studienergebnisse weisen darauf hin, dass eine anhaltende Körpertransfer-Illusion durch kurze Phasen automatischer und synchronisierter visuell-haptischer Stimulation erzielt werden kann - im Gegensatz zum traditionellen Ansatz, der auf manueller Stimulation basiert. Zusätzlich präsentieren wir multimodale Kombinationen von haptischem Feedback, um eine plausible Berührungssillusion zu erzeugen. Unser Ansatz beruht auf der Verknüpfung verschiedener Formen haptischen Feedbacks (kinästhetisch, pseudo und taktil), um Empfindungen für Kontakt, Steifheit und Aktivierung für 3D UIs zu vermitteln.

Abschließend untersuchen wir vibrotaktile Technologien zur Unterstützung von 3D-Navigationsaufgaben in VEs. Wir schlagen drahtlose, am Kopf getragene Geräte vor, die unterstützende vibrotaktile Hinweise bereitstellen und damit die Zeit zum Lokalisieren eines Zielobjekts sowie der entsprechenden Kopfdrehung reduzieren. Darüber hinaus evaluieren wir vibrotaktile Systeme, welche in Schuhsohlen und Handhelds eingebettet sind, in Bezug auf Präsenz, Benutzerakzeptanz und Hinderniserkennung in VEs.

Zusätzlich zu den durchgeführten Studien haben wir ein haptisches Interaktionsgerät entwickelt und evaluiert. Es ist vielseitig einsetzbar und durch das geringe Gewicht sowie die hohe Ergonomie mit natürlichen Interaktions- und Hand-Tracking-Technologien kompatibel. Alle Entwürfe, Spezifikationen und Ressourcen sowie eingebetteter Code und Firmware sind der Arbeit angehängt, um eine Replikation der durchgeführten Experimente zu ermöglichen.

Contents

1. Introduction	1
1.1. Motivation	1
1.2. Scenarios	5
1.3. Research Goals	8
1.4. Outline	9
1.5. Publications	10
1.5.1. Main Authorship	11
1.5.2. Co-Authorship	12
Part I. Fundamentals	15
2. Human Factors	17
2.1. Tactile Modality	18
2.1.1. Mechanoreceptors	18
2.2. Kinesthetic Modality	20
2.2.1. Perception-action Loop	22
2.3. Visual Modality	24
2.3.1. Field of View	24
2.3.2. Depth Estimation	25
2.4. Ergonomics	26
2.5. Psychophysics	27
3. Haptics and 3DUI	31
3.1. Haptic Technology	31
3.1.1. Types of Interactive Haptic Devices	32
3.1.2. Graspable Systems	34
3.1.3. Touchable Systems	36
3.1.4. Wearable and Contactless Systems	37
3.2. Visuo-haptic Illusions	43
3.3. Multimodal Feedback	45
3.4. 3D Interaction	46
3.4.1. Hand Interaction	47
3.4.2. 3D Direct Selection	48
3.4.3. 3D Guidance	50
3.5. Conclusion	50

Part II. Support for 3D Selection	53
4. Proximity-based Patterns	55
4.1. Motivation	55
4.2. Ring-shaped Haptic Device	56
4.3. Vibrotactile Patterns	56
4.4. Usability Study	58
4.4.1. Participants	58
4.4.2. Materials	59
4.4.3. Methods	60
4.4.4. Results	60
4.5. Discussion	61
4.6. Conclusion	63
5. Use of Multimodal Feedback	65
5.1. Motivation	65
5.2. Proximity-based Feedback	66
5.3. Experiment	68
5.3.1. Participants	68
5.3.2. Material	68
5.3.3. Methods	69
5.3.4. Analysis of the Selection Movements	71
5.4. Results	72
5.4.1. Effective Throughput	72
5.4.2. Under/Overshooting	74
5.4.3. Percentage of the Correction Phase	75
5.4.4. Subjective Preference and Questionnaires	76
5.5. Discussion	76
5.6. Conclusion	77
Part III. Perceptual Illusions	79
6. Inducing the Long-Arm Illusion	81
6.1. Motivation	81
6.2. Vibrotactile Glove Device	82
6.2.1. Vibrotactile Display	82
6.3. Experiment	84
6.3.1. Setup	84
6.3.2. Tasks	85
6.3.3. Participants	86
6.3.4. Procedure	86
6.4. Results	87
6.4.1. Subject Reaction	87

6.4.2. Simulator Sickness	88
6.4.3. Presence	89
6.5. Discussion	89
6.6. Conclusion	90
7. Combining Haptics and Pseudo Haptics	91
7.1. Motivation	91
7.2. Experiment 1: Stiffness and C/D Ratio	93
7.2.1. Participants	93
7.2.2. Apparatus	93
7.2.3. Procedure	93
7.2.4. Results	95
7.3. Experiment 2:	
Model of Stiffness and Multi-sensory Integration	95
7.3.1. Participants	96
7.3.2. Apparatus	96
7.3.3. Procedure	96
7.3.4. Results	97
7.4. Experiment 3: Enriching Stiffness with Tactile and Proprioceptive Feedback	98
7.4.1. Participants	98
7.4.2. Apparatus	98
7.4.3. Approach	100
7.4.4. Latency Compensation	101
7.4.5. Procedure	102
7.4.6. Results	103
7.5. Discussion and Conclusion	103
Part IV. Support for 3D Guidance	109
8. Gaze Guidance	111
8.1. Motivation	111
8.2. User Guidance in 3D Environments	112
8.2.1. Vibrotactile Feedback	112
8.3. Cognitive Resources	112
8.4. Experiment	113
8.4.1. Participants	113
8.4.2. Materials	113
8.4.3. Methods	115
8.5. Results	116
8.5.1. Selection Time	117
8.5.2. Memory Task Performance	117
8.5.3. Questionnaires	117

8.5.4. Serial Position Effect	118
8.6. Discussion and Conclusion	119
9. Sound-based Cues on Feet	121
9.1. Motivation	121
9.2. Experiment	122
9.2.1. Apparatus	122
9.2.2. Participants	123
9.2.3. Procedure	123
9.3. Results	124
9.3.1. Sense of Presence	124
9.3.2. Comfort	125
9.4. Conclusion	125
10. Cues for Obstacle Detection	127
10.1. Motivation	127
10.2. Experiment	128
10.2.1. Apparatus	128
10.2.2. Procedure	130
10.2.3. Results	130
10.3. Conclusion	131
Part V. Conclusion	133
11. Summary and Guidelines	135
12. Perspectives	137
Appendix	138
A. Wearable Devices	139
A.1. HapRing	139
A.2. HapFinger	141
A.3. HapBand	142
A.4. HapGloves	145
A.5. HapShoes	146
A.6. HapHandle	147
A.7. HapModule	149
Bibliography	151

List of Figures

1.1. Hand tracking and haptic technology	3
1.2. Use of haptic wearables in VEs	5
1.3. Interaction zones	6
1.4. Scenarios to present the contributions	7
1.5. Thesis structure	10
2.1. Haptics modalities	18
2.2. Skin mechanoreceptors	19
2.3. Density and receptive fields for mechanoreceptors	20
2.4. Kinesthetic organs	21
2.5. Perception-action loop	22
2.6. Neural pathways of the tactile and kinesthetic modalities	24
2.7. Field of view and binocular depth cues	25
2.8. Hand movements	27
2.9. Mixed-grasp taxonomy	28
2.10. Psychometric threshold and JND	29
3.1. Types of interactive haptic devices	32
3.2. Examples of passive haptics	33
3.3. Examples of graspable devices	35
3.4. Examples of touchable devices	36
3.5. Perceived sensations and vibrotactile signals	38
3.6. Finger-worn devices	39
3.7. Hand-worn devices	40
3.8. Examples of electrical stimulation	42
3.9. Examples of contactless feedback	43
3.10. Examples of haptic illusions	44
3.11. Spectrum of interactions within the kinesphere	47
3.12. Fitts' Law standard tasks	49
3.13. Interaction with hands in the VE	50
4.1. Ring-shaped haptic device	56
4.2. Vibrotactile patterns	57
4.3. Experiment setup for testing vibrotactile patterns	59
4.4. Questionnaire results for the vibrotactile patterns	61
5.1. Experiment setup and proximity-based feedback	67
5.2. Vibrotactile fingertip	69
5.3. Selection movement and the velocity profile	70

5.4. Results for the experiment on multimodal feedback for 3D selection	73
5.5. Common velocity profiles for the combinations of modalities	74
5.6. Common velocity profiles for combinations of proximity-based feedback	75
6.1. Participant using the haptic gloves in an VE	82
6.2. User perspective for the long-arm illusion experiment	83
6.3. User perspective for the elongated arm	84
6.4. Plot for scores on proprioception, comfort, and perceived length	88
6.5. Statistical results for the long-arm illusion	89
7.1. Setup for the experiments (stiffness, contact, and activation)	92
7.2. The virtual buttons used for the study	94
7.3. Psychometric function for stiffer responses	95
7.4. Perceived stiffness change by C/D ratio	96
7.5. User wearing the multimodal device	99
7.6. Modules and corresponding technology that convey the different sensations	100
7.7. C/D ratio vs stiffer responses for the tested conditions	104
7.8. Results for the subjective questionnaires	105
8.1. 3DUI for the gaze-guidance experiment	113
8.2. Guidance experiment setup	114
8.3. Radial positions and stimuli	116
8.4. Guidance performance for selection and memory task	118
8.5. Levenshtein distance	118
9.1. Experiment setup to provide cues while walking	123
9.2. Sense of presence and comfort for the tactile cues on feet	124
10.1. Study setup for obstacle detection	129
10.2. Feedback function for obstacle detection	129
10.3. Psychometric function for the obstacle shifting values	131
A.1. Electronics, design and form factor of HapRing	139
A.2. Main components of HapRing	140
A.3. HapRing applications	141
A.4. HapFinger components and tracking setup	141
A.5. HapBand modules	142
A.6. HapBand wearable fingertip	143
A.7. 3D-printable parts of the HapBand fingertip	144
A.8. HapBand Unity Plugin and pins for actuator/sensor connections	145
A.9. HapGloves components	146
A.10. HapShoe components	147
A.11. HapHandle placement of the actuators	147
A.12. HapHandle testing prototype	148
A.13. HapModule components	149

1 Chapter 1

Introduction

“The ultimate display would, of course, be a room within which the computer can control the existence of matter. A chair displayed in such a room would be good enough to sit in. Handcuffs displayed in such a room would be confining, and a bullet displayed in such a room would be fatal. With appropriate programming, such a display could literally be the Wonderland into which Alice walked”

The Ultimate Display
Ivan Sutherland, 1965

1.1. Motivation

More than 50 years ago, Ivan Sutherland shared his vision to create an immersive virtual environment (VE) with his famous “ultimate display” [Sut65]. Since then, academia and industry have made significant efforts to create an immersive computer-generated environment that would be indistinguishable from the real world. The original vision includes displays for different sensory modalities; conveying light, sound, taste, temperature, pressure, and smell into a realistic “wonderland into which Alice walked” [Sut65]. Enormous achievements concerning visual and auditory feedback have been made, and we come closer to a sense of full realism and immersion, whereas, advances with olfactory and gustatory displays are currently in their first stages [Obr+16]. On the other hand, the sense of touch requires the implementation of a haptic display, which has proved to be more challenging regarding the technology required to provide kinesthetic and tactile feedback. However, the interest in adding haptic technology to VEs is on the rise. It has been considered a decisive complement to visual and auditory feedback in creating realistic and immersive environments and improving the user experience.

The study of haptics has been acknowledged as important for the sense of touch as optics has been to sight [Gar08]. Moreover, the usage of haptics in consumer technology is not new. It has been an active field of research for at least 30 years with its inclusion in game consoles and handheld devices,

and currently, in the automotive industry as well as novel technologies related to VEs [Hay19]. Business reports have shown significant growth in the haptics industry for the last five years and an expected market reach of USD 4.8 bn by 2030 [Hay19]. The same notion can be seen in the *Hype Cycle*, created by Gartner [GP20], which projects technologies having the most influence and impact; presenting haptics as *Climbing the Slope* to become mainstream in the field of immersive technologies.

Although the term haptics often refers to the tactile modality and hence to the whole human skin (4 kg and 1.8 m² for an average adult), most of the research regarding immersive technologies is focused on the hands as a universal human interface [AMD17]. The relevance of the hands is highlighted in the *Cortical Homunculus*, showing that a significant proportion of the human brain is dedicated to the processing of hands' motor and sensory functions [RZ18]. We daily use the hands to explore the world with actions integrating skin, muscles, and joints, providing the brain with tactile and kinesthetic input that consequently influences our motor output. A stationary hand being poked by an object acts as a sensory organ for input (i.e., *Passive Touch*). Conversely, a hand pushing an object acts as a motor organ (i.e., *Active Touch* [Gib62]). Accordingly, the human hand is crucial for interactions involving sensing, motor commands, or both.

Regarding the use of technology, most of the human senses (i.e., sight, hearing, taste, and smell) can be stimulated by using head-worn devices like head-mounted displays (HMDs) or smart glasses equipped with displays for the corresponding modalities. However, the sense of touch is composed of skin receptors distributed across the body, directing the design choices to specific and effective body parts, being the hands the typical target for devices featuring haptic feedback. For example, **graspable** interfaces (e.g., robotic arms generating human-scale force feedback, Figure 1.1e), **wearable** interfaces (e.g., gloves providing vibrotactile feedback, Figure 1.1f), and **touchable** interfaces (e.g., touch panels providing haptic cues, Figure 1.1g). Wireless and wearable devices (Figure 1.1i) have received enormous attention because of today's trend of mobility as well as compatibility with hand-tracking and realistic virtual hand representations (Figures 1.1b-d). Such devices enable gesture recognition and higher levels of expressive interactions, taking advantage of the numerous degrees of freedom (DoF) of the human hand. As an additional alternative, contactless tactile feedback can be provided using ultrasonic technology for mid-air interactions. Such technology combined with hand tracking (Figure 1.1j) permits free hands interaction without any controllers (avoiding the use of batteries and offering a more hygienic option). Overall, the use of hands as the primary tool for interaction offers various possibilities to create immersive experiences involving the execution of complex manipulations and the rendering of meaningful sensations in return. In particular, the hands are beneficial because of dexterity, precision, strength, and qualities of its anatomic and functional factors.

Haptic technologies for VEs involving hand tracking and hand interactions can be described in the context of the Reality-Virtuality (RV) continuum defined by Milgram et al. [Mil+94]. This continuum describes Augmented Reality (AR) as a digital representation of the real world (pure reality) using layers to augment/diminish information, defines Augmented Virtuality (AV) as a virtual environment augmented with layered information from the real world, and defines Virtual Reality (VR) or pure virtuality as a digital simulation that immerses the user in a digital environment completely different from the real world. Milgram defines Mixed Reality (MR) as all possible combinations of real and virtual objects within the continuum. Although, this continuum was explicitly envisioned for visual

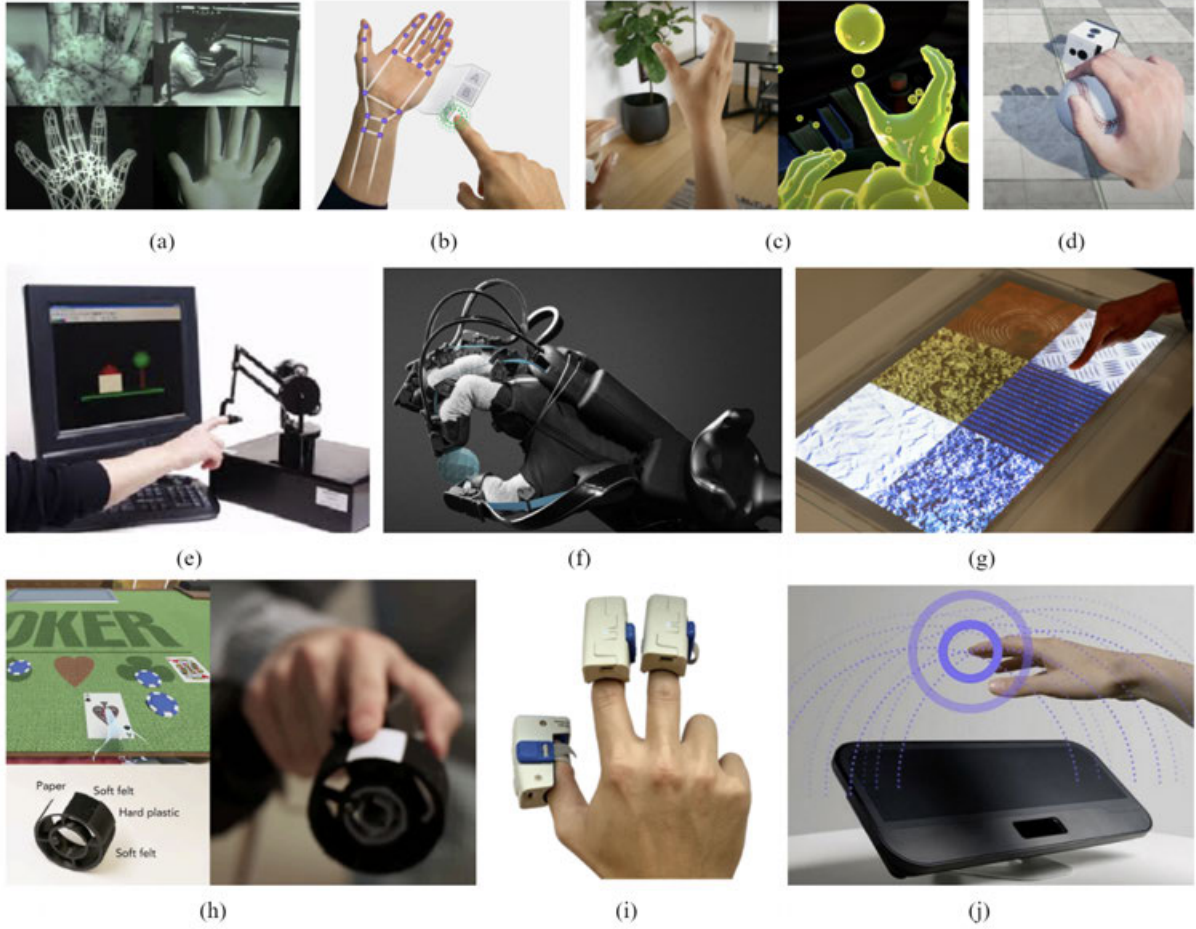


Figure 1.1.: Virtual hand representations and hand-based user interfaces: (a) Primitive representation of a 3D hand was used for the first time in a CGI movie by Ed Catmull in 1972. (b) A virtual hand representation is captured by a time-of-flight depth camera - Ultraleap. (c) Virtual hands are generated by inside-out-tracking with ultra-wide-angle monochrome cameras - Oculus Quest. (d) Physically-based representation of a virtual hand providing realistic grasping interactions with friction and contact forces - ClapXR. (e) Robotic arm providing force feedback [Mas93]. (f) Haptic glove with magnetic tracking capabilities featuring tactile sensations for shape and texture, and kinesthetic sensations for size weight and impact - HaptX. (g) Teslatouch, a touch surface is providing electro-vibration [Bau+10]. (h) Haptic Revolver, a VR controller is featuring touch, shear, texture, and shape rendering [Whi+18]. (i) A wireless finger-worn vibrotactile device - GoTouchVR. (j) A device integrating depth-camera hand tracking and mid-air tactile feedback based on ultrasonic transducers - Ultraleap.

displays, research has considered the inclusion of haptic displays. As an example, a VR user could wear haptic gloves to hand-shake with a hologram of a remote user (3D reconstructed and streamed in real-time) [Ort+16b]. Also, an AR user planning to redesign the living room could be provided with force feedback while pushing augmented virtual furniture [Lop+18].

Although, the studies conducted in this thesis were implemented mainly for VR, the hand tracking technologies and the wearable devices utilized to provide feedback could be easily adapted so that the presented applications can be retargeted to any MR setup. Therefore, for the remainder of this thesis, we will refer to MR as the default target for implementing the experiments. Technology developments

for MR were initially focused on visual and auditory displays, but gradually added haptic displays to enrich the VEs with user input for better interaction. Haptics received more attention when users of MR applications demanded interactive experiences beyond the use of audio-visual output displays and traditional input devices (e.g., mouse, keyboard, or joystick).

MR environments require (i) reliable and real-time rendering, (ii) a realistic representation of the space, and (iii) the use of realistic interaction using different modalities [Bro94; Ste16]. In terms of haptics, an immersive MR environment must provide low-latency multimodal feedback (i.e., visual, tactile, kinesthetic) based on tracked body information, so the VE remains stationary and consistent while the user moves.

The rendering of the environment should be perceived as plausible realism. Also, in terms of interaction, the user must be able to directly select and manipulate virtual objects showing also plausible behavior [Sut65]. For example, applications combining hand tracking as well as haptic technologies can provide kinesthetic and tactile feedback (depicted in Figure 1.1); a MR user could move the real hands and perceive congruent and real-time feedback from the virtual counterparts, resulting in virtual limb and body ownership illusion [Spa+14]. When users grasp a virtual object they should receive force feedback (i.e., feeling of the shape and weight of the object), together with tactile sensations (i.e., temperature, texture, and roughness). Consequently, the requirements for plausible interaction could be fulfilled, and the user could be fully immersed in the VE.

MR setups with haptic technology, involve designing, developing, and evaluating 3D user interfaces (3DUIs). Human-Computer Interaction (HCI) as the discipline concerned with the responsible elaboration of interactive computing systems for human use, has contributed towards such 3DUIs, enabling users to interact within VEs performing selection and manipulation tasks, conveying realistic VEs and interactions, which feel “*natural*”; sometimes denoted as Natural User Interfaces (NUIs) [WW11]. NUIs are based on natural and intuitive human mechanisms like reaching, grabbing, and touching [Ste16] as direct interaction offers performance benefits over indirect manipulation of virtual objects [Shn97]. Furthermore, the interface can be either correspond to behaviors constrained by physics [VCO20], or take advantage of visual dominance to modify a haptic sensation along with a visual illusion (i.e., pseudo-haptics) [Léc09]. Also, enabling the use of perceptual illusions [Kil+12] to provide the user with “supernatural powers” (e.g., precise grasping of out-of-reach virtual objects). The involvement of haptic feedback in NUIs creates emotional connections as the sense of touch is linked with emotions [MWO14], enabling the use of haptic technology to increase the sense of presence and the quality of immersive storytelling. Similarly, the proper integration of visual, tactile, and kinesthetic feedback guarantees the sense of body ownership in VEs [Ehr12].

In general, the integration of wearable haptic technology in MR applications has enormous potential to improve user performance and accuracy while executing 3D selection and manipulation tasks, as well as providing proximity-based guidance during aiming and navigation tasks [Cho+17b; Mar+18]. However, there are limitations related to the devices utilized to visualize VEs, such as the often limited field of view of HMDs [Pal99]. Such issues, in addition to lenses distortion and latencies, can cause misperceptions [Ste+09; Jon+12] (e.g., depth or distance over- and underestimation), as well as decrease the user sense of presence [Lin+02]. Moreover, a lack of haptic feedback has been commonly reported in MR applications, combined with insufficient alternatives to combine feedback for tactile, kinesthetic,

and other modalities in NUIs [BSS13a; BSS; Cha+10; Ort+16a]. Hence, there is a need to develop and evaluate novel haptic technology that circumvents these interaction problems, and contributes to improving user performance by reducing the gap between traditional interfaces and 3DUIs.



Figure 1.2.: Use of haptic wearables in VEs: **(a)** A user with an HMD for VR/AR applications, hand tracking is supported so the user can see a virtual representation of the real hands. The user also has a hand-worn haptic device to feel vibrations every time the virtual hand collides with a virtual object. **(b)** Pictures of the haptic technology that was developed in this thesis. From top-left, a trackable ring with vibrotactile feedback and digital input, a sole supporting pressure sensing and audio-based tactile feedback, a haptic module integrated into an HMD to provide gaze guidance, a wireless fingertip with analog input, gesture detection and vibrotactile feedback, a wireless device incorporating tapping sensations, piezo vibrations, and tendon/muscle electrical stimulation, and wireless haptic gloves providing tactile feedback for the palm and the fingers.

1.2. Scenarios

For the scope of this thesis, we created scenarios to provide an application context for the contributions. In such scenarios, the user is provided with MR technology to interact within a VE (i.e., an HMD, inside-out or camera-based hand tracking, and haptic technology providing tactile and kinesthetic feedback on the hands, head, and feet. Figure 1.2a).

In the scenarios, the user will start the immersion at the center of a virtual room equipped with UI elements (e.g., buttons, dials, levers) attached to walls. Different user actions are required to locate and approach the UI elements, according to the interaction zones (see Figure 1.3a).

The scenarios are based on use-cases for different MR applications involving training, modeling, design, and system control (see Figure 1.3b). In such applications, the UI elements are mostly and conveniently located in the *interaction zone*, within arm-reach and inside the field of view. Some others can be approached with the hands, but require head-turning and visual search because they are located at the extreme of the visual limits (*peripheral zone*). In some cases, larger and structured VEs (e.g., employee training in a virtual refinery, Figure 1.3b bottom-right) could require the use of guidance and navigation techniques to approach not-reachable UI elements located in the *content zone*. All these applications involve the serial execution of atomic interaction procedures to finally accomplish a main complex task.

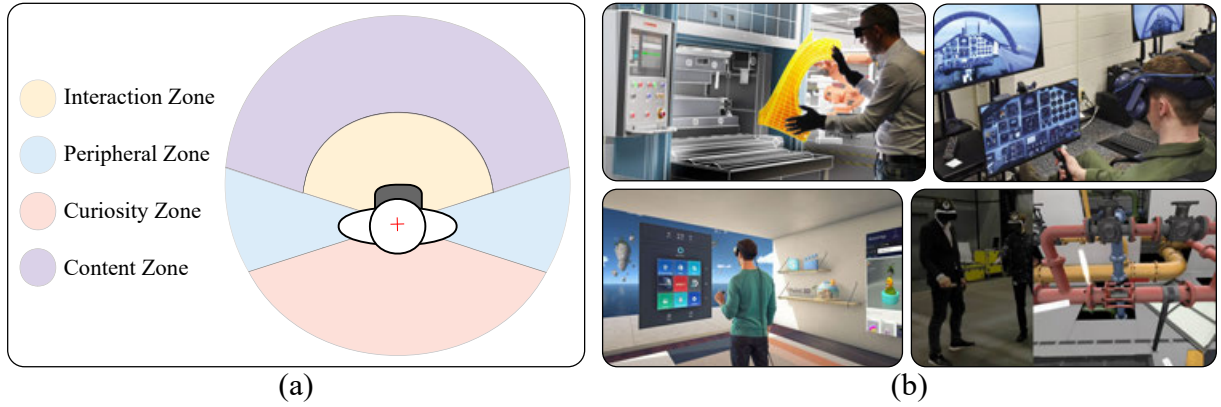


Figure 1.3.: Interaction zones: (a) Top view of the user described in Figure 1.2 showing the different zones to place content and interaction elements inside a VE (the user is looking at the interaction zone). Interaction and content zones are covered by a visual field of 80° , increased to 120° by the peripheral zone. All the content behind the user goes beyond 210° at the curiosity zone. The interaction zone starts at 0.5m away from the center of the head up to 1.3m, and then the content zone goes up to 20m. (b) Examples of real application of VR/AR, including common interactions that were used to define the use case. UI elements surround users; the users must approach them using navigation techniques. Once they are closer, use direct interaction or UI abstractions to manipulate them and perform tasks related to modeling, system control, entertainment, and training (Image credits: Reviatech, FedTech, Microsoft WMR, and Interactive Lab).

We will focus our scenarios (A, B, C, and D), depicted in Figure 1.4) in the task of locating and pressing a virtual button, supporting the user actions with haptic technology.

In scenario A, the user must identify an out-of-sight target button among all the other buttons located either behind the user *curiosity zone* or in the *peripheral zone*, requiring visual search or head-turning. The system provides vibrotactile cues on the back of the head to improve user performance during this process. Once the target button is identified it will be located in the *content zone* or in the *interaction zone*.

In the first case, the button will not be within arm-reach. The user will require either the scenario B with an interaction technique to reach the button while interacting in-place (i.e., supernatural interfaces [Ste16]), or the scenario C featuring vibrotactile feedback on the hand and feet while the user is walking to get closer to the virtual button, improving the realism and providing cues for obstacles. Scenarios B and C represent MR use-cases involving navigation movements and spatial awareness in VEs (e.g., training applications and exergames).

Once the user has arm-reach to the virtual button (*interaction zone*), she must start operating it as quickly and as accurately as possible (Scenario D). In this case, the system provides proximity-based and multimodal feedback to improve user performance in terms of execution time and error rate. Once a task is completed (i.e., the button was fully pressed and released), the user is asked to perform the task again on a different button located in the *curiosity zone*, thus repeating the whole cycle of scenarios.

Scenario D also involves the typical procedure of sitting on a chair in front of the table containing the button and then performing the ballistic and correction movements [LL09] to press and release, thus correctly confirming that the task is completed.

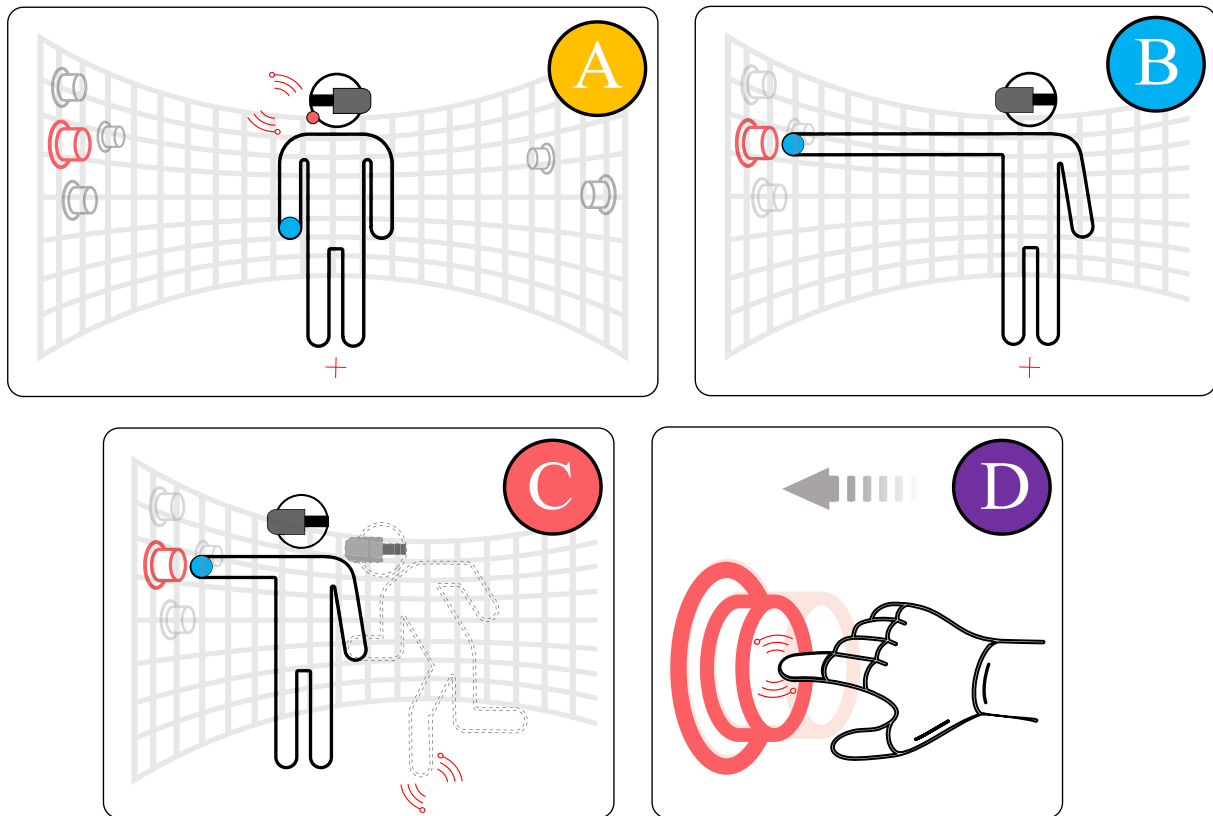



Figure 1.4.: Scenarios to present the contributions: Every scenario represents a usecase supporting the user interaction with haptic technology. **A** Vibrotactile gaze guidance and aiming support to locate out-of-sight 3DUI elements. **B** Embodiment illusions to approach out-of-reach virtual objects. **C** Tactile feedback supporting locomotion and obstacle detection in VEs. **D** Integration of multimodal feedback in 3D selection/manipulation tasks.



In summary, the described scenarios provide haptic technology to support the user during the following interactions:


- A** Guide the head or the body to locate a target 3D button that is out of sight (i.e. curiosity or peripheral zones).
- B** Approach the *interaction zone* by an embodiment illusion elongating the arm so the dominant hand can reach the 3D button.
- C** Approach the *interaction zone* by walking (i.e., natural walking), so the user ends up standing in front of the 3D button.
- D** Perform all the required arm and hand movements to press and release the 3D button.


1.3. Research Goals

The main goal of this thesis is to improve the usability and performance of basic 3D interaction tasks involving guidance and selection of objects in MR by integrating and evaluating wearable haptic technology. Specific challenges are presented in 3 sections.






First, we will explore the use of proximity-based multimodal cues **supporting 3D selection** in the *interaction zone*, specifically, for motions involving ballistic and correction phases during common approaching movements of the human arm [LL09] (Scenario ). Such interactions often suffer from reduced performance due to missing or incongruent feedback provided by MR systems compared to corresponding real-world interactions. Vibrotactile and auditory feedback have been traditionally suggested as additional perceptual cues complementing the visual channel to improve interaction in MR. However, it has rarely been shown that multimodal combinations of tactile and audio-visual cues improve the performance or reduce errors during 3D object selection. Additionally, it is required to investigate how feedback combinations could affect the user's selection movements and the distance/depth perception (under/overestimation), hence influencing the user's performance. A set of finger-worn wireless haptic devices are evaluated among different vibrotactile signal patterns, which can be used to provide proximity-based cues during 3D interaction with virtual objects. Thus, the goal is to investigate how to alleviate the shortcomings of current 3DUIs with the analysis of the selection movements in the peripersonal space and the evaluation of the distance and depth perception during related 3D interaction tasks. Psychophysical experiments are required to analyze the effects of proximity-based multimodal feedback, in which stimulus intensities depend on spatiotemporal relations between the input device and the virtual target object. Also, possible effects of feedback types on ballistic and correction phases of the selection movement, as well as user performance, must be explored.

Second, the use of **perceptual illusions** supported by haptic technology will be evaluated. How a bi-manual wearable device providing vibrotactile feedback could be combined with low-cost technology for hand tracking and gesture recognition to reproduce body-transfer illusions. In this thesis, we used the elongated-arm illusion to enable the user to manipulate 3D objects in the *content zone* while interacting in-place (Scenario ). In particular, we explored whether it is possible to give a person the persistent illusion of body transfer after brief phases of automatic and synchronized visual-haptic stimulation instead of the traditional approach based on manually synchronized stimulation. Additionally, it has rarely been shown how pseudo-haptic illusions can be integrated with multimodal combinations of haptic feedback, even for simple haptic interactions like touching an object in the *interaction zone*. We will test different techniques to improve the haptic realism of simple 3DUI elements such as a button. Our approach proposes a plausible illusion of touch using wearable technology that combines different haptic feedback types (i.e., kinesthetic, pseudo, and tactile) to convey sensations for contact, stiffness, and activation in a 3D button (Scenario .

Third, we will explore vibrotactile technology **supporting 3D guidance** tasks in VEs (Scenario ). Typically, the selection of objects located in the *curiosity zone* requires a visual search, which can reduce the performance of interaction in MR. This thesis explores how wireless and wearable devices, attached to both hemispheres of the user's head, could assistive vibrotactile cues for guidance to reduce the time used to turn and locate a target object. Different vibrotactile patterns for localization tasks must be

tested based on dual-tasking methods to analyze cognitive demands and performance metrics. Besides, this thesis aims to explore the effects of vibrotactile feedback embedded in shoe soles and handles on the sense of presence, user acceptance, and obstacle detection during navigation in VEs (Scenario .

To summarize, the contribution of this thesis addresses the following analyses:

- Effects of proximity-based tactile patterns and combinations of multimodal feedback on 3D selection guidance during ballistic and correction movements. This challenge is related to the scenario .
- Effects of kinesthetic, pseudo, and tactile feedback on body-transfer illusions and holistic touch sensations involving 3DUIs. This challenge is related to the stages  and .
- Effects of vibrotactile feedback, using head and feet-worn devices, as guidance support for gaze-based exploration and immersive walking in VEs. This challenge is related to the scenarios  and .

1.4. Outline

The remainder of this thesis is structured as follows.

Part I presents background information. Chapter 2 describes human factors in the fields of physiology, perception, and performance metrics. Chapter 3 summarizes previous work related to haptic technology and haptic interaction.

Part II explores the use of vibrotactile cues for guidance in 3D selection. Chapter 4 reports the effects of different proximity-based vibrotactile patterns for 3D selection [ALS15; Ari+15]. Chapter 5 analyzes the effects of multimodal feedback on the velocity profile (i.e., ballistic-correction phases) of aiming movements [Ari+18].

Part III presents techniques for inducing perceptual illusions supported by multimodal feedback. Chapter 6 reports guidelines on how to reproduce the Long-Arm illusion with vibrotactile technology [Ari+16]. Chapter 7 introduces a technique and a set of experiments on conveying holistic touch illusions by combining tactile and kinesthetic feedback with pseudo-haptics [AS20].

Part IV reports insights on the use of haptics to support 3D guidance. Chapter 8 evaluates vibrotactile feedback as a gaze guidance helper [Ari+17]. Chapter 9 reports the effects of using sound-based vibration cues while walking in EVs [Fre+20]. Chapter 10 tests vibrotactile feedback for obstacle detection [Her+19].

Part V summarizes the results and concludes the thesis. Chapter 11 includes a summary and a set of design guidelines. Chapter 12 presents the perspective of this thesis and suggests further research.

The Figure 1.5 presents a map of the research goals in the context of the use case.


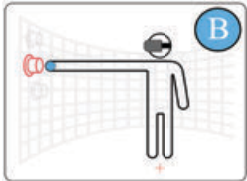


		Use of haptics (Challenges)			
		Support for 3D Selection (Part II)	Perceptual Illusions (Part III)	Support for 3D Guidance (Part IV)	
Fundamentals (Part I)	Scenario			Gaze Guidance (Chapter 8)	Conclusions (Part V)
			Inducing the Long-Arm Illusion (Chapter 6)		
				Sound-based Cues on Feet (Chapter 9)	
			Proximity-based Patterns (Chapter 4)	Combining Haptics and Pseudo-haptics (Chapter 7)	
		Use of Multimodal Feedback (Chapter 5)		Cues for Obstacle Detection (Chapter 10)	

Figure 1.5.: Thesis structure.

In order to conduct studies and analyses, we developed and evaluated different types of haptic technology. Such types feature light-weight, unencumbering, and versatile form factors compatible with natural interaction and hand-tracking technologies. The devices' designs, hardware specifications, embedded code, firmware, and resources were open-sourced to enable practitioners to replicate the conducted experiments (see Appendix A).

1.5. Publications

The main contributions of this thesis have been published in peer-reviewed national and international venues.

1.5.1. Main Authorship

The following publications were mainly created by myself, while co-authors contributed parts of the implementation, writing of paper sections, or supervision. These include five conference papers, one short paper, and one poster ^{1 2}.

- [ALS15] **Ariza, O**, Lubos, P., and Steinicke, F. HapRing: A Wearable Haptic Device for 3D Interaction. In: Mensch Und Computer 2015 - Proceedings, Stuttgart, Germany, September 6-9, 2015. De Gruyter Oldenbourg, 2015, pp. 421–424. URL: <https://dl.gi.de/20.500.12116/7840>.
- [Ari+15] **Ariza, O**, Lubos, P., Steinicke, F., and Bruder, G. Ring-shaped Haptic Device with Vibrotactile Feedback Patterns to Support Natural Spatial Interaction. In: Proceedings of the 25th International Conference on Artificial Reality and Telexistence and 20th Eurographics Symposium on Virtual Environments. Eurographics Association, 2015, pp. 175–181. DOI: [10.2312/egve.20151326](https://doi.org/10.2312/egve.20151326).
- [Ari+16a] **Ariza, O**, Freiwald, J., Laage, N., Feist, M., Salloum, M., Bruder, G., and Steinicke, F. Inducing Body-Transfer Illusions in VR by Providing Brief Phases of Visual-Tactile Stimulation. In: Proceedings of the 2016 Symposium on Spatial User Interaction. Tokyo, Japan: Association for Computing Machinery, 2016, pp. 61–68. DOI: [10.1145/2983310.2985760](https://doi.org/10.1145/2983310.2985760).
- [Ari+16b] **Ariza, O**, Steinicke, F., Lihan, C., and Fanf, F. Visual-Haptic Distance Perception in the Central Fovea and Periphery of the Peripersonal Space. In: International Multisensory Research Forum (IMRF). 2016.
- [Ari+17] **Ariza, O**, Lange, M., Steinicke, F., and Bruder, G. Vibrotactile Assistance for User Guidance Towards Selection Targets in VR and the Cognitive Resources Involved. In: 2017 IEEE Symposium on 3D User Interfaces (3DUI). 2017, pp. 92–96. DOI: [10.1109/3DUI.2017.7893323](https://doi.org/10.1109/3DUI.2017.7893323).
- [Ari+18] **Ariza, O**, Katzakis, N., Bruder, G., and Steinicke, F. Analysis of Proximity-Based Multimodal Feedback for 3D Selection in Immersive Virtual Environments. In: 2018 IEEE Conference on Virtual Reality and 3D User Interfaces (VR). 2018, pp. 327–334. DOI: [10.1109/VR.2018.8446317](https://doi.org/10.1109/VR.2018.8446317).
- [AS20] **Ariza, O** and Steinicke, F. Conveying Holistic Touch Illusions by Combining Tactile and Proprioceptive Feedback with Pseudo-Haptics in VR (in Submission). In: INTERACT, International Conference on Human–Computer Interaction. IFIP, 2020.

¹[Ari+17] is based on a bachelor thesis. The student implemented and ran the experiment under my supervision. I designed the experiment, designed the device, ran the statistics, wrote the embedded code, and wrote the paper.

²[Ari+16] is based on a master project. The students implemented and ran the experiment under my supervision. I designed the experiment, designed and co-built the device, ran the statistics, wrote the embedded code, and wrote the paper.

1.5.2. Co-Authorship

Furthermore, I contributed to the following publications.

- [BAS19] Brauer, C., **Ariza, O**, and Steinicke, F. An Active Tangible Device for Multitouch-Display Interaction. In: Proceedings of Mensch Und Computer 2019. Hamburg, Germany: Association for Computing Machinery, 2019, pp. 439–444. DOI: [10.1145/3340764.3344436](https://doi.org/10.1145/3340764.3344436).
- [Fre+20] Freiwald, J., **Ariza, O**, Janeh, O., and Steinicke, F. Walking by Cycling: A Novel In-Place Locomotion User Interface for Seated Virtual Reality Experiences. In: Proceedings of the 2020 CHI Conference on Human Factors in Computing Systems. Honolulu, HI, USA: Association for Computing Machinery, 2020, pp. 1–12. DOI: [10.1145/3313831.3376574](https://doi.org/10.1145/3313831.3376574).
- [Har+20] Hartfill, J., Gabel, J., Neves-Coelho, D., Vogel, D., Räthel, F., Tiede, S., **Ariza, O**, and Steinicke, F. Word Saber: An Effective and Fun VR Vocabulary Learning Game. In: Proceedings of the Conference on Mensch Und Computer. Magdeburg, Germany: Association for Computing Machinery, 2020, pp. 145–154. DOI: [10.1145/3404983.3405517](https://doi.org/10.1145/3404983.3405517).
- [Her+19] Hertel, J., Schaare, A., Feuerbach, P., **Ariza, O**, and Steinicke, F. STIC - Sensory and Tactile Improved Cane. In: Proceedings of Mensch Und Computer 2019. Hamburg, Germany: Association for Computing Machinery, 2019, pp. 765–769. DOI: [10.1145/3340764.3344905](https://doi.org/10.1145/3340764.3344905).
- [Kat+17] Katzakis, N., Tong, J., **Ariza, O**, Chen, L., Klinker, G., Röder, B., and Steinicke, F. Stylo and Handifact: Modulating Haptic Perception Through Visualizations for Posture Training in Augmented Reality. In: Proceedings of the Symposium on Spatial User Interaction (SUI). Brighton, United Kingdom: Association for Computing Machinery, 2017, pp. 58–67. DOI: [10.1145/3131277.3132181](https://doi.org/10.1145/3131277.3132181).
- [Kat+19] Katzakis, N., Chen, L., Teather, R. J., **Ariza, O**, and Steinicke, F. Evaluation of 3D Pointing Accuracy in the Fovea and Periphery in Immersive Head-Mounted Display Environments. In: *IEEE Transactions on Visualization and Computer Graphics* (2019), pp. 1–8. DOI: [10.1109/TVCG.2019.2947504](https://doi.org/10.1109/TVCG.2019.2947504).
- [Kir+19] Kirsch, K., Schatzschneider, C., Garber, C., Rosenberger, A., Kirsten, K., **Ariza, O**, Steinicke, F., and Bruder, G. KiVR Sports: Influencing the Users Physical Activity in VR by Using Audiovisual Stimuli in Exergames. In: Proceedings of Mensch Und Computer 2019. Hamburg, Germany: Association for Computing Machinery, 2019, pp. 777–781. DOI: [10.1145/3340764.3344907](https://doi.org/10.1145/3340764.3344907).
- [Lub+15] Lubos, P., **Ariza, O**, Bruder, G., Daiber, F., Steinicke, F., and Krüger, A. HoverSpace: Analyses of the Perceived Spatial Affordances of Hover Interaction Above Tabletop Surfaces. In: Human-Computer Interaction (INTERACT). Springer International Publishing, 2015, pp. 259–277.
- [Lub+16a] Lubos, P., Bruder, G., **Ariza, O**, and Steinicke, F. Ambiculus: LED-Based Low-Resolution Peripheral Display Extension for Immersive Head-Mounted Displays. In: Proceedings of the 2016 Virtual Reality International Conference (VRIC). Laval, France: Association for Computing Machinery, 2016. DOI: [10.1145/2927929.2927939](https://doi.org/10.1145/2927929.2927939).

- [Lub+16b] Lubos, P., Bruder, G., **Ariza, O**, and Steinicke, F. Touching the Sphere: Leveraging Joint-Centered Kinespheres for Spatial User Interaction. In: Proceedings of the 2016 Symposium on Spatial User Interaction. Tokyo, Japan: Association for Computing Machinery, 2016, pp. 13–22. DOI: [10.1145/2983310.2985753](https://doi.org/10.1145/2983310.2985753).
- [Mos+19] Mostajeran, F., Katzakis, N., **Ariza, O**, Freiwald, J. P., and Steinicke, F. Welcoming A Holographic Virtual Coach for Balance Training at Home: Two Focus Groups with Older Adults. In: IEEE Conference on Virtual Reality and 3D User Interfaces (VR). 2019, pp. 1465–1470. DOI: [10.1109/VR.2019.8797813](https://doi.org/10.1109/VR.2019.8797813).
- [Mos+20] Mostajeran, F., Steinicke, F., **Ariza, O**, Gatsios, D., and Fotiadis, D. Augmented Reality for Older Adults: Exploring Acceptability of Virtual Coaches for Home-Based Balance Training in An Aging Population. In: Proceedings of the 2020 CHI Conference on Human Factors in Computing Systems. Honolulu, HI, USA: Association for Computing Machinery, 2020, pp. 1–12. DOI: [10.1145/3313831.3376565](https://doi.org/10.1145/3313831.3376565).
- [SAS19a] Schlünsen, R., **Ariza, O**, and Steinicke, F. A VR Study on Freehand Vs. Widgets for 3D Manipulation Tasks. In: Proceedings of Mensch Und Computer 2019. Hamburg, Germany: Association for Computing Machinery, 2019, pp. 223–233. DOI: [10.1145/3340764.3340791](https://doi.org/10.1145/3340764.3340791).
- [SAS19b] Schmidt, S., **Ariza, O**, and Steinicke, F. Blended Agents: Manipulation of Physical Objects Within Mixed Reality Environments and Beyond. In: Symposium on Spatial User Interaction. Association for Computing Machinery, 2019. DOI: [10.1145/3357251.3357591](https://doi.org/10.1145/3357251.3357591).
- [SAS20] Schmidt, S., **Ariza, O**, and Steinicke, F. Intelligent Blended Agents: Reality–Virtuality Interaction with Artificially Intelligent Embodied Virtual Humans. In: *Multimodal Technologies and Interaction* 4 (Nov. 2020). DOI: [10.3390/mti4040085](https://doi.org/10.3390/mti4040085).

The first three publications involved significant contributions from my side and were partly used in this thesis. The remaining publications were mainly created by someone else and are not part of this thesis. However, I contributed critical parts of the implementation, experiment design, device creation, or paper writing ^{3 4 5}.

³In [Fre+20], I co-designed the experiment, designed and built the haptic shoe device, and ran the statistics.

⁴[Her+19] is based on a master project. The students implemented and ran the experiment under my supervision. I designed the experiment, designed and built the device, wrote the embedded code, and co-wrote the paper.

⁵[SAS19] is based on a master thesis. The student implemented and ran the experiment under my supervision. I designed the experiment and wrote the paper.

Part I

Fundamentals

2

Chapter 2

Human Factors

The term Haptic is related to the Greek word $\alpha\pi\tau\iota\kappa\acute{o}\varsigma$ (haptikos) meaning “tactile, or applicable to the sense of touch” [Jon18]. This term has been used to describe the human ability to actively identify and perceive objects’ properties relying on the sense of touch. Haptics, as a research discipline, studies a broad scope, including all the aspects regarding how to manipulate objects and how to acquire information from the environment using the sense of touch. As an example, in the case of grabbing an object from a table in complete darkness, it is not possible to rely on vision to execute the action. Instead, the primary source of feedback would come from the sensory receptors in the skin and the muscles, guiding the hand movements to locate the object and make adjustments according to its texture and weight.

The sense of touch is not localized in a single sensory organ (unlike the senses of sight, hearing, taste, and smell are localized respectively to the eyes, ears, tongue, and nose). Conversely, it is composed of the skin’s sensory organs, joints, tendons, and muscles located across the entire body. All these organs are responsible for tactile sensibility, the perception of our limbs in space, and the stress that they undergo, but also equilibrium, pain, and temperature [KW14].

This thesis is focused on the human hands and the associated arm movements related selection and guidance actions. The relevance of hands is evidenced with the significant proportion of the human brain dedicated to processing the motor and sensory functions involved (i.e., motor and sensory Cortical Homunculus [RZ18]). The evolution of the human hand as a highly adapted tool for exploration and object manipulation is recognized as one of the most critical factors in the phylogeny of humans [BB91]. Additionally, the ability of hands in terms of sensory and motor qualities make human hands extremely efficient at recognizing objects through touch [KLM85].

The sensory information coming from the sense of touch is originated by actively exploring the environment and also from passive contact. In this way, it is much better to understand the properties of an object by palpation or squeezing than the object just being place in our open palm. Haptic sensing requires the use of our limbs to place and explore an object, read its properties with our skin, muscles, joints, and tendons, and construct an idea of it after several scans in a bidirectional way. That means we could change the state of an object in order to sense it properly, like the case of pushing an object to sense the hardness while changing its original shape (i.e., unidirectional sensing like visual or auditory do not change the state of the target object).

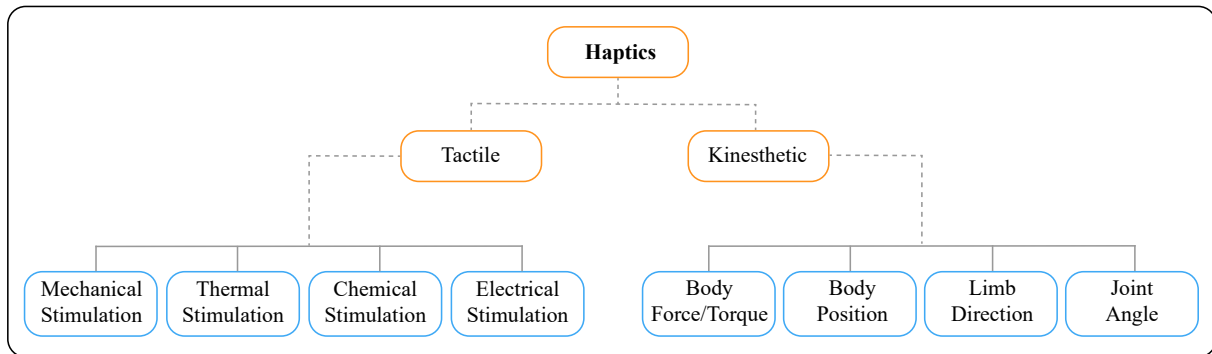


Figure 2.1.: The components of Haptics in terms of feedback for the tactile and kinesthetic modalities [Erp+10].

As every organ senses different signals, Haptics is commonly divided into two modalities: tactile and kinesthetic (Figure 2.1). The following two sections will present the sensory aspects of the human hand and these modalities.

2.1. Tactile Modality

The tactile modality can be defined by the sensations felt in the fingers (or in general on the skin surface). The finger tissue integrates a number of different mechanoreceptors embedded in different skin layers. Tactile sensing is the result of a chain of events that starts when a stimulus such as heat, pressure, shear or vibration, is applied to such receptors. Followed by a response depending on the type, magnitude, and location of the stimuli [Bur96]. Most of the hand receptors are located on the hairless (glabrous) parts of the skin, covering the palm and fingertip regions. The receptors are able to accurately sense mechanical input due to any skin vibration and deformation caused by a tangential movement. As a result, tactile sensing allows for sensations associated with bumpiness, smoothness, roughness, among others [BW11].

2.1.1. Mechanoreceptors

The mechanoreceptors can be initially classified into two large groups according to their adaptation rate, or the transition speed from excited to neutral state:

- **Fast adapting mechanoreceptors (FA)** quickly return to their neutral state. As a consequence, it is not possible to detect material properties of a surface from a single and static observation; instead, we should slide our fingers over a surface to perceive its bumpiness and texture.
- **Slowly adapting mechanoreceptors (SA)** detect if an event is occurring continuously. During grasping movements, we can rely on these receptors to detect and adapt to changes in weight, balance, and slippage.

Mechanoreceptors are also characterized by their input frequency or the speed at which separate stimuli can be detected. Fast adapting mechanoreceptors can respond to events between 20Hz and 300Hz. Slowly

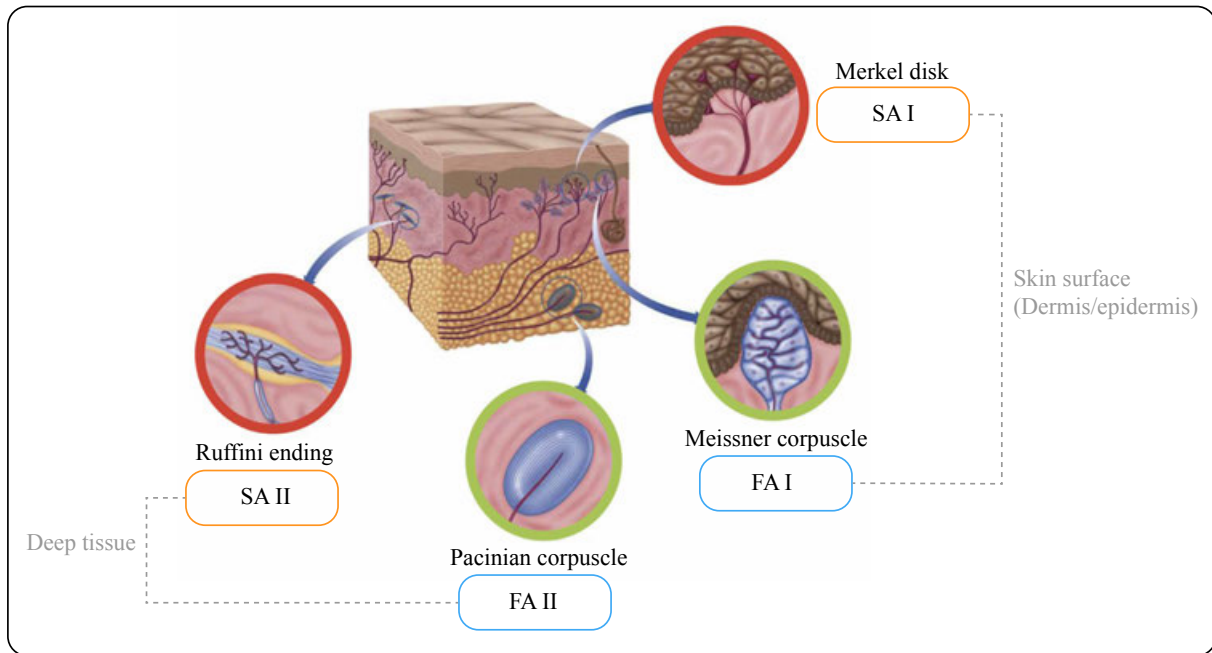


Figure 2.2.: Mechanoreceptors involved in tactile sensing. Cross-section of the skin showing the density and distribution of tactile mechanoreception corpuscles. Adapted from: Thompson Higher Education 2007.

adapting receptors are limited to 10 Hz [BC03]. The glabrous surface of the hand is innervated by four types of mechanoreceptive afferents (associated with specific mechanoreceptors), characterized by their temporal resolution and the size of their receptive fields. Also, due to structural variations, the receptors react to different stimuli [JF09; KW14] (see Figure 2.3):

- **Slowly adapting type 1 (SAI)** rely on **Merkel** disks to detect edges and spatial features. They respond to pressure and low-frequency dynamic skin deformations ($< 5\text{Hz}$), and are sensitive to static force, pressure, and small-scale shapes.
- **Slowly adapting type 2 (SAII)** rely on **Ruffini** endings to sense skin stretch and allow for the perception of the direction of motion. They have low dynamic sensitivity, and are sensitive to static force and tension.
- **Fast adapting type 1 (FAI)** rely on **Meissner** corpuscles that respond to low-frequency vibrations. They are sensitive to dynamic skin deformations of relatively high-frequency (5-50Hz), to local spatial discontinuities (e.g., edge contours, Braille-like stimuli), and are insensitive to static force but sensible to changes in velocity.
- **Fast adapting type 2 (FAII)** rely on **Pacinian** corpuscles to sense vibration and light touch. They are extremely sensitive to mechanical transient and high-frequency vibrations (40-400Hz), but insensitive to static forces. They convey information about distal hand-held events (e.g., vibrations transmitted through a tool).

Besides, the size of the receptive field indicates the skin area in which a single receptor is sensible to stimuli (i.e., two-point discrimination or the distance where the two points can be felt as separate). The size of the receptive field is proportionally inverse to the spatial resolution [VJ84].

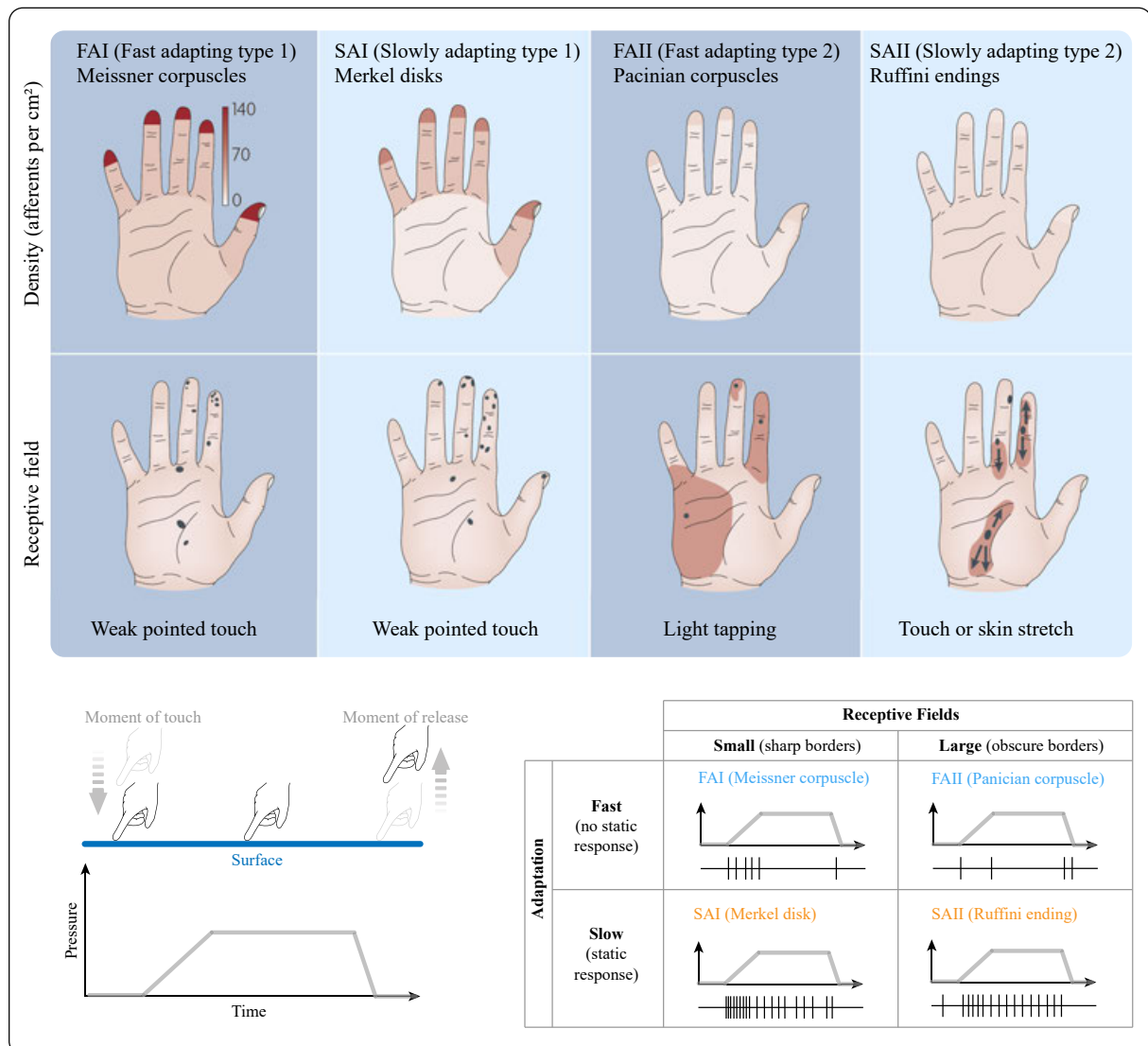


Figure 2.3.: Density and tactile sensory innervation of the hand mechanoreceptors (Adapted from [JF09]).

In addition to the mentioned mechanoreceptors for vibration and pressure. There are additional cutaneous submodalities for temperature, pain, and itch. Temperature receptors provide information on warm and cold surfaces. Pain receptors or nociceptors protect the skin against potential damage and are triggered by thermal, mechanical (i.e., high friction), or chemical stimuli. Finally, itch receptors are triggered by mechanical stimuli related to transient sensations like coarse wool [Jon+12].

2.2. Kinesthetic Modality

Haptics also include proprioception and kinesthesia. Both terms are often used interchangeably, but some literature considers proprioception as containing both the kinesthetic and the vestibular systems, while others consider them as two separate modalities with the kinesthetic modality as related to movements

Feature	Meissner corpuscle	Pacinian corpuscle	Merkel disk	Ruffini ending
Rate of adaptation	Fast (FAI)	Fast (FAII)	Slow (SAI)	Slow (SAII)
Location	Superficial dermis	Dermis and subcutaneous	Basal epidermis	Dermis and subcutaneous
Mean receptive area	$13mm^2$	$101mm^2$	$11mm^2$	$59mm^2$
Spatial resolution	Poor	Very poor	Good	Fair
Frequency response	10-200 Hz	70-1000 Hz	0.4-100 Hz	0.4-100 Hz
Sensitive to temperature	No	Yes	Yes	at > 100 Hz
Physical parameter sensed	Skin curvature	Vibration	Pressure	Skin stretch
	Velocity	Slip	Skin curvature,	Local force
	Local shape	Acceleration	Local shape	
	Flutter, Slip			

Table 2.1.: Properties of the different types of mechanoreceptors. The adaptation rate is the speed for a receptor to go back to its neutral state, the input frequency corresponds to the frequency at which separate stimuli are distinguished, and the receptive field is the area in which a single receptor is sensible to stimuli [RH93].

and proprioception (as well as vision and the vestibular system) is responsible for balance [RZ18].

A common distinction is that proprioception informs us about awareness and position of the body in space (the cognitive component), and kinesthesia provides useful information on how we move in space (the behavioral component). As mentioned, the vestibular system supplies information about balance, the position of the head and body in relation to the earth's surface [RZ18].

The kinesthetic modality is responsible for perceiving the mechanical forces related to the weight and resistance (i.e., stiffness, squeeziness) of objects and the relative position of our extremities in relation to our body (i.e., where are the body parts and what are they doing) [BW11]. Figure 2.4 depicts the musculoskeletal organs associated with the kinesthetic modality. The muscle spindles sense muscle movement, skeletal muscle length, and stretch reflex. The Golgi tendon organs (GTO) detect tendon tension. Finally, joint capsules are responsible for pressure and tension detection at a particular limb's joint.

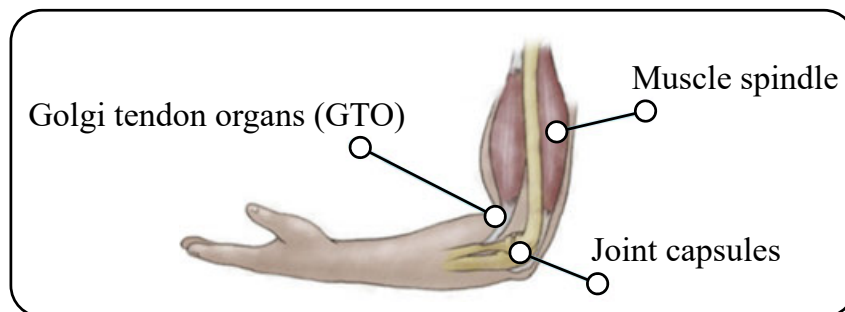


Figure 2.4.: The kinesthetic modality relies on internal organs to provide information about stretching, tension and pressure of our limbs relative to the body. In the picture, muscle spindles, Golgi tendon organs, and joint capsules.

As an example, in the case of lifting a rock from the floor using our dominant hand, kinesthetic signals come from mechanoreceptors, joints, tendons, and muscles of the limbs involved. The frequency of the signal generated by joint receptors indicates the angular velocities between limbs, and the amplitude of the signal is proportional to the angle between limbs connected at a specific joint [Bur96]. GTOs (positioned as a link between tendons and muscles) are responsible for sensing the stress caused by internal and external forces on muscles, iteration over tension-measurement, and stabilization cycles to adapt dynamically according to the weight of the lifted rock.

Additional properties of the rock, like shape and rigidity, are estimated with reference to the muscle length as measured by the muscle spindles (located inside at the center) [KW14]. The overall sensation is enriched with information coming from the tactile modality. As the rock is lifted, skin mechanoreceptors sensing bulging and stretching of the skin are activated indirectly by flexion and extension movements in the arm limbs. Additionally, the vestibular system contributes with a global perception of orientation and position for the limbs (i.e., fingers, hand, forearm), as well as proprioceptive links between head, neck, trunk, and limbs [Ach15].

2.2.1. Perception-action Loop

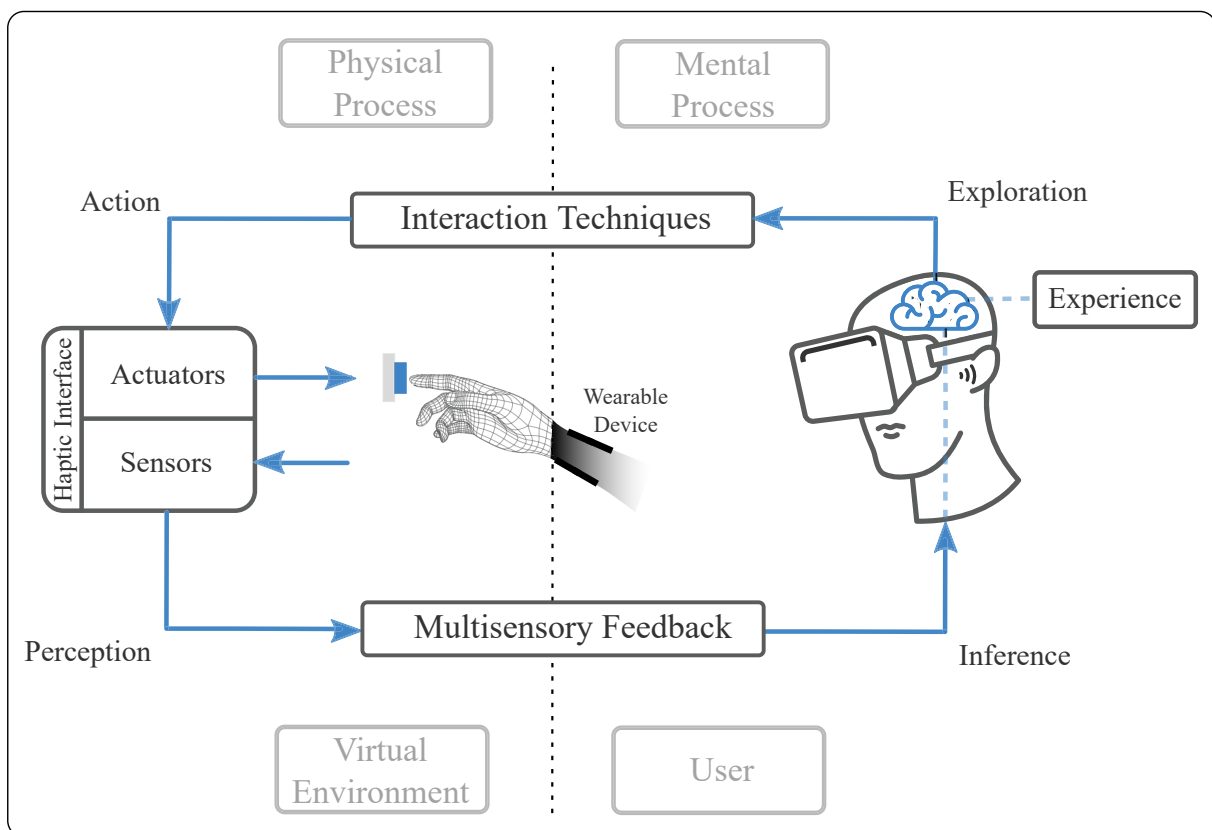


Figure 2.5.: Model for human motor action and reaction in interactive VEs.

In the interaction process between user and VE, the user can exploit different techniques (e.g., selection, manipulation, or navigation) to interact with the VE. The user is equipped with sensors and actuators,

which allow for tracking actions and for providing actuation accordingly. The system provides tactile and kinesthetic feedback, which is perceived by the user. The brain starts the inference process, analyzes the cues, and integrates all signals, which finally represents the user experience. In this section, we explain the perceptual and cognitive mechanisms [GL17; MD15; KEE19] that enable a system to convey sensations using haptic feedback. When a 3D object (representing a physical object) is pushed with a finger, visual, tactile, and proprioceptive feedback is experienced simultaneously and in a congruent way. Such user actions are typically performed as follows:

1. The user starts to reach the target object; therefore, the brain sends a motor command (efference) to forearm muscles and creates the efference copy.
2. In parallel:
 - a) The motor command arrives at muscles (i.e., the muscle spindle is the efferent receptor), and the index finger travels in mid-air, getting close to the target object.
 - b) The efference copy arrives at the cerebellum to predict the sensory input consequences (intended movement) using a *forward model*.
3. Then, the user comes across a collision with the object surface, and three afferent signals are triggered by the somatosensory system:
 - a) First, the user sees the contact between the finger and the object, which is sent to the brain as a visual afferent signal.
 - b) Second, a change in input is detected by the tactile mechanoreceptors in the fingers, which is sent to the brain as a tactile afferent signal.
 - c) Third, a change input is detected by the GTO as the *Extensor Indicis* muscle (flexion antagonist) is contracted because the index finger is slightly extended during the collision with the object. As a result, the GTO sends a proprioceptive afferent signal to the brain.
4. Then, the brain receives the afferent signals caused by the last motor behavior (actual movement) and compares them to the predicted signals (intended movement). Differences between the signals are used to adapt the behavior of the user:
 - a) The tactile afferent signal is attenuated as it matches the predicted signal from the efference copy. This happens because of priors (earlier perceptions related to associative learning) as the user pushed similar objects before. Therefore, self-generated touch sensations, which are somatosensory consequences of the user reaching movement (reafferent), are less important for the brain.
 - b) The proprioceptive afferent signal should be more relevant when it can not be predicted. This signal is taken as produced by external forces (exafferent), forming a perception residual that requires an action.
5. Then, based on the exafferent, the brain plans a change in the manipulative behavior of the user while interacting with the object: sending motor commands (efference) to push the object and compensate for the increasing force according to the object weight.

Haptic perception is based on the integration of afferent proprioceptive and tactile signals. In a common VE scenario, only a fraction of the afferent signals are rendered; in particular, there is a lack of tactile feedback. Mostly, whenever the user approaches and collides with the virtual object, the user

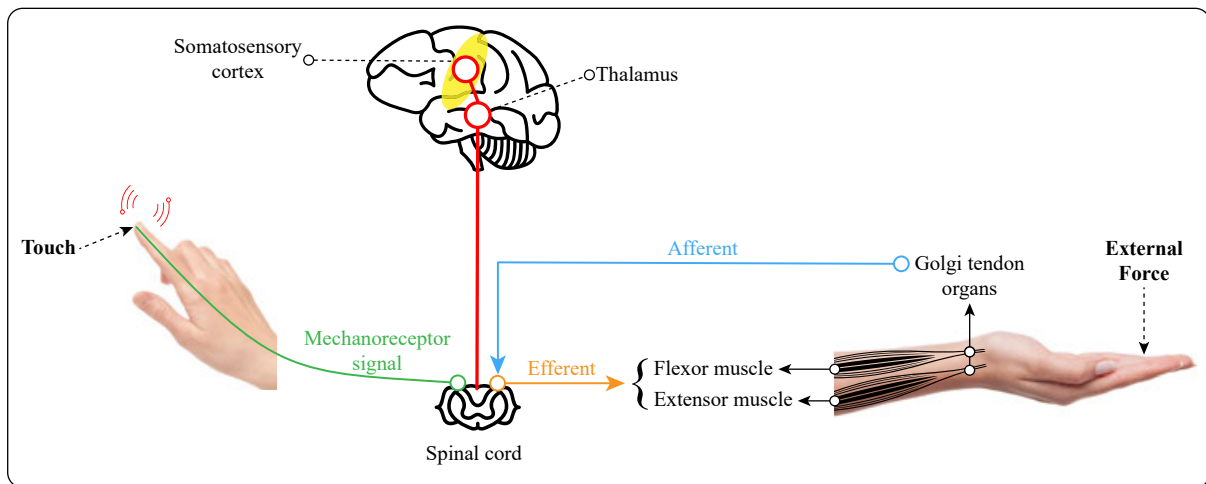


Figure 2.6.: Neural pathways of the tactile and kinesthetic modalities.

perceives visual feedback accordingly. Still, the fingertip tactile sensation of the collision and also the kinesthetic sensation of the movement being interrupted are lost, producing large sensory conflicts. Such conflicts are crucial for human-computer interaction in VEs as they can induce breaks in presence, reduce task performance, require higher cognitive efforts during the multisensory integration process, and finally degrades the overall user experience in the VE [Ins01].

2.3. Visual Modality

Vision is based on photoreceptor cells located on the retina. When photoreceptors are stimulated with visible light, they transmit electrical signals through the optical nerve to the brain. Cone photoreceptors enable color and high light vision, and rod photoreceptors allow for low light and peripheral vision [Lam15].

2.3.1. Field of View

The field of view (FOV) is the horizontal and vertical extent of the observable environment. In MR applications, the FOV is a key aspect to improve the sense of presence [Lin+02]. The human vision is described by two types of FOV (Figure 2.7 left). First, the horizontal Monocular FOV describes the field of view for every eye independently, consisting of both the nasal FOV (angle from the pupil to the nose 60° - 65°), and the temporal FOV (angle from the pupil to the head side 100° - 110°). Second, the horizontal Binocular FOV is the combination of the two monocular fields. The combination of both Monocular and Binocular FOVs, provide a viewable area of 200° - 220° . Also, the overlapping FOV or stereoscopic binocular FOV enables the perception of 3D content in VEs with an approximate angle of 114° .

The effects of the FOV in VEs and specifically with the use of HMDs have been studied. Pointing tasks as perceived as easier with an unrestricted FOV in comparison to a narrow FOV (i.e., 40°) [RB04]. However, there is no such effect for searching tasks [LR05]. Also important regarding the use of HMDs

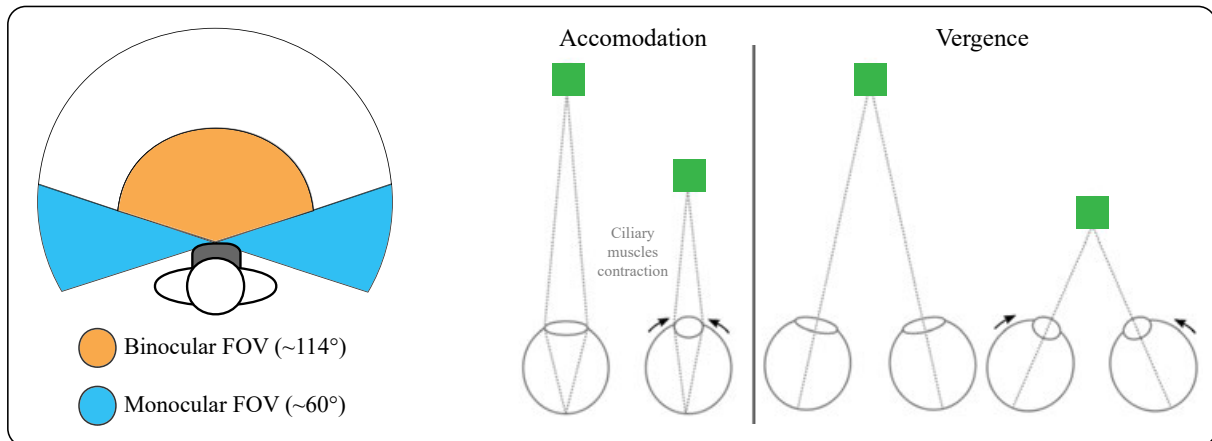


Figure 2.7.: Field of view and binocular depth cues: **(left)** The field of view represents the extend of observable environment. **(right)** Binocular depth cues for accommodation and vergence to focus on close objects (Adapted from [Lub18]).

in VEs, the interpupillary distance [Mil04] (distance between the eye pupils) plays an important role for calibration and usability purposes. Better user experience scores were reported when the IPD was calibrated to match the focal point of the HMD lenses (i.e., avoiding FOV reduction and distorted images) [Ras09].

Finally, concerning commercial advances, HMD designers have the lenses as a limiting factor to get a better FOV. Current explorations include either move the lenses closer to the eyes with mechanical actuators or increase the size of the lenses while maintaining an ergonomic and lightweight design. As an alternative, fabricants could use a shorter focal length for a stronger magnification (i.e., using thicker and heavier lenses, or Fresnel lenses to reduce weight) and move the display closer. However, geometric distortion and chromatic aberration became more difficult to tackle. Also, the HMD display requires a higher resolution display to reduce the apparent individual pixels (i.e., screen door effect).

2.3.2. Depth Estimation

Human eyes are situated approximately $64mm$ apart, providing two signals, and hence, two different images, which are combined by the brain into a single 3D image. The size of the disparity between the images indicates the size of the three-dimensional effect. Thus, far-away objects (with less disparity) are perceived as flat, and closer objects (providing large disparity) appear with more depth cues. Appropriate depth estimation in VEs is important for 3DUIs featuring selection and manipulation tasks. Such estimations assure the users can execute proper ballistic and correction movements [LL09], avoiding false selections and overestimations resulting in interaction issues (i.e., intersected objects and occluded fingers).

Depth perception is supported by visual and non-visual depth cues [How12]. Monocular depth cues can be perceived with a single eye and presented on a single display. Binocular depth cues (disparity and vergence) require both eyes to see a different image on independent displays [WRM95].

Disparity cues enable humans to estimate depth due to the distance between the eyes and the fact that both eyes look in a similar direction [Col96]. Such cues can be categorized as oculomotor cues because

are sensed from muscle actions (i.e., instead of photoreceptors) in the visual system to achieve a crisp image [LaV+17]. Vergence is defined as the simultaneous movement of both eyes in opposite directions to maintain binocular vision. Thus, eyes turning inward will focus closer objects (convergence), and eyes turning outward will focus objects farther away [GJ84]. Vergence movements are closely connected to eye accommodation (i.e., how much the ciliary muscles contract to increase the lens refraction due to diverging light rays from a close object). Changing the eyes focus of the eyes to look at an object at a different distance will automatically cause vergence and accommodation (i.e., convergence-accommodation reflex).

One of the major sources of distance estimation problems in VEs is the so-called vergence-accommodation conflict [Hof+08]. The conflict is evident when accommodation and vergence are evaluated in common HMD setups. The user's eyes have to accommodate at the display plane while converge to focus on a target 3D object, causing discomfort and fatigue. Additionally, regarding the influence of the FOV for distance estimation in VEs, the use of a wider FOV and proper IPD calibration presented a significant positive effect on distance judgment while using an HMD [Jon+12; Kel+12].

2.4. Ergonomics

This section presents the function of the human hand in terms of its anatomic features and capabilities. This information is vital to facilitate and motivate the design of hand-worn haptic technology.

The human hand is a complex structure integrating bones and joints with a high degree of articulation (27 individual bones; 8 carpal, 5 metacarpal, and 14 phalanges are connected by joints and ligaments) [NT93]. The wrist connects the hand to the forearm comprising eight small bones. The palm holds metacarpal bones, creating an arrangement of joints to the fingertips. Every finger is a branch composed of the proximal, medial, and distal phalanx. The whole structure has a small volume due to thin tendons (going through the wrist up to the fingertips) connecting remote muscles located in the forearm, and enabling the hand with finger curling and thus powerful and tight grips [TS55]. The remote muscles (i.e., flexors and extensors), as well as the muscles supporting wrist rotations, are mainly arranged in the humerus, near the elbow. Additional local muscles for lateral finger movements (i.e., adduction and abduction) are located between the metacarpal bones. In particular, the movement of the thumb is controlled by remote muscles (i.e., extension and abduction) and local muscles (i.e., flexion and opposition) [Mor89].

The DoFs of the hand have anatomic constraints. Medial phalanxes can reach 110° , and proximal phalanxes can approximately rotate 90° at a maximum. Additionally, distal joint bending affects the preceding joints (the effect is also notable while curling the ring and little fingers), evidencing in this way, muscular interdependencies between adjacent parts of the hand [JYH00]. In summary, the human hand supports 27 DoF distributed as follows. The wrist has six DoF defining position and orientation in space. The thumb has five DoF due to a special joint for rotations toward the palm (i.e., prehension grasp). Every finger root is provided with flexion/extension and abduction/adduction summing up two DoF, plus one flexion DoF for both the medial and distal joints; giving a total of four DoF per finger [ES03; NT93].

Interaction taxonomies present the mechanical configurations of the hand to interact with our environment. In the real world, typical interactions involve a reduced number of all the possible manipulation postures. In the context of this thesis, we contextualize our studies following the mixed-grasp taxon-

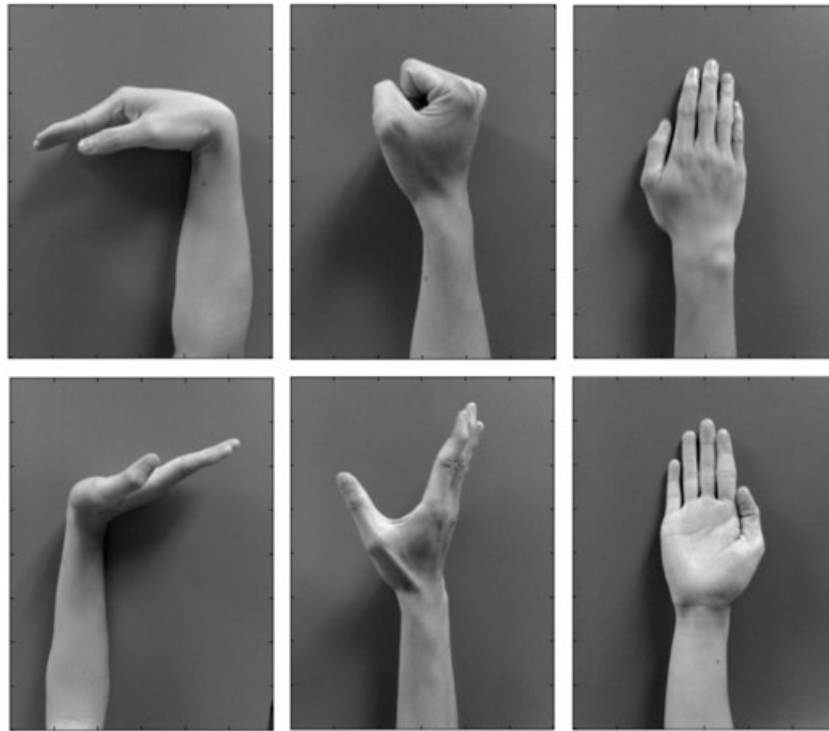


Figure 2.8.: Types of hand movement: (in columns from left to right) Wrist flexion, wrist extension, hand close, hand open, forearm pronation, forearm supination [PLP09].

omy [BD11] in order to describe the hand postures required to use haptic wearables and to perform selection and manipulation tasks in VEs. The selected taxonomy is very versatile and classifies the tasks regarding hand motion, contact with target objects, gestures involved as well as prehension, the and the relative motion of the manipulated object (Figure 2.9). Additionally, the selection tasks evaluated in this thesis constrain the contact patterns between hand and object [Cut89]. Specifically, finger-object (for no-motion-at-contact tasks, see *writing* in Figure 2.9), as we use the gesture of a pointing index finger (i.e., on the dominant hand) to provide multimodal feedback whenever the finger interacts with 3DUI elements, paying attention to dexterity (high DoF between finger and object) and precision (accurate collision/intersection detection).

2.5. Psychophysics

Psychophysics is defined as the relationship between the subjective sensation and the objective physical stimulus [Sno+85]. The main objective is to find the relationship between the intensity of the physical stimulus and the perceived stimulus intensity. The methodology is based on measuring the ability of participants to consciously discriminate between two physical intensities. As a result, perceptual limits indicate the way humans interpret increases in the stimulus intensity to produce increases in the sensory experience.

The just noticeable difference threshold (JND) measures the sensitivity for the discrimination or the smallest amount of stimulus necessary to produce a sensation. According to Weber's law, [Web+96] the

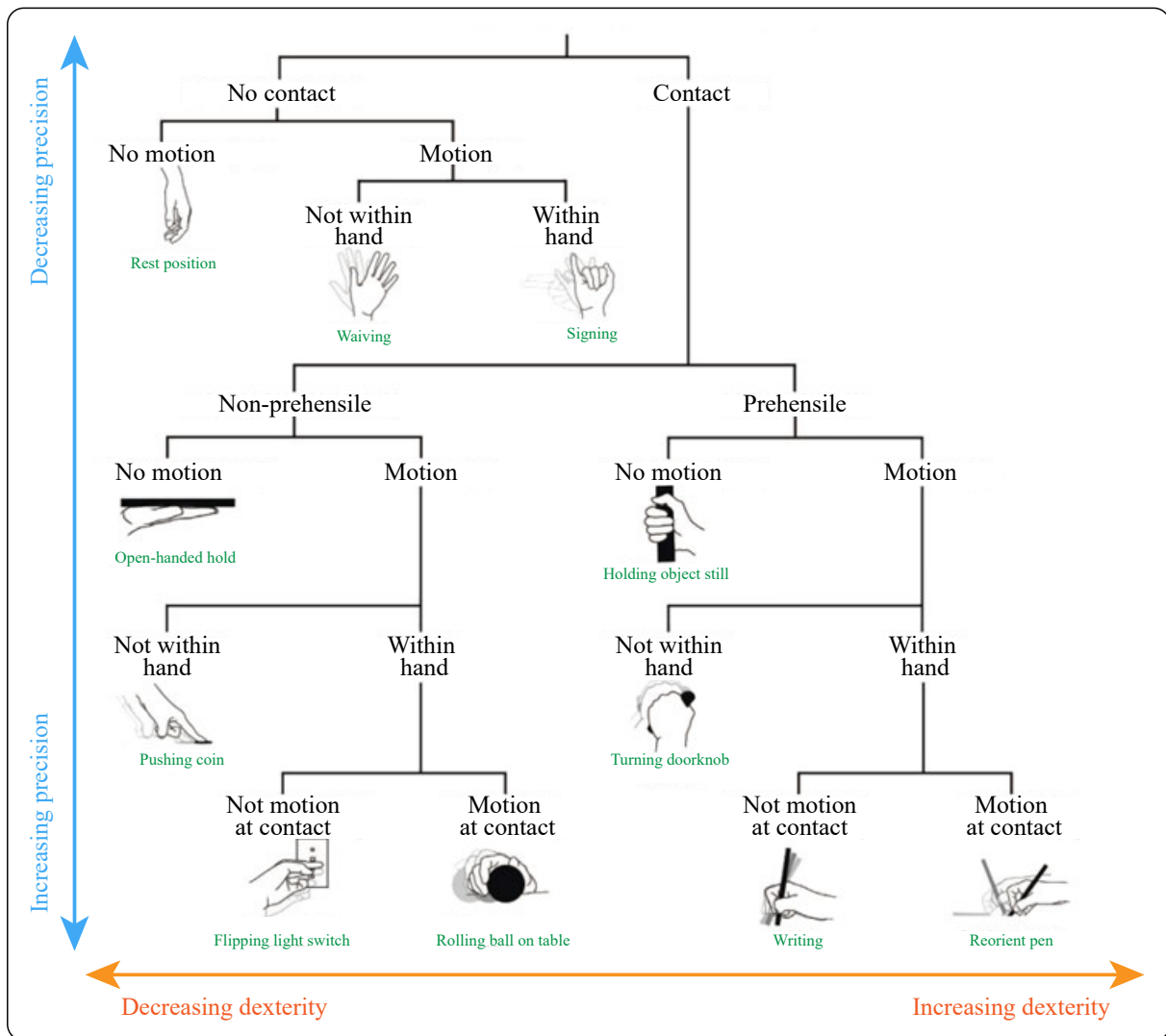


Figure 2.9.: Mixed-grasp taxonomy, including within-hand motions and gestures (Adapted from [BD11]).

JND is a constant proportion of the original stimulus, describing the relation between stimulus intensity and the perceived intensity. In other words, JND is the smallest amount of detectable difference between two stimuli intensities that an individual can perceive. In the same way, we can define a threshold as the lower limit at which a stimulus (or the difference between two stimuli) ceases to be perceptible [Ges13]. Ideally, there is a specific stimulus intensity at which an observer could not (below) or could (equal or greater) detect a stimulus change (Figure 2.10 left-top). In real and controlled experimental conditions (i.e., with response variability due to attention, sensitivity, and subjective conditions), the responses are spread near the stimulus threshold (Figure 2.10 left-bottom). For example, if a stimulus is presented to an observer and then the intensity is slowly increased. If the intensity has to be increased several times to reach level 10 before the observer could identify that the stimulus had changed, the JND would be ten levels. Using this information, you could then use Weber's law to predict the JND for other intensity levels.

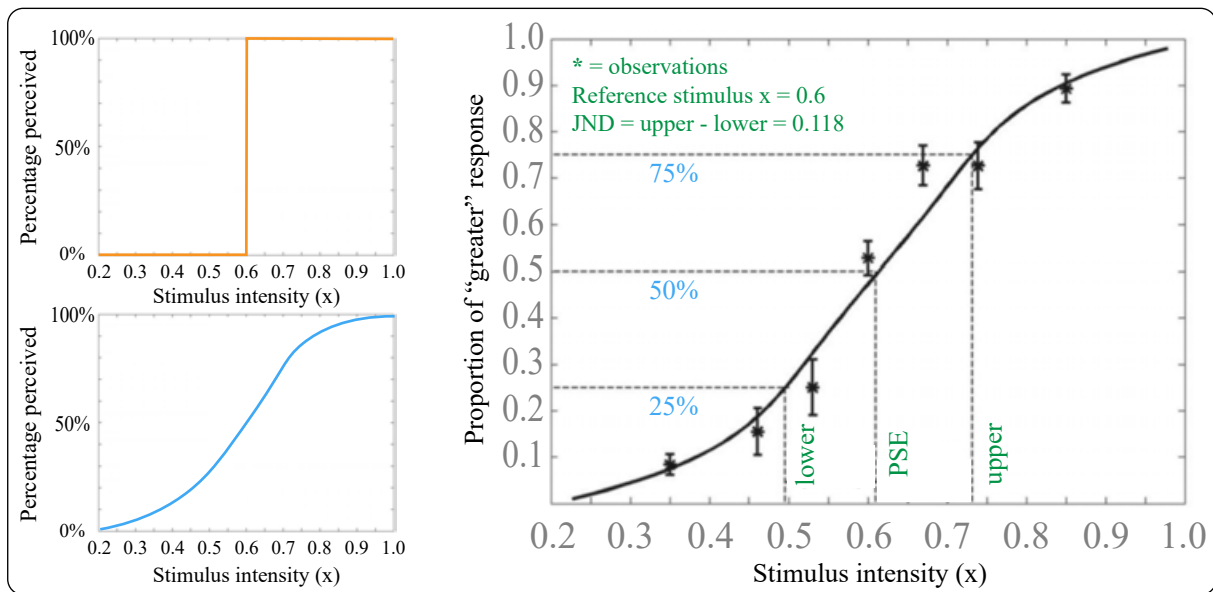


Figure 2.10.: Psychometric threshold and JND: **(left top)** Ideal psychometric function. **(left bottom)** Expected psychometric function. **(right)** Example of psychometric function using the method of constant stimuli.

Due to the variability of responses to the same stimulus, the threshold will never be absolute and must be defined statistically. If an observer detects a stimulus of a certain intensity for only 25% of the time, the detection probability increases with the intensity of the stimulus. As a standard procedure, the detection threshold is the intensity at which the person correctly detects the stimulus 75% of the time (Figure 2.10 right). The observer discrimination is influenced by stimulus intensity changes and sensitivity, but also by multimodal background noise and biased perception associated with prior experience and learning effects [Sno+85].

There are several different methods for measuring detection thresholds through psychophysical experiments. In this thesis, we used the methods of adjustment [Ste58], the method of constant stimuli [Spe08], and the two-alternative forced-choice task method (2AFC) [Bog+06] to determine detection thresholds:

- **Method of adjustment**

In this method, the subject is asked to change the stimulus level until it is the same as the level of a comparison stimulus, or it is just barely detectable against the background noise. The adjustment requires several trials for the subjects to control themselves the magnitude of the variable stimulus, starting with a level evidently different (“greater” or “lesser”) than a standard stimulus and vary it until they find subjective equality between them. The stimuli difference is recorded per adjustment, providing at the end an average error (i.e., sensitivity measurement).

- **Method of constant stimuli**

In this method, the levels of the stimulus are not related from one trial to the next but presented randomly, reducing errors of habituation and expectation by preventing the experiment subject from being able to predict the level of the next stimulus. The method can

test an absolute threshold (i.e., binary answer), requesting the subjects to report whether they are able to detect the stimulus. Also, a difference-threshold can be tested by constant comparison of a base stimulus against a set of others with varied levels.

- **2AFC**

In this method, the experiment subjects are exposed to intensities couples of a stimulus. In each trial, subjects/participants are forced to pick one of two choices related to the comparison of a random intensity against a standard reference intensity (e.g., shorter or longer, smaller or greater). Neutral answers are not allowed, and subject guesses will be taken by chance (i.e., correct in 50% of the cases). With the resulting data for the two choices available, a psychometric function plots the proportion of “greater” responses against the value of the comparison stimulus (Figure 2.10 right). Next, the Point of Subjective Equality (PSE), or the level at which the comparison stimulus appears equal to the standard, is obtained as the value at the 50% proportion. As an example, at the PSE, all the subjects will find a stimulus “larger” 50% of the time and “smaller” the other 50%. The JND is then calculated to be the average of the upper and lower difference threshold values (taking levels for the 25% and 75% proportions, respectively).

3

Chapter 3

Haptics and 3DUI

3.1. Haptic Technology

Haptic technology has been explored to improve task performance, mimic or expand sensory capabilities, and make interactions more compelling and satisfying [CSO18]. Humans have kinesthetic limitations related to absolute position control. However, humans excel at producing small variations in force resistance. In other words, humans can accomplish tasks involving motor precision when the limbs involved are supported by a solid and stable anchor (i.e., world-grounded; hand supported by the table while writing vs. writing with no hand support). In haptics, stability or resistance is usually supplied by robotic-arms or passive objects as kinesthetic feedback. On the other hand, when precision is not needed, tactile (un-grounded) feedback can be provided by mechanical-electrical actuators arranged as tactile display on-skin in the limb of interest [CSO18]. Haptic feedback can also provide spatial guidance, actively guiding the body with force feedback, or providing tactile cues to orient the visual attention or specific limb postures. The development of haptic technology also has great challenges; most of them related to the hardware displays utilized to provide feedback. The use of inadequate dynamic range or refresh rate is a common cause of jittery feedback [Cho+17a]. Haptic rendering of realistic and compliant human-scale forces is problematic due to motors and actuators with issues and compromises related to size, weight, responsiveness, and latencies. Additional problems are associated with the form factor (mainly because of the limited workspace of small haptic displays), inadequate or not enough DoFs, insufficient affordances, and lack of support for anatomical diversity [Mac08]. Haptics is also studied in the context of the interaction between machines and humans in real environments, VEs, and even tele-presence systems [Ran+10]. This thesis will focus on the study of both computer and machine haptics in VEs. Computer haptics conceives (in the same way as computer graphics does for the vision sense) the rendering and representation of touch sensations. On the other hand, machine haptics comprehends the development and evaluation of technology to simulate or supplement the sense of touch. The design of haptic devices crosses different approaches, from grounded systems to wearables as well as hybrid systems. All of these approaches offer different features and are classified into different categories [CSO18].

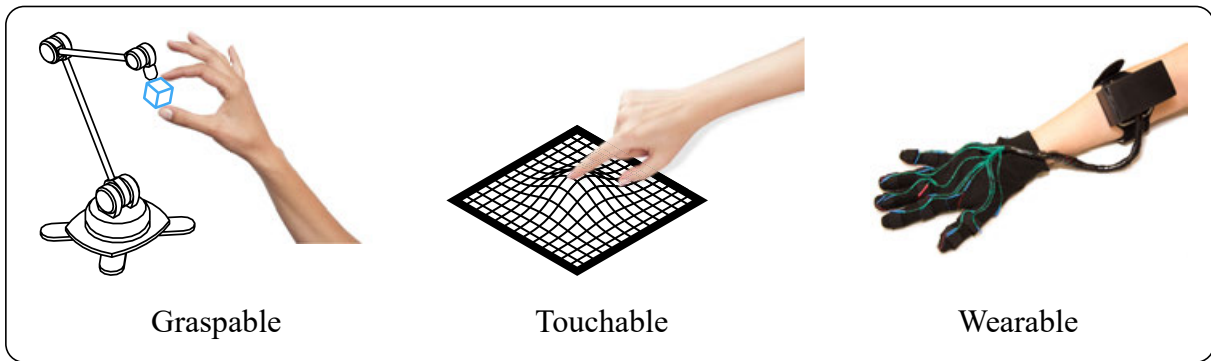


Figure 3.1.: Types of interactive haptic devices for kinesthetic and tactile stimulation: Graspable, touchable, and wearable (Based on [CSO18]).

3.1.1. Types of Interactive Haptic Devices

This chapter is based on recent taxonomies for interactive haptic devices [CSO18; Pac+17] to explore the main characteristics of haptic systems. We consider the following taxonomy with three main categories and sub-categories (Figure 3.1):

Graspable systems. Such as hand-held tools, pens, or handles connected to

- world-grounded devices providing kinesthetic feedback (push-pull forces),
- ungrounded devices providing kinesthetic feedback (inertial forces), or
- ungrounded devices providing tactile feedback.

Touchable systems. Which are encountered-type active surfaces to provide

- tactile feedback based on location, or
- tactile and kinesthetic feedback for changes in
 - shape,
 - mechanical properties, or
 - surface properties.

Wearable and contactless systems Which are

- hand-grounded devices or exoskeletons providing kinesthetic feedback,
- world-grounded tactile devices for mid-air contactless sensations, and
- hand-mounted or limb-mounted on-skin devices to provide
 - vibrotactile feedback,
 - lateral skin stretch,
 - normal skin deformation, or
 - muscle or tendon stimulation.

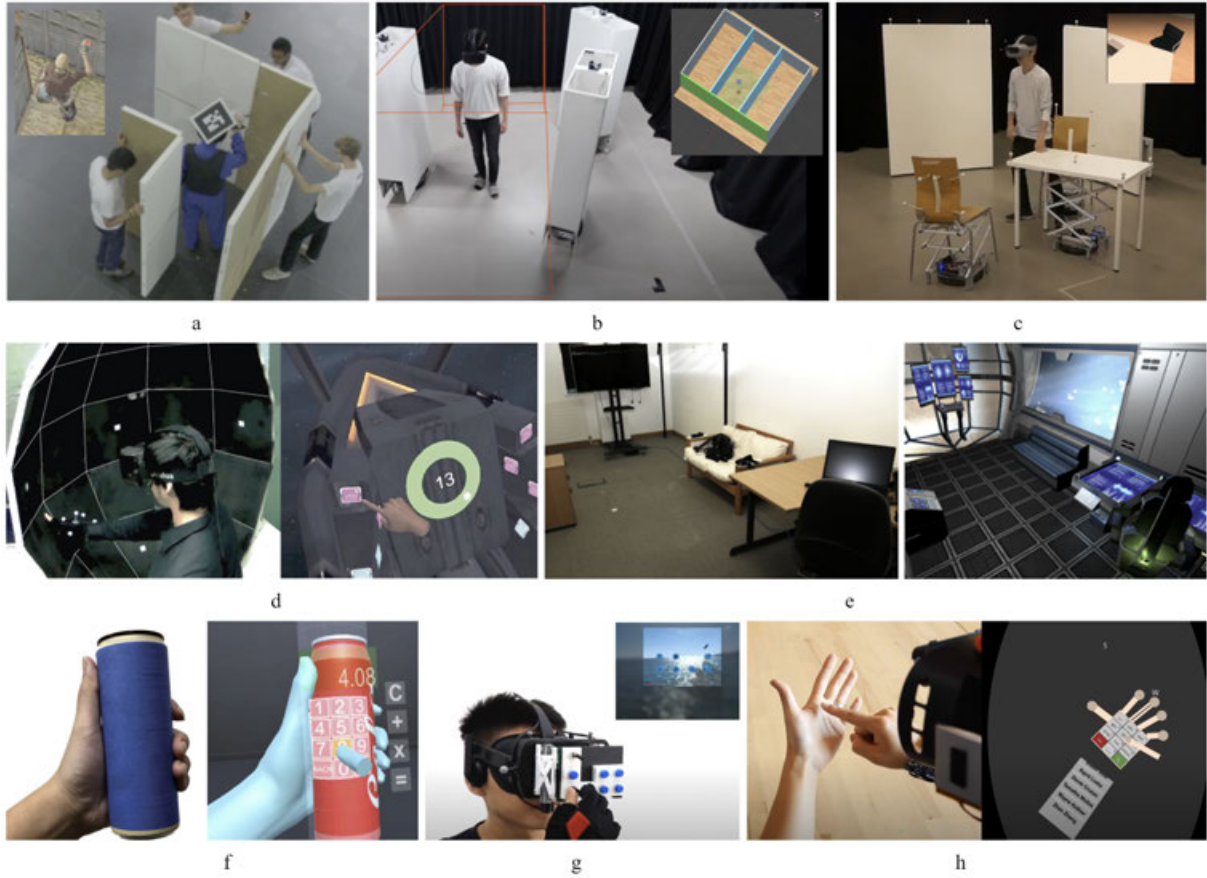


Figure 3.2.: Examples of passive haptics: (a) TurkDeck [Che+15], (b) ZoomWalls [Yix+20], (c) RoomShift [Suz+20], (d) Sparse Haptic Proxy [Che+17], (e) Substitutional reality [SVG15], (f) Gripmarks [Zho+20], (g) FaceWidgets [TWC19], and (h) ActiTouch [Zha+19].

Additionally, high-level classifications propose the concepts of passive and active haptics. Passive haptics is related to interactions in which the devices are in motor control. In the case of passive tactile feedback, the device deforms or stimulates the skin, and the user is not required to perform any movement in order to perceive the feedback. In passive kinesthetic feedback, a device or object imposes forces to restrict the user's movements. Examples of passive haptics can be seen in Figure 3.2: Users touching or manipulating objects in VR can simultaneously interact with corresponding objects in the physical world [Che+15] (see Figure 3.2a).

Two similar approaches for room-scale VR relies on multiple autonomous robots (i.e., robotic swarms) that dynamically adapt to the user movements to provide passive feedback with encounter-type wall-shaped props for both walls [Yix+20] (see Figure 3.2b) and furniture [Suz+20] (see Figure 3.2c). A proxy of physical geometric primitives can simulate touch feedback in VEs, simulating detailed 3DUIs by redirecting the user's hand to a matching primitive of the proxy [Che+17] (see Figure 3.2d). The substitutional reality in VR pairs every physical object surrounding the user to a virtual counterpart, plus intentionally adding some discrepancy [SVG15] (see Figure 3.2e).

Also, regarding substitution, passive feedback can be provided associating a particular handgrip, a physical object, and an activation gesture to enable the object to be used as input for 3DUIs (i.e.,

no object recognition nor instrumenting needed) [Zho+20] (see Figure 3.2f). Physical widgets can be grounded on HMDs, and VR controllers to provide passive haptics for tangible interactions [TWC19] (see Figure 3.2g). Going beyond, computer vision and electrical methods can be combined to perform on-skin touch segmentation and enable the skin as a passive surface for tactile interaction in VR/AR [Zha+19] (see Figure 3.2h).

Conversely, active haptics is related to interactions in which the user is in motor control, and the devices respond accordingly with feedback. In the event of active kinesthetic feedback, the device simulates forces in response to user conscious motions. The device creates a natural experience operating human-scale forces (i.e., 0.1N-20N) with reactive actuation and low latency (i.e., <20ms). The active kinesthetic feedback can be either motor-driven or brake-like to convey sensations of friction and resistance, respectively. Finally, active tactile feedback is provided in response to user motions (i.e., detected by hand tracking). For example, when a system tracks a finger being slid over a virtual surface, the device renders the roughness properties as vibrotactile patterns on the skin.

The remaining sections briefly show the categories for active haptics. As this thesis is focused on haptic wearables, the corresponding last section will present more details in order to motivate the following chapters.

3.1.2. Graspable Systems

Grounded devices can provide kinesthetic force feedback with three or six DoFs of human-scale force and high-bandwidth for medium to large workspaces. A surrounding platform can be world-grounded, but also use a motorized turntable that rotates to deploy hand-held devices providing different types of feedback depending on the AR task being executed [Hua+20] (see Figure 3.3a). However, grounded devices are mainly based on robotic arms using admittance control systems to provide resistive forces and high-quality haptic rendering [BR19] (see Figure 3.3b). Kinesthetic ungrounded devices in the shape of electro-mechanically actuated physical connections can provide variable stiffness feedback for bi-manual interactions in VR [Str+18] (see Figure 3.3c). An ungrounded handle for tool-based interaction in VR is able to provide kinesthetic feedback for the perception of size, shape, and stiffness of virtual objects [Sun+19] (see Figure 3.3d). Some other graspable alternatives are active props. Such devices support ungrounded kinesthetic feedback and are able to provide inertial forces. For example, a graspable device for VR/AR capable of affording the users a realistic haptic sensation of fluid behaviors in vessels by actively relocating the center of gravity to emulate the moving center of gravity [Sag+19] (see Figure 3.3e). An ungrounded prop to provide kinesthetic feedback with propeller-induced force provides continuous force feedback in any direction regardless of the device's orientation [Heo+18] (see Figure 3.3f). Ungrounded weight-shifting devices can combine active and passive haptics to construct proxies that automatically adapt their haptic feedback [ZK17] (see Figure 3.3g). An ungrounded active prop can also be a shape-changing device providing kinesthetic feedback based on air resistance, weight shift, and rotational inertia by dynamically adjusting its surface area [ZK19b] (see Figure 3.3h). A similar device can drive weight on a 2D planar area to alter mass properties of the hand-held controller to provide shape perception in VR [Shi+18] (see Figure 3.3i).

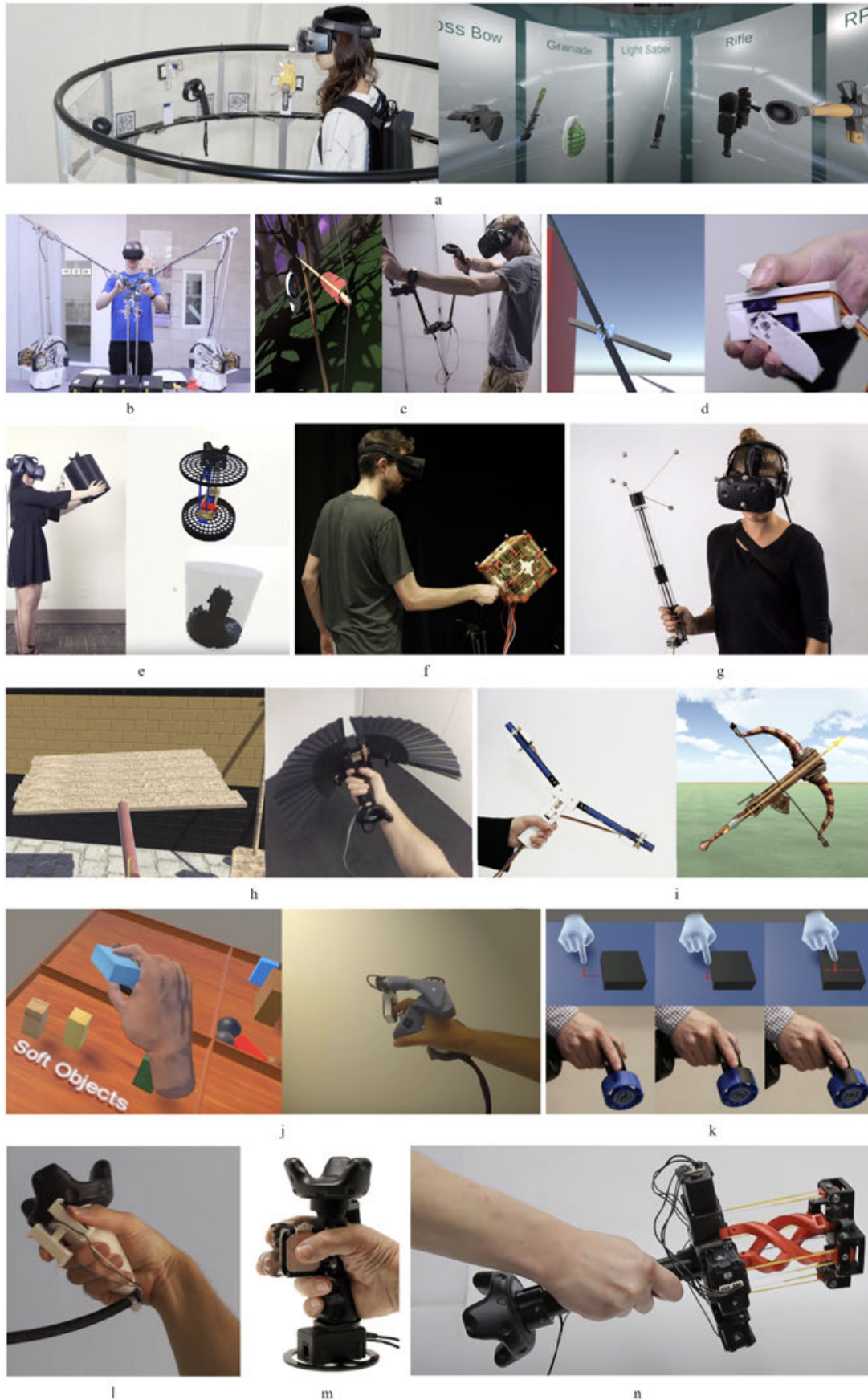


Figure 3.3.: Examples of graspable devices: (a) Haptic-Go-Round [Hua+20], (b) Mantis [BR19], (c) Haptic Links [Str+18], (d) PaCaPa [Sun+19], (e) SWISH [Sag+19], (f) Thor’s Hammer [Heo+18], (g) Shifty [ZK17], (h) Drag:on [ZK19b], (i) Transcalibur [Shi+18], (j) CLAW [Cho+18], (k) Haptic Revolver [Whi+18], (l) DualVib [THC20], (m) TORC [Lee+19], and (n) ElaStick [Ryu+20].

Handheld VR controllers can be enhanced with kinesthetic feedback and actuated movement to the index finger to support interactions for grasping virtual objects, touching virtual surfaces, and pull triggers [Cho+18] (see Figure 3.3j). Hand-held controllers can provide tactile sensations when a user touches a virtual surface, simulating different sliding and friction effects with a wheel raising-lowering mechanism [Whi+18; Lo+18] (see Figure 3.3k). Devices reacting to hand movements can provide feedback for manipulating dynamic mass (i.e., shaking a container object). The simulation is done by simultaneously delivering asymmetrical vibrations to provide kinesthetic feedback and acoustic vibrations to provide tactile feedback related to material properties [THC20] (see Figure 3.3l). A similar handheld renders texture and compliance by holding and squeezing the thumb and two fingers while operating a trackpad. As a result, the device supply vibrotactile feedback for the sensations of squeezing, shearing, or turning virtual objects [Lee+19] (see Figure 3.3m). Finally, a hand-held VR controller uses four custom elastic tendons along a joint to modulate the perception of stiffness when VE users are shaking/swinging flexible virtual objects [Ryu+20] (see Figure 3.3n).

3.1.3. Touchable Systems

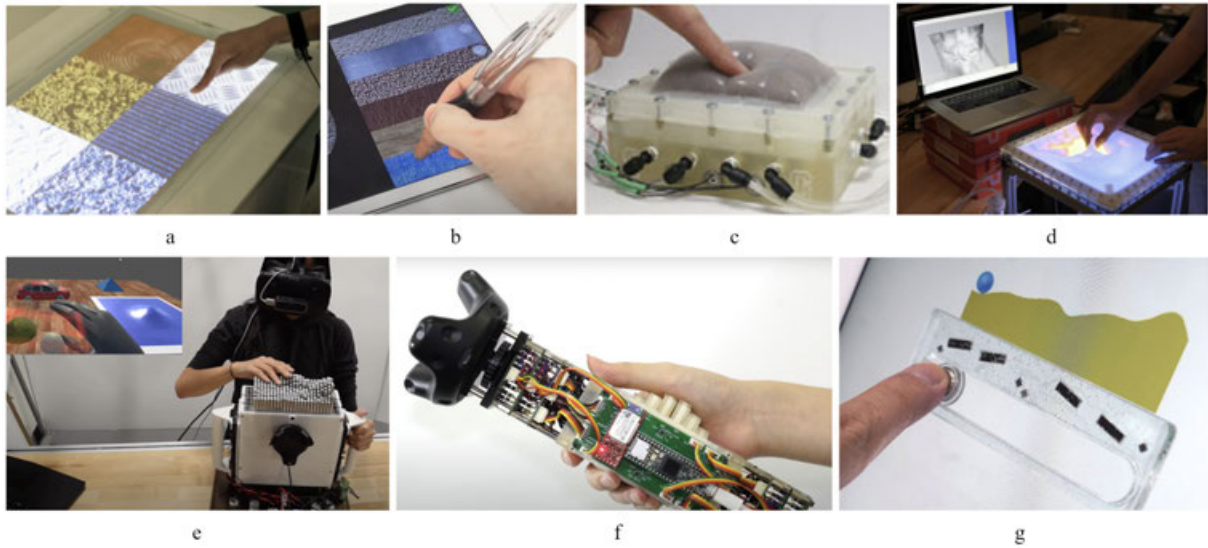


Figure 3.4.: Examples of touchable devices: (a) TeslaTouch [Bau+10], (b) TactGAN [BU18], (c) Controllable Surface Haptics [SO15], (d) Jamming User Interfaces [Fol+12], (e) ShapeShift [Siu+18], (f) PoCoPo [YSK20], and (g) Magneto-Haptics [Oga18].

Most of the touchable haptic systems can be categorized as active surfaces, providing tactile and kinesthetic feedback to communicate texture properties as well as forces and shape to the whole hand. Vibrations on surfaces can be used to simulate friction. For instance, the perceived friction can be modulated by using electrotactile feedback. In this case, the normal force on the touching point and hence the effective friction depends on the electrostatic attraction between the surface and the finger [Bau+10] (see Figure 3.4a). Vibrotactile feedback can also be recorded from physical interaction with a real surface (i.e., Haptography [KRM11]) and then recreated in simulated scenarios (e.g., active surfaces). Alternative approaches let users design vibrotactile signals using tactile impressions from user-defined parameters and

images. The resulting vibrotactile signals can be presented in surfaces offering vibrotactile stimuli for UI components and textures [BU18] (see Figure 3.4b). Deformable crust devices rely on dynamic topologies or particle jamming to enable the user for continuous surface control at higher resolutions. Pneumatic systems feature control of shape in a tactile display. Such display contains silicone membranes and a vacuum that enables molding and switching from flexible to rigid states [SO15] (see Figure 3.4c). Particle jamming devices can use material stiffness to create malleable and organic user interfaces supporting 3D modeling with digital clay. This type of system uses low-power pneumatic jamming, hydraulic-based actuation, and optical shape sensing [Fol+12] (see Figure 3.4d). A touchable display can also provide resistive kinesthetic feedback by using permanent magnetic patterns during active touch. This approach distributes magnetic force along paths of motion to convey sensations (e.g., motion difficulty related to slope) [Oga18] (see Figure 3.4e). Another approach for touchable haptics is the pin-array devices, allowing for un-tethered interaction and providing kinesthetic feedback by controlling the stiffness of surfaces. In this way, such arrays can render 3D models physically. Pins are usually arranged in a bed in which a surface point or area unit is represented by a pin physically attached to a linear actuator moving up and down. Pin-headed robots can provide kinesthetic feedback to make the user feel virtual shapes with bare hands (i.e., bimanual interaction) [Siu+18] (see Figure 3.4f). Pin-based real-time shape displays can also be handhelds for VR, providing contact sensations for palm and fingers with high rates of shape recognition and acceptable perception of the virtual objects size [YSK20] (see Figure 3.4g).

3.1.4. Wearable and Contactless Systems

This thesis presents evaluations and studies based on wearable devices providing haptic and kinesthetic feedback. Design implications of such technology aim for a balance between addressing 3DUI requirements and hand capabilities. The most appropriate input device for an interactive task must rely on the control properties of the device and the perceptual structure of the task [Jac+94]. Thus, wearable haptics with tactile and kinesthetic feedback allows for recreating real-world tasks relying on hand dexterity in VEs. Following this guideline, we present some examples of related technologies supporting interactions on VEs with virtual hands and using wearables providing active haptic feedback that responds to the user's motions. User interactions must have clear states for initiation, performance, and completion of tasks, and the feedback must eliminate ambiguity between states so the users can perform successful interactions more efficiently.

Wearable technology is restricted by form factors such as size and weight associated with the limb the device is attached to regarding mobility and musculoskeletal strength. In terms of ergonomics, device comfort and support for diversity of anthropometric profiles are essential. Additionally, the device requires acceptable autonomy in terms of power usage and connectivity. Wearable devices also require meaningful feedback related to precision, accuracy, intensity, latency, duration, and fidelity [BH17]. Haptic wearables are mainly selected to eliminate typical workspace restrictions that are common in grounded devices. Are also targeted for mobile VEs (i.e., untethered) where users require to be free and unencumbered to explore and manipulate the 3D environment. Wearables are versatile enough to provide tactile sensations, kinesthetic feedback, or both. However, the exerted forces are low-scale in comparison to grounded alternatives. Moreover, actuation power can be limited due to weight and power consumption. Vibrotactile

feedback is the most common type of feedback in haptic wearables. The perceived surface properties for virtual textures (i.e., texture, geometric patterns, forces, and tension/vibration) can be characterized by the use of different alternate-current signals [HI17]. Similarly, properties related to stickiness, smoothness, and friction can be modulated with frequency and amplitude parameters [Bau+10] (see Figure 3.5).

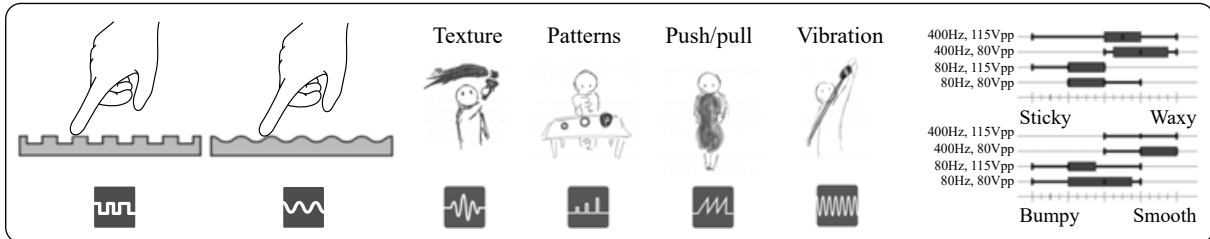


Figure 3.5.: Perceived sensations and vibrotactile signals (Adapted from [HI17; Bau+10]).

The electronic components of haptic wearables (i.e., actuators and sensors) are predominantly located on the fingertips and palmar regions. These regions are chosen because of their high sensibility for feature discrimination and grip/force capabilities, respectively. Control hardware components are usually attached to fingers while keeping the mobility but could also be attached to the wrist for ease of attachment.

Finger-worn Devices

Previous research on finger-worn devices focused mainly on the creation of input devices. For instance, uTrack [Che+13] is a self-contained 3D pointing device composed of magnetometers similar to Finger-Pad [Cha+13] which uses the index finger and thumb to provide a 2D touchpad. RingMouse [Bow+04], a ring-like device, uses ultrasonic tracking to generate position information only. FingerFlux [Wei+11] provides simulated haptic feedback to the fingertip during touch panel operation. Ergonomic and wireless haptic devices [Sch+10] provide collision feedback or guidance information to the human arm when interacting in VEs. Symmetrical haptic interaction systems with virtual creatures in MR [Tak+09] have been proposed, using vibration elements to provide haptic or vibrotactile feedback. Recent research work produced a solution for visually impaired people, providing a finger worn device that assists them in reading a text while providing real-time auditory and vibrotactile feedback [Shi+14].

Thimble-based wearable devices provide feedback on the pulp of the fingertips. A device with 3-DoF and two platforms connected by three articulated legs actuated by motors can simulate contact sensations by changing the orientation of the platforms (i.e., RRS Revolute-Revolute-Spherical kinematic chain) [Chi+15] (see Figure 3.6a). Tactile feedback manipulating both contact area and contact force in fingers has been achieved with a fabric-based display. It provides both active and passive tactile feedback by modulating the stretching state of fabric through motors to convey stiffness, as well as a lifting mechanism to convey softness stimuli [Fan+16] (see Figure 3.6b). Skin deformation in wearables is also possible. Such devices are instrumented with sliding parts actuating on the fingers to render virtual objects with varying mass, friction, and stiffness. The device can be used in the index finger and the thumb, supporting 3DUIs for manipulation and exploration such as grasping, squeezing, pressing, lifting, and stroking [SO17] (see Figure 3.6c). A wearable device can provide trajectory-dependent effects

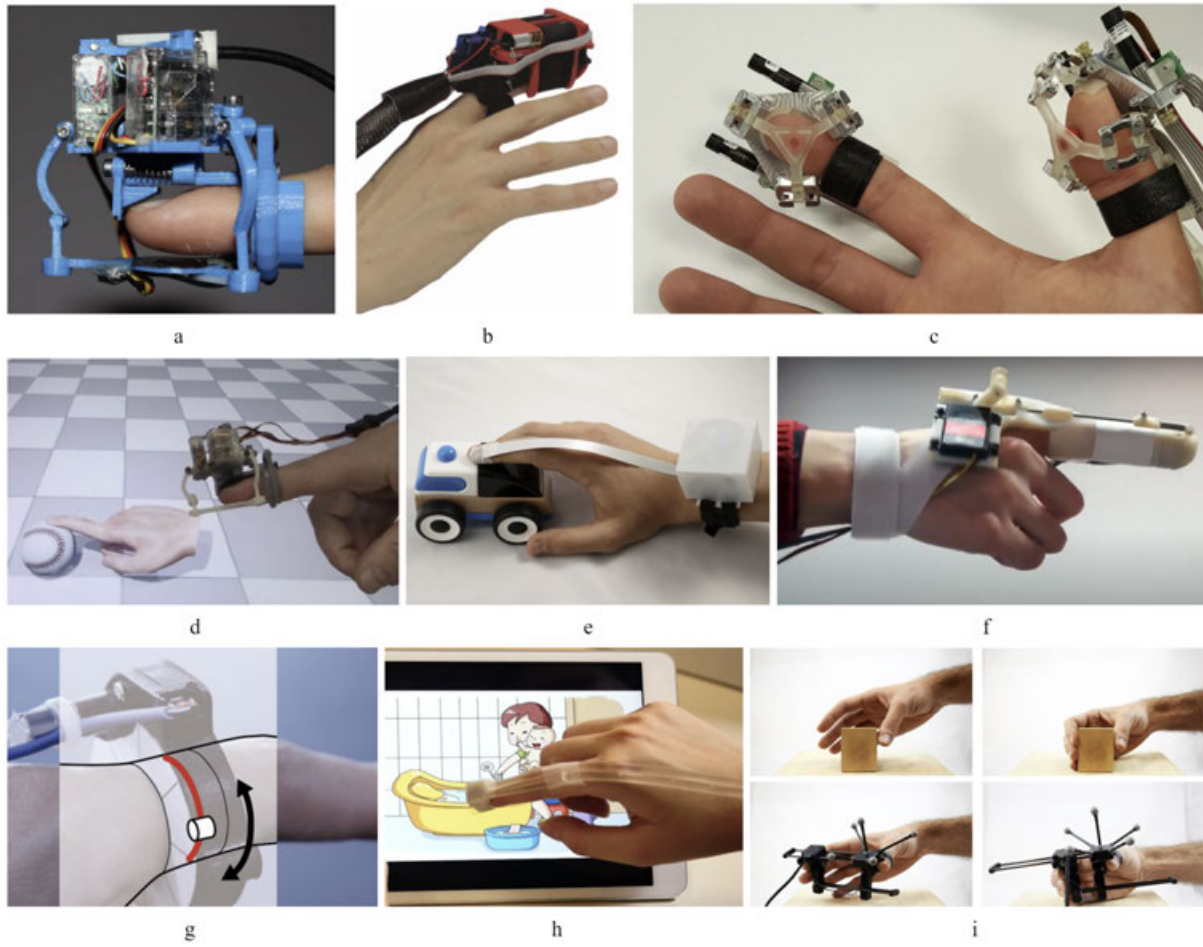


Figure 3.6.: Finger-worn devices: (a) RRS Thimble [Chi+15], (b) W-FYD [Fan+16], (c) Fingertip Tactile Devices [SO17], (d) Skin Stress Optimization [VCO20], (e) Tacttoo [WGS18], (f) HapThimble [KKL16], (g) TactoRing [Je+17], (h) HydroRing [Han+18], and (i) Grabity [Cho+17b].

with real-time tactile feedback for smooth rolling, contact with edges, or frictional sensations [VCO20] (see Figure 3.6d). Electrotactile feedback on fingers can be supplied with temporary tattoos. This approach represents a thin and ergonomic form factor that is scalable to other body locations. It provides high-density tactile output to augment surfaces in VEs [WGS18] (see Figure 3.6e). The perceptions of softness-hardness and stickiness while touching virtual objects can be provided with wearables enabled with electrotactile feedback [Yem+18]. Interaction with virtual touch screens is possible with wearables delivering tactile, pseudo-force (see Section Visuo-Haptic Illusions), and vibrotactile feedback [KKL16] (see Figure 3.6f). Smart rings are a wearable alternative suitable for notifications based on skin dragging. The device drags a tactor around the finger to provide accurate tactile cues and poking sensations [Je+17] (see Figure 3.6g). Also, a ring device enabled for ubiquitous interaction, is equipped with liquid flow actuators to provide tactile sensations of pressure, vibration, and temperature on the fingertip [Han+18] (see Figure 3.6h). Finally, a wearable device can be mounted on the index finger and thumb to provide kinesthetic and vibrotactile feedback for precision grasps. It is designed to simulate grip forces and weight, using a brake mechanism and two voice coil actuators for skin deformation [Cho+17b] (see Figure 3.6i).

Hand-worn Devices

Hand-worn devices are a common choice for wearable haptic devices to supply stimuli for tactile and kinesthetic sensations in grasping and manipulation of virtual objects. Related research includes prototypes of haptic hand-worn devices comprising vibrating actuators and bending sensors to test the effects of intensity and length of activation on the feeling of objects [Kra93], as well as the use of vibration motors in perception experiments [MNT12]. More recent work proposed vibrotactile gloves providing tactile sensations in order to evaluate texture discrimination [Mar+16] and shape recognition [GPS12]. Other approaches are based on vibrotactile displays providing navigation cues in computer-aided surgery systems [HB07] and assistance in teleoperated assembly processes [Deb+02]. In contrast, recent research also based on haptic gloves [Hum+16] uses electro-tactile displays instead of vibration actuators to provide tactile feedback on grasping tasks in a VR environment, and other studies are focused on cutaneous and kinesthetic feedback with active thimbles [SFB10].



Figure 3.7.: Hand-worn devices: (a) DextrES [Hin+18], (b) Dexmo [Gu+16], (c) TacTiles [Vec+19], (d) Wireality [Fan+20], and (e) CapstanCrunch [Sin+19].

Anthropomorphic exoskeletons as hand-grounded devices can provide kinesthetic feedback to constraint the DoF of the human hand. This type of devices is usually grounded on the wrist and use link-rod structures with sensors and actuators to supply resistive forces when the user is grasping a virtual object [Gu+16] (see Figure 3.7b). Newer approaches reduce the bulky setup of electromechanical gloves by using electrostatic brakes or clutches. The device uses articulated guides for the index finger and thumb finger to let the brakes glide and exert forces up to 20 N. Such strength is enough to provide kinesthetic feedback in grasping tasks as well as generating electrically-controlled friction force [Hin+18]

(see Figure 3.7a). Gloves with electromagnetic actuation present a light and low power alternative. These wearable gloves contain haptic arrays of micro solenoids to provide localized tactile feedback for contact and pulse sensations. The latter can be used in exploration tasks by using spatial haptic patterns [Vec+19] (see Figure 3.7c). Kinesthetic feedback can also be applied by a wearable shoulder-grounded device that uses retractable wires. The wires are attached to fingers and wrist to constraint the hand motion and enable tangible interactions with complex geometries [Fan+20] (see Figure 3.7d). Furthermore, palm-grounded devices can also provide kinesthetic feedback for touching and grasping actions in VEs. This solution is based on a friction-based capstan-plus-cord actuator that generates resistive forces [Sin+19] (see Figure 3.7e).

Electrical Stimulation

Electrical muscle stimulation (EMS) or electromyostimulation is the elicitation of muscle contraction using electric impulses. EMS has been used for controlling the user's hand (i.e., 16 joints) by applying electrical stimulus to the muscles around the forearm, generating controlled movements for the extension, flexion, adduction, and abduction [TMR11]. This original work evolved into a multi-channel wearable device supporting fine-grained hand movements [DPR17]. Other explorations of EMS studied the affordance of objects and how they communicate dynamic uses like motion or behaviors [LJB15] (see Figure 3.8a). In recent work, muscles were stimulated to simulate a limb being hit by pushing or pulling selected muscles to create a compelling sensation of impact, inducing a proprioceptive reaction as *muscle-propelled force feedback* [LB13; LIB15] (see Figure 3.8b). EMS in multiple arm muscles can be used to add haptic feedback in VEs to prevent virtual hands from passing through walls and heavy objects, creating a counter force that pulls the user's arm backward [Lop+17] (see Figure 3.8c). A similar setup has been used in cutscenes to enhance the storytelling with higher perceived presence, and realism [Kha+19] (see Figure 3.8d). In mid-air interaction with 3D objects, like selection and manipulation in space, traditionally, the illusion of touch has been provided by visual or auditory feedback; more recently, vibrotactile feedback has been used as well. When vibrations are replaced by or combined with EMS to supply cues regarding contact and material texture, the users reported better experiences as EMS offered a more comprehensive range of strengths and qualities of haptic feedback [Pfe+14].

Alternatively, force sensation could also be generated by tendon electrical stimulation (TES) on the skin surface, stimulating sensory nerves instead of motor nerves (EMS). TES works around any joint where muscles do not overlap the tendon. Also, TES can present a force sensation of around 250 *gf* and deliver proprioceptive feedback without generating muscle contractions, which is convenient for VEs with limited interaction space. When tapping a virtual object in mid-air, the sensation of contact has been conveyed by combining electrotactile feedback and TES, using psychophysical tools to deal with different inter-delays and perceive the two stimulations as simultaneous [Miy+15]. Recent research [TTK18] suggests that the combination of TES, visual, and vibration stimulation enables the adequate perception of force using multimodal feedback, and also found that the direction of the force sensation is opposite to the motion elicited by EMS. Additionally, TES is suitable for momentary sensations (i.e., subtle short sensations due to collisions) when properly combined with other modalities [TTK19].

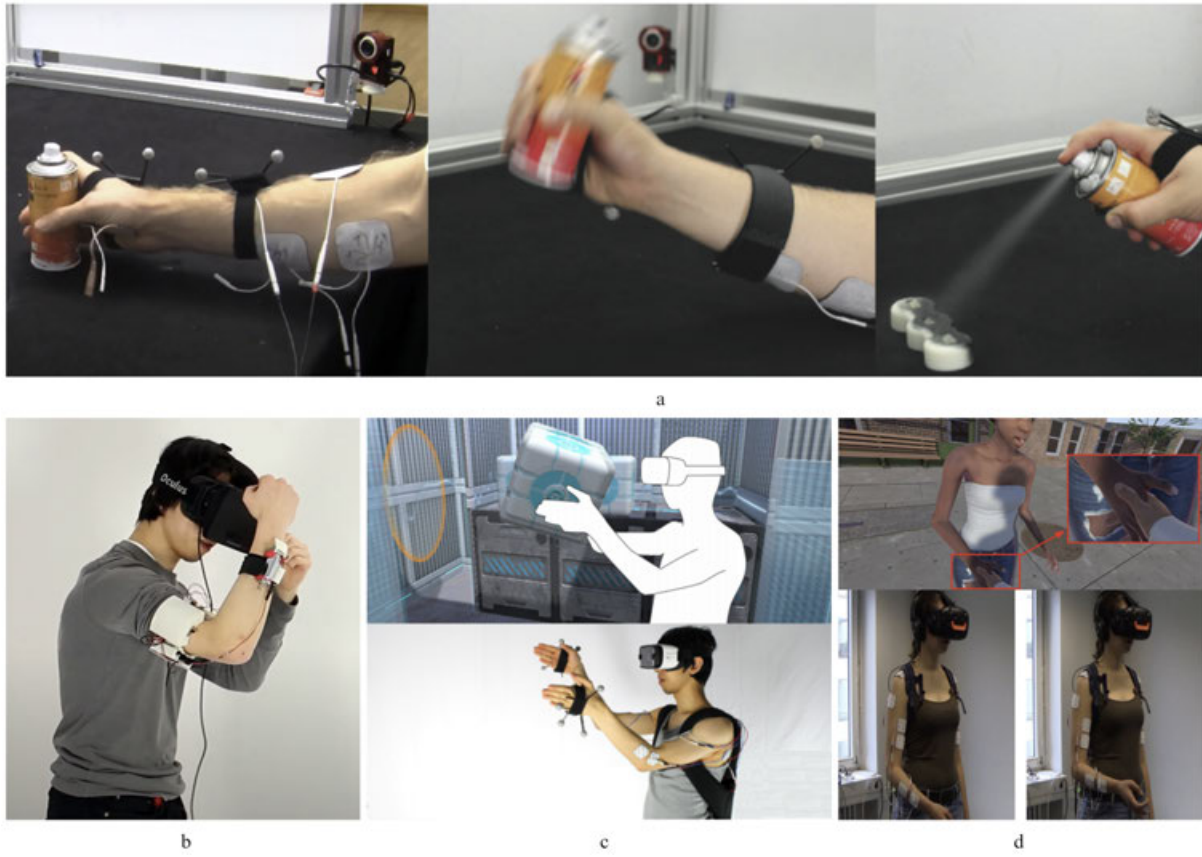


Figure 3.8.: Examples of electrical stimulation: (a) Affordance++ [LJB15], (b) Impacto [LIB15], (c) Providing Haptics to Walls & Heavy Objects [Lop+17], and (d) ElectroCutscenes [Kha+19].

Mid-air Contactless Feedback

Novel technologies in the field of haptic feedback use ultrasonic transducers to create focused ultrasound at a specific target (e.g., fingertip or palm) to provide tactile feedback in mid-air [Lon+14] (see Figure 3.9a). This approach is based on acoustic principles of non-audible radiation forces that are strong enough to elicit tactile sensations (perception of discernible geometric shapes on the skin). The implementation requires un-instrumented hand tracking to keep the hand skin uncovered and ready to be stimulated by the ultrasonic signal.

The main benefit of this technology is the ability of free-hand interaction with no device attachments. Recent studies are based on the generation of air vortexes by using a flexible nozzle to provide tactile feedback. The device is actuated to throw a vortex with a spatial resolution of 8.5cm at up to 1 meter with a FOV of 75 degrees [Sod+13] (see Figure 3.9b). Finally, a similar technology uses air vortex rings due to slow dissipation. Vortex rings can travel several meters and still provide perceptible feedback (tested at different body areas) with a spatial resolution of less than 10 cm at a distance of 2.5 meters [Gup+13b] (see Figure 3.9c).

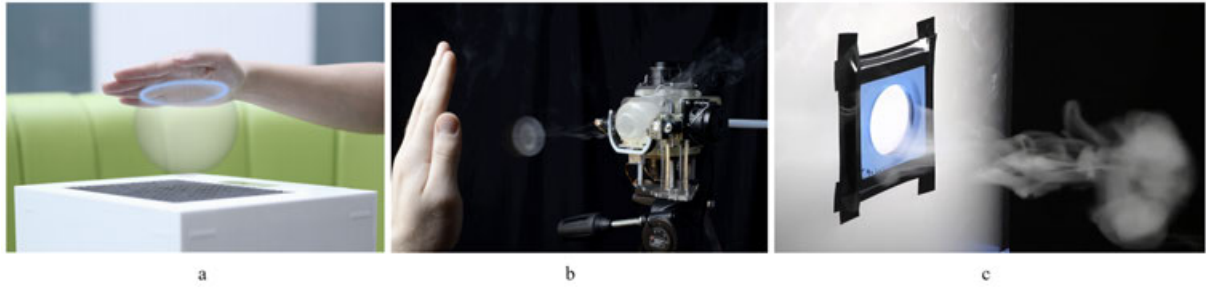


Figure 3.9.: Examples of contactless feedback: (a) Rendering Volumetric Haptic Shapes in Mid-Air Using Ultrasound [Lon+14], (b) AERIAL [Sod+13], and (c) AirWave [Gup+13b].

3.2. Visuo-haptic Illusions

As the visual sense provides the most reliable cues in many situations, it often dominates other senses in cases of conflicting multisensory input [Bur+05]. In this context, discrepancies between visual and tactile/proprioceptive feedback go unnoticed, relying mostly on the visual perception during the multi-sensory integration process [RV64]. This characteristic of the human perceptual system facilitates three main categories of visuo-haptic illusions: (i) retargeting, (ii) redirection, and (iii) scaling with control to display (C/D) ratio.

Haptic retargeting allows for using a single real object to provide passive haptic feedback for multiple virtual objects; however, the physical properties of a virtual object, like size and shape, must be identical (or at least similar) to the repurposed counterpart. It is possible to manipulate the representation of the virtual hand, warp the virtual world coordinate system to modify the perceived location of the virtual objects, or both [Azm+16; Che+17] (see Figure 3.10e). Ungrounded haptic retargeting has been studied for precise object selection and manipulation with grabbing tools (i.e., training chopsticks). In this case, the tool provides passive feedback, and the system performs dynamic visual adjustments of the position of the chopstick in VR in order to create the illusion of grabbing virtual objects with different sizes [Yan+18] (see Figure 3.10f).

Hand redirection has been used to create illusions during surface explorations, dynamically manipulating both the position of the virtual hand and the visual representation of an object providing passive haptics [Koh13]. The concept was initially proposed for redirected walking [RKW01; Ste+10], creating the illusion of walking along a real path that is visually incongruent with the virtual one. Lower-bound detection thresholds for unnoticed hand redirection have been studied [ZK19a], contributing thresholds for vertical, horizontal, and gain offsets for conservative and realistic VEs. The redirection has also been applied as finger translation gains to manipulate the perceived size of real objects during a grasping gesture [BMK19].

C/D ratio is the proportion between the displacement of the real and the virtual hand. Increasing or decreasing the ratio has often been used to provide pseudo-haptic feedback [Lec+00; LB05], modulating the perceived physical properties of a virtual object (e.g., sliding a finger over materials with a C/D ratio greater than one creates the illusion of higher friction). This approach is often used as a mechanism for hand redirection [AF18], enabling passive shape displays to manipulate the perceived resolution. Additional research explored the combination of pseudo and passive haptic feedback to create an illusion

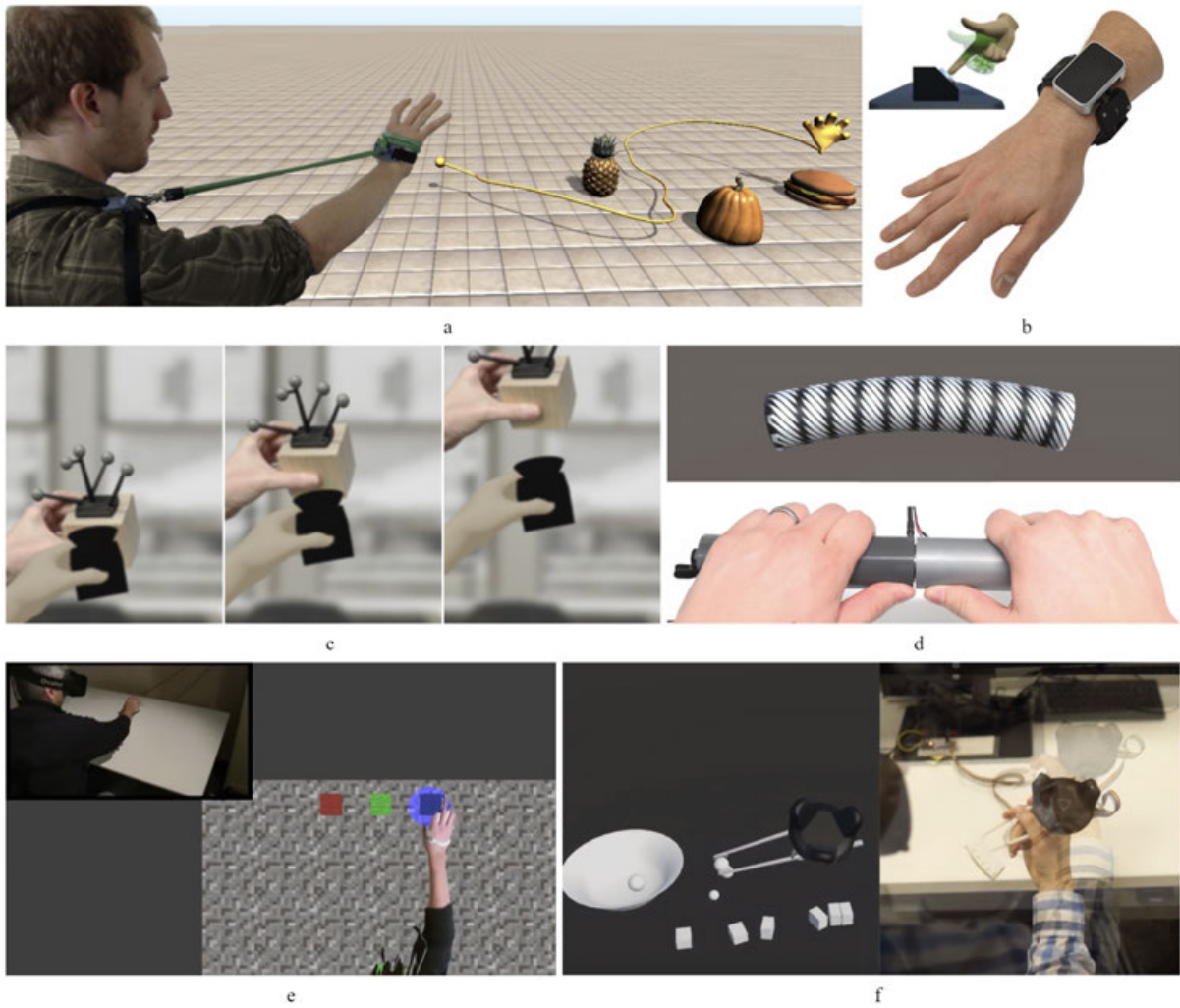


Figure 3.10.: Examples of haptic illusions: (a) Elastic-Arm [Ach+15], (b) Tasbi [Pez+19], (c) Pseudo-Haptic Weight [Sam+19], (d) PseudoBend [HLW19], (e) Haptic Retargeting [Azm+16], and (f) VR Grabbers [Yan+18].

of grip and elastic forces with spring devices [Ach+14; Ach+17], and the combination of pseudo-haptics and redirected touching to provide human-scale passive feedback as progressive resistance force when extending the arm [Ach+15] (see Figure 3.10a).

Regarding the use of C/D ratio manipulation to change the perception of physical properties in VEs, recent work-induced genuine weight and mass-distribution perception without kinesthetic feedback while preserving the sense of ownership of the virtual hand and producing high levels of presence, immersion, and enjoyment [Sam+19; Rie+18; YB20] (see Figure 3.10c). In the case of stiffness or compliance perception, research has led to the exploration of haptic displays based on multisensory feedback to compensate for the limitations of traditional haptic devices in bandwidth and exerted force. Visual cues can be used to modify or deform the visual dimensions to simulate stiffness, taking advantage of visuo-haptic cross-modal transfers experienced by VE users [Lec+00; Léc09; BKC01]. Auditory cues can provide the same illusion, producing impact sounds when tapping virtual objects with a force-reflecting haptic interface; however,

the effect diminished as participants became familiar with the task [DBS97; AC06]. Also, the strong interrelationship between physical stiffness and perceived roughness has been demonstrated [Geo14]. Similarly, reliable stiffness discrimination with wearable vibrotactile devices has been achieved [Mae+17]. Physical objects providing passive feedback can be instrumented in order to create the illusion that the virtual object counterpart is being stretched, bent, or twisted. The instrumentation includes a 6-DoF sensor to measure object changes on force and torque and a vibrotactile actuator to simulate the tactile cues produced by deformations [HLW19] (see Figure 3.10d). Finally, an approach featuring squeeze and vibrotactile feedback combined with pseudo-haptics can provide sensations of contact and stiffness in VR [Pez+19] (see Figure 3.10b).

Beyond creating devices to provide haptic feedback, some studies explored illusory tactile feedback techniques using arrangements of vibrational elements, like Funneling and Saltation illusions [Hay08; Lee+12], haptic stimulation of the feet to induce vertical illusory self-motion [Nor+12] and alteration of the perceived distance from hitting an object [OH14].

Well-known perceptual illusions like the rubber-hand illusion, aiming to induce in the participant the sense of being touched on a fake arm behaving as if it would be part of their body [BC98] and the elongated-arm illusion [Kil+12], aiming to extend the body space by means of elongated virtual limbs. Related research studied the neural mechanisms which are responsible for perceptual illusions, in particular, the integration of tactile and visual feedback [Cru+92; ESP04; Gra99].

There have been discussions in the literature about how the fake limb should look like in comparison with the real one. Prior research claims that there must be some correlation between the fake arm and the real one [TH05]. Newer investigations show that the illusion can be reproduced in VR and, in addition, it does not appear important whether the fake arm has the correct skin color or garments as the participant's arm, and the illusion effect can even be achieved under controlled distortions between proprioceptive and visual information. However, the effect is negated when an abstract representation of the arm (such as an arrow) is displayed [YS10].

Further research shows that a perceptual illusion of body-swapping can be induced for the whole body with an HMD showing stereoscopic real-time video imagery [PE08]. Investigations in HMD-based immersive virtual environments argued that a virtual body is a critical component and that it has a major effect on the users [Hee03; SS00], even for embodiment in body-representation illusions [Spa+14]. In investigations by Slater et al., participants showed a higher sense of presence by using their virtual body to touch than by those who just pressed a button to confirm actions during experiments [Sla+98].

3.3. Multimodal Feedback

Multisensory feedback during the selection of objects has been thoroughly studied in 2D graphical user interfaces (GUIs) [AMH95; CB05]. In particular, a vast amount of studies has been conducted with a focus on adding sound to GUIs. For example, previous work used auditory display of so-called earcons as auditory cues while the cursor was over a target object or initiated some actions. However, previous work could not find any significant improvements in the overall selection time [AMH95], whereas the combination with an additional earcon providing feedback when the target was successfully selected lead to a reduced mean selection time [CB05]. For VEs, the addition of auditory feedback is preferred by

users, and depending on the selection metaphor, it can also speed up the interaction process [VRC06].

Previous research has also focused on the effects of different forms of force feedback (such as texture, friction, recess, and gravity) in 2D GUIs [Léc09]. The results show that force feedback during 2D selection has the potential to reduce error rates and decreased task completion times [CB05]. In the context of VEs, previous work has shown that additional haptic feedback can improve the accuracy in the selection of objects in 3D [Wal+02; Kat+17]. The importance of spatial multisensory cues on target selection performance has also been examined [Mat+12]. For most of the previous work on 3D selection performance with haptic feedback, the Geomagic Haptic Device¹ was used to provide force feedback. Recently, different hardware prototypes and commercial products have been presented, which can provide users with unimodal or multimodal feedback during interaction in 3D space. While visual and auditory displays and feedback have been studied for quite a long time, the combination with vibrotactile feedback has gained enormous interest in recent years [AA13].

Multimodal feedback in VEs must be adequately and timely provided to avoid the uncanny valley of haptics [Ber+18]. Spatiotemporal issues could decrease the subjective experience's quality if the VE fails to keep up with the increased expectations when the user is provided with complex haptic cues. The sense of presence can be affected by using multimodal feedback in VEs, increasing in this way the subject attribution of credibility, especially with the use of vibrotactile feedback combined with passive haptics [Gon+19]. Studies in multimodal feedback have highlighted how the addition of modalities to the traditional visual feedback can reduce sensory conflicts, improve the sense of presence in VEs, and improve user performance. Incorporating mechanoreceptive feedback is essential in tasks involving virtual hands manipulating virtual objects. It facilitates the perception of contact when collisions with virtual objects are aligned with the most salient sensory feedback [Lee+17]. Additional haptic feedback also reduces the detection of visuo-proprioceptive illusions because it inflates the detection threshold [LJL15]. Furthermore, previous research investigated the effect of visual, auditory, and kinesthetic (i.e., force-displacement model) feedback but not any tactile cues while pressing a virtual button. The results suggest that unexpected effects related to underestimation may emerge when feedback modalities are combined [FH14].

3.4. 3D Interaction

Designing haptic experiences requires taking into account the pre-existing behaviors of the user and technological limitations. It also requires the use of body-centered design supported by technologies like hand/body tracking and gesture recognition. In this regard and in the context of this thesis, the following sections will present considerations on how the interaction space and 3DUIs can take advantage of the hands as a universal input mechanism and interactive sensors.

Interaction in VEs requires the users to understand their own personal space or their *kinespheres* [Lub+16]. The term evolved from the field of ergonomics and defines a kinesphere as the with-in reach, surrounding space for interaction (also known as peripersonal space or workspace) while being static. A kinesphere constitutes the boundaries and the context of interaction design to define 3DUIs in terms of body, action, and interactivity. The spatial and the postural extent of the human kinespheres

¹Originally distributed as Sensable Tech PHANTOM Omni model.

are important to define the ecologically-valid attributes for visual, tactile, and kinesthetic stimuli in VEs [Ser+18]. Figure 3.11 presents the spectrum of interactions regarding reach levels determined by the kinespheres. *Near reach* enables interaction with wearables and the use of hand gestures. *Medium reach* enables the user to perform indirect manipulations with arm gestures and controllers. Finally, the *far reach* level is good for proprioceptive interaction with body gestures or poses. Regarding comfort and content, virtual objects and interactive elements must be placed between desk height and eye level, being the ideal ergonomic height at the breastbone level. Locating content above produces gorilla-arm syndrome [Jan+17], neck strain as well as hand occlusion. On the other hand, placing content below is uncomfortable for standing users and present occlusion problems for sitting users.

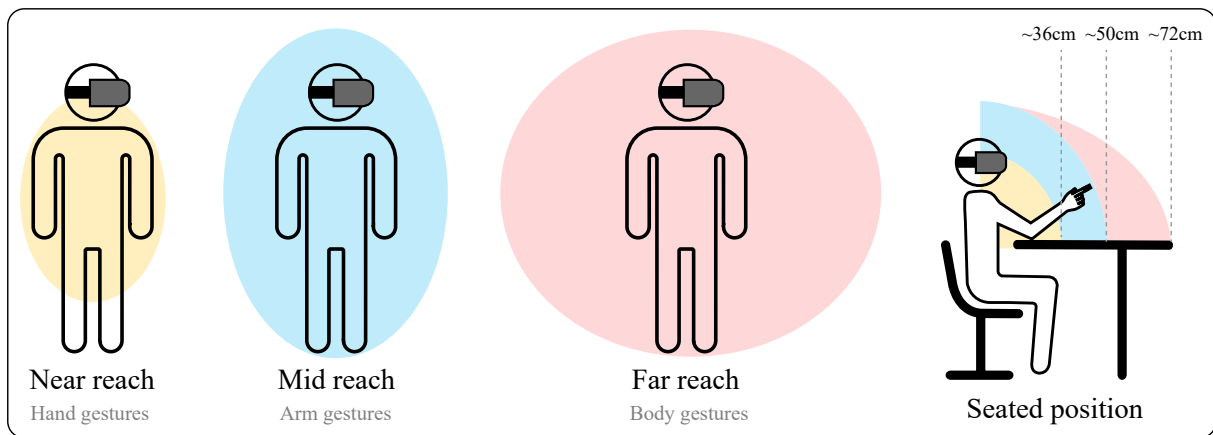


Figure 3.11.: Spectrum of interactions within the kinesphere for standing and sitting postures.

3.4.1. Hand Interaction

Interaction in VEs requires virtual representation for the human hands. Articulated hand models are beneficial for natural 3DUIs. Such interfaces present virtual counterparts of the user's hands while executing manipulation tasks, with real-time 6-DoF visual feedback from a hand tracking system [AMD17]. More advanced implementations include anatomical details like realistic skin textures, deformable hand models, and physically-based rendering for actions such as pulling, grasping, or even dexterous manipulations such as spinning objects [Höl+18].

Interacting with hands and natural gestures in 3D space open up new possibilities for exploiting the richness and expressiveness of natural interaction. Users can control multiple DoFs simultaneously and replicate familiar real-world actions. However, as a matter of fact, interaction in the 3D mid-air is physically demanding and, therefore, often hinders user satisfaction and performance [Cha+10]. The increase in the DoFs that have to be controlled simultaneously as well as the absence of passive haptic feedback and resulting interpenetration and occlusion issues when "*touching the void*" are often responsible for reduced performance [BSS13b; Cha+10]. Additional issues include the necessity to keep hands in range to guarantee acceptable tracking conditions and avoid interactions that might require the user to occlude their own fingers.

3DUIs usage is tied to user capabilities during task execution. If the user is engaged in 3D direct interaction, the user's hands are busy, and as a consequence, the use of the remaining modalities to extend the user's abilities is required. Interaction models like gaze-and-commit are useful to enable the user to select target objects or options by gazing, followed by triggering commands to confirm the task [LaV+17]. Confirmation actions vary from timers to the use of natural language and voice commands. An ideal solution should support multimodal interactions. The system must track the motion of hands or provide input with controllers to perform a 3D spatial task while supporting contextual interactions by the use of voice recognition and hand-free techniques.

3.4.2. 3D Direct Selection

3D hand tracking technologies capture the user's hand or finger movements, enabling the selection of (stereoscopically-displayed) objects in space. The kinematics of point and grasp gestures in 3D space and the underlying cognitive functions have been widely studied [GCE08; Mac+87; WWG03]. For instance, it has been shown that the arm movement during reach-to-grasp or selection consists of two distinct phases [Liu+09] [Liu11]:

- (1) ***Ballistic phase***: During this phase, the user's attention is focused on the object to be grasped, selected, or touched. In this initial phase, the motion is essentially controlled by proprioception.
- (2) ***Correction phase***: This phase reflects refinement and error correction of the movement, incorporating particularly visual feedback in order to minimize the error between the hand or finger and the target [LCE08].

According to Mine et al. [MJS97], direct interaction leads to significantly higher performance than manipulation of objects at a distance from the user's hand. Most results from similar studies agree on the point that optimal performance may be achieved when visual and motor spaces are superimposed or coupled closely [Dja98; LL07; WM99]. Previous research explored different approaches to analyze reaching and grasping movements in 3D environments under different conditions for visuomotor control and perceptual effects [HG00]. MacKenzie et al. [Mac+87] investigated real-time kinematics of limb movements and showed that humans decelerate the motion sooner if the target seems to require more precision in the correction phase. Such changes of the kinematics and control for reaching tasks within VEs have been further investigated in [DKK07; Via+04].

Although, 3D selection by touch and grasp gestures provides an intuitive interaction technique, touching an intangible object, i.e., “*touching the void*” without haptic feedback, leads to confusion and a significant number of overshoot errors [Cha+10; BSS13a]. This is due to the often observed situation that depth perception is less accurate in virtual scenes compared to the real world, which might be caused by problems of diplopia or vergence-accommodation conflicts [BSS13a]. Studies revealed that as long as the participant is performing 3D selection tasks, 3D visual cues perform better than 2D counterparts [CB04].

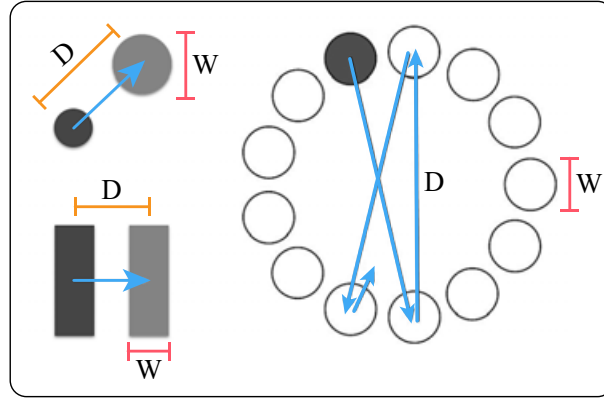


Figure 3.12.: Fitts' Law standard tasks according to the ISO 9241-9.

Fitts' Law

Fitts' Law [Fit54] is an empirical model for user performance in selection tasks. The model predicts the movement time MT for a given target distance D and size W :

$$MT = a + b \cdot \log_2(D/W + 1), \quad (3.1)$$

where a and b are empirically derived. The long term defines the *index of difficulty (ID)* and indicates overall task difficulty. This implies that the smaller and farther a target object appears, the more time is required to select it accurately. A valuable extension supported by an international standard [Sta00] is the use of “effective” measures. This post-experiment correction adjusts the error rate to 4% by re-sizing targets to their effective width (W_e). This enables the computation of effective throughput, a measure that incorporates both speed and accuracy, by “normalizing” the accuracy as effective scores. This *effective throughput* is computed as:

$$TP = \log_2(D_e/W_e + 1)/MT, \quad (3.2)$$

where D_e is the effective distance (average of measured movement distances), and W_e the effective width (standard deviation of error distances multiplied by 4.1333 [MI08]). Previous work [TS11] suggests that one should use the point closest to the target along the ray to compute an accurate representation of the effective width W_e , as using the actual 3D cursor position would artificially inflate the effective measure [Mac18]. In essence, this suggestion projects the 3D task into 2D before computing throughput for touch-based interaction techniques. Even more recent work revealed that the distortion due to perspective also has an effect [TS13]. As a conclusion, it is suggested the use of the 2D projections of sizes and distances to compute a screen-projected throughput for all *remote-pointing* techniques, such as ray-pointing. Pfeiffer and Stuerzlinger have found that vibration feedback in 3D Fitts' Law tasks does not significantly differ from visual feedback [PS15] and some studies have indicated the positive impact of vibration feedback on detection-reaction times [Cha+14].

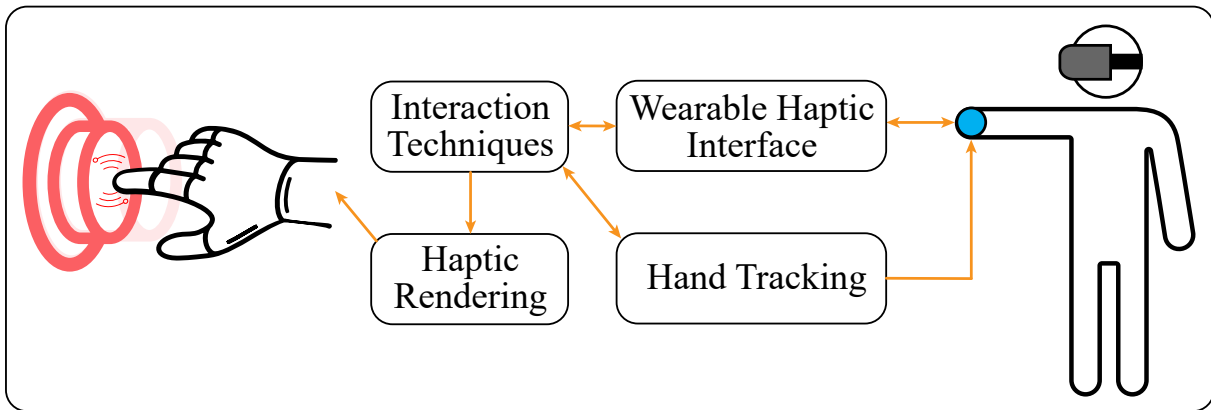


Figure 3.13.: Interaction with hands in the VE.

3.4.3. 3D Guidance

Guidance systems use technology to stimulate different modalities to provide encoded cues and intuitively help the user to change directions while performing selection, aiming and navigation tasks. Previous research showed that auditory cues for orientation could increase navigation performance in real-world scenarios [Con+13]. Studies on navigation tasks found the effectiveness of directional vibrotactile cues [Lin+05]. Recent research proposed the use of dynamic vibrotactile warning signals in different contexts; collision avoidance [Men+15] and prevention [SG08] during simulated driving. Research focused on vibrotactile feedback showed that a vibration belt, featuring cues per cardinal direction, can provide assistance to avoid the collision with obstacles in a VE, or in addition to verbal and visual guidance, can decrease the task error rate [Woe+09]. A similar study providing vibrotactile cues in the north direction presented better navigation performance in real-world environments [Kae+12]. The *Pocket-Navigator* device was able to successfully provide assistance for per-segment navigation using vibration patterns to encode cardinal directions and assist the user to follow a correct path [PPB10]. Some studies explored the development of helmet-mounted actuators [MK10], indicating cues for movement direction in GPS-supported navigation and providing the locations on the head that are most sensitive to vibration stimulation as well as optimal frequencies for tactile feedback. The effect of actuator density on vibrotactile HMDs has also been studied [J O+16], showing a positive effect on user performance for 3D selection tasks. When vibrotactile feedback is provided with guidance purposes, the cognitive load can be reduced with short repetitive vibrations when haptic stimulation is provided in order to inform users of pointing inaccuracies, by guiding their gaze in the direction of nearby interactive objects; the feedback should be activated sequentially and not simultaneously [PRI15].

3.5. Conclusion

In this thesis, we use hand tracking to present virtual representations of the user's hands and enable natural interactions (Figure 3.13). We develop wearable and ergonomic haptic interfaces that are functionally compatible with hand tracking modules. The system features interaction techniques to support the user while performing tasks using 3DUIs. Such techniques evaluate user actions and produce haptic

responses that are rendered through the visual modality (i.e., HMD) and the wearable devices (i.e., actuator commands). Overall, the system supports haptic feedback for direct physical interactions based on real-world experiences (e.g., pressing a button), as well as high-level interactions based on haptic cues communicating contextual information (e.g., obstacle detection). In summary, our approach is able to provide low-latency haptic feedback (i.e., tactile and kinesthetic) in response to user interactions during selection and manipulations tasks in VEs.


The motivation behind the use of (finger- and hand-worn) wearables for haptics relies on using wireless and ergonomic technology to use the skin as a medium of communication, to offload the overworked visual and auditory modalities [Jon18]. Our approach avoids the use of world-grounded and bulky devices with workspace limitations in favor of user mobility and the current trend of ubiquitous and spatial computing. The main objective is the creation of wearable tactile and kinesthetic devices that go beyond simple vibrations and provide more meaningful feedback. Such devices should provide vibrotactile patterns and kinesthetic cues instead of simple alerts and notifications. Furthermore, our techniques make use of visuo-haptic illusions and multimodal feedback. We exploit such combination under the premise that vision-dominance leverage facilitates manipulations of the user hands motion to induce illusions enriched with tactile and kinesthetic feedback [Sam+19]. We believe that all this leads to believable experiences instead of hyper-realistic interaction designs that often produce low-rated usability.

Part II

Support for 3D Selection

4 Chapter 4

Proximity-based Patterns

This chapter is related to the scenario  (see Section 1.2).

4.1. Motivation

Vibrotactile or kinesthetic information can be conveyed by a wide range of technologies such as devices composed of sets of actuators [Buz+13; Lee+12; OH14; Sch+10; Shi+14]. If combined with tracking technologies, such haptic feedback devices can be dynamically controlled according to interaction conditions to ensure spatially sensitive feedback such as collision responses or warnings or may be used to elicit physiological responses or behavior [SG08; Cha+14]. Even though new and varied input and output devices are constantly released for application domains that require interaction with VEs, such as wands, gamepads or touch-sensitive surfaces for video games or entertainment, few of these incorporate more complex haptics technologies than on/off vibration feedback [Gup+13a; Mon+14]. Moreover, few of these devices have a light-weight, unencumbered, and versatile form factor that supports haptic feedback during spatial interaction in mid-air, while keeping the fingertips free to use other tools or devices, such as touch-sensitive surfaces [Lub+14]. In this chapter we describe a ring-like haptic device for which we designed spatially sensitive vibrotactile stimuli to effectively convey spatial information in the shape of timely responses [SG08; Cha+14; Men+15], elicited as dynamic feedback patterns that can be combined with auditory and visual signals, producing improved user performance on 3D interactive tasks. This form of active haptic feedback for spatial interactive applications uses a set of proximity-based vibrotactile patterns to provide dynamic feedback signals. We also present the vibrotactile patterns, as well as a usability study, in which we evaluated the proposed patterns to support selection feedback when selecting 3D virtual objects by touching them with a fingertip. In the usability study we used a HMD as visual output and tracked the user's finger by using an optical system to track the infrared (IR) LED embedded in the device.

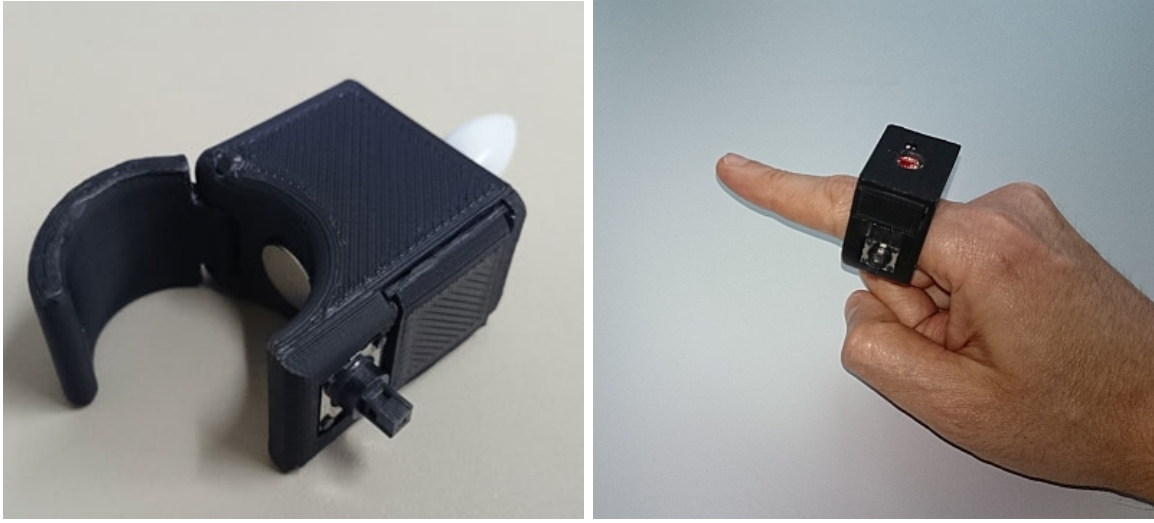


Figure 4.1.: Our ring-shaped haptic device featuring a light-weight form factor, actuator for vibrotactile feedback and IR LED for optical tracking.

4.2. Ring-shaped Haptic Device

Our finger-worn device is designed in the shape of an adjustable ring and it is completely autonomous, i. e., avoiding cables using a wireless Bluetooth connection, a SoC micro-controller, a digital micro joystick for input commands, a small form factor rechargeable 2-hour battery and an IR LED with omnidirectional diffusor cap for external reference support (i.e., optical tracking systems). It also contains an on-skin vibration element, managed and controlled by embedded software, which can be activated at different frequencies according to signals received from the computer to provide haptic feedback. Taking into account the designs of other finger-based wearables [CM06], we decided to place the ring on the first joint of the user's index finger. This allows for comfortable pointing gestures in VEs, natural multi-touch gestures when using touch-sensitive interfaces, as well as comfortable control of the joystick. The prototype is illustrated in Figure 4.1. Specific details of the device can be found in the Appendix (see Section A.1) and [ALS15].

4.3. Vibrotactile Patterns

In order to provide feedback when the user is interacting with a 3D object, we defined a sphere-shaped interaction space which contains the object and matches its center. The interaction space exceeds the size of the 3D object, providing a threshold that enables the haptic ring to provide vibration cues when the user's finger is approaching, penetrating or moving inside the 3D object.

The haptic feedback changes accordingly to a vibrotactile signal pattern that varies the vibration frequency depending on the distance from the tracked finger to the center of the interaction space. Our proposed interaction space is also intended to offer haptic feedback in 3D interaction as in a typical 3D aimed movement [LL09]. In this way, with variations on the threshold and the radius, it is possible to provide vibrotactile feedback during the ballistic and corrective phases or any detected and significant

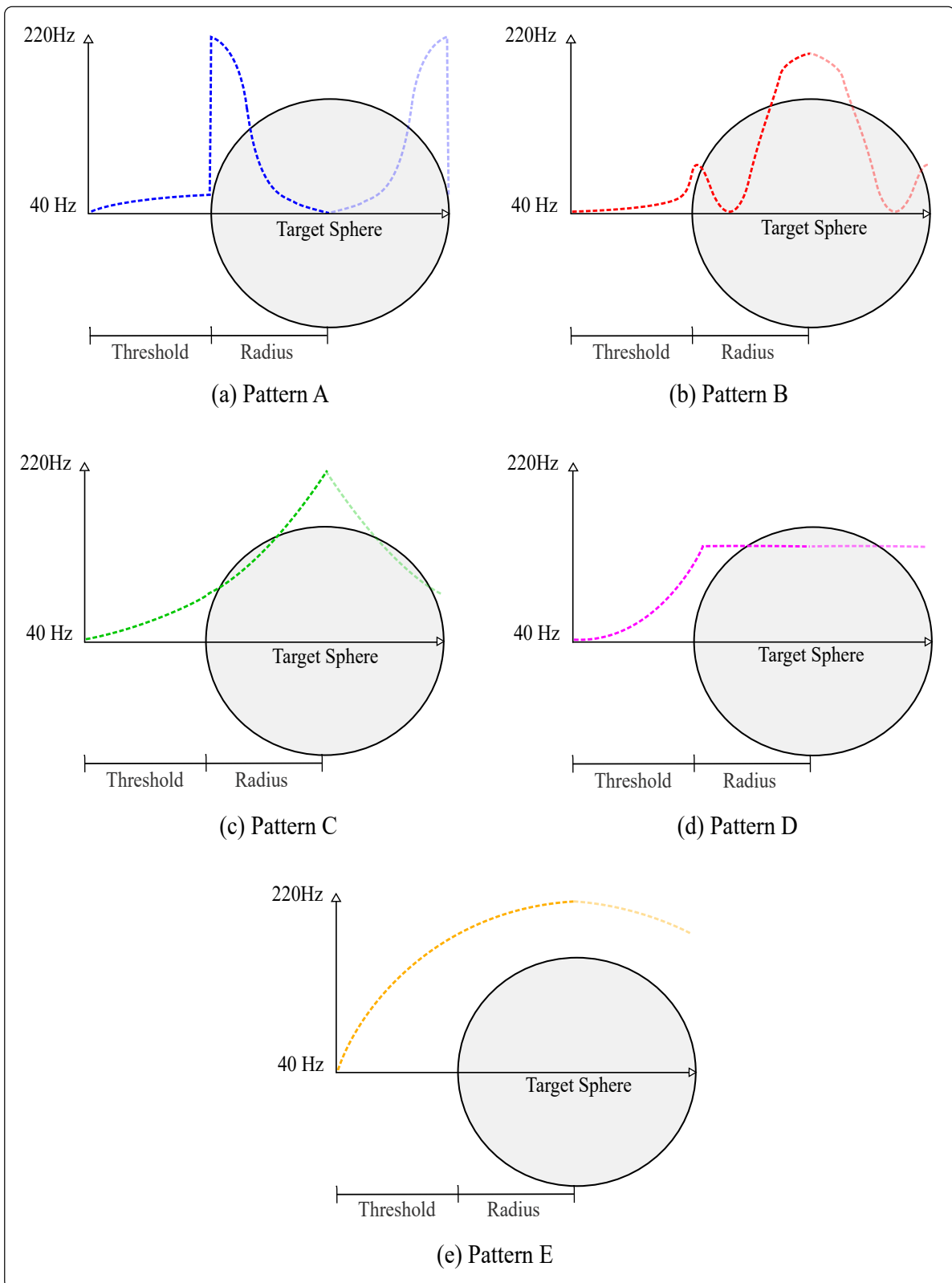


Figure 4.2.: Illustrations of the interaction space and the signal patterns used to provide haptic feedback.

sub-movement. The positive effect of the haptic feedback (e.g. the reduction of the error rate) in related 3D interaction tasks has been tested recently [PS15].

As shown in Figure 4.2, the threshold part of the signal pattern is used to define the behavior of the frequency when the finger is approaching the 3D object (a sphere in our test case), the rest of the signal could define that behavior for penetration and movements inside the sphere (e.g. if the user should receive specific feedback when touching the sphere's center). For the experiment, the radius of the sphere was defined in terms of the user's ergonomic space, enabling the user to interact comfortably. Consequently, the size of the threshold was defined as twice the radius in order to define a wide enough interaction space and elicit meaningful haptic feedback.

We defined five vibrotactile signal patterns (Figure 4.2) representing different cues in terms of the feedback provided in three phases: moving towards the sphere, penetrating the sphere and moving inside the sphere. For all of the patterns, the outcome frequencies range goes from 40Hz to 220Hz according to the capabilities of the device. The following listing shows a qualitative description of the patterns:

Pattern A This signal provides a subtle vibration during the approaching phase, then reaches the maximum vibration frequency when the finger is close to the sphere's bounds according to a steep peak. Then inside, the frequency decreases softly until no feedback is provided on the sphere's center.

Pattern B This signal provides an increasing and soft vibration during the approaching phase, goes until 55Hz on the sphere's bounds, then softly goes to zero to then increase quickly, providing the maximum frequency on the sphere's center.

Pattern C This signal increases softly according to an exponential function from the minimum to the maximum vibration frequency. No distinguishable changes between the three movement phases.

Pattern D This signal behaves as an exponential function during the approaching phase (0Hz to 110Hz), then provides the last reached frequency (110Hz) over the whole volume occupied by the sphere.

Pattern E This signal increases softly according to a logarithmic function. No distinguishable changes between the three movement phases.

4.4. Usability Study

In this section we describe the study we conducted to evaluate the qualitative effect of the different signal patterns used to provide haptic feedback, as described in the previous section. The participants were asked to judge the quality of each curve for different purposes. The task was performed in a VE and consisted in approaching a virtual target object with the index fingertip.

4.4.1. Participants

We recruited 16 participants for our experiment. Ten of them were male and 6 were female (ages 21–36, $M = 26.38$, $SD = 4.272$). The participants were professionals or students in the fields of human-computer interaction or computer science, who received class credit for the participation in the experiment. Two participants were left-handed, the others were right-handed. All but one of them had normal or corrected

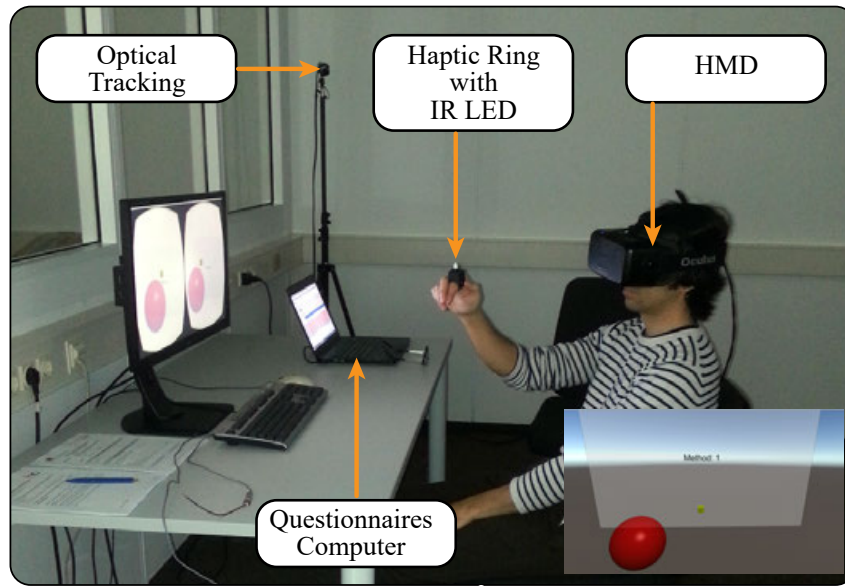


Figure 4.3.: Participant during the experiment with annotations explaining the setup. The inset shows the visual stimulus the user saw during the experiment.

vision. One reported having Dyschromatopsia. We measured the interpupillary distance (IPD) [Wil+08] before the experiment ($M = 6.394$ cm, $SD = 0.386$ cm). We calibrated the VE for each subject to ensure comfort. All but two subjects reported at least some experience with 3D video games (rating scale 1 = yes, 5 = no, $M = 1.875$, $SD = 1.455$). All subjects reported at least some experience with stereoscopic 3D, such as cinemas or TV (rating scale 1 = yes, 5 = no, $M = 1.750$, $SD = 1.065$). Twelve subjects reported that they had participated in HMD studies before. All participants were naïve to the experimental conditions. The mean of the total time per subject, including questionnaires and instructions was about twenty minutes. Participants were allowed to take a break between the training and the main trials.

4.4.2. Materials

As illustrated in Figure 4.3, users wore an Oculus Rift DK2 HMD and our haptic device on the index finger of their dominant hand, tracked in 3 DoF with an optical WorldViz Precision Position Tracking (PPT X4) system with sub-millimeter precision. The Oculus Rift offers a nominal field-of-view of 100° at a resolution of 960×1080 for each eye. The visual stimulus consisted of a 3D scene (see Figure 4.3 inset), which was rendered with Unity3D on an Intel computer with a Core i7 3.4GHz CPU and Nvidia GeForce GTX780TI. The participant's finger was represented by a yellow cube and the target was a semitransparent sphere. The sphere was red when the cube was outside and green when the cube was inside. During both the training and the experiment phases there was just one target in the scene. The targets were located depending on the calibrated finger position. The participants received haptic feedback through the *device* depending on the distance of their finger to the center of the target sphere, as illustrated in Figure 4.2. The diameter of the target sphere was 21.876 cm, calculated by taking into account a distance of 40 cm and an index of difficulty of 1.5, and the size of the finger cube was 2.5 cm.

4.4.3. Methods

We used a within-subject design testing the five different patterns in an order given by a 5×5 Latin Square. After familiarizing themselves with all the patterns twice in a training part, the main trials followed. The training was excluded from the results. For each trial, the participant was instructed to move their finger through and around a sphere as long as they liked to acquire an understanding of the technique. After a selection by pressing a button in the ring's joystick, the participants had to take off the HMD and answer a questionnaire evaluating the last used technique. The subjects were asked to evaluate the last used technique by the following sentences (rating scale 1 = Agree, 5 = Disagree):

- The haptic feedback provided is helpful to feel how the finger **penetrates** the sphere.
- The haptic feedback provided is helpful to feel how the finger **approaches** the sphere.
- The haptic feedback provided is helpful to keep the finger at the **center** of the sphere.
- The haptic feedback provided is appropriate in terms of **intensity**

Hypotheses

We evaluated the following three hypotheses:

- H1** Vibrotactile feedback patterns influence the user's awareness of virtual objects.
- H2** Providing vibrotactile feedback around an object increases awareness of proximity.
- H3** Lack of vibrotactile feedback in an object increases the awareness of the object's center.

4.4.4. Results

One subject misunderstood the task and was excluded from the results, so the results from the remaining 15 subjects were taken into account for the evaluation and were normally distributed according to a Shapiro-Wilk test at the 5% significance level. We analyzed the results with a repeated measure ANOVA and Tukey multiple comparisons. Degrees of freedom were corrected using Greenhouse-Geisser estimates of sphericity when Mauchly's test indicated that the assumption of sphericity had been violated. The results of the questionnaires are shown in Figure 4.4.

We found a significant main effect of the used pattern on penetration ($F(4, 56)=9.306$, $p<.001$, $\eta_p^2=.399$). Post-hoc tests with Bonferroni correction revealed that pattern A was significantly better for penetration than patterns B ($t(14) = 2.229$ $p < .05$), C ($t(14) = 3.5$ $p < .05$), D ($t(14) = 3.228$ $p < .05$) and E ($t(14) = 4.83$ $p < .05$). Pattern E was also worse than B ($t(14) = 2.828$ $p < .05$), C ($t(14) = 3.552$ $p < .05$) and D ($t(14) = 3.287$ $p < .05$).

We found a significant main effect of the used pattern on range ($F(4, 56)=9.243$, $p<.001$, $\eta_p^2=.398$). Post-hoc tests with Bonferroni correction revealed that pattern E was significantly better for range than patterns A ($t(14) = 3.190$ $p < .05$), B ($t(14) = 1.586$ $p < .05$) and C ($t(14) = 4.3226$ $p < .05$). Pattern D was significantly better than patterns A ($t(14) = 3.251$ $p < .05$) and B ($t(14) = 3.761$ $p < .05$). Pattern C was better than pattern B ($t(14) = 2.747$ $p < .05$).

We found a significant main effect of the used pattern on center ($F(2.091, 29.269)=9.426$, $p<.001$, $\eta_p^2=.402$). Post-hoc tests with Bonferroni correction revealed that pattern B was significantly better for

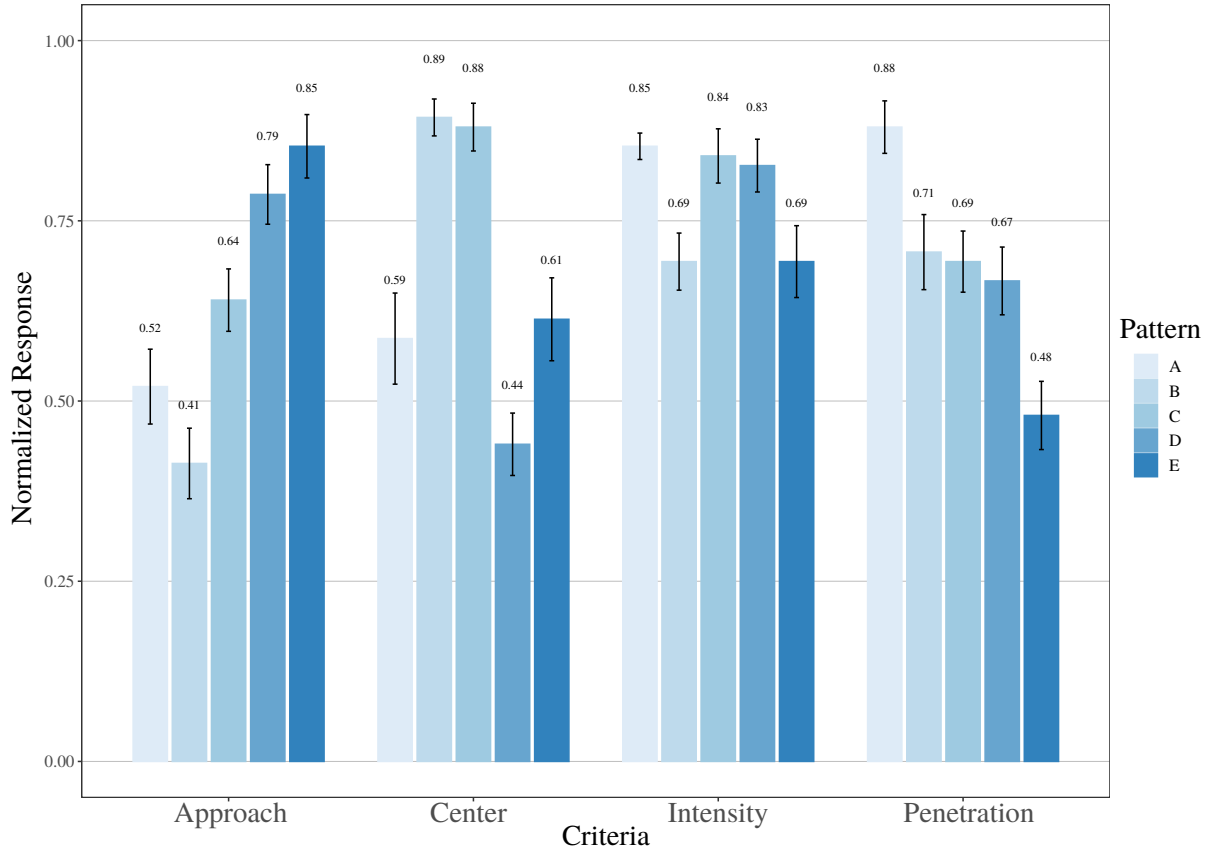


Figure 4.4.: Experiment questionnaire results for each pattern concerning the questions described in Section 4.4.3 (normalized response 1 = Agree, 0 = Disagree).

center than patterns A ($t(14) = 3.286$ $p < .05$), D ($t(14) = 5.906$ $p < .05$) and E ($t(14) = 3.862$ $p < .05$). Pattern C was significantly better than patterns A ($t(14) = 1.6556$ $p < .05$), D ($t(14) = 5.145$ $p < .05$) and E ($t(14) = 4.394$ $p < .05$).

We found a significant main effect of the used pattern on intensity ($F(4, 56) = 3.598$, $p < .001$, $\eta_p^2 = .204$). Post-hoc tests with Bonferroni correction revealed that pattern E was significantly worse for intensity than patterns A ($t(14) = 2.567$ $p < .05$), C ($t(14) = 2.750$ $p < .05$) and D ($t(14) = 2.197$ $p < .05$). Pattern A was also significantly better than pattern B ($t(14) = 3.055$ $p < .05$).

Additionally, before and after the experiment, we asked subjects to judge their level of simulator sickness with the Kennedy-Lane SSQ questionnaire [Ken+93]. While we measured an average pre-SSQ score of $M = 10.721$ ($SD = 18.853$), the post-SSQ score was $M = 12.467$ ($SD = 14.531$). We found no significant increase in simulator sickness over the time of the experiment ($t(14) = .401$ $p = .694$).

4.5. Discussion

Overall, the feedback patterns significantly influenced the subjective awareness of the users, which supports our hypothesis H1. The results show that every feedback pattern has their strengths in different

	A		B		C		D		E	
	M	SD	M	SD	M	SD	M	SD	M	SD
Approach	3.400	1.298	3.933	1.223	2.800	1.082	2.067	1.033	1.733	1.100
Center	3.067	1.580	1.533	.640	1.600	.828	3.800	1.082	2.933	1.438
Intensity	1.733	.458	2.533	.990	1.800	.941	1.867	.915	2.533	1.246
Penetration	1.600	.910	2.467	1.302	2.533	1.060	2.667	1.175	3.600	1.183

Table 4.1.: Questionnaire Results: Mean and standard deviation for the vibrotactile patterns (rating scale 1 = Agree, 5 = Disagree).

areas. Pattern A appears to be the best for the simulation of penetration. While some participants thought pattern B offered a good sense of penetration, others did not indicate that sensation. However, pattern A was judged badly for sensing the center of an object. Pattern E showed the highest ratings for the sense of range, or being close to the object, as it offered relatively strong vibration throughout the threshold. However the sense of penetration was rated badly and especially the intensity received the worst ratings, as expected. Nevertheless, the haptic feedback increased the participants' awareness of proximity to the objects, supporting our hypothesis H2. Patterns C and B equally gave the participants a good awareness of where the center is. The patterns offer different advantages. Pattern B offers a reasonable sense of penetration and a good hint for the determination on where the center is. This could enrich selection tasks and allow the execution of various tasks without the necessity to keep visual contact with the interactive object. The fact that users gave mixed and negative ratings for the center question at pattern A indicated that the participants were inclined to focus on the active vibrotactile feedback and not the lack thereof. Despite being able to determine clearly when they penetrated the object, allowing them to stay within the target, they did not actively feel the center of the object as it offered no vibrotactile feedback, which disagrees with Hypothesis H3.

Being actively able to feel objects and their centers might have an influence on the distance perception and the errors caused by distance overestimation and underestimation in VE tasks, e.g., in selection tasks [LBS14]. It is thus necessary to further tune the parameters, depending on the desired use-case. However, a few recommendations for the use of vibrotactile feedback patterns can be derived:

- Vibrotactile peaks at the outline of objects allows users to feel the outline and the penetration thereof.
- Lack of vibrotactile feedback does not get detected as easily as vibrotactile peaks.
- Decoupling of vibrotactile feedback from visual cues can guide users to objects.


Some combinations of the patterns were used but in some cases produced misinterpretations related to the number of objects felt by users (i.e. some signal combinations behaved like the signals related to several objects close to each other). While the pilot study was conducted with spheres as targets, it is possible to determine the depth of arbitrary watertight 3D objects and thus calculate a center and the distance thereto for the determination of the correct signal strength based on the current pattern.

4.6. Conclusion

We presented a novel ring-shaped wireless haptic feedback device for spatial user interfaces, and we presented a usability study evaluating different vibrotactile feedback patterns. These feedback patterns differ from the common on/off approach for vibrotactile feedback used by most similar devices as they offer different strengths of feedback depending on the distance to a target or its hull. Our usability study showed that these vibrotactile patterns can improve the user's subjective awareness of a virtual scene, enriching it by providing haptic feedback when objects are penetrated or when their center is reached. Moreover, the results showed that there is no overall optimal pattern as each pattern provides advantages in different situations. We discussed recommendations for user interface designers to decide which pattern should be chosen for particular interfaces depending on their goals. Future work should evaluate the feedback patterns during pointing, touching, grasping or dexterous manipulation and determine how they may further support 3D selection and manipulation tasks (e.g., by designing a controlled Fitts' Law experiment which could also take into account error and performance measurement, as well as the comparison with the visual and even the audio feedback). Also, further studies should take into account the amplitude as another variation value of the vibrotactile pattern.

5 Chapter 5

Use of Multimodal Feedback

This chapter is related to the scenario  (see Section 1.2).

5.1. Motivation

In this chapter we analyze the effects of unimodal and bimodal feedback provided through the visual, auditory and tactile modalities, while users perform 3D object selections in VEs, by comparing both binary and continuous proximity-based feedback. We conducted a Fitts' Law experiment and evaluated the different feedback approaches. The results show that the feedback types affect ballistic and correction phases of the selection movement, and significantly influence the user performance.

Multisensory integration describes how information from different sensory modalities, such as vision, audition, and somatosensation are integrated by the human central nervous system [Ern06]. Congruent representations of such multisensory stimuli allow us to have meaningful perceptual experiences. Earlier work has shown that the addition of multisensory feedback can improve interaction in VEs as it increases the bandwidth of information that can be transferred to the user [VRC06]. While most VEs traditionally focus on audio-visual feedback, e. g., to avoid extensive user instrumentation with gloves or similar, current advances in 3D digital fabrication enabled the effective design and construction of unencumbering haptic input devices, which have the potential to enrich the user's experience and improve the feedback.

However, significant performance gains of using multimodal feedback, such as vibrotactile or auditory feedback, have rarely been shown for typical interaction tasks such as 3D object selection or manipulation [Eri+08]. In particular, 3D object selection is one of the most essential tasks for natural interaction in VEs. In order to select the target object in the 3D space, the user needs to use devices or perform hand gestures, such as grasping or pointing. If no additional feedback is provided during the selection process, the user has to rely on the internal body senses only, i. e., proprioception and kinesthesia, to ensure that the result of the selection process is indeed the intended virtual object. While proprioceptive and kinesthetic cues can be sufficient for objects close to the user [MJS97], previous work suggests that interaction performance is reduced for distant objects with such limited feedback.

Most direct 3D selection techniques provide at least visual feedback, which user perceive in addition to the proprioceptive and kinesthetic cues. In addition, when the user performed the selection of an object (e. g., with a button press or pinch gesture), the selected 3D object is often highlighted (e. g.,

changing color), which further allows the user to ensure that the corresponding object is the intended one. From a naive perspective, it seems reasonable to assume that the provision of redundant information via multiple feedback modalities, might have the potential to improve user performance. On the other hand, however, it has been shown that increasing the quality of visual feedback does not necessarily improve user performance [Pou+98] and might even reduce selection performance [WB05].

Although it is not clear that additional sensory feedback results in performance gains, users often tend to prefer multimodal feedback. For instance, auditory feedback has often been used in combination with visual feedback in 3D selection tasks to reinforce a user's actions, e.g., to inform the user when a target has been highlighted or successfully selected [VRC06]. In addition, providing touch feedback in spatial interactive applications through haptic technology, e.g., by using devices composed by sets of actuators, makes more meaningful experiences possible. In addition, haptic feedback can be dynamically adjusted according to interaction conditions to provide more significant information such as cues and warnings [Cha+14; SG08]. Hence, so far only little research has been conducted to adapt non-visual (e.g., vibrotactile and auditory) feedback with different stimulus intensities and frequency ranges to inform user about spatio-temporal relations between the virtual input device and the target object.

In this chapter we present and compare different multimodal feedback types to provide the user with additional spatio-temporal cues during the 3D selection process based on the proximity of the virtual input device and the target object. We analyze the effects of multimodal feedback, while users perform 3D object selection tasks in a Fitts' Law experiment.

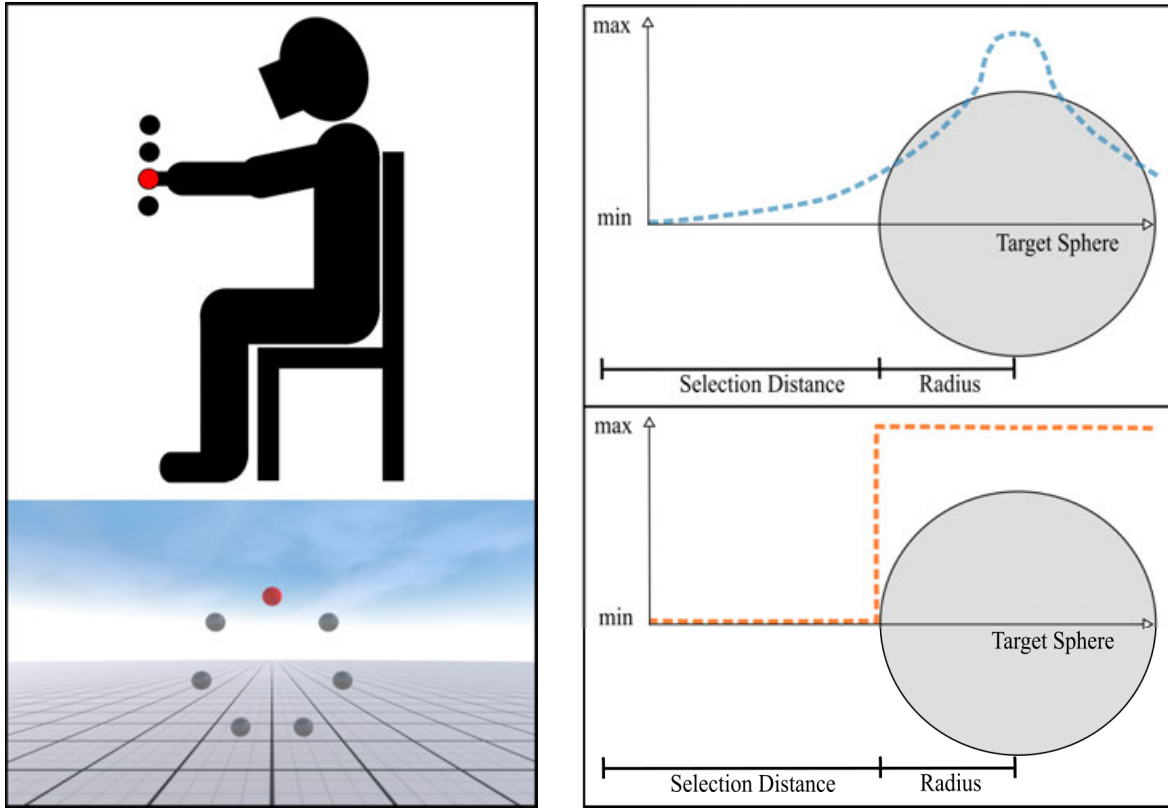
The contributions of this chapter are:

1. A comparison of unimodal and bimodal feedback, combining the visual, auditory and tactile modalities for user guidance during 3D selection tasks.
2. Performance analysis of proximity-based dynamic feedback patterns with traditional binary (on/off) feedback in a Fitts' Law experiment.
3. An analysis of the ballistic and correction phases of the selection movements to evaluate how are effected by the presented multimodal and feedback types.

5.2. Proximity-based Feedback

Most previous work on 3D user interfaces for object selection tasks incorporated some kind of feedback (e.g., visual, auditory and/or vibrotactile) according to the position of a virtual cursor and the position of a target object intended to be selected, in order to help a user to perform the selection faster and/or more precise. We classify these types of feedback following a basic distinction between two main approaches, which can be modeled with proximity-based transfer functions:

- (1) ***Continuous Proximity-Based Feedback***: The feedback continuously increases or decreases according to the distance from the user's finger to the target's center. The user experiences the maximum feedback level when the finger is at the target's center (Figure 5.1b(top)).
- (2) ***Binary Proximity-Based Feedback***: The feedback is activated when the user's finger is inside the target. Otherwise, no feedback is provided as shown in Figure 5.1b(bottom). This solution is the classic approach, going instantaneously from min to max feedback.



(a) Position of the participant while performing the Fitts' Law selection task. The inset shows the participant's view in the VE. For details regarding target sizes and calibration see Section 5.3.3.

(b) Transfer functions: Proximity-based binary feedback (**bottom**) or continuous feedback (**top**) can be applied to the fingertip based on distance to virtual targets.

Figure 5.1.: Experiment setup and proximity-based feedback.

We deliver the feedback using an in-house developed 3D-printed wireless device (see Section 5.3.2), which is shown in Figure 5.2. With this wearable interface it is possible to track the pose of the finger in 3D space and to present vibrotactile feedback adapted to the proximity of the virtual representation of the device to virtual target. Moreover, by using a head-mounted display (HMD) and headphones we can present additional sensory feedback to the user. Table 5.1 shows details about the possible combinations of sensory modality, feedback type and transfer function. The columns *Min* and *Max* are related to the signal levels shown in Figure 5.1b.

In the case of a continuous proximity-based haptic feedback, the device starts to deliver a subtle vibration when the virtual input device is at a given distance (cf. Section 5.3) from the target object. While approaching the virtual object the intensity slowly increases until the finger is close to the target's bounds and then increases quickly, providing the maximum intensity on the target's center (Figure 5.1b). This pattern has been preferred by participants in a pilot study described in [ALS15].

For continuous proximity-based auditory and visual feedback, the same gradual change is applied to the frequency of the tone (from 0 Hz to 900 Hz) and the color (from Red to Green) of the target respectively. In the case of the binary proximity-based auditory and visual feedback, the *Max* is provided as soon as the finger intersects the target, but no changes in color, frequency or intensity are provided while the





Feedback	Modality	Change	Min	Max
Binary (B)	Visual	Color		
	Auditory	Freq.(Hz)	0	900
	Haptic	Intensity	0	128
Continuous (C)	Visual	Color		
	Auditory	Freq.(Hz)	0	900
	Haptic	Intensity	30	128

Table 5.1.: Configuration for proximity-based feedback.

user is approaching the target. The target selection circle is presented to the participant as shown in Figure 5.1a. (following the guidelines of ISO 9241) and the selection approaches as well as the target selection positions are recorded for all the conditions presented in the experiment.

5.3. Experiment

In this section we describe the Fitts' Law, within-subjects experiment conducted to analyze 3D selection performance using different types of feedback and sensory modalities.

5.3.1. Participants

Participants were recruited through academic mailing lists. 18 subjects (14 male, 4 female) took part in the study (mean age 26.4 years, SD=5.19). 14 participants had experienced a VR headset before and 11 had used a haptic device before. No displacements of equilibrium or motor disorders were reported by the participants. We collected informed consent from all participants and received IRB approval for our experiment. After removing participants who misunderstood the task, the data from the remaining 15 participants was analyzed. The experiment lasted approximately one hour including training trials to get the participants familiarized with the task and the devices.

5.3.2. Material

Participants sat on a static chair (see Figure 5.1a) wearing an HMD to display the visual stimulus during the experiment, which was a 3D scene rendered with the Unity3D engine on an Intel computer with a Core i7 4.0 GHz CPU, 16 GB of main memory and an Nvidia Quadro K5200 graphics card. The HMD used during the experiment was an Oculus CV1 offering a nominal diagonal FOV of approximately 120 degrees at a resolution of 1080×1200 pixels for each eye. Participants also wore a pair of headphones to provide auditory feedback at 60 dB (with a sampling frequency of 48000 Hz and a gain of 0.025 decibels) and a wireless haptic device (see Figure 5.2) in order to provide vibrotactile feedback. In addition, this self-made device enables user input with a momentary button which can be effortlessly clicked in order to avoid the Heisenberg effect [Bow+01], and was used by the participants to confirm selections. Specific details of the device can be found in the Appendix (see Section A.2).

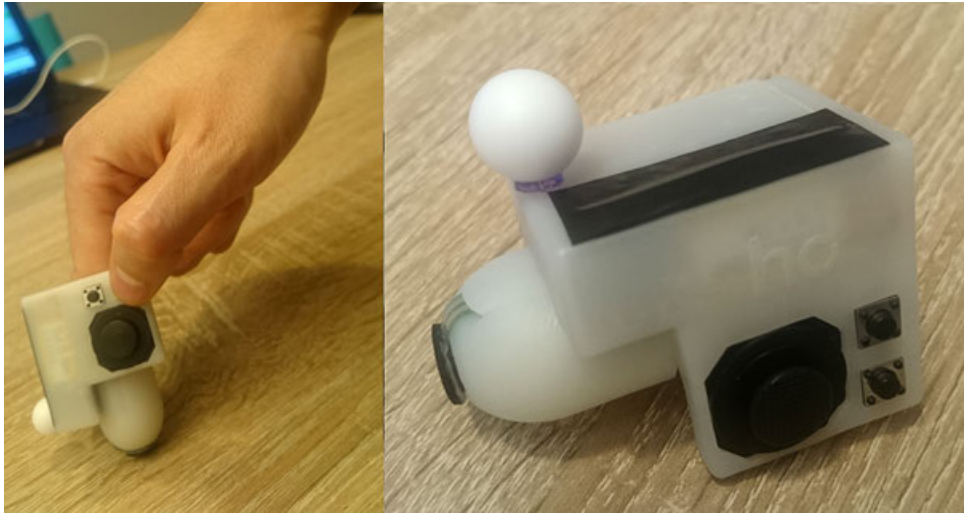


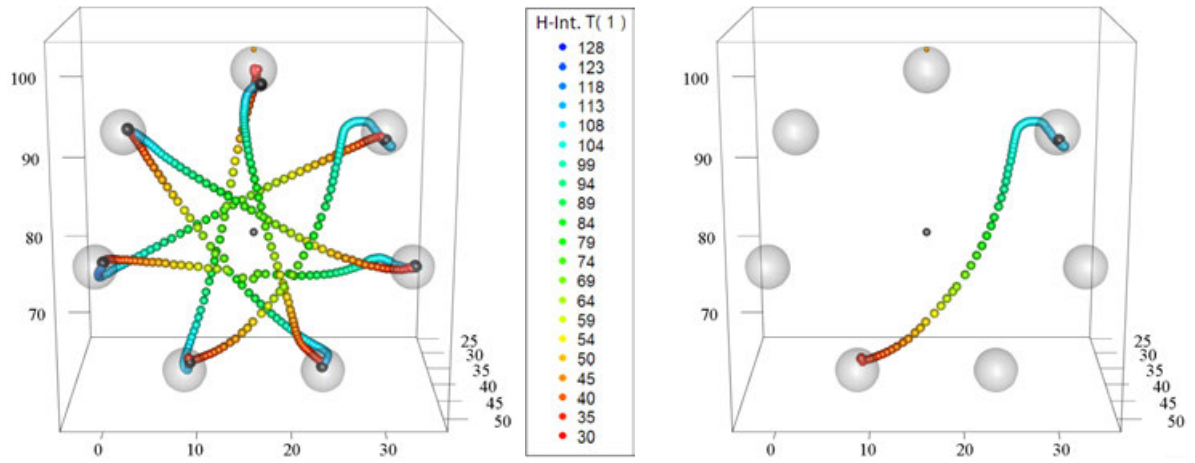
Figure 5.2.: Self-made wireless vibrotactile fingertip to provide haptic feedback and confirm participant's selections.

We used an IR marker attached to the haptic device to track the position of the index finger of the participant's dominant hand in order to show a cursor in the VE shaped as a 10 mm wide orange sphere. The marker was tracked by an optical WorldViz Tracking System (PPT X4) with sub-millimeter precision, which was chosen to offer high precision for the Fitts' Law experiment. The participant's head was also tracked using the PPT system. The 3D scene for the Fitts' Law experiment was designed taking into account considerations for this kind of task [ST14]. Settings like target transparency, target shape, target arrangement and depth cues in the VE were defined accordingly to avoid problems such as the non-spherical distribution of hit points in 3D VEs and to enable direct comparisons between 2D and 3D pointing results.

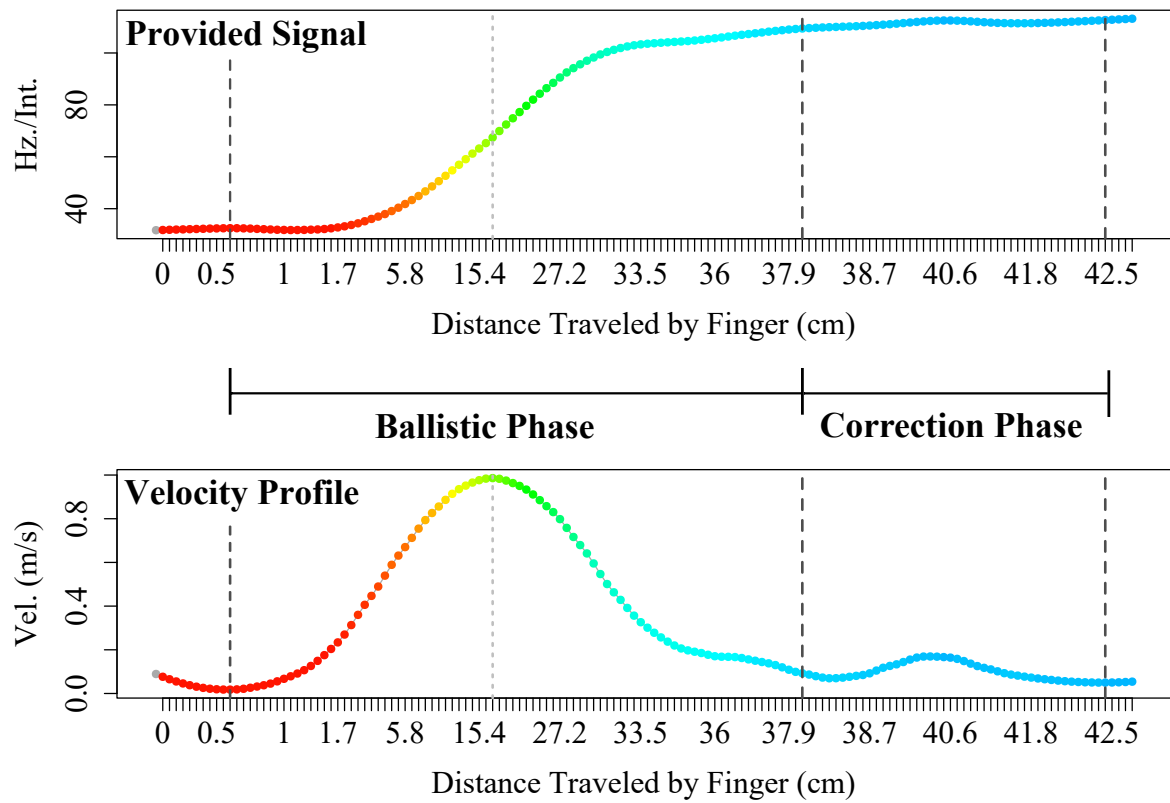
5.3.3. Methods

The task required to move the cursor as fast and as precisely as possible to the center of a target sphere making part of a circular arrangement of 7 targets as defined in the ISO 9241 Part 9 for evaluating pointing tasks using Fitts' Law [Sta00]. The next target to be selected was always colored in red. Selection was confirmed using the small digital button located on the side of the haptic device. A selection was deemed successful if the button was pressed when the cursor was intersecting the target sphere. However, it was not necessary to successfully hit the target in order to enable the next target and to continue with the pointing task until all the 7 trial targets were selected.

To position the target circles in a comfortable pose for each participant, a process of calibration was executed at the beginning of the experiment. Participants were asked to extend their dominant arm forward and the index finger position was saved as a calibration point. The circle was positioned at a distance of about 80% the participant's arm length as described in [Val+11; Lub+16] as an optimal distance for vertical pointing tasks, providing a comfortable position according to ergonomic guidelines when seated [Sta00]. We tested 6 different combinations of Index of Difficulty (ID) and Target Width (W), with ID s uniformly ranging from 2.5 to 3.5 bits, and testing



(a) 3D reconstruction of the selection movements for a complete trial (7 targets), showing the variation on feedback intensity along the path followed by the participant's finger. (b) Example of a common selection movement, the black sphere inside the target represents the selection point.



(c) The perceived signal as a function of vibrotactile intensities over time (**top**), and the corresponding velocity profile of the selection, showing the ballistic phase followed by the correction phase (**bottom**).

Figure 5.3.: Visualizations of the selection movement and the velocity profile.

target sizes from 2.9 to 7.5 cm, representing a valid range of difficulties for this particular setup. Each condition was tested with 5 repetitions and their order was fully randomized. The repetitions were aggregated by D/W Fitts-Law values, according to ISO 9241-9 procedure for throughput calculation.

The system provided different types of visual, audio and/or vibrotactile feedback according to the distance from the cursor to the geometric center of the target sphere as described in Section 5.2. In total, we considered a set of 13 different conditions including a baseline condition without feedback, i.e., neither visual nor auditory or haptic cues informed the participant when her/his finger was within the target sphere. The remaining conditions were split into two factors. The first factor provides six combinations of modalities (*MODALITY*) as three unimodal conditions (i.e., Audio, Haptic, Visual), and three bimodal conditions (i.e., VisualAudio, VisualHaptic, AudioHaptic). The second factor includes two types of proximity-based *FEEDBACK* providing binary and continuous feedback for every *MODALITY*, summing up a total of 12 more conditions in addition to the baseline.

We recorded the movement time from one target to the next in the Fitts' Law task, we further measured the error rate as a percentage of the amount of target selections by clicking the device button when the target was not successfully selected by the participant, i.e., when the cursor was outside the target sphere. Additionally, we measured the 3D error distance over the selections by computing the Euclidean distance from the target center to the selection point. Finally, we computed our first dependent variable as the effective *THROUGHPUT* metric incorporating both errors and time into an overall estimate of performance.

5.3.4. Analysis of the Selection Movements

In order to add more dependant variables to analyze the effect of the presented conditions on the quality and the accuracy of the movements performed by the participants to select a 3D target, we implemented a procedure to reconstruct all the actions performed (i.e., target approaches and selections) by using the 3D tracking data recorded during all trials for all the subjects (see Figure 5.3a). In this way, we performed an off-line analysis of the trajectories traveled by the participants' finger to intersect the target object and confirm the selection. Furthermore, we also recorded the variations on feedback (i.e., color, intensity, or frequency) along the path followed by the participant's finger, according to the parameters defined in Table 5.1 and depicted in Figure 5.3a-right. The perceived signal (defined by the proximity-based feedback) over time is presented on Figure 5.3c-top, enabling the analysis of the movement phases and the transfer functions of the feedback simultaneously.

Ballistic and Correction Phases

As described in Section 3.4.2, we can analyze a single selection movement (see Figure 5.3b) extracting the velocity profile which shows the velocity of the participant's finger as a function of time (see Figure 5.3c-bottom) in order to detect the ballistic and correction phases of the movement. We implemented a classifier algorithm to process our trials data and set a dependant variable with the percentage of *CORRECTION* phase in the selection movement (i.e., ballistic and correction percentages are comple-

mentary), based on the local minima/maxima and zero jerks (i.e., derivative of acceleration with respect to time) detected in the velocity profile [Liu+09].

Undershooting and Overshooting

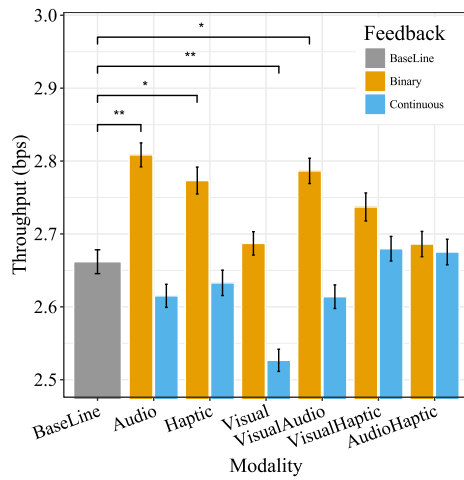
Based on the sub-movements detected by the classifier algorithm on the velocity profile, we are able to discriminate among the ballistic phase, correction phase, returning to the target after overshooting, undershooting and re-accelerating to the target, and inflection points in the profile in general. We created an additional dependant variable (*UNDERSHOOTING*) to store the under/overshooting distance along the vector defined by the positions of the last target and the current target being selected. To do this, we projected the selection vector on the target vector and recorded negative values for undershooting selections and positive values for overshooting selections.

5.4. Results

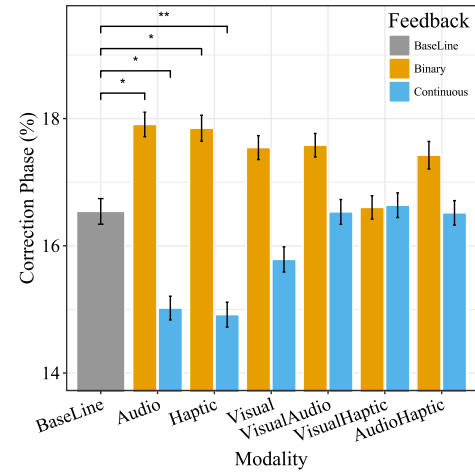
We analyzed the results with RM two-way ANOVAs for the two factors (i.e., *MODALITY* and *FEEDBACK*) on the dependant variables (i.e., *THROUGHPUT*, *CORRECTION* and *UNDERSHOOTING*), followed by post-hoc analyses with pairwise T-test comparisons with Bonferroni's correction at the 5% significance level. We confirmed the assumptions of the ANOVA for the experiment data; a Shapiro-Wilk's test did not indicate that the assumption of normality had been violated. Degrees of freedom were corrected using Greenhouse-Geisser's estimates of sphericity when Mauchly's test indicated that the assumption of sphericity had been violated. One-way RM ANOVAs were used to compare the *MODALITY* regarding the number of modalities involved (i.e., Unimodal and Bimodal) on all the dependant variables and no significant differences were found. On this section, only significant comparisons are mentioned and the whisker bars shown on the different plots present the standard error of the mean.

5.4.1. Effective Throughput

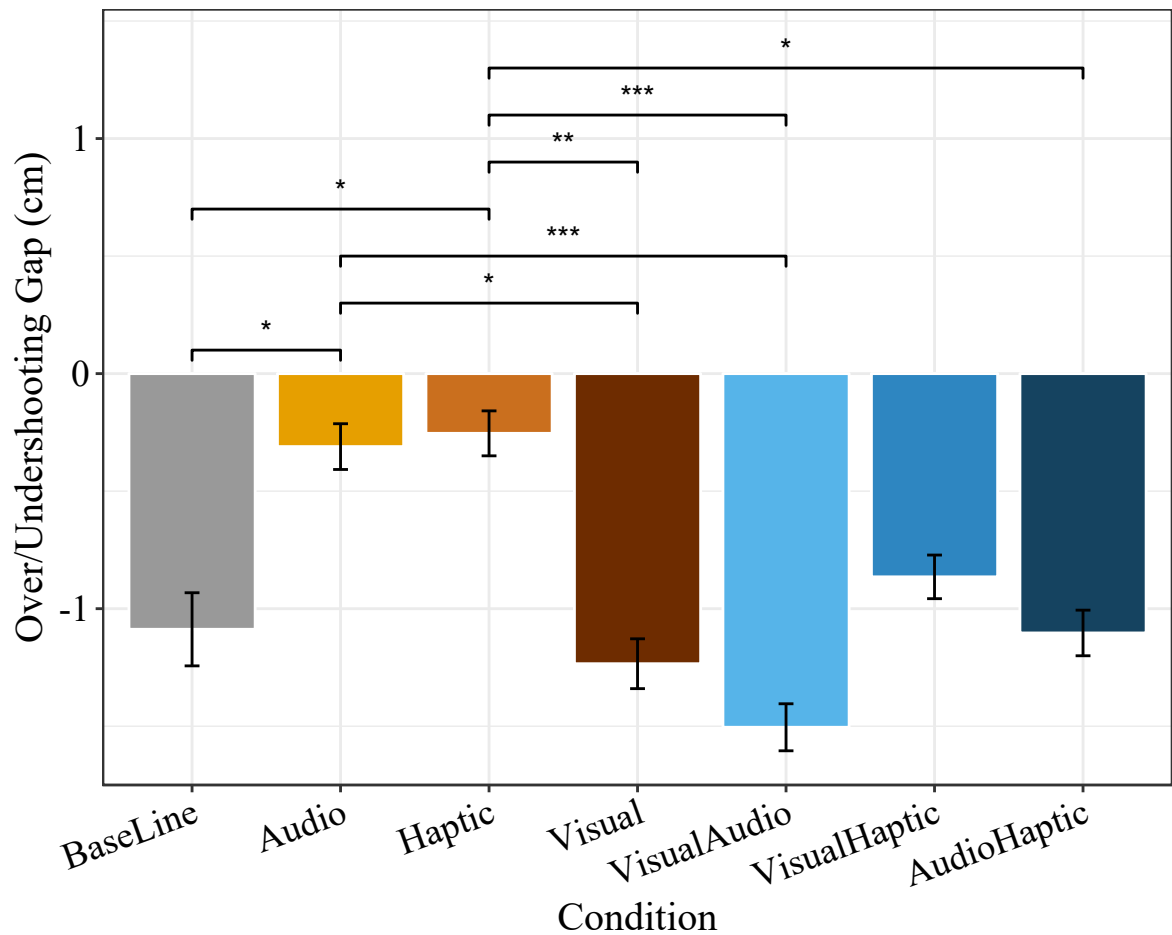
The RM two-way ANOVA showed a significant main effect of *FEEDBACK* ($F(1, 14) = 6.673$, $p < 0.05$) but not for *MODALITY* on *THROUGHPUT*. No significant interaction of *FEEDBACK* and *MODALITY* was found. Post-hoc tests revealed significant differences between Binary and BaseLine ($p < 0.05$), and between Binary and Continuous ($p < 0.001$), with Binary feedback ($M=2.747$, $SD=0.656$) having higher throughput than both Baseline ($M=2.662$, $SD=0.594$) and Continuous ($M=2.624$, $SD=0.613$) conditions. Regarding the Baseline condition, pairwise comparisons revealed a significantly better *THROUGHPUT* for Binary-Audio ($M=2.808$, $SD=0.616$, $p < 0.01$), Binary-Haptic ($M=2.773$, $SD=0.691$, $p < 0.05$), and Binary-VisualAudio ($M=2.787$, $SD=0.654$, $p < 0.05$). On the contrary, *THROUGHPUT* was significantly lower for the Continuous-Visual condition ($M=2.526$, $SD=0.566$, $p < 0.001$). Figure 5.4a summarizes the results, showing that the *THROUGHPUT* is higher when Binary-Audio, Binary-Haptic and Binary-VisualAudio feedback are provided.



(a) Effective throughput is better in Binary conditions (i.e., Audio, Haptic).



(b) Binary-Audio and -Haptic feedback presented longer correction phases.



(c) Audio and Haptic conditions presented very low undershooting.

Figure 5.4.: Results for the experiment on multimodal feedback for 3D selection.

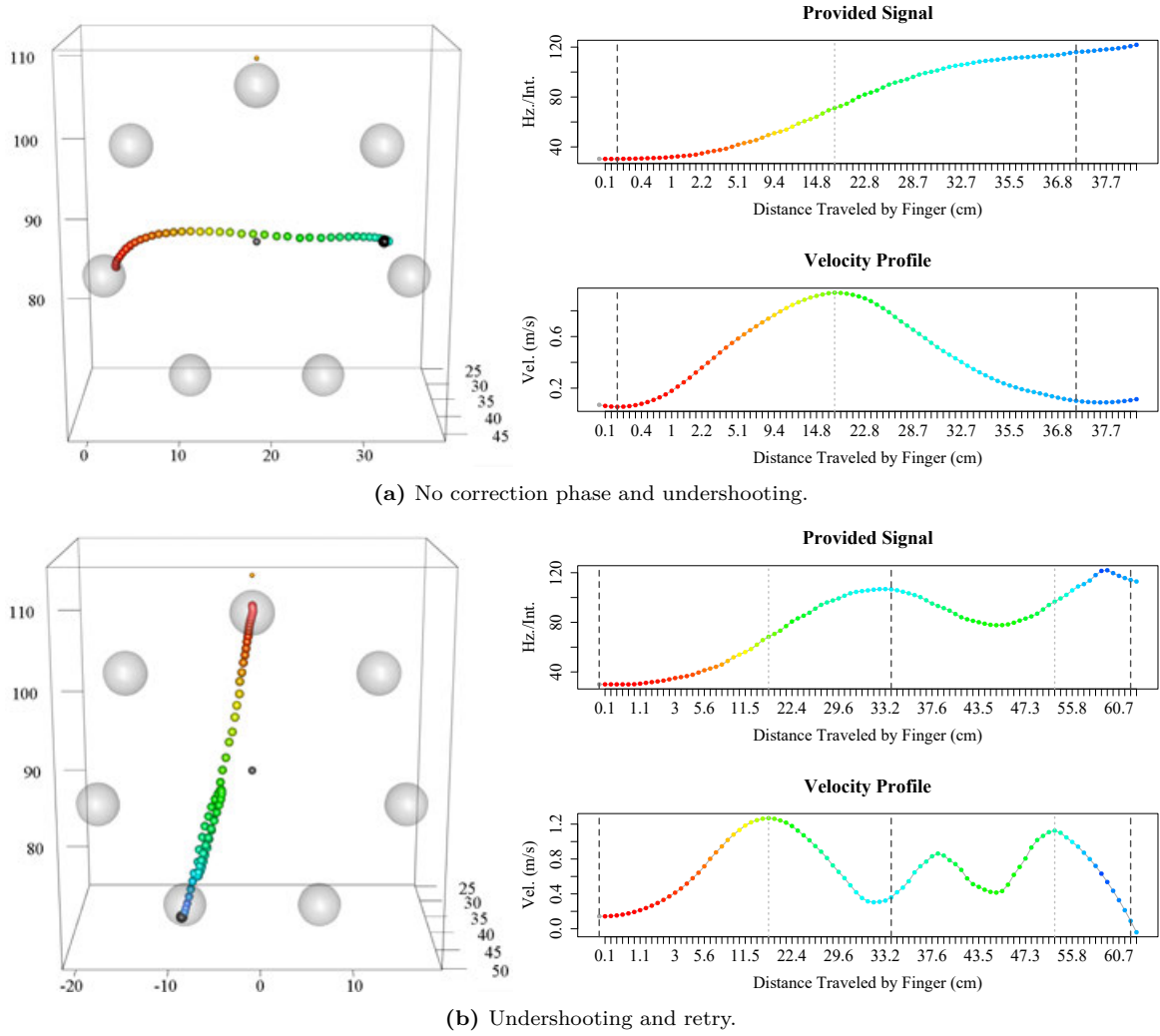


Figure 5.5.: Common velocity profiles for the combinations of modalities.

5.4.2. Under/Overshooting

The RM two-way ANOVA showed a significant main effect of *MODALITY* ($F(1, 14) = 2.932, p < 0.05$) but not for *FEEDBACK* on *UNDERSHOOTING*. No significant interaction of *FEEDBACK* and *MODALITY* was found. Regarding the condition, the pairwise comparison revealed that the Audio condition ($M = -0.310, SD = 5.145$) is significantly better (i.e. prevented the undershooting) than BaseLine ($M = -1.088, SD = 5.652, p < 0.05$), Visual ($M = -1.234, SD = 5.600, p < 0.05$) and VisualAudio ($M = -1.505, SD = 5.254, p < 0.001$). The same test also revealed that the Haptic condition ($M = -0.254, SD = 5.031$) is significantly better than BaseLine ($M = -1.088, SD = 5.652, p < 0.05$), Visual ($M = -1.234, SD = 5.600, p < 0.05$), VisualAudio ($M = -1.505, SD = 5.254, p < 0.001$) and AudioHaptic ($M = -1.103, SD = 5.113, p < 0.05$). Figure 5.4c summarizes the results. As a main outcome, a general undershooting problem was observed (i.e. even the BaseLine condition was affected), only Audio and Haptic feedback could prevent this distance estimation problem.

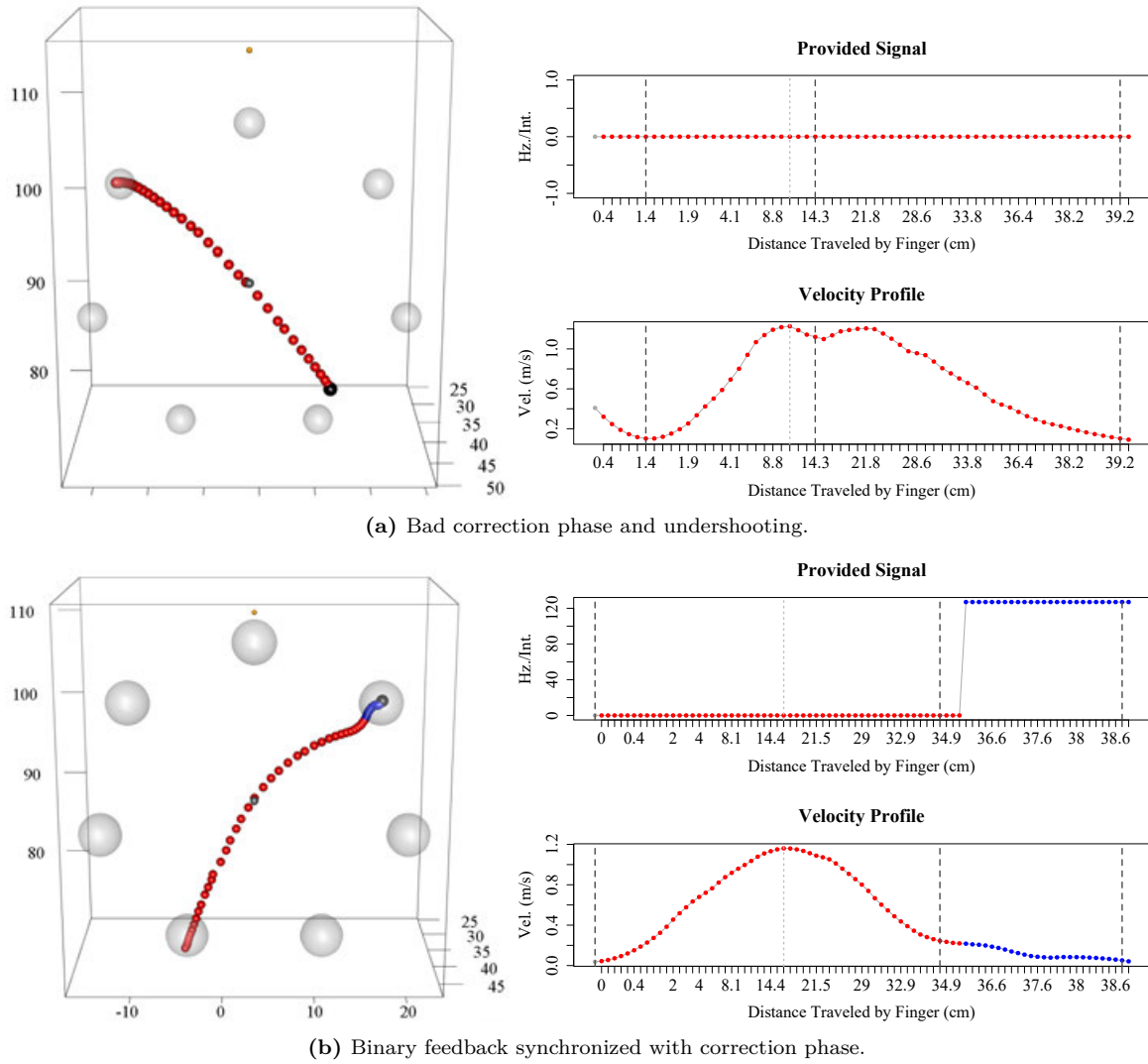


Figure 5.6.: Common velocity profiles for the combinations of proximity-based feedback.

5.4.3. Percentage of the Correction Phase

The RM two-way ANOVA showed a significant main effect of *FEEDBACK* ($F(1, 14) = 6.961$, $p < 0.05$) but not for *MODALITY* on *CORRECTION*. No significant interaction of *FEEDBACK* and *MODALITY* was found. Post-hoc tests revealed significant differences between Binary and both Baseline ($p < 0.05$) and Continuous ($p < 0.001$), with Binary feedback ($M=17.486\%$, $SD=7.231$) having a longer correction phase than Continuous feedback ($M=15.899\%$, $SD=7.099$) and BaseLine ($M=16.541\%$, $SD=7.258$). Regarding the Baseline condition, pairwise comparisons revealed significantly longer *CORRECTION* phase for Binary-Audio ($M=17.908$, $SD=7.160$, $p < 0.05$) and Binary-Haptic ($M=17.848\%$, $SD=7.561$, $p < 0.05$). On the contrary, *CORRECTION* phase was significantly shorter for the Continuous-Audio ($M=15.021\%$, $SD=6.780$, $p < 0.05$) and Continuous-Haptic ($M=14.918\%$, $SD=7.142$, $p < 0.01$). Figure 5.4b presents the results. In summary, Binary-Audio and Binary-Haptic conditions presented longer correction phases, conversely, Continuous-Audio and Continuous-Haptic presented the shortest correction phases.

5.4.4. Subjective Preference and Questionnaires

At the end of the experiment we asked subjects to judge if the different types of feedback were useful by giving subjective values on a scale of 0 (not useful at all) to 10 (very useful). For visual feedback the score was $M = 7.33$ ($SD = 1.91$), for haptic feedback the score was $M = 5.63$ ($SD = 2.63$), for auditory feedback the score was $M = 7.53$ ($SD = 1.06$) and for the combinations of different types of feedback the score was $M = 9.33$ ($SD = 0.81$). A Friedman test revealed a significant effect of the feedback combinations on the scores ($E(2)=17.365$, $p < 0.001$). A post-hoc test using Wilcoxon-rank with Bonferroni correction showed a significant difference between haptic feedback and bimodal feedback ($p < 0.05$); participants preferred the bimodal conditions over the unimodal haptic feedback. In the same way, some of the comments given by the participants show the same tendency: “*I liked the combination of visual and audio elements in the experiment*” and “*Precise positioning in the center of the sphere was easiest with additional audio pattern feedback*”.

Although the participants kept a seated position during the experiment, we asked the participants to answer the Simulator Sickness Questionnaire (SSQ) before and after the experiment. We analyzed the data with a non-parametric Wilcoxon Signed-Rank test at the 5% significance level. There were no significant increases in the condition of the participants before ($M=5.150$, $SD=3.23$) and after the experiment ($M=6.213$, $SD=6.67$). The participants had also to judge their level of presence on the basis of the Slater-Usuh-Steed presence questionnaire after the experiment ($M=4.911$, $SD=1.259$) indicating a good sense of presence.

5.5. Discussion

Our experiment revealed that the overall effective throughput that can be reached with proximity-based feedback differs significantly in favor of binary feedback over continuous feedback for unimodal conditions. In particular, we made the following observations in the proportion of the ballistic and correction phases and undershooting for the feedback types:

- *Continuous* feedback (for all the conditions) presented the same or less level of *THROUGHPUT* and *CORRECTION* as our base condition. Additionally, many selection movements with continuous feedback presented undershooting problems caused by velocity profiles with no correction phase at all (Figure 5.5a), maybe associated with too-fast approaches when compared with related research [Liu11]. Also, we detected common selection movements with a premature correction phase leading to undershooting, then a retry over a very short distance, which produced small overshooting in most cases (Figure 5.5b).
- *Binary* feedback for the visual modality was in general no different from the BaseLine condition, presenting the same undershooting problem and in many cases the finger approached the target region but the usual corrective behaviors to locate the center of the target were completely lost or erratic (Figure 5.6a).
- *Audio and Haptic* conditions with continuous feedback could prevent the undershooting with short correction faces as the associated movements produced low *THROUGHPUT* (i.e., the effective

throughput was below the Baseline) due to very slow but precise approaches. This behavior can be explained by the cognitive load needed to interpret proximity-based feedback based on intensities or frequency changes [Ari+17]. In contrast, *Audio and Haptic* conditions with binary feedback, produced high *THROUGHPUT*, very low *UNDERSHOOTING* and longer *CORRECTION* phases, beneficial in order to achieve a selection performance similar to real-world selections as presented in [Liu+09]. Many selection movements in this category, could even elicit velocity profiles highly synchronized with the feedback signal (vibrotactile and audio); the correction phase movement improves with the binary feedback (Figure 5.6b).

Moreover, our results showed that participants subjectively preferred the *bimodal* over *unimodal* feedback, and that bimodal feedback significantly reduced error rates (there was a significant difference ($p < .05$) in error rate for unimodal ($M=9.76$, $SD=15.33$) and bimodal ($M=8.01$, $SD=14.11$) conditions. This result is contrasted with studies showing continuous visuo-haptic feedback reducing the error rate in comparison with a binary alternative [Ach+14].

Considering that it is essential for some application domains to keep a balance between minimizing errors and achieving faster selections, we believe that our suggestions will provide valuable options that can be leveraged by practitioners to improve their 3D user interfaces. We propose the following guidelines:

- Avoid bimodal combinations if the user interface must provide advantages in terms of throughput and preventing undershooting.
- Choose binary proximity-based feedback over continuous feedback for faster movement times and overall higher throughput in 3D selection tasks.
- Choose bimodal over unimodal feedback for reduced error rates in 3D selection tasks and higher subjective user acceptance.
- The best deal among throughput, under/overshooting distance and the proportion of the correction phase is *binary-unimodal-haptic* feedback. With this profile, is it possible to significantly increase the correction phase (i.e., 12%), prevent over/undershooting almost completely while having a higher throughput in comparison with the BaseLine condition. Although *binary-unimodal-audio* feedback offers the same advantages, we recommend haptic feedback (i.e., vibrotactile in this case) because audio cues could interfere with common environmental sounds in VEs.

Finally, the context of the presented study is related to 3D selections on a Fitts' Law experiment with an interaction space restricted to a circular layout of targets. Is it necessary further research to evaluate the conditions, the hardware developed, and the guidelines suggested on different interaction spaces and techniques for VR (i.e., different depth levels, fovea/periphery, pulse-based tactile feedback, etc.).

5.6. Conclusion

In this chapter, we presented proximity-based feedback types that can be used, in particular, during 3D selections. We applied these feedback types to three sensory modalities (i.e., visual, auditory, and tactile), leveraging an HMD, headphones and a vibrotactile finger-wearable device. Moreover, we changed


the intensity, frequency, and color according to the distance traveled during selection, which provides localization cues to improve overall performance. We analyzed the types of feedback using a Fitts' Law experimental design. Our Fitts' Law experiment revealed significant benefits of binary proximity-based feedback over continuous feedback in terms of higher effective throughput and less undershooting. The overall effective throughput that can be reached with proximity-based feedback differ significantly in favor of binary feedback. We found that binary feedback is also offering better benefits preventing undershooting when selecting 3D targets in comparison with the continuous counterpart. Furthermore, we analyzed the proportion of the ballistic and correction phases of the selection movements and we found that binary feedback produce movements with larger correction phases, usually related to accurate selections. Moreover, bimodal feedback was subjectively preferred over unimodal feedback. Finally, we discussed guidelines for practitioners in this field to improve their 3D user interfaces.

Part III

Perceptual Illusions

6 Chapter 6

Inducing the Long-Arm Illusion

This chapter is related to the scenario  (see Section 1.2).

6.1. Motivation

Current developments in VR allow numerous users to experience VEs in a broad range of application fields. However, most traditional VEs are focused solely on the visual and auditory modalities, which often limits the user's sense of body ownership and embodiment in virtual environments. Research has shown novel advances in wearable devices to provide vibrotactile feedback which can be combined with low-cost technology for hand tracking and gestures recognition. In this way, it is possible to reproduce perceptual illusions involving tactile sensations, in which the stimulation of the sense of touch can be provided with an actuated device instead of using a real object, extending the interaction possibilities of the user, creating compelling illusions and, for instance, even creating the sense of having bigger, shorter or elongated limbs [Kil+12; TH05]. However, so far there are no conclusive results about the effects of replacing the traditional approach to provide the tactile feedback i.e., manual and synchronized tapping, with automatic vibrotactile stimuli using a wearable device. By combining HMD-based VEs with head, hand and body tracking, with haptic feedback devices enables the creation of interactive experiences providing embodied visual, auditory and haptic feedback in response to user actions. Additionally, current technology provides low-energy, wearable and wireless components to create ergonomic and low-latency vibrotactile devices, reliable enough to automate the creation of perceptual illusions in VEs and possibly inducing effects similar to real-world demonstrators. Body-transfer illusions, such as the rubber-hand illusion or elongated-arm illusion, have shown that it is possible to give a person the persistent illusion of body transfer after only brief phases of synchronized visual-haptic stimulation. The motivation of this chapter is to induce such perceptual illusions by combining VR, vibrotactile and tracking technologies, offering an interesting way to create new spatial interaction experiences centered on the senses of sight and touch. We present a pair of self-made gloves featuring vibrotactile feedback that can be synchronized with audio-visual stimulation in order to reproduce an illusion of body-ownership providing automatic tactile stimuli, instead of the traditional approach based on manually synchronized stimulation, and finally measured the physiological responses to a sudden event in order to evaluate if the illusion effects could be properly induced.



Figure 6.1.: (left) Images of the glove with the electronic case attached to the forearm, and (right) participant interacting with the VR application, wearing the pair of gloves and the Oculus Rift DK2 with the Leap Motion attached in front to facilitate the hand tracking.

6.2. Vibrotactile Glove Device

We designed our device as a glove to recreate the sense of touch with vibrotactile feedback while the user is exposed to a VR visual stimulus involving body-transfer illusions. In this section, we detail the concepts and the implementation details of a pair of tactile devices (for bimanual interaction), which offer a wireless, lightweight and responsive tactile display solution, able to provide synchronized visual-tactile stimuli in VEs.

6.2.1. Vibrotactile Display

There is a wide range of methods to provide tactile feedback (i. e. temperature, vibration, pressure). Our approach is based on coin-type linear resonant actuators (LRAs), used to create vibrations by powering a voice coil, which moves a magnetic mass and vibrating at a resonant frequency in one dimension; in this case, the normal direction to the hand's palm surface.

The proposed glove consists of 14 actuators. The quantity of actuators was defined as a balance between device mobility and power usage while still offering a comfortable wearable device. The positions were chosen regarding neurological aspects; the density of actuators on individual parts of the hand depends on the size of the area in the somatosensory cortex. We concentrated on the fast adapting Pacini corpuscles (PC) described by Stark et al. [Sta+98] in the fingers and palm of the hand. The receptors are primarily reacting to vibration so it is easy to stimulate them with LRA actuators [CK13; Kur+07]. The receptive fields of cortical neurons on the fingertips are smaller than the one on the palm. Therefore, each finger has two actuators, which are placed on the fingertip and above the metacarpophalangeal joints. The palm has only four actuators: Two on the ball of hand and two on the palmar surface, renouncing on placing one vibration motor in the middle of the palm, as it could not touch the skin under certain hand postures [GPS12]. Israr and Poupyrev [IP11] proved with their tactile brush algorithm, that it is possible to create continuous, high-resolution tactile stimuli with a low-resolution grid of vibrating actuators by using the apparent motion and the phantom illusion.

For the resonance frequency Kuroki et al. chose 240 Hz for their mechanical feedback to stimulate the PC [Kur+07]. In general PC stimulate in an interval of 10 -500 Hz with a minimal threshold of 150-300

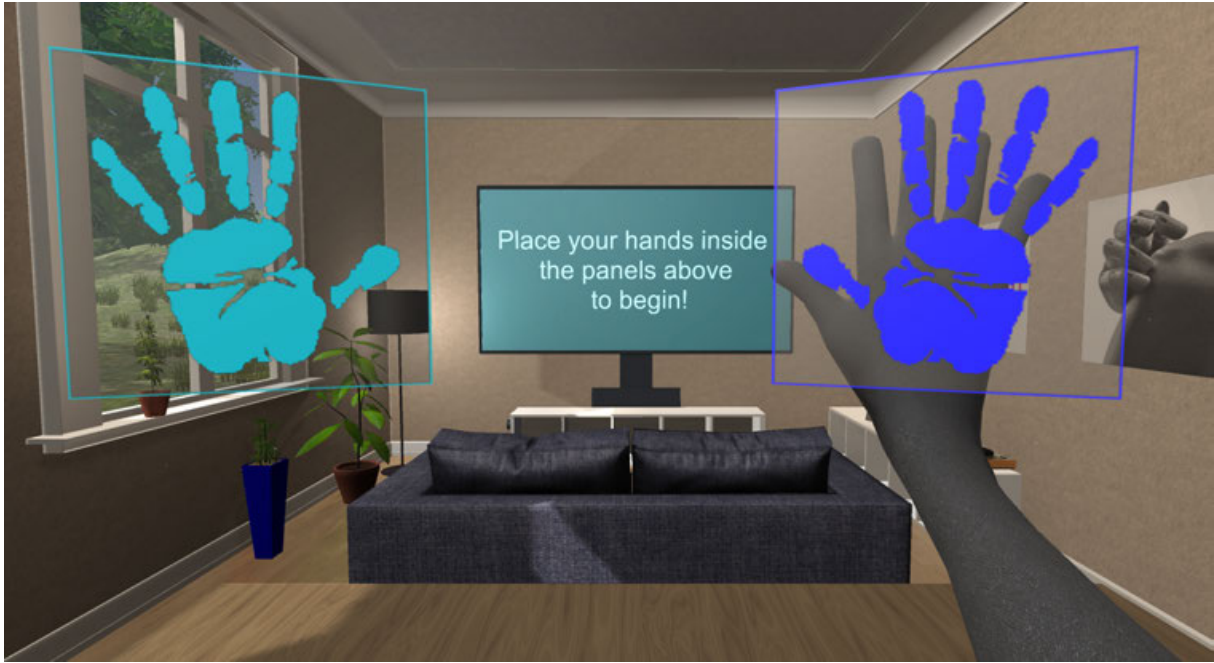


Figure 6.2.: View of the 3D user interface used to navigate through the experiment tasks.

Hz [CK13]. If the frequency is high, the localization of the single signal gets more difficult because the stimuli are propagated. After a test to detect stimuli overlapping, we set a frequency of 175 ± 5 Hz so the vibration is not too strong for sensitive people and keeping the source still distinguishable.

As a result, our grid of actuators can stimulate the hand in a detailed manner that is enough to provide the touch sensations required in perceptual illusions experiments, emitting vibration stimuli between the acceptable range [Kur+07]. The vibration motors are attached with a rubber band to a thin fabric glove. Previous prototypes of our device have shown that normal gloves do not create enough tension to produce the same vibration on different hand sizes. With regards to Choi and Kuchenbecker we included rubber bands to “ensure signal transmission” [CK13] and that the motors are nearly on constant places for a wide range of hand sizes. Specific details of the device can be found in the Appendix (see Section A.4).

When emitting signals to the vibration motors, we address the motor independently with values to define the intensity of vibration. Before emitting signals, we have to determine the intensity for each vibration motor. We do this by attaching Tactile Control Points (TCPs) to the avatar’s hand bones at specific locations, which represent the real vibrators’ locations on the gloves. Instead of using full vibration intensity when in contact with a surface, following an on-off approach, TCPs inherit an intensity value dependent on their distance to the nearest touchable collider in the scene. The used distance function is defined by $(1 - x/0.01)^4$ and returns values greater than zero for distances between zero and one centimeter. The “actual distance” refers to the size of the depicted hand, while the graph is only valid for the examined point on the surface at the coordinate (0,0). After determining the intensity for each TCP, all the data is collected and sorted by a central organizer unit. This unit puts all the intensities into an encoded-data packet and sends it to the experiment computer.

The choice to emit an intensity based on distance rather than contact, stems from the way the tracked hands interact with virtual objects. It is because of our inability to detain the user’s real hands from

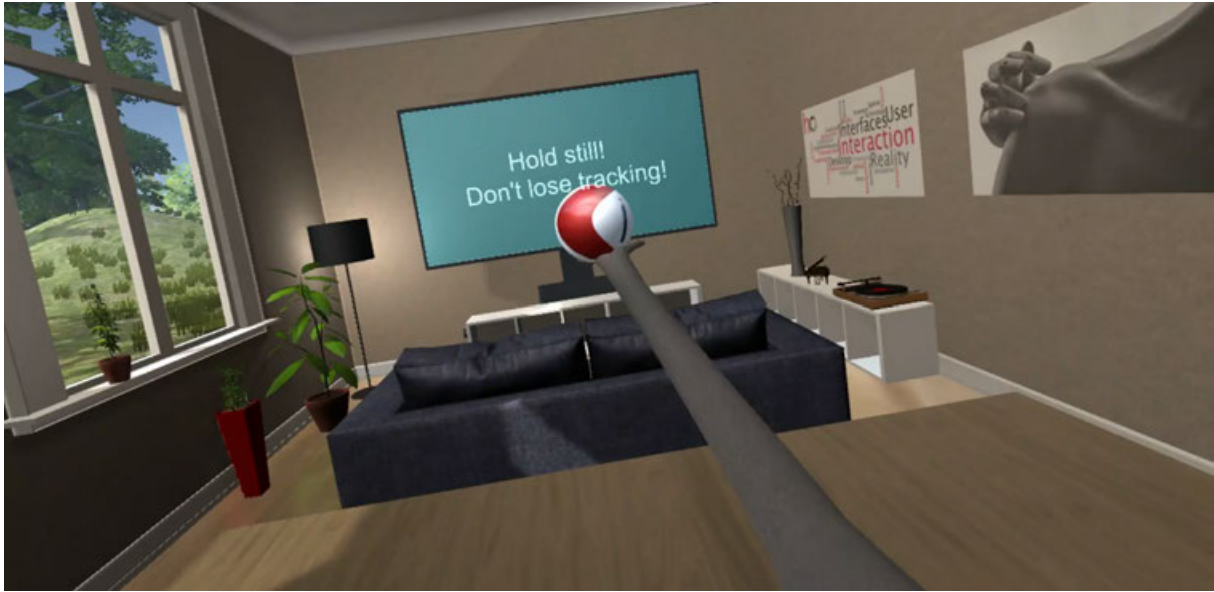


Figure 6.3.: User perspective for the elongated arm.

moving when the correspondent virtual hands should, due to collisions. If we stopped the virtual hands from moving further in a direction because of an obstacle, we could not synchronize this behavior to the user's real hands, which are free to move in any direction at any time in our setup. Since it is a delicate task to maintain a hand position that actually provides tactile feedback while touching a static surface, we defined a certain range around the surface that would trigger a vibration on our glove. This eventually led to the implementation of the distance function to provide a more elaborate sensation.

We integrated the vibrotactile glove into a VR setup using the Unity3D engine and an Oculus Rift DK2 head-mounted display with a Leap motion controller for hand tracking. The tracked pose of the glove can be used to induce vibrotactile feedback, for example, when collisions with virtual objects are detected.

6.3. Experiment

In this section we describe the within-subject experiment conducted to analyze whether the vibrotactile feedback condition, using our proposed device, can reach a similar effect strength as the traditional reference condition, in which tactile stimulation is applied manually with a real-world object as commonly used to induce the elongated-arm illusion in psychological experiments.

6.3.1. Setup

The virtual environment was designed with the Unity3D engine and deployed on an Intel computer with a Core i7 hexacore at 3.5 GHz CPU with 32 GB RAM and two Nvidia GeForce GTX 980 graphics cards in an SLI array. We used an Oculus Rift DK2 as a fully immersive display and a Leap Motion for hand tracking. In order to guarantee a reliable hand tracking for rested-forearm tasks and according to our

experiences, the Leap Motion was tilted down by approximately 13 degrees using a 3D printed mount. Also, noise cancelling headphones were used to increase the immersion and filter out background noises.

As we wanted to make the experience as little irritating for the participants as possible, we chose to create a neutral environment in which a participant's avatar is seated in a desktop setup, looking from the avatar's point of view. This scene recreates the actual constellation of the participant to the chair, table and screen in the physical experimental setup. We ensured that sufficient free space was available between the participant and the screen in order to let them interact with their hands with virtual objects or interfaces (see Figures 6.2 y 6.3).

A simple 3D user interface was included so that the participants could advance through the different experimental steps at their own pace. This was carried out via two hand panels, hovering above the table, which could be touched simultaneously to indicate that the participant was ready to be given the next instruction. The virtual room was refined by adding details in the form of furniture, windows, plants and decorative assets to reproduce the impression of the real place uses for the study.

6.3.2. Tasks

The experiment consisted of three phases. The first phase introduced the participant to the sensation of the vibrotactile feedback. This included being exposed to visual-haptic stimuli on the hands and recognizing basic shapes like a cube or a sphere. In the second phase, the participant's arm was stabilized in a comfortable position on a wedge of foam, and the participant was asked to hold the physical arm still while concentrating on the virtual arm, which was slowly elongated and after reaching twice-and-a-half of its original length was slowly retracted again to its normal length. While doing so, a virtual ball was bouncing on the virtual hand to attract the attention of the participant. The sensation of touch provided by the bouncing ball was assigned randomly and produced according to our two experiment conditions:

1. Through vibrotactile feedback activating the vibrating actuators in the gloves according to the collisions detected between the virtual hand and the virtual bouncing ball (further called *Vibrotactile Condition*).
2. Through a real ball which was bounced synchronously on the participant's real hand by a member of the team, tapping gently the real hand of the participant every time the virtual hand was touched by the virtual bouncing ball (further called *Tapping Condition*).

Once the second phase was finished, the participant was asked to answer a survey regarding the feeling and sensation of having an elongated arm. Also, the participant had to estimate the length of the perceived elongated arm. For the third phase, the participant had to repeat the same procedure as in phase two, but received feedback according to the remaining condition. Again the arm was elongated, but in contrast to phase two, it was threatened with a sudden event occurring when it was fully elongated, which consisted of a heavy object falling from the ceiling. Finally, the fourth phase gathered the same subjective data as the second phase.

6.3.3. Participants

In a time span of two weeks, 37 participants were recruited through academic mailing lists to test the experiment. All of them gave their informed consent and the study was approved by and conducted in accordance with the local Ethics Committee. The variety of age was between 10 and 54 years old ($M = 28.0$, $SD = 9.1$).

The aspect of gender was distributed with 26 male and 11 female participants, mostly computer science students and IT professionals and all of them had normal or corrected vision. Two-thirds of the participants reported no prior experience with experiments involving vibrotactile devices. The mean time per subject, including questionnaires and instructions, was about fifty minutes. After removing a participant who failed the stereoscopic vision test, the analysis employed data of 36 remaining participants.

6.3.4. Procedure

The participation started with a demographic questionnaire and the Titmus test [SH84] for stereo-blindness assessment. The participants sat on a static chair in front of a table. Two computers were used for this experiment. The first one was only used for the testing environment and measuring the interpupillary distance (IPD). The monitor was needed to synchronize the stimulation with the real ball at phases two and three. Unused devices (including keyboard, mouse, connector etc.) were moved away to not be a hindrance to the participant during the experiment. The second computer was used only for answering questionnaires. The table was covered with an infrared light absorbing material to support the tracking of the Leap Motion. For the experiment itself, the participants were asked to wear multiple devices: The Oculus Rift DK2 HMD with the attached Leap Motion sensor, the noise-cancelling headphones and the pair of haptic gloves (see Figure 6.1).

For the stimulation with the real ball, a matching-size sphere was glued to a stick, so the member of the research team would not touch and distract the participant. In order to achieve higher accuracy in the *Tapping Condition*, the same experimenter performed all the tapping actions during the whole experiment. In addition, training sessions were conducted apriori to reduce the variance on timing and intensity, thus achieving a synchronous and believable movement comparable to the *Vibrotactile Condition* that consistently matches the visual feedback. During and after the experiment, the results were collected in three different ways. First, a questionnaire was answered by the participant. As a second result, an attending member of the research team subjectively evaluated the reaction to the sudden event of a heavy object falling from the ceiling on a scale from 0 to 10 (being 10 the highest score), according to reflex reactions of the participant's body avoiding the threat and offering insights about the achieved sense of body ownership. To avoid experimenter bias, the evaluation was quantified according to predefined guidelines to score reactions like going back with their head and arms, twitching, faster breathing or comments made by the participants. Lastly, the participants were asked to judge their own feeling and reaction towards having his arm elongated and threatened by the sudden event.

Directly after the elongated-arm stimuli (phase two and three), the participants were asked to answer different questions regarding their feeling of ownership of the virtual arm (scale 0 to 10 for the first three questions):

1. Please judge your sense of having an elongated arm.
2. Did the elongated arm feel like a part of your body?
3. How comfortable did you feel with an elongated arm?
4. How long do you think your elongated arm was (in %)?
5. Additional comments (I liked..., I didn't..., because...)

The four dependent variables, defined as *Ownership*, *Proprioception*, *Comfort* and *Perceived Length* from the first four questions, focus on the feeling of body ownership. If the corresponding answers show a trend towards high values, we can conclude that the elongated-arm illusion could be correctly induced [Kil+12]. The additional comments were used to comprehend and confirm the participant's answers.

6.4. Results

The results of the experiment are shown in Figure 6.4. For the analysis we ran comparative tests to measure the effects of the long-arm illusion induced with our vibrotactile condition in comparison with the traditional tapping condition. We ran a Wilcoxon Signed-Rank test at the 5% significance level for the *Ownership*, *Proprioception* and *Comfort* variables, and a paired t-test at the 5% significance level for the *Perceived Length* variable. Table 6.5 lists all the calculation details related to the following findings:

- We found a significant influence of the elongated arm on **ownership** for the *Tapping Condition* ($M=6.5$, $SD=2.171$) and the *Vibrotactile Condition* ($M=7.028$, $SD=2.210$), reporting an effect of medium size (0.247).
- We found a significant influence of the elongated arm on **proprioception** for the *Tapping Condition* ($M=5.778$, $SD=2.520$) and the *Vibrotactile Condition* ($M=6.50$, $SD=2.299$), reporting an effect of medium size (0.348).
- We found no significant influence on the **comfort** variable for the *Tapping Condition* ($M=6.555$, $SD=2.104$) and the *Vibrotactile Condition* ($M=6.833$, $SD=2.236$).
- We found a significant effect of the elongated arm on the **perceived length** for the *Tapping Condition* ($M=142\%$, $SD=0.991$) and the *Vibrotactile Condition* ($M=170\%$, $SD=1.267$), the effect size is 0.350, with a standardized mean confidence interval of [-0.554; 0.010].

6.4.1. Subject Reaction

As described above, to draw further conclusions regarding the body ownership, a sudden event was presented to the participants at the end of the third phase. While doing the experiment, every participant

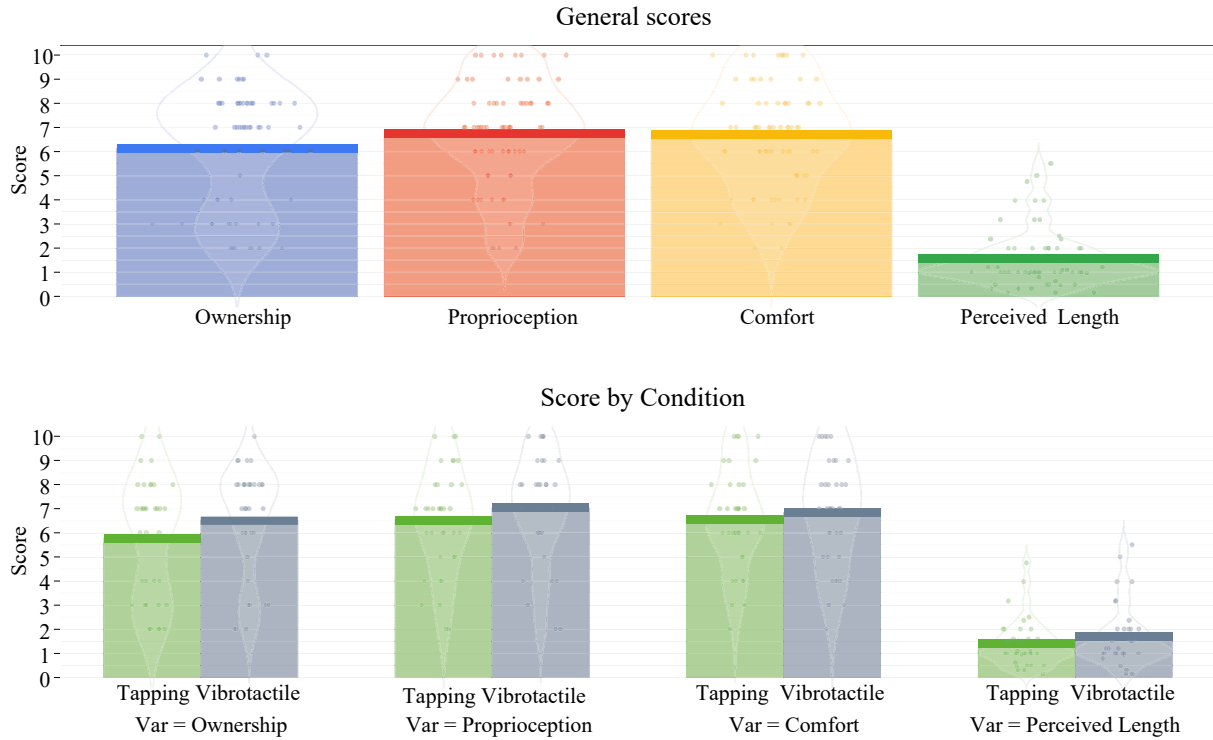


Figure 6.4.: Plot corresponding to the dependent variables (**ownership**, **proprioception**, **comfort** and **perceived length**) showing the general scores (**top**), and the scores ranked by experiment condition (**bottom**).

(if previously agreed) was filmed to offer the possibility to recapture missed reactions during the study reviewing the video footage. The shown reactions were put into a scale from 0 to 10. If the participant did not show any signs of reaction, the value equals 0. If the participant showed a full reaction, like trying to protect his arm or showing full surprise reactions, like heavy breathing, then the value equals 10. The team did not only look at the twitching of the arm, but also included the surprise and fear reactions like laughing anxiously into the value. The presented reactions were noted as a comment to differentiate the values. The values of this subjective variable, indicate that almost 50% of the participants reacted noticeably to the sudden event ($M=5.25$, $SD=2.872$), while the *Tapping Condition* ($M=4.4$, $SD=2.746$) presented a lower reaction level than the *Vibrotactile Condition* ($M=5.857$, $SD=2.869$).

6.4.2. Simulator Sickness

Although the participants kept a seated position during the experiment and were instructed to look forward avoiding fast head movements to reduce nausea among other simulator effects, we asked the participants to answer the Simulator Sickness Questionnaire (SSQ) [Ken+93] before and after the experiment. We analyzed the data with a non-parametric Wilcoxon Signed-Rank test at the 5% significance level. There are no significant increases in the condition of the participants between before ($M=0.187$, $SD=0.143$) and after the experiment ($M=0.131$, $SD=0.065$).

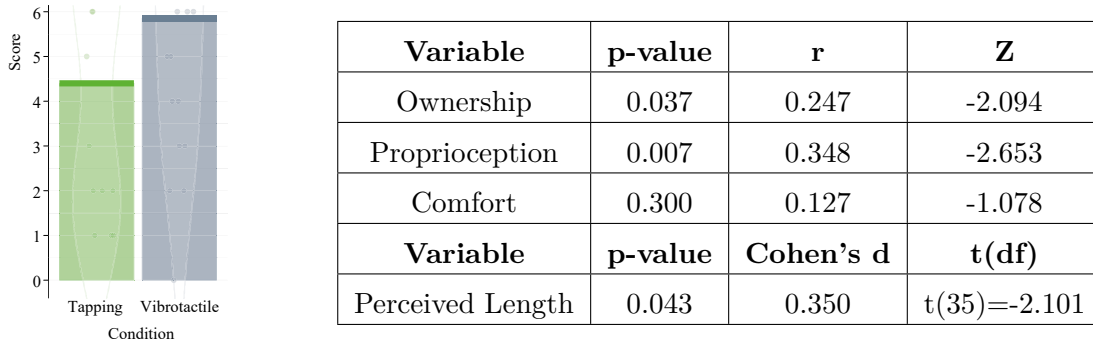


Figure 6.5.: Plot corresponding to the the reaction levels (**left**) and results for the significance tests (**right**).

6.4.3. Presence

The participants had to judge their level of presence on the basis of the Slater-Usuh-Steed presence questionnaire [Uso+00] after the experiment ($M=4.828$, $SD=0.259$) indicating a good sense of presence in addition to positive comments from some participants about the quality of the VR experience.

6.5. Discussion

The results of the study indicate that the elongated-arm illusion was produced under both experimental conditions, which shows that the brief phases of matching visual-vibrotactile feedback could induce a compelling illusion. Moreover, the results show significant differences for the variables *ownership*, *proprioception* and *perceived length* between the conditions (see Figure 6.4), slightly benefiting the *Vibrotactile Condition*. This effect is most noticeable on the *perceived length*, showing a higher value by approximately 20% in this condition (although, as the virtual arm was elongated to double the starting size, most participants underestimated the length of the elongated arm in both conditions). The same trend is also present in the subject reaction measurements, where the *Vibrotactile Condition* resulted in behavior more closely matching natural threat responses with high body ownership.

We believe that an explanation of these differences is that our low-latency vibrotactile stimulus could be presented with less sensory discrepancy than the manually synchronized tapping. Although several efforts were made to provide high accuracy in the manual stimulation, the higher scores on the *Vibrotactile Condition* might be attributed to this discrepancy. In order to remove this confounding factor, it is needed to track the position of the physical ball (i.e. IR-LED marker tracking) and transfer this onto the virtual ball in our 3D scene. Going further, other question could also be addressed regarding the vibrotactile device: ¿Could non-realistic (in terms of intensity) or non-synchronous feedback still be effective to support the body-transfer illusion in VR?

It is an interesting finding that the vibrotactile feedback was not just comparable to haptic feedback with a real ball in terms of the body-transfer illusion in this experiment, but even supported the illusion. Moreover, the automatic contact detection and feedback generation in the Unity3D implementation allows us to induce or reinforce such body-transfer illusions with brief phases of synchronized visual-tactile feedback at any time during a VR experience, without the need for a trained operator standing by to provide manual tapping feedback. We believe that this will allow us to reach similar effects in other

illusions as well, such as the rubber-hand illusion [BC98]. Informal preliminary testing being conducted at our laboratory seems to support this impression.


Regarding our device, we are considering different technologies and techniques to improve the feedback, like haptic cues or dynamic vibration patterns [Ari+15]. Although we had a shape-recognition task to familiarize the participants with our device, it is still necessary to integrate more sensors and actuators to enable the feeling of textures, weight and detailed shapes. For example, recent studies focused on electro-tactile devices [Hum+16] and reported good results in terms of precision and performance for grasping tasks using tactors, which could offer a good alternative to address some issues related to location acuity and location sensitivity in order to implement effective shape-recognition techniques. In the same way, our experiment relied on the hand tracking provided by the Leap Motion sensor, but an approach in combination with optical LED marker tracking might further improve the device.

6.6. Conclusion

We presented a technology framework featuring a device able to provide brief phases of vibrotactile feedback synchronized at low latency with visual feedback for the goal to enable and simplify the process to induce and reinforce body-transfer illusions in VR. We provided evidence from an experiment showing that the automatic visual-vibrotactile feedback can be used to induce a similar elongated-arm illusion as that which traditionally requires an operator to be present in order to stimulate the user with synchronized visual-haptic tapping feedback. Our results suggest that the approach may be transferred to other body illusions as well, thus providing the means to improve VR experiences of users in a variety of application fields (e.g., VR games [Har+20; Kir+19]). We plan to test other materials, to support the contact between the skin and the actuators. Also, in order to sense subtle user reactions, we plan to measure skin conductance as a stress response [AR03], with the integration of galvanic skin response (GSR) sensors and include fingertip heart rate monitors. Finally, further work will be mainly focused in the integration of other perceptual illusions with the purpose of use the gained experience in the creation of perceptually inspired user interfaces for VR.

7 Chapter 7

Combining Haptics and Pseudo Haptics

This chapter is related to the scenario  (see Section 1.2).

7.1. Motivation

In this chapter, we propose non-intrusive wearable haptic technology and multimodal cues to combine pseudo-haptics, tactile, and proprioceptive feedback to convey sensations for contact, stiffness, and activation, respectively, while interacting with realistic 3DUIs. Our experiments are based on a use case with 3D buttons. They are universal-known UI elements, making it easy to distinguish the working mechanism and the hand movement required to operate them. Hence, the user quickly implies the button's ergonomics and affordances (i.e., the user knows what can be done). A button also resembles common 3DUI elements for VR training apps when the user must feel softness, hardness, contact, and stiffness (e.g., organs exploration for surgeon training).

Mid-air direct interaction happens during the arm's ballistic reach to approach the button until the index finger touches the button. Our approach conveys the sensation of contact with tactile and proprioceptive feedback, providing both a fingertip tap and electrical stimulation in the finger tendons. Metaphorical interaction occurs when the user perceives stiffness and is provided with vibrotactile active feedback when the button is activated. The system provides the sensation of pseudo-haptic stiffness by visually modulating the C/D ratio on the axis of the arm's movement towards the movement, redirecting the virtual hand whenever the user is touching the surface of the button (i.e., the user knows if the interaction element is working). Then, while the user is pushing the finger until it goes beyond the operation threshold, the system renders the button according to a force-displacement curve providing vibrotactile cues at the fingertip to convey the sensation of activation (i.e., the user knows when the action/task is complete).

We make the following contributions:

- Introduction of a novel method to simulate the stiffness of interactable objects in VEs manipulating the C/D ratio.
- Reporting of the results from a study combining pseudo-haptics, tactile, and proprioceptive feedback for 3DUIs.
- Provision of guidelines to convey contact, stiffness, and activation in 3DUIs based on user acceptance, sense of agency, and performance metrics.

This work is motivated by the concept of *Specificity* [BF05]. It states that instead of using generalized 3D interaction techniques, new specific approaches could be designed, implemented, and evaluated to take advantage of novel 3D technologies and prior knowledge on how to map between I/O devices and interaction in VEs. We consider that novel uses of haptic feedback in 3DUIs improve VEs presence, sense of agency, and user performance [Mar+17], also taking advantage of how our hands have evolved for manipulating objects [NT93]. In summary, there has been numerous work recently, which focuses on providing compelling touch illusions in VEs. However, we are not aware of previous research that introduced non-intrusive all-in-one wearable haptic technology and multimodal cues, which combine pseudo-haptics, tactile, and proprioceptive feedback to convey sensations for contact, stiffness and activation of 3DUI elements.

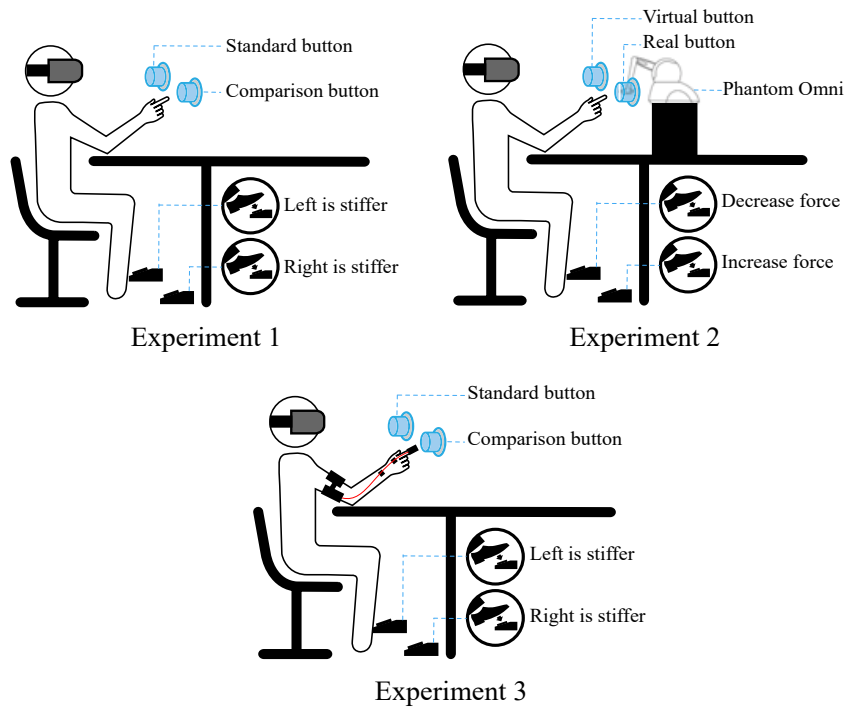


Figure 7.1.: Setup for the experiments.

7.2. Experiment 1: Stiffness and C/D Ratio

In this experiment, we focus on visual feedback only to induce the illusion of stiffness. Therefore, we used pseudo-haptics to find a valid range of C/D ratio manipulation that alters the perception of stiffness in a 3D button, focusing on visual feedback.

7.2.1. Participants

For this study, we recruited 12 participants (age: $M=26.1$, $SD=3.66$, four left-handed), mainly students and employees from our computer science department. According to the pre-questionnaire, 5 participants took part in a study involving VR for the first time. None of the participants reported any visual impairments that could affect the results of our experiment.

7.2.2. Apparatus

The experiment setup included a table measuring 140 cm by 70 cm placed in the center of a tracking space composed of four OptiTrack Prime 13W cameras at 240 FPS and calibrated with a 3D mean error of 0.213mm, providing reliable 6-DoF tracking for the participant's index fingertip of the participant's dominant hand. We used a PC Workstation equipped with an Intel processor i7, an Nvidia GTX1080, and an Oculus Quest HMD interconnected via Link technology, rendering the VE using Unity 3D. The participant performed the experiment in a seated position. The coordinate systems of both the Oculus Quest and the Optitrack system were registered by the operator at the beginning of every session as soon as the subject was seated comfortably. After registration, the subject was able to feel passive haptic feedback from the virtual table. Under the table, the participant pressed two pedals using the feet, enabling left/right answers while focusing on the hand-based experiment task. The visual stimulus presented a virtual 3D replica of the real table registered at the same position and orientation. Also, a 3D pointing hand was rendered matching the position and the orientation of the participant's index finger. On top of the table, two virtual buttons with 18 cm diameter front and 15 cm displacement depth (see Figure 7.2 left). Upon collision between the button and fingertip, the virtual fingertip of the participant was always projected onto the button surface to avoid confusing visual interpenetrations, following the "God Object" constraint/based method defined by Zilles et al [ZS95]. In order to prevent bias and confounding effects related to crossmodal references for color, size, and physical properties in general, both buttons were rendered with precisely the same material shader, mesh, size, and displacement depth [Par15].

7.2.3. Procedure

In this experiment, we used pseudo-haptics to find a valid range of C/D ratio manipulation that alters the perception of stiffness in a 3D button. With changes in the C/D ratio, we created a discrepancy in the displacements of the real and the virtual hands while pressing the button. To perceive a stiffer button in VR, a longer displacement in the real world was required (see Figure 7.2 left). For this, we conducted 2AFC experiment; the participant was asked to choose for the stiffer button using the feet pedals after

exploring a standard and comparison buttons for up to 20 seconds. The C/D ratio was manipulated, so one of the buttons presented the standard stimulus (i.e., $C/D = 1.0$) and the other one gave the comparison with one of the following values: 0.2, 0.4, 0.6, 0.8, 1.2, 1.4, 1.6, 1.8. The presentation order of the buttons and the C/D ratios were randomized per trial, presenting ten repetitions per C/D ratio, completing 1080 data samples for all the participants.

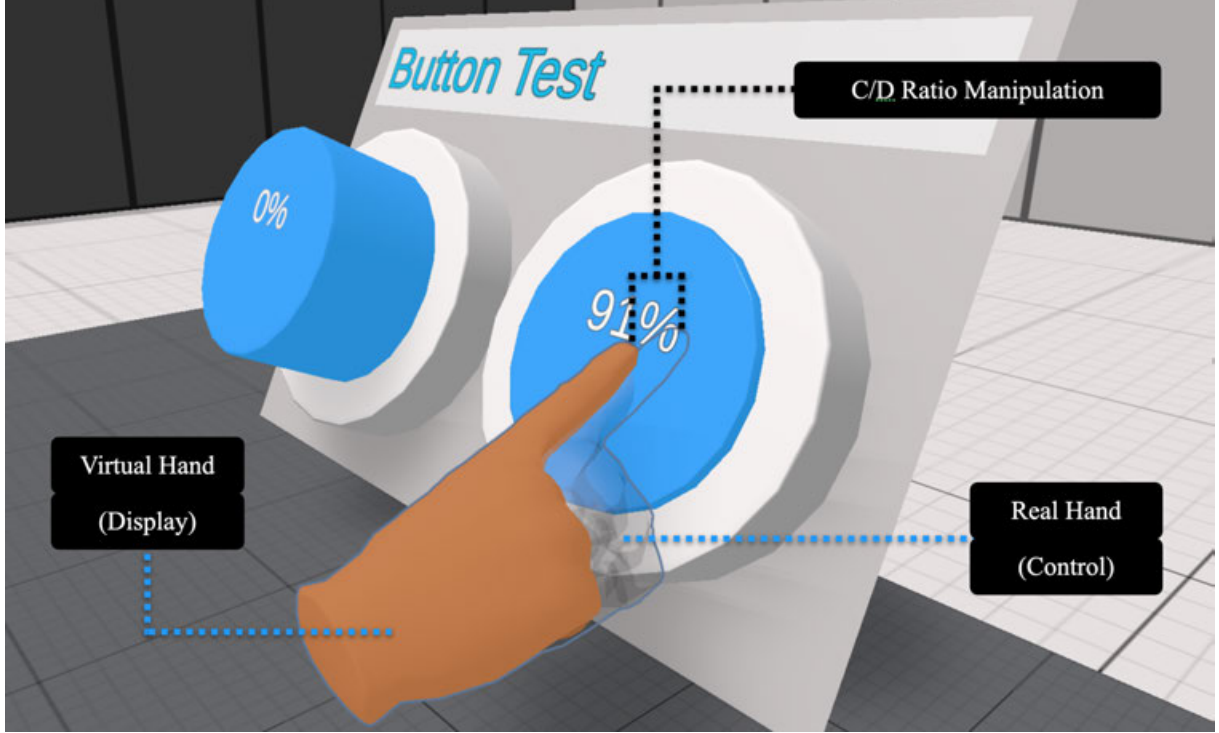


Figure 7.2.: The virtual buttons used for the study.

The subjects were provided with a white-noise loop sound during the whole experiment in order to keep the focus on visual, tactile, and proprioceptive feedback. As the experiment requires exhaustive arm movements, the subjects were asked to operate the buttons supporting the elbow on an ergonomic rubber pad to make interactions more comfortable and prevent the gorilla-arm syndrome [Jan+17]. Subjects could ask for breaks whenever they felt fatigued. The mean time per participant to complete the experiment was about 60 minutes.

The data were fitted with the psychometric function with real numbers a and b , according to the procedure explained in [Ste+10]:

$$f(x) = \frac{1}{1 + e^{ax+b}} \quad (7.1)$$

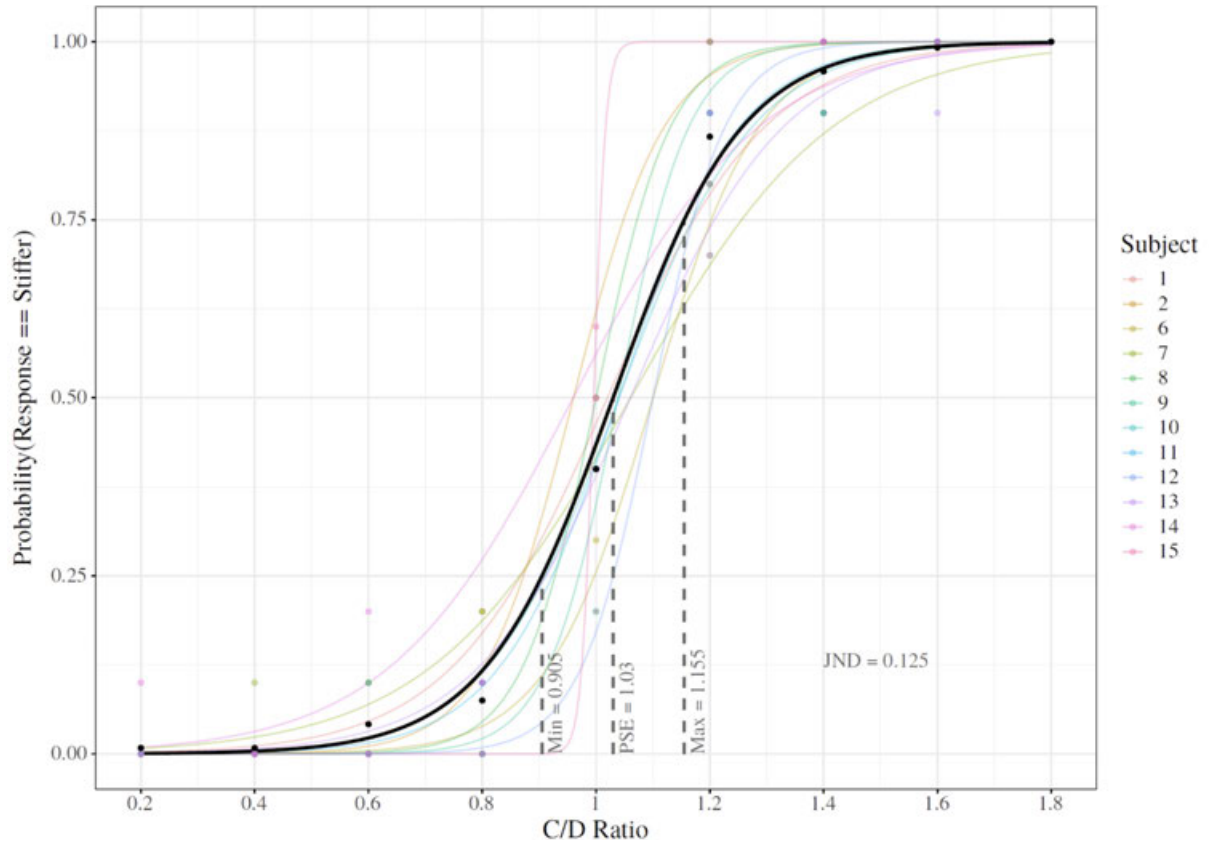


Figure 7.3.: Experiment on stiffness perception manipulating the C/D ratio. Psychometric function for stiffer responses.

7.2.4. Results

Detection thresholds for the C/D ratios are given by the upper- and lower-bound gains at which participants can reliably identify the smaller or larger C/D ratios; according to standard 2AFC procedures, this is the case when participants answer 75% of the cases. The results show that the range of $0.905 - 1.155$ for C/D ratios can be applied to simulate stiffness in 3D buttons while providing a believable illusion for the users. Also, the analysis reported a PSE of 1.03 and a JND of 0.125.

7.3. Experiment 2:

Model of Stiffness and Multi-sensory Integration

In this experiment, we compared real stiffness provided by a physical button with the stiffness simulated via the pseudo-haptics implementation described in Experiment 1. Based on real proprioceptive feedback provided by a robotic arm, we use multisensory integration theory [EB02] to create a model to predict the perceived stiffness for a specific C/D ratio.

7.3.1. Participants

12 Participants (age: $M=24.8$, $SD=3.53$, two female, two left-handed) participated in this experiment, mainly students and employees from our computer science department. According to the pre-questionnaire, none of the participants reported any visual impairments that could affect the results of our experiment.

7.3.2. Apparatus

The apparatus for this experiment builds upon the first experiment, adding a Panthom Omni device to provide force feedback and dynamically simulate stiffness for virtual button counterparts. The participants were able to increase or decrease the stiffness by 0.1 N/m using the right and left pedals, respectively. The left virtual button was co-located with the Omni effector tip, so the center of the button surface provided corresponding stiffness whenever the user touched the virtual button with the virtual hand providing real stiffness perceivable via the user's real index finger.

7.3.3. Procedure

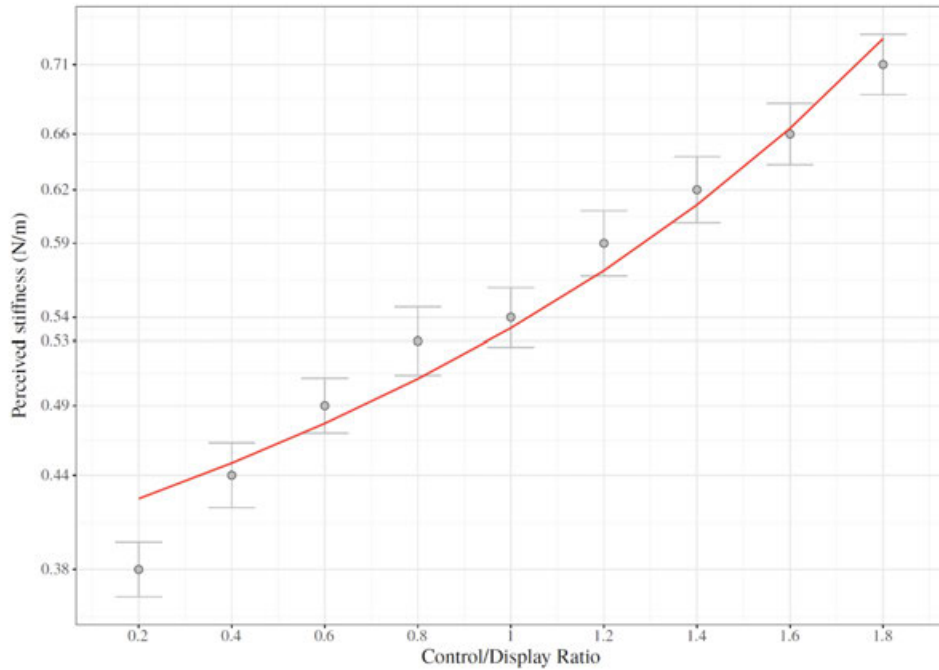


Figure 7.4.: Perceived stiffness change by C/D ratio.

We used the method of adjustments, so the participants used the left hand on the Omni effector tip to operate the left virtual button and the right hand to operate the right virtual button, which provided stiffness by modifying the C/D ratio with one of the following values: 0.2, 0.4, 0.6, 0.8, 1.2, 1.4, 1.6, 1.8. Then, in every trial, the participants were asked to adjust the stiffness of the left button using the pedals until they perceived a match with the stiffness of the left button; they could adjust it for up

to 30 seconds, followed by a confirmation to record the data using gaze pointing on a virtual button and the start of the next trial. We used psychophysical methodologies [Sam+19] to compare stiffness between pseudo-haptics (C/D ratio manipulation) and real force feedback (Phantom device), using the *forced fusion* strategy [HE07] of multisensory integration [EB02] to create a predictive model for perceived stiffness in VR given a C/D ratio. To do this, we solved the integration calculations for the proprioceptive and visual signals. First, we assume that subjects were asked to push completely the virtual button co-located with the Phantom Omni, with a displacement (d) of $15cm$, moving the real index finger by $0.15/\lambda m$, where λ is the C/D ratio so we can define the proprioceptive displacement as $d_{proprioceptive}$. We can also define $s_{proprioceptive}$ as the proprioceptive *Stiffness* felt in the same finger. Now, we can measure the force applied by the button to the fingertip (equation 7.2). $d_{proprioceptive}$ could differ from the visual displacement (d_{vision}) when λ is manipulated but the multisensory signals are integrated with ($\alpha + \beta = 1$) as the combination for proprioceptive and visual weights. Thus, the perceived displacement is a combination of the two cues (Equation 7.3). Perceived *Stiffness* can also be defined in terms of $d_{proprioceptive}$ (Equation 7.4, 7.5, 7.6), and substituting the known terms, we get the equation for the perceived stiffness (Equation 7.7).

$$F = d_{proprioceptive} * s_{proprioceptive} \quad (7.2)$$

$$d_{perceived} = (\alpha * d_{proprioceptive}) + (\beta * d_{vision}) \quad (7.3)$$

$$s_{perceived} = \frac{F}{d_{perceived}} = \frac{d_{proprioceptive} * s_{proprioceptive}}{(\alpha * d_{proprioceptive}) + (\beta * d_{vision})} \quad (7.4)$$

$$s_{perceived} = \frac{(\frac{0.15}{\lambda}) * s_{proprioceptive}}{(\alpha * (\frac{0.15}{\lambda})) + (\beta * 0.15)} \quad (7.5)$$

$$s_{perceived} = \frac{s_{proprioceptive}}{\alpha + \beta \lambda} \quad (7.6)$$

7.3.4. Results

Equation 5 is fitted with the proprioceptive stiffness data from the experiment to get the integration weights. Figure 7.4 shows the perceived stiffness according to the experimental data and the red fitting curve of the integration model ($R=0.959462$). As a result, we got the predictive model equation that enables the calculation of perceived stiffness in VR buttons for a given C/D ratio (Equation 6). Besides, based on the psychometric results from experiment 1, we can use the identified range of C/D ratios (i.e., $\lambda = (0.905 - 1.155)$), and use the equation to get a range of perceptually congruent stiffness values going from $0.524N/m$ to $0.568N/m$, which are valid stiffness values for finger forces[Geo14].

$$Stiffness(N/m) = s_{perceived} = \frac{0.54}{1.32 - (0.32 * \lambda)}, \quad (7.7)$$

The unit of stiffness is Newtons per meter (N/m), it delivers the counterforce provided by the button in Newtons per meter, and λ is the used C/D ratio.

7.4. Experiment 3: Enriching Stiffness with Tactile and Proprioceptive Feedback

The third experiment builds on the results from experiments 1 and 2, enhancing a virtual button with plausible stiffness following multisensory integration and psychophysics principles. When pressing a real button, visual, tactile, and proprioceptive feedback are experienced simultaneously. We want to cover this gap by providing tactile and proprioceptive feedback to convey the missing sensations. Table 1 shows the sensations we want to convey and the feedback we are providing.

Feedback	Stimuli	Conveys	ID
Visual (Pseudo-Haptics)	Hand Redirection	Stiffness	S
Tactile	Tap	Contact	C
Proprioceptive	TES	Contact	C
Tactile	Vibration	Activation	A

2

Table 7.1.: Multisensory feedback.

The sensation of stiffness (S) is provided by C/D ratio manipulation using the results from experiments 1 and 2. These experiments delivered a solid apparatus to quantify the perceived stiffness within valid perceptual limits. Contact (C) sensation is provided by tactile and proprioceptive signals triggered whenever the subject fingertip is touching a virtual button. Finally, the sensation of activation (A) is provided with a piezo element, vibrating according to the inner mechanisms of a button to deliver dynamic cues while pressing/displacing and finally actuated/activated.

7.4.1. Participants

8 Participants (age: $M=29.3$, $SD=4.3$, four female, two left-handed) participated in this experiment, mainly students and employees from our computer science department. According to the pre-questionnaire, none of the participants reported any visual impairments that could affect our experiment's results.

7.4.2. Apparatus

The apparatus for this experiment builds upon the first experiment. We incorporated a wearable and wireless haptic device, enabling tactile feedback (i.e., tapping feedback, vibrotactile feedback by piezo actuation), and proprioceptive feedback by electric stimulation (i.e., TES).

The device provides redundant but congruent signals to enrich our VR setup and simulate the whole range of sensations offered by a real button. It makes part of a framework for haptic experiments,

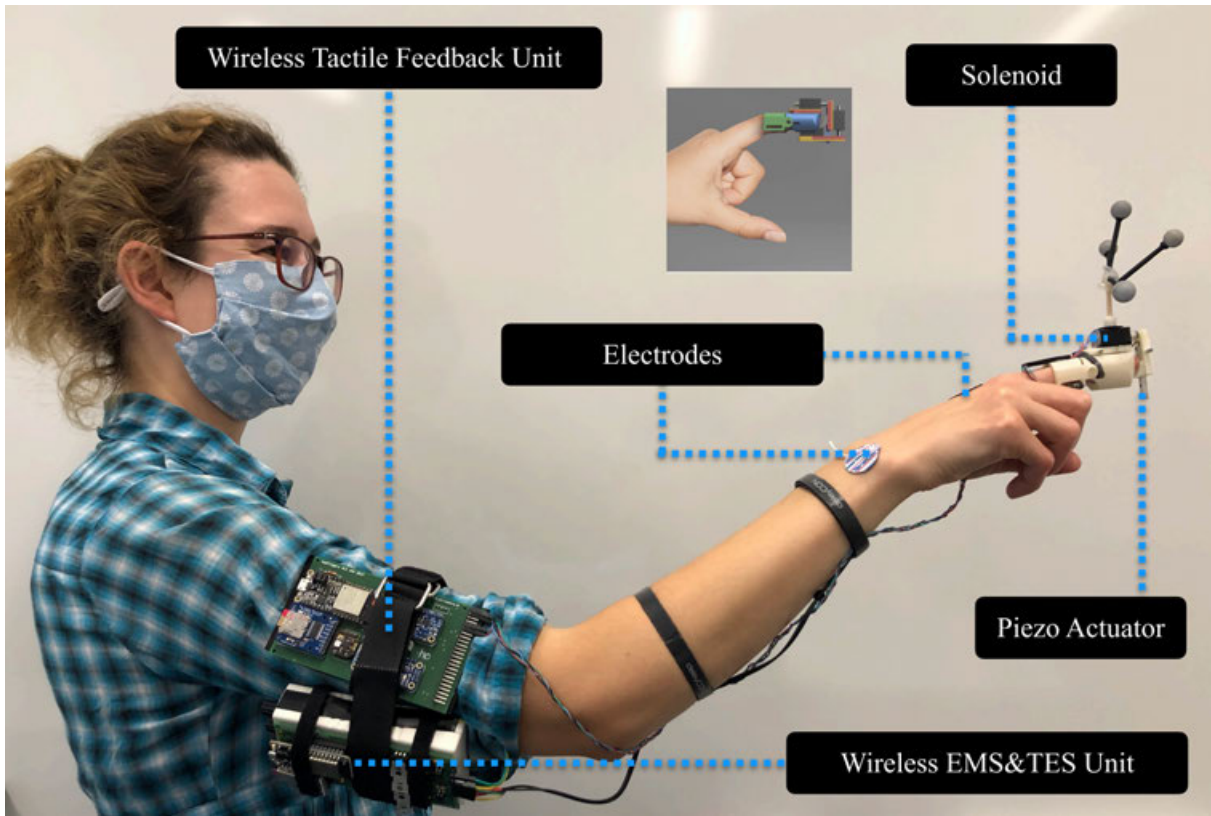


Figure 7.5.: User wearing the device with annotations for the actuation elements.

providing a Unity plugin to wirelessly control solenoids, piezo elements, audio-based haptic transducers, EMS/TES electrodes. Specific details of the device can be found in the Appendix (see Section A.3).

3D Button Design

In traditional 3DUIs, a button as an input element can be activated by a collision between simple colliders assigned with the button and the user's hand. Finally, it provides vibrotactile cues, for instance, delivered via a controller. However, its simulation is much more complex as the haptic feedback rendering relies on force-displacement curves and velocity profiles [KL13; LKO18]. In this way, is it possible to provide timely sensations for the activation [KLO18], the press-release movements, as well as vibration and velocity-dependent characteristics [Lia+20]. The same approach has been used in VEs, simulating buttons providing pseudo-forces and tactile feedback [KKL16].

In mid-air interactions, it is possible to represent realistic buttons by always projecting the virtual fingertip onto the button surface to avoid incongruent visual interpenetrations, following the 'God Object' constraint [ZS95]. Regarding the neuromechanics of a button, it is possible to predict the user's performance based on motor-control models and mechanical design parameters, minimizing the error between the expected and perceived button activations [OKL18]. Also, traditional input methods with 3D buttons (i.e., keyboards) in VEs, with matching VR representations and providing passive haptic feedback, have proven to deliver intuitive interactions and improve user performance [Sch+19].

7.4.3. Approach

In a common VE scenario, whenever a user approaches and collides with virtual objects, the visual feedback is correct but only a fraction of the haptic sensations are rendered. Still, the fingertip tactile sensation of the collision and also the proprioceptive sensation of the movement being interrupted are lost, producing large sensory conflicts. Such conflicts are crucial for human-computer interaction in VEs as they can induce breaks of presence, reduce task performance, require higher cognitive efforts during the multisensory integration process, and finally degrades the overall user experience in the VE. The goal of our research is to provide a holistic touch sensation by providing tactile and proprioceptive feedback together with the visual illusion of touch. We provide signals to improve the stiffness perception as well as tactile (finger) and proprioceptive (hand tendons) cues related to contact and activation of a 3D button.

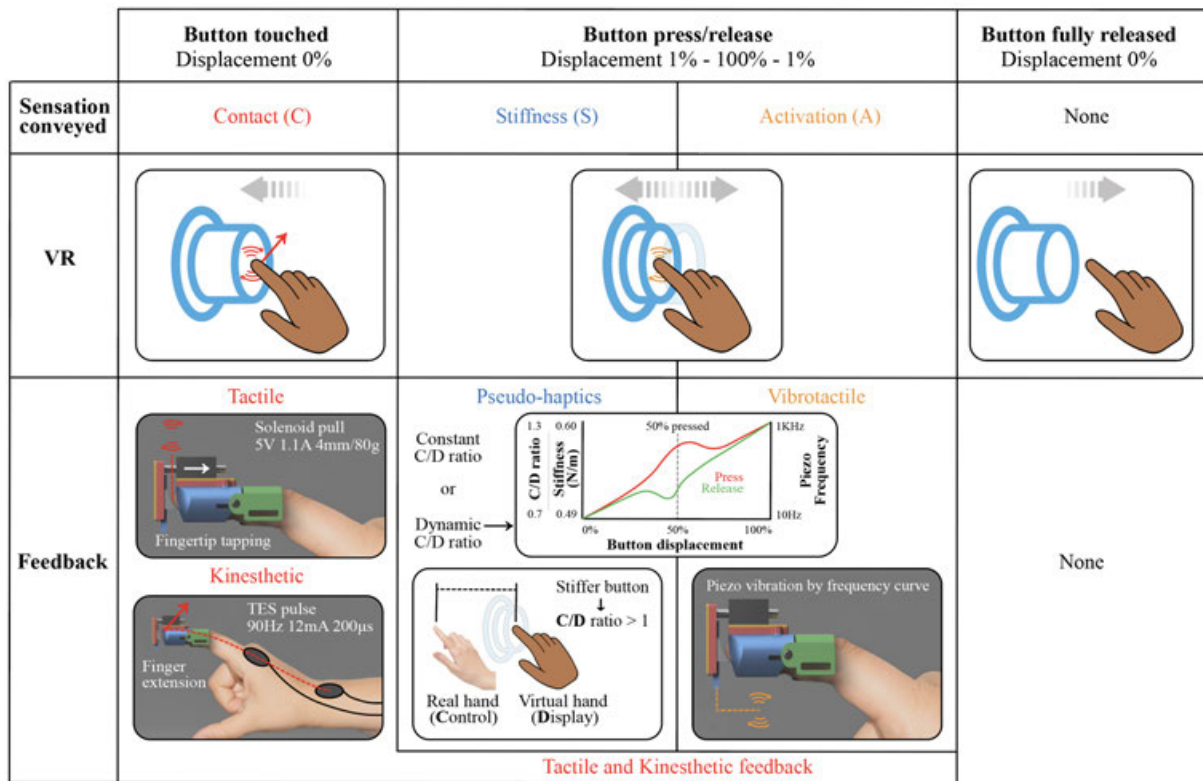


Figure 7.6.: Modules and corresponding technology that convey the different sensations.

Figure 7.5 describe the modules and corresponding technology that convey the different sensations step-by-step as follows: Starting with the VR user approaching a virtual button with her index finger causing our system to provide tactile (tapping) and kinesthetic (extension) feedback to convey the illusion of contact. While pushing the button, the pseudo-haptics induce a sensation of stiffness, and the changing frequency of vibrotactile feedback indicates the (press/release) activation. Finally, after the button is released all feedback is disabled.

The activation sensation is rendered by the use of frequency/displacement curves [LKO18; Lia+20; KKL16]. The curve can be easily adapted to define different buttons' behaviors for press/release movements. To this end, the curves define dynamic changes of frequency according to the button displacement.

Additionally, we could use the curves to simultaneously change C/D ratios for pseudo-haptics to render variable stiffness.

We use an approach to simulate impact decomposing the resulting sensations in tactile and proprioceptive feedback, as explored before [LIB15]. However, we use TES [Miy+15] because it is more compatible with the sensorimotor frameworks that make VR illusions possible [GL17]. In our case, the sense of agency (i.e., volition) helps the user to internalize the VR experience as real, whenever the user is the initiator of the action (i.e., efference; ballistic-correction arm movement to press the button) and is artificially provided with afferent feedback from the Golgi tendon on the *extensor indicis* muscle. Besides, TES is beneficial to convey contact sensations while avoiding unwanted small movements (i.e., Heisenberg effect [AA13]) during 3D interaction. Such movements can deteriorate the quality of the experience because an abrupt hand movement would be noticed immediately as the C/D ratio manipulation drives the user's stiffness perception.

7.4.4. Latency Compensation

Non-simultaneous multimodal feedback represents problems for motor control, producing temporal asynchrony and inadequate cue integration. For this reason, synchronization of the feedback is essential to deliver a compelling and plausible experience; time gaps between feedback signals could require time prediction of triggering events to compensate and finally convey all the multimodal sensations in unison for the user.

The Minimum Jerk (MJ) movement model [FH85], predicts the ballistic phase in arm movements, assuming that the primary goal of motor coordination is to produce the smoothest possible movement of the hand in extracorporal space. The model has been tested in VEs with teleoperation purposes, showing that the model can deal with delays up to 100ms [BSC07]. The model can also be used locally in VEs to compensate for delays and latency, with an average error of 290ms with hand redirection and 30 ms with normal hand reach [GAF19]. A user could reliably detect the asynchrony if haptic feedback were presented less than 50ms after visual stimuli [DM19]. Prior solutions involved the use of larger bounding volumes (i.e., 25%) for collision detection, delivering early feedback (i.e., 30 ms) to compensate for the EMS latency Lopes2015.

Regarding our use case, relevant research provides some guidelines. Physical contact with a button occurs in about 100 ms [Kim+13]; however, it is too brief for real-time corrections [Gom08]. TES and EMS are prone to latencies involving the propagation of the motor signals in limbs; for this reason, using multimodal combinations of TES and electrotactile feedback requires an early activation of TES, starting 25 ms before the tactile signal to guarantee the perception of simultaneity [Miy+15]. We implemented the MJ model to reduce the latency of our TES unit using data from our real-time velocity profile module. Thus, the TES stimulation is not triggered by the button collider but by the prediction algorithm based on the velocity profile of the ballistic approach and the MJ output. As a result, we can calibrate the model at the beginning of the experiment session and reduce the latency to be compatible with the perceptual limits described above, achieving compelling sensations of multimodal feedback with our approach.

7.4.5. Procedure

Sensation Conveyed	Condition ID
Stiffness	S
Stiffness + Activation	SA
Stiffness + Contact	SC
Stiffness + Contact + Activation	SCA

Table 7.2.: Conditions and sensations conveyed.

Table 7.2 shows the conditions of the experiment. We want to test how the additions of modalities affect the perceptual limits and user acceptance.

In the beginning, the TES analog stimulator is calibrated for every participant to guarantee that every subject is comfortable with the current levels applied on the electrodes. TES calibration was performed per subject and lasted 5 minutes; the *extensor indicis* muscle was contracted ten times to guarantee a reliable and constant level of stimulus. Electrodes were located along with the hand and wrist, following the oblong structure of the muscles. The anode was located on the tendon and the cathode on the muscle spindle. The stimulus was intended to produce a sensation of force traveling in the direction opposite the side to which the electrode was affixed so that the subject could feel a subtle index-finger extension. During the calibration process, participants practiced the reaching movement to press the virtual button to guarantee homogeneous velocities and reliable prediction of the collision time to compensate for latencies.

We conducted a two-alternatives forced-choice(2AFC) experiment again; the participant was asked to choose the stiffer button using the feet pedals after exploring a standard and comparison buttons for up to 20 seconds. Both buttons provided the sensations dictated by the current condition. The C/D ratio was manipulated, so one of the buttons presented the standard stimulus (i.e., $C/D = 1.0$). The other one gave the comparison with one of the following values: (0.7, 0.8, 0.9, 1.1, 1.2, 1.3). The presentation order of the buttons and the C/D ratios were randomized per trial.

We collected subjective data from questionnaires on user acceptance using a 7-point Likert scale (1, disagree, 7 agree) for all the questions. We measured the *sensations conveyed*:

- **Q1** I felt stiffness in the buttons.
- **Q2** felt when I touched the buttons.
- **Q3** felt I was pressing the buttons.
- **Q4** had the feeling of manipulating real buttons.

And *limb ownership and realism*:

- **Q5** The virtual hands appeared in the same location as my hands.
- **Q6** The virtual hands seemed to belong to my body.
- **Q7** The buttons that I pressed were the same buttons that I saw.
- **Q8** The buttons that I saw were in the same location as the buttons I felt.

7.4.6. Results

In this section, we will report the results for the experiment. We used four conditions (see table 2), six C/D ratios, and six repetitions to get 144 data samples per participant and 1152 data samples for the whole experiment.

First, we fitted again the data regarding C/D ratios and the probabilities of perceiving stiffer buttons for the different conditions (see Figure 7.7, condition S is presented in Figure 7.3). Condition SA presented a PSE of 1.0238, a JND of 0.1186, and 85.05% correct choices for the stiffer button. Condition SC gave a PSE of 1.0624, a JND of 0.1032, and 85.42% correct choices for the stiffer button. Finally, the condition SCA presented a PSE of 1.0155, a JND of 0.0716, and 93.75% of correct decisions for the stiffer button. The condition S, providing only pseudo-haptics for the stiffness condition, presented 70.49% correct choices for the stiffer button. Knowledge about the range of C/D ratios, which can be applied without users noticing the discrepancy, is essential to provide a plausible "God Object" constraint for 3DUI elements. The C/D ratios found for the conditions SA, SC, and SCA are in line with prior findings on hand-redirection gains in the depth axis [ZK19a], which found that a range of 0.88 - 1.07 (-6.18% - 13.75%) can go unnoticed.

Second, we processed the data from the subjective questionnaires (see Tables 7.3 and 7.4). Main differences were tested with an ordinal logistic regression, and pair-wise comparisons were performed with the Tukey test.

The answers for the questions evaluating the sensations conveyed show significantly higher scores for the condition SCA over S, with overall higher scores for user acceptance on all sensations. Condition SC presented high scores for the sensation of contact, and the condition SA showed high scores for the sensation of activation compared with condition S only. The scores for the subjective acceptance of limb ownership and realism were mainly high for all conditions, with significant differences related to visuo-haptic mismatches in the condition S compared to SC, SA, and SCA.

7.5. Discussion and Conclusion

With this work, we wanted to go beyond providing abstract vibrotactile feedback in such a way that haptics could realistically convey sensations. The conducted experiments examine the effects of conveying sensations for contact, activation, and stiffness sensations while pressing virtual buttons building upon recent research [Pez+19; Sam+19]. The choice of sensations unifies premises in related research, looking for rich 3DUI elements supporting useful affordances. Hence, the user knows what can be done, whether the interaction element is working, and when the action/task is complete. Also, an essential requirement, the objective evaluation of how haptic technology produces motor and sensory signals in the human pathways between the proprioception/tactile mechanoreceptors and the brain. And also, whether these signals are produced in a timely manner, so all possible latencies are compensated to guarantee a successful multisensory integration. Our proposed technology and multimodal feedback could be used in VR and AR environments enabling the user with instinctual interactions. As we mentioned, we aim to supply interactive elements with the right affordances to be quickly learned and used with different interaction models. For example, the user could interact with virtual hand representations operating controllers or

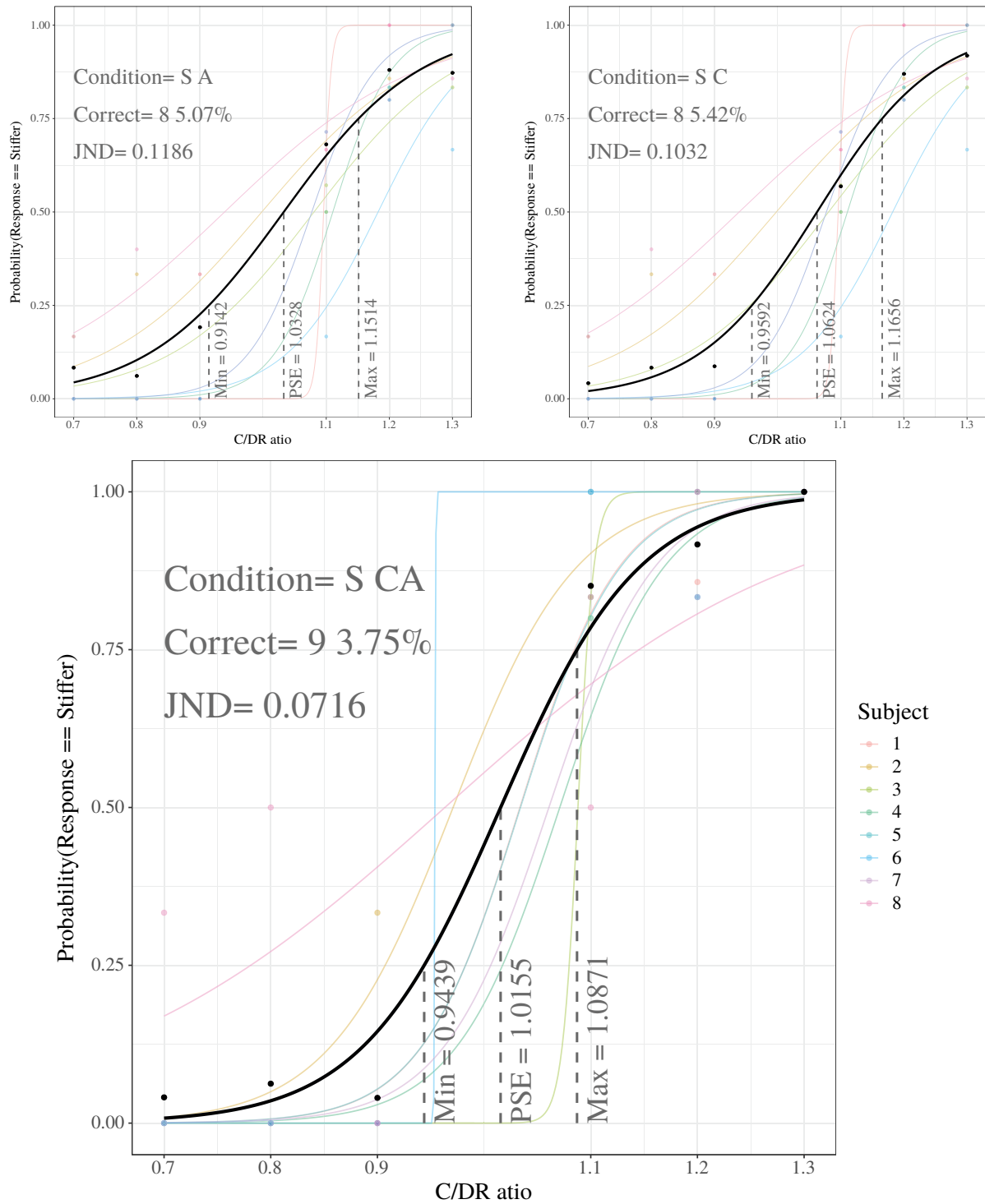


Figure 7.7.: C/D ratio vs stiffer responses for the tested conditions.

hand-free natural interaction.

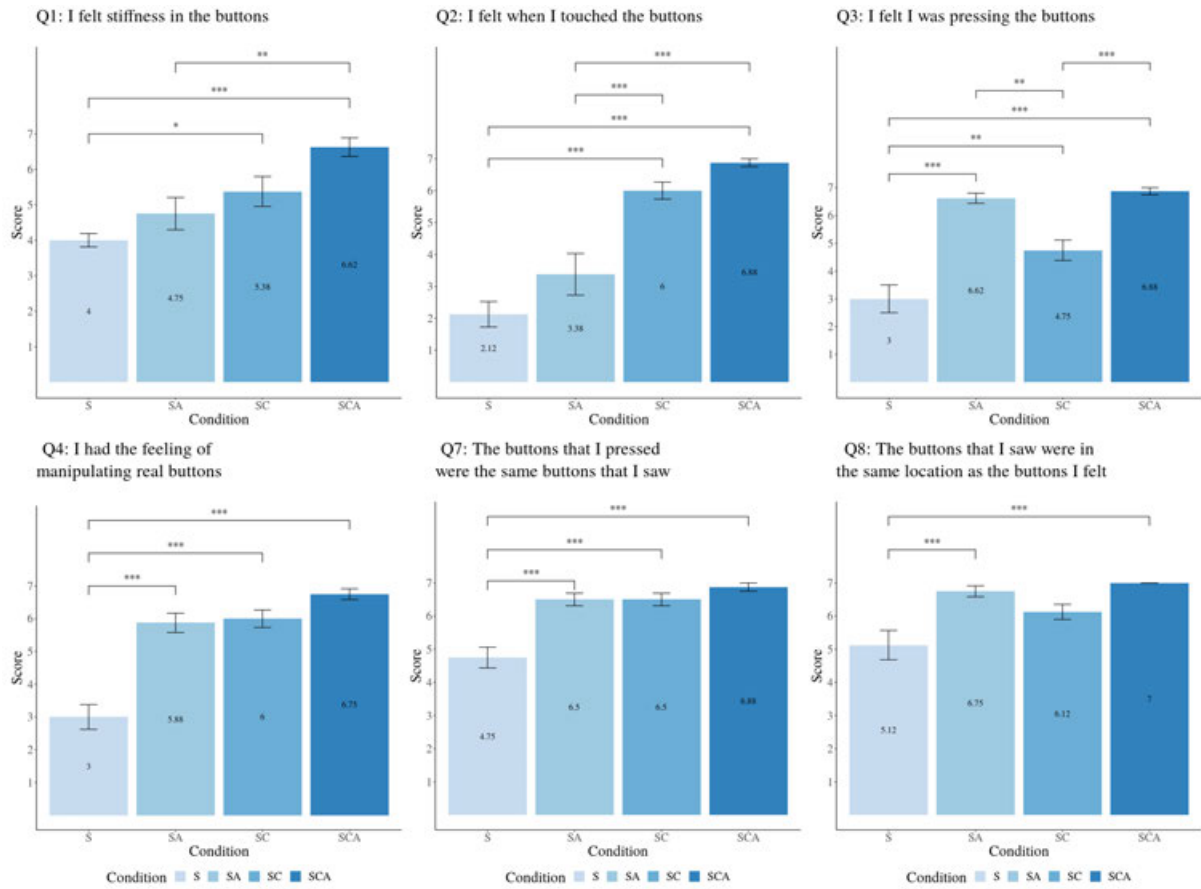


Figure 7.8.: Results for the subjective questionnaires.

These models could also be combined with a *gaze and commit* technique using voice commands for confirmations, enabling a seamless and performant interaction environment. Besides, we found that the PSE, giving the point where a physical stiffness is estimated of equal size as a virtual counterpart, was closer to the identity when other sensations were added. The JND decreased, increasing the sensitivity to stiffness changes when sensations of contact and activation were added. These findings evidence the advantages of multimodal feedback and dispense guidelines for 3DUI elements involving designs with multimodal feedback. We believe that the combination of feedback tackles the problem of under/over-estimation while pressing a virtual button, in comparison with prior research, which reported depth perception problems [FH14]. This was enabled by the aggregation of the sensation of button hysteresis in the activation sensation, as we implemented the mechanism to render curves displacement/force, replacing the force with dynamic changes of frequency and amplitude on the piezo element used in the condition for activation (A). Also, the subjective results show significant scores in favor of this approach.

We introduced different techniques to improve the haptic realism of simple 3D user interface elements such as a 3D button with wearable technology that combines different types of haptic feedback to provide tapping and vibrotactile feedback, and a method to simulate the stiffness by manipulating the C/D ratio. We reported the results of 3 studies combining pseudo-haptics, tactile, and proprioceptive feedback for 3DUIs, providing guidelines to properly convey contact, stiffness, and activation in 3DUIs based on user

Sensations Conveyed

Q1 : I felt stiffness in the buttons

Condition	N	Mean	SD	SE	CI
S	8	4.00	0.54	0.19	[3.62, 4.38]
SA	8	4.75	1.28	0.45	[3.84, 5.66]
SC	8	5.38	1.19	0.42	[4.54, 6.22]
SCA	8	6.62	0.74	0.26	[6.10, 7.15]
Main Effect					
<i>LR Chi-Square</i>			Df	<i>P-Value</i>	<i>p<.05</i>
23.511			3	0.00003	***
Post-hoc Test (Tukey)					
Pair	Diff	Lower	Upper	P Adj	<i>p<.05</i>
SA-S	0.750	-0.5967	2.0967	0.4391	*
SC-S	1.375	0.0283	2.7217	0.0440	***
SCA-S	2.625	1.2783	3.9717	0.0001	***
SC-SA	0.625	-0.7217	1.9717	0.5908	
SCA-SA	1.875	0.5283	3.2217	0.0038	**
SCA-SC	1.250	-0.0967	2.5967	0.0762	

Q2 : I felt when I touched the buttons

Condition	N	Mean	SD	SE	CI
S	8	2.12	1.13	0.39	[1.33, 2.92]
SA	8	3.38	1.85	0.65	[2.07, 4.68]
SC	8	6.00	0.76	0.27	[5.47, 6.54]
SCA	8	6.88	0.35	0.13	[6.63, 7.13]
Main Effect					
<i>LR Chi-Square</i>			Df	<i>P-Value</i>	<i>p<.05</i>
41.658			3	0.000000	***
Post-hoc Test (Tukey)					
Pair	Diff	Lower	Upper	P Adj	<i>p<.05</i>
SA-S	1.250	-0.3325	2.8325	0.1604	
SC-S	3.875	2.2925	5.4575	0.0000	***
SCA-S	4.750	3.1675	6.3325	0.0000	***
SC-SA	2.625	1.0425	4.2075	0.0006	***
SCA-SA	3.500	1.9175	5.0825	0.0000	***
SCA-SC	0.875	-0.7075	2.4575	0.4454	

Q3 : I felt I was pressing the buttons

Condition	N	Mean	SD	SE	CI
S	8	3.00	1.41	0.50	[2.00, 4.00]
SA	8	6.62	0.52	0.18	[6.26, 6.99]
SC	8	4.75	1.04	0.37	[4.02, 5.48]
SCA	8	6.88	0.35	0.13	[6.63, 7.13]
Main Effect					
<i>LR Chi-Square</i>			Df	<i>P-Value</i>	<i>p<.05</i>
43.122			3	0.000000	***
Post-hoc Test (Tukey)					
Pair	Diff	Lower	Upper	P Adj	<i>p<.05</i>
SA-S	3.625	2.3545	4.8955	0.0000	***
SC-S	1.750	0.4795	3.0205	0.0042	**
SCA-S	3.875	2.6045	5.1455	0.0000	***
SC-SA	-1.875	-3.1455	-0.6045	0.0021	**
SCA-SA	0.250	-1.0205	1.5205	0.9497	
SCA-SC	2.125	0.8545	3.3955	0.0005	***

Q4 : I had the feeling of manipulating real buttons

Condition	N	Mean	SD	SE	CI
S	8	3.00	1.07	0.38	[2.24, 3.76]
SA	8	5.88	0.84	0.30	[5.29, 6.46]
SC	8	6.00	0.76	0.27	[5.47, 6.54]
SCA	8	6.75	0.46	0.16	[6.42, 7.08]
Main Effect					
<i>LR Chi-Square</i>			Df	<i>P-Value</i>	<i>p<.05</i>
37.49			3	0.000000	***
Post-hoc Test (Tukey)					
Pair	Diff	Lower	Upper	P Adj	<i>p<.05</i>
SA-S	2.875	1.7691	3.9809	0.0000	***
SC-S	3.000	1.8941	4.1059	0.0000	***
SCA-S	3.750	2.6441	4.8559	0.0000	***
SC-SA	0.125	-0.9809	1.2309	0.9896	
SCA-SA	0.875	-0.2309	1.9809	0.1593	
SCA-SC	0.750	-0.3559	1.8559	0.2714	

Table 7.3.: Descriptive statistics and omnibus/post-hoc tests results for the subjective questionnaires on *Sensation Conveyed*. The condition acronyms stand the sensations; *Stiffness*, *Contact*, and *Activation* (Significance codes: 0 *** 0.001 ** 0.01 * 0.05).

acceptance and performance metrics. Besides, we used a multisensory integration model to facilitate an equation to predict perceived stiffness given an specific C/D ratio.

Limb Ownership and Realism

Q5 : The virtual hands appeared
in the same location as my hands

Condition	N	Mean	SD	SE	CI
S	8	6.50	0.54	0.19	[6.12, 6.88]
SA	8	6.62	0.74	0.26	[6.10, 7.15]
SC	8	6.25	0.46	0.16	[5.92, 6.58]
SCA	8	6.25	0.71	0.25	[5.80, 6.75]
Main Effect					
<i>LR Chi-Square</i>		Df	<i>P-Value</i>	<i>p<.05</i>	
3.3198		3	0.3449		

Q6 : The virtual hands seemed
to belong to my body

Condition	N	Mean	SD	SE	CI
S	8	6.12	1.13	0.40	[5.33, 6.92]
SA	8	6.88	0.35	0.13	[6.63, 7.13]
SC	8	6.38	0.74	0.26	[5.85, 6.90]
SCA	8	6.62	0.52	0.18	[6.26, 6.99]
Main Effect					
<i>LR Chi-Square</i>		Df	<i>P-Value</i>	<i>p<.05</i>	
4.2693		3	0.2338		

Q7 : The buttons that I pressed were
the same buttons that I saw

Condition	N	Mean	SD	SE	CI
S	8	4.75	0.89	0.31	[4.12, 5.38]
SA	8	6.50	0.54	0.19	[6.12, 6.88]
SC	8	6.50	0.54	0.19	[6.12, 6.88]
SCA	8	6.88	0.35	0.13	[6.63, 7.13]
Main Effect					
LR Chi-Square			Df	P-Value	p<.05
33.034			3	0.000000	***
Post-hoc Test (Tukey)					
Pair	Diff	Lower	Upper	P Adj	p<.05
SA-S	1.750	0.9190	2.5810	0.0000	***
SC-S	1.750	0.9190	2.5810	0.0000	***
SCA-S	2.125	1.2940	2.9551	0.0000	***
SC-SA	0.000	-0.8310	0.8310	1.0000	
SCA-SA	0.375	-0.4560	1.2069	0.6123	
SCA-SC	0.375	-0.4560	1.2060	0.6123	

Q8 : The buttons that I saw were
in the same location as the buttons I felt

Condition	N	Mean	SD	SE	CI
S	8	5.12	1.25	0.44	[4.24, 6.00]
SA	8	6.75	0.46	0.16	[6.42, 7.08]
SC	8	6.12	0.64	0.23	[5.67, 6.58]
SCA	8	7.00	0.00	0.00	[7.00, 7.00]
Main Effect					
LR Chi-Square			Df	P-Value	p<.05
25.495			3	0.000012	***
Post-hoc Test (Tukey)					
Pair	Diff	Lower	Upper	P Adj	p<.05
SA-S	1.625	0.6175	2.6325	0.0008	***
SC-S	1.000	-0.0075	2.0075	0.0523	
SCA-S	1.875	0.8675	2.8825	0.0001	
SC-SA	-0.625	-1.6325	0.3825	0.3457	
SCA-SA	0.250	-0.7575	1.2575	0.9047	
SCA-SC	0.875	-0.1325	1.8825	0.1062	

Table 7.4.: Descriptive statistics and omnibus/post-hoc tests results for the subjective questionnaires on *Limb Ownership and Realism*. The condition acronyms stand the sensations; *Stiffness*, *Contact*, and *Activation* (Significance codes: 0 *** 0.001 ** 0.01 * 0.05).

We provided objective and subjective evidence on how combinations of proprioceptive, pseudo, and tactile feedback improve the conveyed sensations for contact, stiffness, and activation of 3D buttons. Providing these sensations by using congruent feedback as redundant multisensory information enabled our approach to create a plausible illusion of touch, delivering a holistic feeling when interacting with 3D buttons. As a result, the use of multimodal feedback enhanced the overall perception of stiffness while operating 3DUI elements in VEs, while maintaining good levels for the sense of body ownership and presence, as well as positive subjective feedback for user acceptance.


Part IV

Support for 3D Guidance

8

Chapter 8

Gaze Guidance

This chapter is related to the scenario  (see Section 1.2).

8.1. Motivation

Current HMDs provide large binocular FOVs for natural interaction in VEs. However, the selection of objects located in the periphery and outside the FOV requires visual search by head rotations, which can reduce the performance of interaction in VR. Providing gaze guidance in VEs could help the content creators to increase the control over where users are looking, which could improve the user experience and efficiency in general [MK10]. As an alternative to traditional solutions, vibrotactile technology featuring wireless and wearable devices represents a useful feature, and has potential to increase the performance of the user in navigation and selection tasks. Vibrotactile feedback can provide spatial cues (complementary to the traditional alternatives based mainly on visual and auditory modalities) when target objects are located outside the user's field of view, and thereby improving common 3D interaction tasks related to pointing, selection, and grasping of virtual objects. Regarding the use of HMDs with arrays of vibrotactile actuators, the density of the array is proportional to the user performance in detecting directional cues [JO+16]. Moreover, physical activities can be guided by the use of devices providing tactile feedback. Such tactile instructions have higher recognition accuracy and faster user response in comparison with corresponding instructions provided with auditory feedback [Spe+09]. Previous research also found significant benefits of HMDs with vibrotactile feedback in combination with reduced peripheral lighting for spatial and social presence [Ric+19].

We found inspiration and ideas to build a wireless vibrotactile display which could be located properly on the back side of the head (and also attachable to existing HMDs) to provide useful cues in order to improve the performance of users while locating and selecting targets in VEs. We believe that there is still room to explore more on the creation of versatile and affordable devices to provide vibrotactile feedback for simple spatial interaction tasks while using HMDs. We found the motivation to study how other user cognitive resources could be affected during a selection task when vibrotactile feedback is provided. This chapter explores the use of a pair of self-made wireless and wearable devices, which once attached to both hemispheres of the user's head provide assistive vibrotactile cues for

guidance in order to reduce the time used to turn and locate a target object. Although the proposed vibrotactile solution does not interfere with stimuli related to the visual and auditory modalities, such an assistive technology might consume additional cognitive resources, which may be required by other tasks executed by the user in the virtual environment. We present an experiment based on a dual-tasking method to analyze cognitive demands and performance metrics during a set of selection tasks followed by a working memory task.

8.2. User Guidance in 3D Environments

One of the challenges for VE users is the navigation of complex and unknown 3D worlds, and the selection of objects in unknown positions. In order to facilitate those 3D interaction tasks, computer-supported guidance can be provided in the shape of visual cues and in some cases auditory cues which help users to find not-visible locations or objects of interest. Common guidance capabilities are implemented as visual constraints and warning sounds provided when the user is not following the navigation path correctly. Usually, visual cues for guidance represent invasive content which can occlude the visual representation of the virtual environment and in the same way, auditory cues provided for navigation guidance require sound effects or speech synthesis which are presented to the user in addition to the auditory stimuli produced by the interaction of the user with the environment. In the other hand, vibrotactile feedback can be provided as assistance cues, presenting information to locate places or objects without interfering with the interaction flow as the tactile modality is not used actively in common VEs.

8.2.1. Vibrotactile Feedback

Most traditional VEs are focused mainly on audio-visual feedback, which often limits the user sense of body ownership and embodiment in virtual environments. However, combining HMDs and tracking functionalities with tactile feedback devices, enables the creation of interactive experiences providing embodied visual, auditory and tactile feedback in response to user actions. Additionally, current technology provides low-energy, wearable and wireless components to create ergonomic and low-latency vibrotactile devices, reliable enough to provide additional cues during the execution of interaction tasks and even able to encode tactile patterns representing distances to target objects [Ari+16].

8.3. Cognitive Resources

3D interaction involve simultaneous spatial tasks competing for the limited cognitive resources of users, related to theoretical models which usually distinguish between verbal and spatial resources of cognition and working memory. Although, interpretation of vibrotactile cues for guidance might be a subconscious process, it could consume cognitive resources in addition to other manipulation or locomotion tasks executed simultaneously. Some research explored the effects of learning while using a vibrotactile handheld device for navigation assistance. The results showed that the navigation condition using the device performed better at rehearsal [Gac+16]. Additional research on virtual environments navigation showed that visual cues were significantly more efficient than a group without signals and the cognitive load



Figure 8.1.: 3DUI for the gaze-guidance experiment: **(left)** Unselected target. **center)** Selected target turned into green color after the participants kept the line-of-sight on the cube for 2 seconds. **(right)** Message panel with instructions for letter sequence input.

can be significantly reduced [Nel+14], and cognitive tasks which activate working memory and spatial attention can consume resources needed to accomplish physical tasks [Nad+10]. Furthermore, spatial attention and short term memory are shared and limited neural resources that can be affected when a task involving the tactile modality is executed [KAM14]. We analyze the mutual influence of tactile cues for 3D selection assistance and a memory task. We conducted an experiment to show how a selection task assisted by vibrotactile feedback affects the verbal working memory demands.

8.4. Experiment

In this section we describe the experiment in which we analyzed how a selection task assisted by different types of vibrotactile feedback could affect the verbal working memory demands.

8.4.1. Participants

12 subjects (2 female, ages 23 – 41, $M = 28.4$) participated in the experiment. The participants were students or members of the local department of computer science, who obtained class credit for their participation. All of our participants had normal or corrected-to-normal vision. Four participants wore glasses and two participants wore contact lenses. One of our participant reported a disorder of equilibrium. Two of our participants reported eye related disorders, Dyschromatopsia and Color-blindness respectively. Nine participants had participated in an experiment involving HMDs before. The total time per participant, including pre-questionnaire, calibration, instructions, experiment, breaks, post-questionnaire, and briefing was 1 hour. Participants wore the HMD for approximately 40 minutes and they were allowed to take two breaks between the conditions.

8.4.2. Materials

We performed the experiment in a $4m \times 2m$ laboratory room. Subjects wore a Oculus Rift CV1, which provides a resolution of 1080x1200 pixels per eye with a refresh rate of 90Hz and an approximate 110° diagonal field of view. We used an Intel computer with 3.4GHz Core i7 processor, 16GB of main memory and a Nvidia GeForce 980Ti graphics card. The stimuli were rendered with the Unity 3D engine.

We built the vibrotactile devices in the shape of two small wearable boxes completely autonomous,

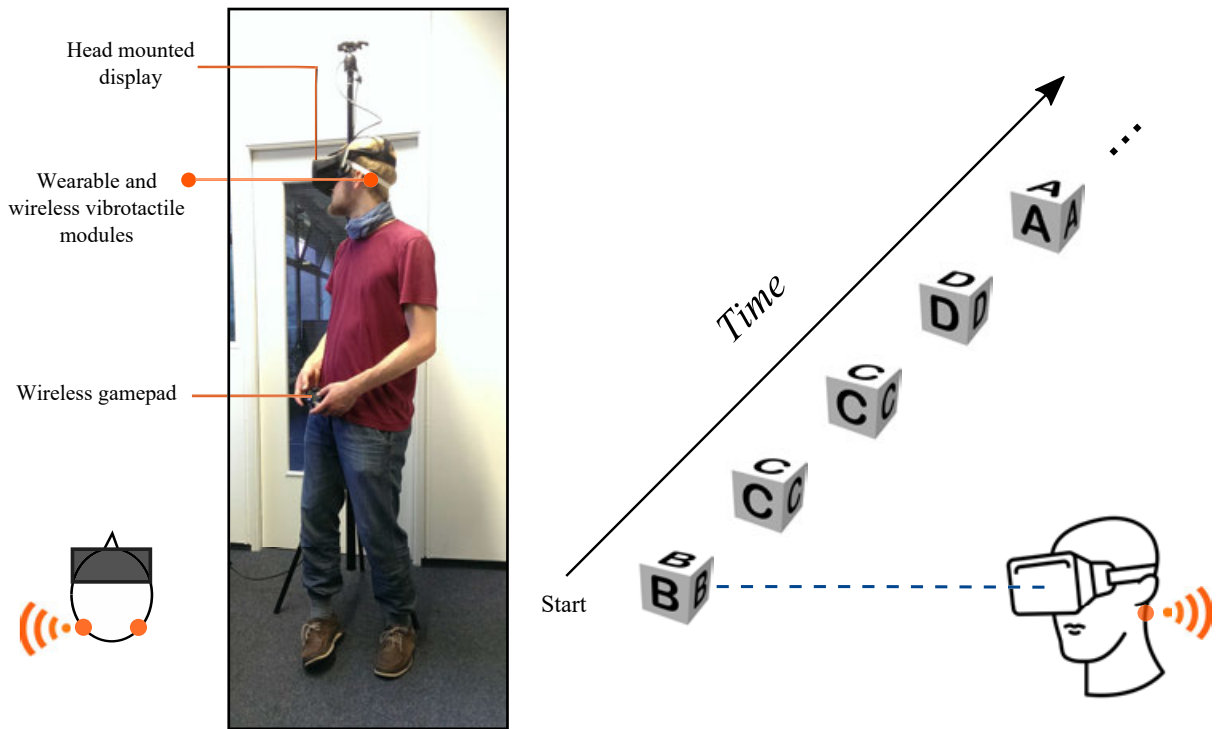


Figure 8.2.: Left: Experiment setup. Right: Sketch of the task stimuli.

using a wireless enabled microcontroller. Specific details of the device can be found in the Appendix (see Section A.7). The two modules were attached on the back side of the head, located on the left and right sides of occipital lower zone (see Figure 8.2), using rubber bands (ranging from 35cm to 55cm) covering different head sizes of the subjects. Location on the occipital region and over the temples is appropriate according to [MK10]. The vibrotactile feedback was always provided at 100Hz., which is correct in terms of the comfortable range (32Hz.-150Hz.) [MK10]. The device latency is $28\text{ms} \pm 4.166$, was measured according to the technique used in [Ari+16], and the end-to-end latency makes a total of 46ms, which is still compatible with common tolerance between sensations corresponding to visual and tactile modalities [Shi+10]. The visual stimulus consisted of a simple VE consisting of a grass landscape with a blue sky and a few clouds. All the task instructions were presented with a 2D message board on the HMD. Participants performed the selection inputs for the task via button presses on a XBox wireless gamepad (see Figure 8.2, left). The pair of vibrotactile modules are connected via Bluetooth to the computer, where two UDP servers decouple the connection management between the Unity application and the wearable modules. In this way, the Unity application is mainly focused on the HMD rendering and subject interaction with the XBox controller. There was no measurable difference in latency between one or two modules because of the buffering settings in our embedded code and our multi-threaded approach on the client side. During the experiment, no communication between experimenter and subject was performed, so the participants could be focused on the task.

8.4.3. Methods

To analyze the cognitive resource demands during a selection task, we made use of a within-subjects experimental design in which the participant must select objects located randomly at not visible positions, while memorizing a sequence of letters displayed over the current object being selected (see Figure 8.2). We evaluated three conditions, presenting different vibrotactile guidance techniques (i.e., increasing, decreasing, no feedback) with 10 repetitions each, producing 210 data records per participant (3 conditions \times 7 targets \times 10 trials). The presentation order of the conditions was balanced according to a Latin square pattern.

Participants were instructed to perform the task to the best of their ability. Before the experiment, all participants filled out an informed consent form and received detailed instructions to perform the task. A calibration process was also performed to set the range of vibrotactile intensities (from 0 to 127) in order to provide comfortable and effective feedback; every participant used a keyboard to increase or decrease a level in order to find a minimum intensity ($M=36.417$, $SD=14.945$) and a maximum intensity ($M=94.667$, $SD=11.703$). Furthermore, they filled out the Kennedy-Lane simulator sickness questionnaire (SSQ) [Ken+93] immediately before and after the experiment, further the Slater-Usch-Steed (SUS) presence questionnaire, and a demographic questionnaire.

Selection Task

For every trial, the participants were asked to locate and select 7 yellow cubes sequentially. Every object was randomly located behind the participant in order to guarantee that it was not on the field of view provided by the HMD, requiring the participants to rotate the whole body in order to locate and then select the target object by keeping the line of sight over it for two seconds. All the objects were always displayed 2m away and at the same elevation as the virtual head. An example of the arrangement is displayed on Figure 8.3. The position of every target was set randomly on predefined positions every 16 degrees and could not be predicted. After each completed selection, visual feedback was provided turning the cube color into red and then the next yellow cube was displayed, always behind the participant following the procedure explained above, until the seventh cube is selected completing in this way the selection task for the current trial and starting with the memory task.

Memory Task

Every target cube presented in the selection task was displayed with one of the letters A, B, C, or D on it. The letters were assigned randomly so whenever the participants selected the seventh target cube on a trial, they were required to recall the seven letters in the same order the sequence was displayed, using a controller (see Figure 8.2). The participants had unlimited time to enter and edit the sequence until they were sure enough to confirm the sequence with a button and continue with the next trial. For every trial, the correct sequence, the answered sequence and the corresponding Levenshtein's distance [SK83] were stored for further analysis. As an example, the figure is presenting a cube on the left back side of the user, the intensity will start at the maximum and will decrease, according to the blue curve, while the user body is rotated clockwise.

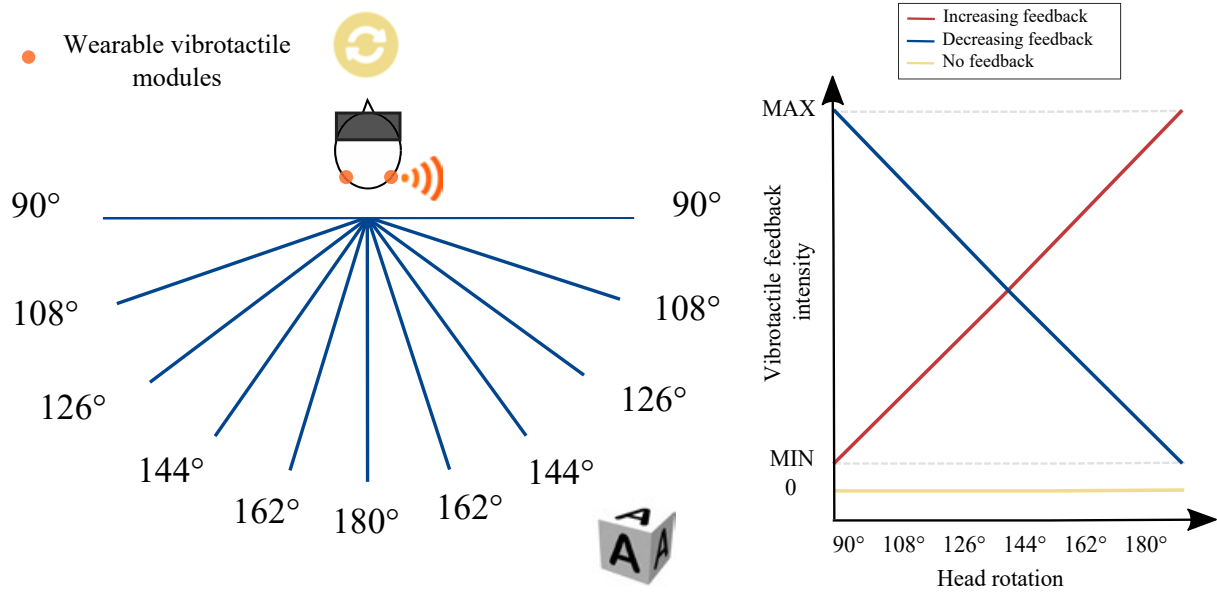


Figure 8.3.: Radial positions and stimuli: **(left)** Predefined angular positions for the targets. **(right)** Vibrotactile feedback intensity as a function of the body angle.

Conditions

For every trial and according to the rotation of participant body to locate the targets (using his/her line of sight), changes on the vibrotactile feedback intensity were applied dynamically according to a function of the angle (see Figure 8.3, right). We considered three methods of controlling the intensity to provide guidance assistance:

- **Increasing Feedback.** The intensity increases as the participant approximates to the target object, from the starting position (0 degrees) providing the minimum calibrated intensity to the target angle, providing the maximum calibrated intensity.
- **Decreasing Feedback.** Vice versa to the previous condition, the intensity decreases as the participant approximates to the target.
- **No Feedback.** In this condition, there was no vibrotactile feedback and hence no guidance assistance was provided.

8.5. Results

The results were normally distributed according to a Shapiro-Wilk test at the 5% level. We analyzed the results with a repeated-measures ANOVA and Tukey multiple comparisons at the 5% significance level with Bonferroni correction. Degrees of freedom were corrected using Greenhouse-Geisser estimates of sphericity when Mauchly's test indicated that the assumption of sphericity had been violated.

8.5.1. Selection Time

The mean time needed to select a target cube on the conditions providing vibrotactile feedback (increasing and decreasing conditions) were smaller than the selection time with no feedback (see Figure 8.4, left), spending in average 0.43 seconds less. We found a significant main effect of condition on the selection time ($F(2, 22)=18.2, p<.001$). A deeper analysis of the selection times for every angular position revealed that the highest improvement on selection time for the increasing and decreasing conditions was achieved for smaller angular distances (from 90° to 108°), reducing the time in approximately 1 second.

8.5.2. Memory Task Performance

We measured the percentage of correctly recalled trials (i. e., the participant was able to recall the complete sequence of 7 letters) in order to compare the performance for all the conditions. As an opposite result compared with the selection time, the performance was slightly better with the no-feedback condition in comparison with the increasing and decreasing feedback. Additionally, we calculated the Levenshtein's distance based on the recalled sequence of letters given by the participants (see Figure 8.4). This metric indicates how many editing operations are required to get the same string. The lower the value, the better the participant could remember the correct sequence. Again, the no-feedback condition achieved slightly better results in comparison with the increasing and decreasing feedback. However, we did not found a significant main effect of these two variables ($F(2, 22)=0.72, p<.5$ and $F(2, 22)=0.53, p<.6$).

8.5.3. Questionnaires

We measured a mean score for SSQ of $M=4.99$ ($SD=5.6$) before the experiment, and a mean SSQ-score of $M=32.10$ ($SD=39.27$) after the experiment. Both results showed the SS effect was significantly bigger than before ($T(11)=-2.711, p=0.02$), due to repetitive rotations of the body while wearing the HMD. The mean SUS score for the sense of feeling present in the VE was $M=3.667$ ($SD=0.61$), which indicates a high sense of presence (where a score of 7 represents a normal experience of being in a place). A 0-5 Likert scale (being 5 the best score) was used to evaluate subjective questions related to the usefulness and the comfort provided for all the conditions tested, as well as a subjective question to evaluate the favorite condition. The result matches the data collected (see Figure 8.4) and is summarized as mean values in the following table:

	Decreasing	Increasing	No Feedback
Useful	4,75	4,25	0,25
Comfortable	4,08	3,75	2,25
Favorite	67%	25%	8%

Table 8.1.: Subjective scores for the guidance conditions.



Figure 8.4.: Mean values for every condition on the dependant variables (i.e., selection time, selection error, and memory task performance).

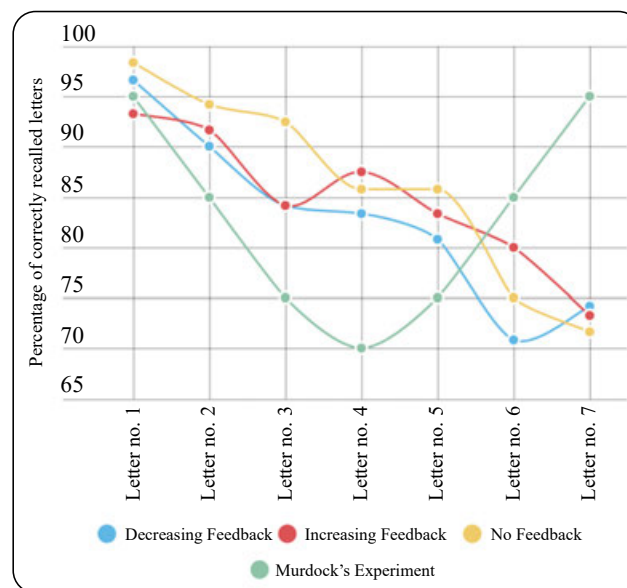


Figure 8.5.: Levenshtein distance: Pooled results of the experiment with the percentage of correct recall for all the sequence of letters in all the trials.

8.5.4. Serial Position Effect

We measured the percentage of correct recall for every letter in the sequence on all the trials. The results are displayed in Figure 8.5 (on the right) and can be used to study the serial position effect proposed by [Jah63] which presented a tendency to remember the first few (primacy effect) and last few letters (recency effect), and more likely to forget those in the middle of a sequence. The cited study suggested

that the primacy effect is related to store items in the long term memory (LTM) and that the recency effect would be related to store items in the short term memory (STM), typically limited to about 7 items. As can be depicted, the recency effect or STM allocation was prevented in all of our conditions in comparison with the normal behavior predicted by Murdock, which is shown in green color.


8.6. Discussion and Conclusion

The results show that the vibrotactile feedback improves the selection performance but, as a consequence, the metrics related to correct memory recalls for a sequence of 7 letters presented lower scores. Regarding the analysis of the serial position effect, the good performance achieved by the participants to recall the first letters can be explained as the expected outcome for LTM storage. However, the performance dropping could not be explained using the same framework as usually the STM buffer has an approximated capacity of 7 items and should be enough to produce the recency effect. One possible explanation could be given using the results obtained by [GC66], where a delay of about 30 seconds is produced before the recall process, then the recency effect is prevented and the STM storage is lost. This tendency could be explored in more detail evaluating the conditions over longer time spans and using more complex working-memory tasks, which could involve longer sequences and the use of words instead of letters so the requirements for cognitive resources could be higher and hence the resources pulled between tasks could show a more clear interaction.

In this chapter, we introduced the development of an affordable, wireless and wearable vibrotactile device. We presented a technique to provide selection guidance by dynamic changes on the vibration intensity as a function of the angular distance to the target when the user turns their head trying to locate the object. We also presented the results of an experiment showing the significant influence of a set of vibrotactile feedback conditions on the selection performance. However, the same conditions do not influence significantly the cognitive load variables. Future work should involve a larger study using further variables for selection errors, a more intense task in terms of cognitive resources consumption. We suggest the evaluation of vibrotactile feedback in different scenarios like vehicle operation, warning signaling and the use of vibrotactile patterns to provide richer and more detailed guidance feedback in VR. In addition, further research could include the analysis of cognitive performance based on verbal memory [BLS15].

9 Chapter 9

Sound-based Cues on Feet

This chapter is related to the scenario  (see Section 1.2).

9.1. Motivation

In the context of this thesis, we want to enable the user to move in small virtual spaces by real walking in order to approach 3DUI elements and perform selection and manipulation tasks. Walking is enough to keep good presence and usability levels in comparison to other navigation techniques for VEs in terms of spatial tasks and cognitive demands [RL09; RVB11; Mar+13]. Additionally, navigation support by controllers have limitations related to the sense of presence, spatial cognition, and more prone to produce simulator sickness [BC19].

Regarding the sensation perceived by users by real walking, such activity provides multimodal feedback including visual, kinesthetic, and vestibular cues [Ste+13]. Previous studies have shown that the use of auditory, visual and vibrotactile feedback is essential to convey the walking sensations and to produce plausible levels of self-motion and distance traveled [Kru+16]. Moreover, related research have evaluated haptic technology to provide friction forces on feet to reproduce sensations associated the user motion while walking [Kat+18]. A similar approach uses audio-based tactile feedback on stepping by the synthesis of ground surface by the use of inertial and pressure sensors, and therefore influence the user gate with rehabilitation purposes [Zan+14].

We propose in this chapter a wearable sound-based vibrotactile pair of actuated soles. Such device conveys sensations related to surface texture for real walking while users are immersed in VEs. Our approach aims to improve the sense of presence while the user navigates in limited areas to accomplish tasks involving the use of hands and 3DUIs. We performed a user study to compare our proposal with a base condition with no tactile feedback. Also, we collected subjective data regarding the sense of presence, comfort and acceptance of the technique.

9.2. Experiment

In this section we describe the user study that we conducted to evaluate the users' perception of self-motion and the sense of presence while walking in a VE. We compared a condition providing visual feedback for the floor surfaces (i.e., representing different materials and textures) with a condition incorporating also auditory and tactile feedback on the user feet. The two conditions were tested with a within-subject design. We expected the condition involving tactile feedback to be the most significant factor in the subjective perception of presence and acceptance rate.

9.2.1. Apparatus

The proposed technology involves the use of different modalities in order to incorporate as much as possible the aspects of the natural human gait whilst supplying an unencumbered device. We used avatars to represent the user body and walking actions. The implementation does not require position trackers of feet in order to detect contact with the virtual floor as our device contains a grid pressure sensors to detect different step stages and animate the avatar feet accordingly. For the study presented in this chapter, we used a walking-in-place (WiP) tracked device [Fre+20]. Unity3D was used to render the scene on an HTC Vive Pro.

Vibrotactile and Auditory Feedback

The device consists of a pair of anatomic soles. Every sole is connected to a small electronics compartment (i.e., wireless module) that can be comfortably attached on each ankle. Every sole contains an arrangement of pressure sensors (i.e., to detect gait stages) and an embedded audio-based tactile actuator. Specific details of the device can be found in the Appendix (see Section A.5).

The soles establish a wireless connection with the experiment PC receiving commands to activate the actuator and reproduce pre-recorded audio files matching the properties of the material the user is walking on. As an example, if the user is walking over virtual grass, the sole actuator reproduces an amplified audio stream of steps on grass. Simultaneously, the same audio feedback is provided to the user by headphones. The intensity of the feedback streams is proportional to the walking speed (see Figure 9.1).

Additional Visual Cues

As the user can move around the interactive area by real walking, all the subtle visual cues related to head cadence movements and leaning of the body (i.e., when starting, stopping, and turning) are naturally provided by the user movements (i.e., muscle and joints involved in real walking). We assumed that real walking while using an HMD would minimize the visual-proprioceptive sensory conflicts that are a common cause of simulator sickness [LaV00].

In the case of using a WiP device, the realism of the walking avatar can be guaranteed by adding visual effects. We added a head-bumping effect that creates horizontal and vertical organic movements of the virtual camera. As a result, it simulates the subtle head motions that occur during real walking [SCL17]. Additional visual cues include changes on the avatar leaning as the user is starting to walk, moving

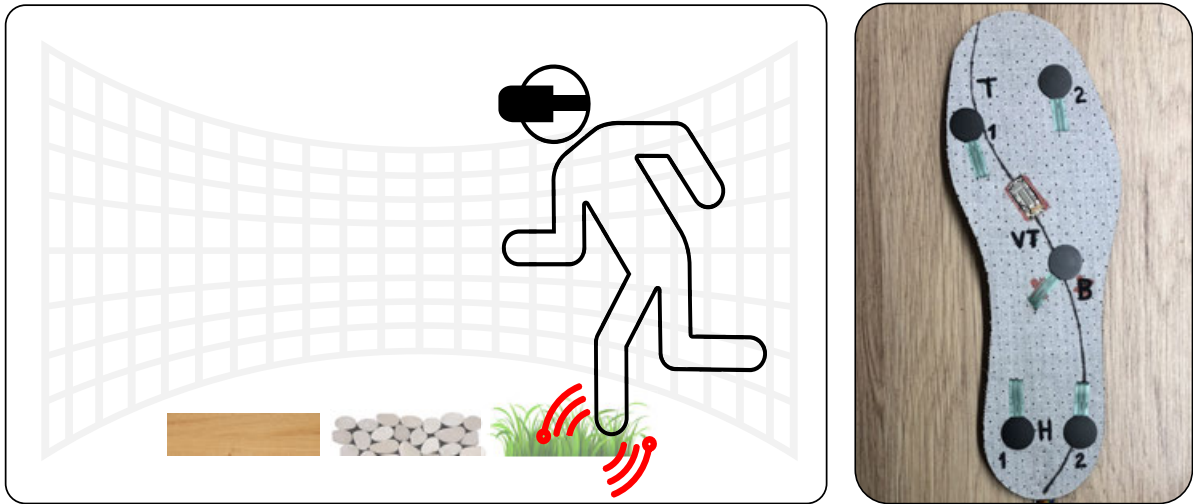


Figure 9.1.: Experiment setup to provide cues while walking: **(left)** The user is represented with an avatar and provided with matching visual, auditory, and tactile feedback on their feet whenever a foot lands on different surfaces (i.e., grass, stones, wood). **(right)** A picture of the sole device. It contains pressure sensors to detect foot contacts, and also an audio-based actuator to provide tactile feedback according to the surface the user is currently walking on.

forward, or stopping. The leaning angle depends on the virtual legs dimensions and the averaged speed over the last 30 frames [Fre+20]. Consequently, the effect conveys real-walking sensations of inertia when starting and leaning forward when going fast which brings the virtual feet into the FOV more often.

9.2.2. Participants

20 subjects ($M = 30.6$, $SD = 6.82$, 7 female) took part in the experiment. The participants were professionals or students in the fields of human-computer interaction or computer science, who received class credit for the participation in the experiment. Two participants were left-handed, the others were right-handed. All them had normal or corrected vision. Four participants were excluded from the analysis because of dizziness. In all cases they stated to generally be susceptible to motion sickness.

9.2.3. Procedure

The experiment started with a demographic and PRE simulator sickness questionnaire (SSQ) [Ken+93], which consists of 16 items categorized in nausea, oculomotor and disorientation scales. The procedure was followed by a briefing about the nature of the experiment.

The order of conditions was randomized while keeping a balanced number of trials. During the 10 trials for every condition, the participants were asked to walk on connected and straight paths in the shape of triangles with sides having 5 to 10 meters. Along the walking paths, the floor was composed by tiles of different materials. As the subjects walked on different tiles, the auditory feedback (provided with headphones) and the tactile feedback on the stepping foot changed accordingly to match the visual feedback of the rendered texture. The intensity of the feedback was proportional to the walking speed. The participants were asked to walk at a normal pace. Good to feel the changes on materials and adequate

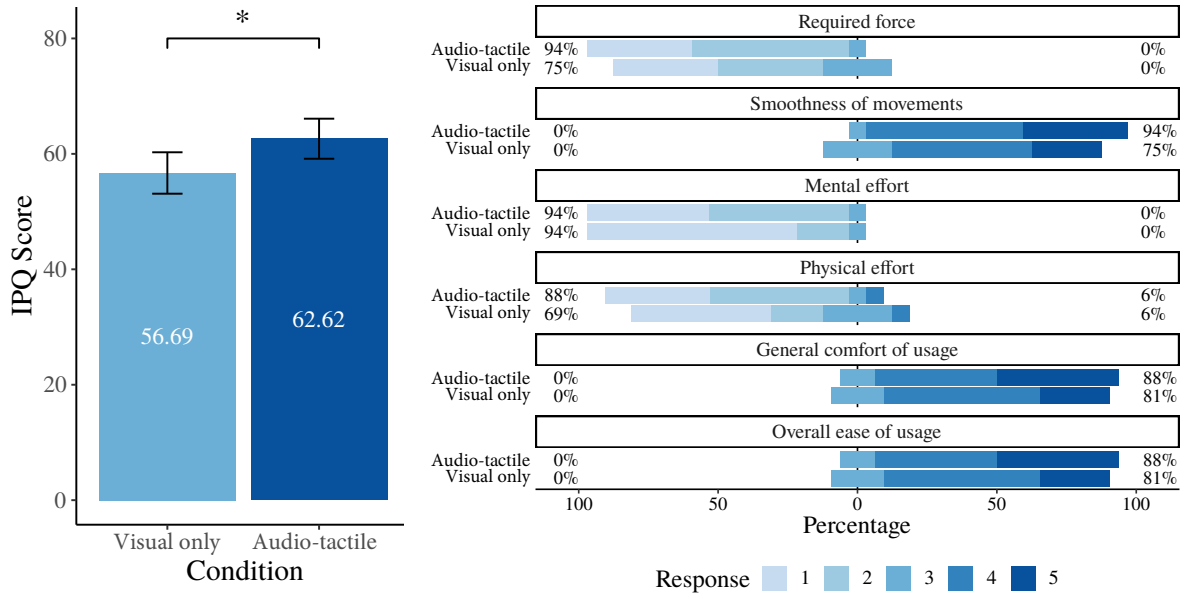


Figure 9.2.: Results for the tactile cues on feet: **(left)** Sense of presence for walking with no feedback and vibrotactile feedback, respectively. **(right)** Comfort scales for the tested conditions. The significance codes for figures are as follows: *** $\leq .001$, ** $\leq .01$ and * $\leq .05$.

to avoid inducing simulator sickness. Once the trials ended, the subjects were asked to fill out a POST SSQ. Then, The sense of presence was reported with the Igroup Presence Questionnaire (IPQ) [SFR01]. It consists of 14 items, categorized in spatial presence, involvement and experienced realism scales. Finally, comfort data was collected with the Device Assessment Questionnaire (DAQ) [DKM99]. It consists of 13 items, that can be rated on a 5-point Likert scale ranging from 1 to 5.

9.3. Results

In this section, we summarize the results from the experiment. Results were normally distributed according to a Shapiro-Wilk test at the 5% level. For the SSQ, we compared the differences from the questionnaire results gathered before and after every condition (POST-PRE). The differences were compared with a Wilcoxon signed-rank test. Although the *Audio-tactile* condition got lower SSQ scores, we found no significant increase in simulator sickness over the time of the experiment; *Visual only* ($M = 1.17$, $SD = 25.1$), *Audio-tactile* ($M = -6.54$, $SD = 27.3$).

9.3.1. Sense of Presence

For the IPQ, we used a Wilcoxon signed-rank test to compare the differences between conditions. We found a significant difference; *Audio-tactile* feedback ($M = 62.6$, $SD = 13.9$) presented the highest score, being better than *Visual only* ($M = 56.7$, $SD = 14.4$, $p = 0.018$). This finding confirms that leg proprioception and tactile feedback on feet have a strong impact on the sense of presence. The IPQ scores are illustrated in Figure 9.2 (left).

Condition	N	Mean	SD	SE	CI	Min	Max
Required force							
<i>Visual only</i>	16	1.88	0.806	0.2016	[1.472, 2.278]	1	3
<i>Audio-tactile</i>	16	1.69	0.602	0.1505	[1.386, 1.989]	1	3
Smoothness of movements							
<i>Visual only</i>	16	4	0.730	0.1826	[3.635, 4.365]	3	5
<i>Audio-tactile</i>	16	4.31	0.602	0.1505	[4.011, 4.614]	3	5
Mental effort							
<i>Visual only</i>	16	1.31	0.602	0.1505	[1.011, 1.614]	1	3
<i>Audio-tactile</i>	16	1.62	0.619	0.1548	[1.315, 1.935]	1	3

Condition	N	Mean	SD	SE	CI	Min	Max
Physical effort							
<i>Visual only</i>	16	1.88	1.02	0.2562	[1.363, 2.387]	1	4
<i>Audio-tactile</i>	16	1.81	0.834	0.2085	[1.395, 2.23]	1	4
General comfort of usage							
<i>Visual only</i>	16	4.06	0.680	0.17	[3.722, 4.403]	3	5
<i>Audio-tactile</i>	16	4.31	0.704	0.176	[3.96, 4.665]	3	5
Overall ease of usage							
<i>Visual only</i>	16	4.06	0.680	0.17	[3.722, 4.403]	3	5
<i>Audio-tactile</i>	16	4.31	0.704	0.176	[3.96, 4.665]	3	5

Table 9.1.: Descriptive statistics for the DAQ scores.

9.3.2. Comfort

We analyzed the DAQ Likert ratings related to comfort with an ordinal logistic regression in order to find differences between conditions. There are no significant differences for the scores related to required efforts and ease of usage. However, the results show that the use of the device did not reduce comfort levels in comparison with the walking condition providing no feedback. Although the subject where using a wearable sole and had an electronics module attached to the ankle, there were no complaints nor negative scores regarding the weight, ergonomics or unpleasant vibrotactile feedback. Figure 9.2 (right) illustrates the distribution of responses and the corresponding descriptive statistics for all the scores are presented in Table 9.1.


9.4. Conclusion

We found no significant differences for the self-reported simulator sickness or comfort for the tested conditions. In general, both conditions did not present increased incidences of nausea, disorientation nor oculomotor related symptoms. The use of the proposed technology did not reduce the acceptable scores for cybersickness of the base condition, showing it as safe to use as the condition of real walking with no feedback. Regarding the sense of presence (IPQ questionnaire), we found the condition providing sound-based tactile feedback to be significantly better than not providing feedback at all. As a result, the vibrotactile soles feature an increased sense of presence by conveying the sensation of stepping on ground surfaces that match the visual representation. The overall sensation was conveyed by the combination of auditory and vibrotactile feedback sourced from the same audio pattern representation for specific ground materials. Considering that our device requires more hardware setup (i.e., place a pair of wearable soles inside the shoes and attached electronics to the ankles), the results show that we did not reduce comfort levels. Conversely, we received positive subject comments about how compelling/reactive was the feedback, as well as good ergonomics. In summary, we presented a technique to improve realism and presence for real walking in VEs. We contributed the implementation and a user study that shows that our approach significantly improves the sense of presence and features acceptable comfort rates.

10

Chapter 10

Cues for Obstacle Detection

This chapter is related to the scenario  (see Section 1.2).

10.1. Motivation

User interaction in VEs involves navigation [LaV+17]. Hence, the user could collide with obstacles that are either approaching moving objects or static objects placed on the current path. This chapter is an exploration on how wearable technology could support the user to detect such obstacles while navigating. We aim to avoid the use of visual and auditory modalities because the corresponding senses are used actively while performing selection and manipulation tasks in VEs. Therefore, vibrotactile feedback could provide cues for obstacle detection while the user is performing primary tasks in VEs (e.g., receive a tactile cue communicating the distance of an approaching object while the user is manipulating a virtual object with a hand-operated VR controller).

In order to focus on the perception of tactile cues to detect obstacles, eliminating the use of eyes and ears, this chapter is motivated in previous research on technologies to determine the position of obstacles for visually impaired persons (VIPs). However, in addition to contribute with a wearable technology for VIPs, we believe that the same technology principles could be applied in VEs requiring support for obstacle detection (e.g., real/physical walls providing passive kinesthetic feedback). Vibrotactile support for guidance has been explored before using different form factors and actuator densities. Previous results have presented improvements in user performance for detecting directional cues, recognition accuracy and faster user response [J O+16; Spe+09].

A white cane is the typical tool for VIPs to avoid crashes and navigate through the environment more safely. Nevertheless it lacks the ability to detect objects above floor level. Therefore white canes are augmented with certain sensor devices [KC13]. Typical augmented white canes are referred to as smart canes. These smart canes make use of ultrasonic sensors, infrared sensors or cameras which obtain obstacle information such as distance and position. Auditory or vibrotactile feedback patterns encode and deliver the relevant information to the user. It is crucial to use common design guidelines and well known methods from HCI research which map and encode signals to a comprehensible feedback stimuli. This

chapter introduce a haptic handle that can be integrated in smart canes but also could be integrated in current VR controllers. We use affordable components and vibrotactile feedback based on piezo actuation.

In a previous study, subjects used both an auditory guidance device compared to vibration device whilst being subjected to street noise. Participants wore either headphones to receive auditory or a harness to receive vibrotactile guidance commands. Results indicate a comparable performance while using either of those methods [GBC07]. It shall be noted that the use of regular headphones imposes a danger to subjects in a walking situation because important auditory cues can not be perceived. A possible solution could be bone-conduction headphones which do not cover the outer ear because they create sound through vibrating skull bones [WL05]. Still there remains the question of an auditory overload caused by many auditory cues. Finally, working memory plays an important role in interpreting the feedback mechanisms designed by the researchers. Due to working memory restrictions vibrotactile, spatial feedback is expected to interfere less likely with already existing auditory stimuli imposed by the environment [Bad92].

In summary, wearable devices to support obstacle detection while walking must feature free-hands interaction or be integrated to handheld interfaces. Also, the technology must not cover the ears for the sake of echolocation and related cues. Finally, the device must be minimalist and communicate good affordances and easy learning curves [DB10]. The remaining of the chapter presents the design and evaluation of wearable technology according to the presented guidelines.

10.2. Experiment

We conducted a study to analyze the psychometric thresholds related to vibrotactile feedback for obstacle detection on predetermined distances. Feedback was given by a handle provided by vibrotactile feedback used by subjects to estimate obstacle distances along a linear path towards the user. The psychometric analysis determines the minimum change in stimulus intensity that is consciously or subconsciously perceptible by the subjects. The expected outcome is the minimum distance change that still let the subjects make reliable judgments (i.e., at least 90% certainty) on whether the obstacle moves towards or away from the user. Figure 10.1 shows the experiment setup.

10.2.1. Apparatus

An augmented handle was constructed using an infrared and an ultrasonic sensor which were connected to an Arduino-compatible microcontroller. The handle was created using a clay imprint of a right hand in handle-grasp posture. Next, the handle was 3D-scanned and finally 3D printed. Specific details of the device can be found in the Appendix (see Section A.6).

Feedback Function

The range to provide meaningful tactile feedback is constrained by a minimum and maximum distances, which are related to the interaction and content zones. The minimum distance is given by 20cm since the ultrasonic sensor can only provide noise free signals for this distance upwards. The maximum was

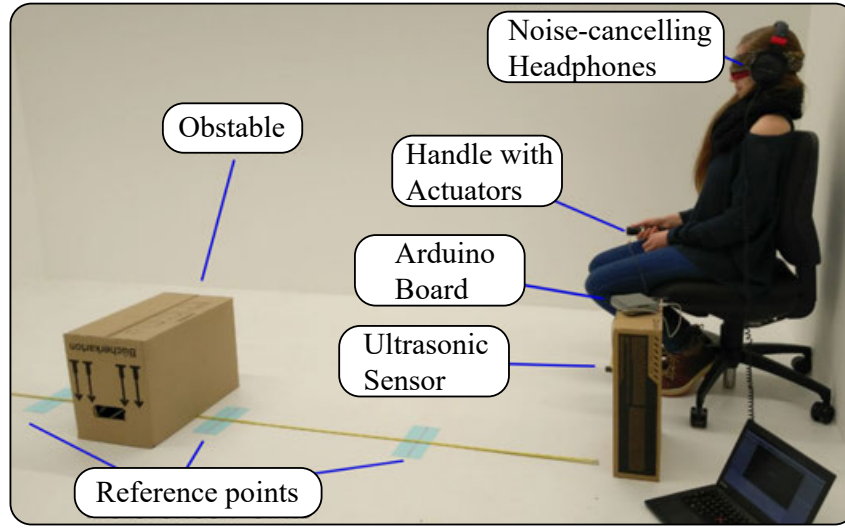


Figure 10.1.: Study setup: Blindfolded subject receiving feedback via actuators on the handle relative to the obstacle distance. The handle was held, such that the thumb could be placed on the top actuator to perceive the feedback.

Distance	Exponential (Hz)	Linear (Hz)
20 cm	7.00	7.00
90 cm	4.30	5.50
160 cm	2.65	4.00
230 cm	1.63	2.50
300 cm	1.00	1.00

$$f(x) = a_{max} \cdot \left(\frac{a_{min}}{a_{max}} \right)^{\frac{x-d_{min}}{d_{max}-d_{min}}}$$

Figure 10.2.: Distance discrimination for obstacle detection: **(left)** Feedback function mapping the current distance from the sensors to actuated frequencies. **(right)** Corresponding frequency values for linear and exponential distributions.

set to 300cm to encapsulate the immediate surroundings while still providing a reasonable resolution for distance discrimination. Figure 10.2 shows the mathematical function for distance discrimination, mapping the distance information from the sensors to actuator frequencies (left). The function applies for the maximum and minimum activation frequency a_{max} , a_{min} as well as the maximum and minimum distances d_{max} , d_{min} . The figure also presents a table with the corresponding frequencies for the selected distances (right).

The function maps the minimum distance to the maximum activation frequency and vice versa. The selected minimum and maximum activation frequencies are $1Hz$ and $7Hz$, respectively. The minimum activation frequency convey a discernible base feedback for the maximum distance according to a pilot study. The maximum activation frequency is limited by the micro-controller software. According to the table, at far-apart distances, the linear frequencies produce a change from $1.0Hz$ to $2.50Hz$ which is more recognizable than a frequency change from $1.0Hz$ to $1.63Hz$ for a distance offset of $70cm$. Conversely, the exponential frequencies supply more resolution in the interaction zone, which is more convenient. Additionally, perceived differences of activation frequencies correspond exponentially with the measured distances.

10.2.2. Procedure

The study was conducted in a room with enough space according to the distance covered by the ultrasonic sensor. Selected distances for the obstacles were marked on the floor (see Figure 10.1). Four reference points from near to far were determined to cover the whole spectrum of possible object distances. Reference points were marked at 55cm, 125cm, 195cm and 265cm. The closest possible obstacle distance was 25cm, the farthest possible was 295cm respectively. A box was placed on the respective reference point and shifted by 5, 10, 15, 20, 25 or 30 centimeters closer to the subject (negative shift) or further apart (positive shift). After each shift the subject had to decide whether the box was shifted further away or closer in depth.

The subject was blindfolded and received white noise over noise-cancelling headphones to prevent auditory hints (e.g., box shifting). The only cue presented was feedback given by the piezo actuator on the handle. Every subject was instructed to place the dominant-hand thumb on the actuator. Proper feedback levels and sensitivity were calibrated at the beginning of the study. Before shifting the box for the next trial, it was placed back on the reference point (current distance) to offer subjects the opportunity to recall the corresponding tactile pattern once again. Subjects estimated distances twice per shifting point (i.e., two repetitions) in both the negative and positive direction. Order was always the same, starting from the closest reference point at 55cm up to the last reference point at 265cm. After 24 decisions the reference point was changed and the subject could have a short break if preferred. A total of 96 decisions have been recorded per subject; 48 positive and 48 negative shifts.

10.2.3. Results

Data from six subjects was collected (age $M = 26.33$, $SD = 4.93$, 2 female) for a total of 576 data entries. We tested for data normality using the Shapiro-Wilk test, for negative shifts ($W = 0.85$, $p > 0.05$) and for positive shifts ($W = 0.92$, $p > 0.05$). A paired T-Test comparison for the shifting directions resulted in no significant differences ($t(5) = -1.22$, $p < 0.05$) for positive ($W = 0.91$, $SD = 0.08$) and negative ($W = 0.93$, $p > 0.08$) shiftings. As a result, we computed a Pearson correlation with the absolute shift values ($W = 0.92$, $SD = 0.08$). The result indicates a strong correlation ($r(4) = 0.91$, $p < 0.05$). The mean number of wrong answers was 7.33 ($SD = 2.92$) for all subjects. The best and worst performing subjects had an error rate of about 4% and about 12% respectively. Each distance of the object to a reference point had 48 corresponding trials. The mean of the number of errors across all distance differences was 3.67 ($SD = 3.59$). Besides, feedback irregularities for very close objects have been reported by subjects. Although it is not significant, ($\chi^2(3) = 5.95$, $p > 0.1$), the collected data shows a high error rate for the first reference point at 55cm.

Regarding the psychometric function, a probabilistic distribution allowed to compute the threshold at which at least 90% of forced choices were expected to be correct. Since there is no difference assumed between negative and positive shift, the psychometric function for absolute shifts was calculated, with threshold at 13.58cm ($M = 5.94$, $SD = 9.08$, $CI [11.64\text{cm}, 15.56\text{cm}]$). The figure 10.3 presents the psychometric function for the obstacle shifting values.

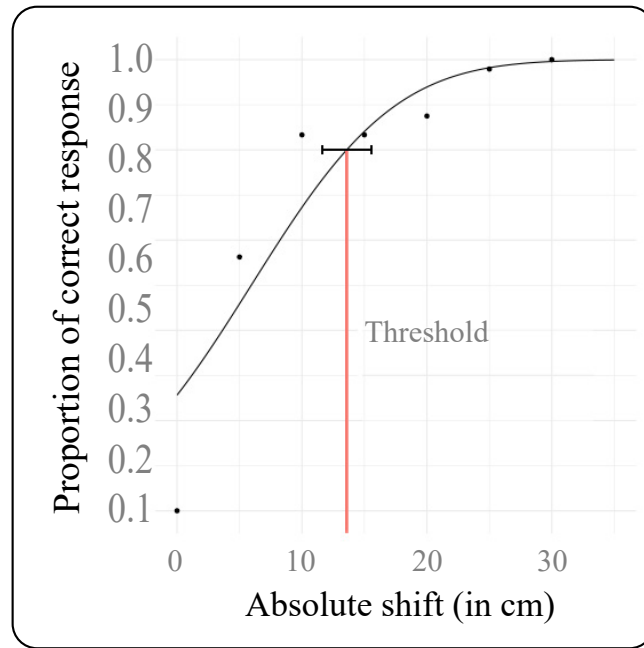


Figure 10.3.: Psychometric function for absolute shiftings. Dots mark the ratio of correct answers given by subjects regarding the reference point.

10.3. Conclusion

Our approach uses a constant frequency for the vibrotactile feedback on static obstacles. This limitation is prone to an adaption effect [Van02]. In this case, the user's subjective magnitude could decrease which could lead to weakened perception of obstacles. However, such an adaption effect is avoidable by switching to a variable tactile pattern whenever the distance to the obstacle remains constant for a predetermined amount of time.

We have presented the design and implementation of a wearable device for obstacle detection while walking. The device features an ergonomic handle with good affordances and is comfortable to hold. Our approach makes use of ultrasonic distance sensors and piezo tactile actuators to continuously measure the distance to static and approaching obstacles in VEs. The feedback is provided by encoding the distance of detected objects as an activation frequency of the piezo actuators. The results indicate a high rate of correct answers. Given a minimum distance shift of 13.58cm the subjects could determine the direction of shifts with a probability of 90% on a total spectrum ranging from 20cm to 300cm.

Part V

Conclusion

11

Chapter 11

Summary and Guidelines

The use of wearable haptic technology in VEs has enormous potential to improve user performance and accuracy while executing 3D selection tasks, as well as providing proximity-based guidance to compensate for vision perception problems. However, nowadays VEs often lack proper haptic feedback, combined with insufficient alternatives to incorporate feedback for the tactile and the kinesthetic modalities in 3DUIs.

In this thesis, we developed and evaluated wearable haptic technology that circumvents the mentioned limitations, improves usability, and reduces the performance gap between traditional interfaces and 3DUIs.

Part I presented fundamentals on haptics and background information on physiology, perception, and performance metrics regarding the tactile and kinesthetic modalities. Furthermore, we explored previous work related to haptic technology and haptic interaction, including taxonomies and comparisons.

Part II explored the use of vibrotactile cues for guidance in 3D selection. First, we presented a ring-shaped wireless haptic device for spatial user interfaces, and we reported the effects of different proximity-based vibrotactile patterns. We showed that such patterns can improve the user's subjective awareness of a virtual scene, enriching it by providing haptic feedback when virtual objects are touched or intersected. Moreover, the results showed that there is no overall optimal pattern but that design implications can exploit the advantages and issues for each pattern. Furthermore, we presented a vibrotactile finger-wearable device providing proximity-based feedback in the fingertip. We built upon the vibrotactile patterns tested with the first device with a study testing a Fitts' Law 3D selection task. We tested three sensory modalities (i.e., visual, auditory, and tactile), changing the intensity, frequency, and color according to the distance traveled during selection. The results revealed significant benefits of binary over continuous feedback and higher subjective preferences for bimodal feedback. Regarding the proportion of the ballistic and correction phases of the selection movements, we found that binary feedback produces movements with larger correction phases, usually related to accurate selections. As a main result, we proposed a set of guidelines for 3DUI designers: (i) avoid bimodal combinations if the user interface must provide good throughput and should prevent undershooting, (ii) choose binary proximity-based feedback over continuous feedback for faster selections and overall higher throughput in 3D selection tasks, (iii) choose bimodal over unimodal feedback for reduced error rates in 3D selection tasks and higher subjective user acceptance, and (iv) the best deal among throughput, under/overshooting distance, and the proportion of the correction phase is binary-unimodal feedback. With this profile, it is possible to

significantly increase the correction phase (by more than 12%) and prevent over/undershooting almost completely while keeping a higher throughput.

Part III studied techniques for inducing perceptual illusions supported by multimodal feedback. First, we presented a pair of wearable vibrotactile gloves able to provide brief phases of vibrotactile feedback. Such feedback was synchronized at low latency with visual feedback in order to reproduce the Long-Arm illusion with vibrotactile technology. Results of our experiment showed that visual-vibrotactile feedback can be used to induce the illusion while simplifying and automating the process, which traditionally requires an operator to be present in order to manually stimulate the user with synchronized visual-haptic tapping feedback. Our results suggest that the approach may be transferred to other embodiment illusions as well, thus providing means to improve the VE experiences of users in a variety of application fields. Second, we presented wearable technology that conveys holistic touch illusions by combining tactile and kinesthetic feedback with pseudo-haptics. We reported the results of 3 studies providing guidelines to properly convey contact, stiffness, and activation in 3DUIs. Overall, our approach creates a plausible illusion of touch, delivering a holistic feeling when interacting with 3D buttons, and maintaining good levels for the sense of body ownership and presence, as well as positive subjective feedback for user acceptance. In addition, we provided a model to predict perceived stiffness given a specific C/D ratio.

Part IV explored the use of haptic technology to support 3D navigation. As a first exploration, we introduced affordable wearable devices to provide vibrotactile feedback on the backside of the head (i.e., attachable to HMDs). We showed that such feedback is beneficial for the selection of objects located out-of-sight. Our technique guides the user's head to locate an object by providing dynamic changes on the vibration intensity as a function of the angular distance to the target. The results revealed a significant effect on selection performance, being the feedback decreasing in intensity the most effective. Furthermore, we discussed the implications of the cognitive resources involved. In this part, we also presented a pair of soles with embedded sensors and audio-based tactile actuators. These haptic soles are easily attached to shoes and provide vibration cues while walking in EVs. Such cues were combined with congruent auditory feedback indicating the texture properties of the floor (i.e., grass, wood, or stones), and also matching the visual representation. We conducted a study comparing a soles condition with a no-haptic-feedback condition for participants performing real walking in a VE. Results indicated that there are no significant differences for the self-reported simulator sickness or comfort, showing that our approach is as safe and usable as the condition providing no feedback. Regarding the sense of presence, we found that the sound-based tactile feedback was significantly better than not providing feedback at all. Finally, we introduced a wireless handle with vibrotactile feedback for obstacle detection in VEs. The device makes use of ultrasonic distance sensors and piezo tactile actuators to continuously measure the distance to static and approaching obstacles and provide tactile feedback accordingly. The design of the device was motivated by the possibility of detecting approaching or static obstacles in VEs without relying on vision or, while the user is focused on selection or manipulation tasks. We moved obstacles along the line of sight of the user (ranging from 20cm to 300cm) and they managed to reliably detect obstacle shiftings larger than 10cm, as well as the shifting direction (90% of correct trials).

12

Chapter 12

Perspectives

We presented a set of wearable haptic devices and interaction techniques to support users while operating 3DUIs in VEs. The contributions of this thesis could be further improved with the use of novel technologies and integrated with novel solutions for mobile MR. We believe the technology proposed in this thesis could be further miniaturized to be integrated with headsets or motion controllers, or even adapted to improve the compatibility with inside-out hand tracking solutions. Moreover, pseudo-haptic techniques could be further optimized and combined with multimodal feedback to convey more compelling force sensations. Future work should evaluate more vibrotactile feedback patterns for grasping or dexterous manipulation. Also, the context of the presented studies is related to 3D selections on a Fitts' Law experiment with an interaction space restricted to a circular layout of targets and hence is necessary for further research to evaluate different interaction spaces.

As a main goal, haptic technology should be wearable, wireless, lightweight, and power-efficient haptic devices able to convey tactile and kinesthetic feedback in VEs. Although haptic technology is still in an early stage of development ("might be 30 years behind graphics" [Sch+17]), we believe that haptic research is accelerating to overcome the current challenges and integrating contributions on actuators engineering, haptic design, and haptic rendering [Mue+20; Sch+17]. In addition to the fact that hardware solutions become more affordable, promising perspectives for haptics are starting to explore better couplings between skin receptors and actuator/sensors. Extremely thin devices could stimulate skin mechanoreceptors with electrical activity [WGS18], and be combined with novel epidermal, transdermal, and subdermal implants to augment the human hand/body with unencumbered sensing and tactile actuation [Mue+20]. Regarding new engineered materials, electroactive polymers for haptics allow interaction designers to use shape-changing surfaces and structures. Such polymers are interactive and create organic and subtle movement of semi-transparent membranes which is useful to provide dynamic passive haptic feedback in VEs [FF19]. Similar materials have dual functionalities of force sensing and vibrotactile actuation. This kind of polymers can be manipulated with vibrotactile waveforms while sensing changes in capacitance from contact forces [Yoo+19]. Furthermore, novel mechano-tactile interfaces are thin and flexible skin stickers with silent operation and changing shape. Such stickers provide tactile patterns like pinching, directional stretching, pressing, pulling, dragging, and expansion. The patterns have been tested in interactive experiences like physical guidance, health interfaces, and VR gaming [Ham+19].

As future work, one could improve wearable devices with a new set of haptic sensations relying on

audio-based tactile feedback in order to support high-definition effects in 3DUI elements. Current testing is ongoing with novel diegetic user interfaces for VR. Moreover, tactile feedback could take advantage of physically-based audio modelling [ARR02]. For example, a VE user provided with our haptic shoes (see Chapter 9) could feel vibrations produced by virtual objects falling and colliding with the virtual floor. Nowadays, it is possible to receive auditory feedback produced by the synthesis of collision audio effects corresponding to the material properties of the falling objects and the floor. Additionally, physics propagation effects can be applied to finally render spatialized audio in VEs. We believe that the same synthesized audio patterns could be reproduced with audio-based tactile actuators to convey multimodal sensations and improve even more the sense of presence in VEs^{1 2}. Additionally, we suggest the use of 3D engine features to set the physical characteristics of the 3D object (i.e., stiffness, friction coefficients). Such characteristics have been traditionally used for simulations, but could be used to configure interactive virtual objects in VEs and improve the realism of the generated audio patterns. Spatial and temporal resolution parameters (i.e., frequency, resonant frequencies, and curve shapes) could be extracted from the texture/bump maps and synthesize audio samples with that information [BU18; KRM11] so they can be streamed to the same audio-based tactile actuators. As a result, the audio patterns can be reproduced on the skin, activating the tactile mechanoreceptors to convey sensations of contact whenever our finger collides or slides over a virtual surface. At some point, such profiles could be collected, distributed, and integrated into the VE design process similarly to audio assets. In general, we aim for improving devices with a new set of haptic sensations relying on audio-based tactile feedback in order to support high-definition effects and the development of new 3DUI elements. Current testing is ongoing with novel diegetic user interfaces for VR, enriching 3DUI elements [SAS19] and tangible passive interfaces [BAS19] with tactile feedback in order to improve the user performance.

Ultimately, we believe that haptic technology, and in general, the use of multimodal feedback might be the key to success for super-immersive VEs that close the gap to achieve the ultimate display. A display that could control the existence of matter, with virtual chairs we can sit on and virtual bullets that would be fatal [Sut65].

¹<https://tech.alpsalpine.com/prod/e/html/haptic/>

²<https://lofelt.com/>

A Appendix A

Wearable Devices

This appendix introduces the wearable technology we developed to conduct the studies presented in this thesis. The following sections provide technical details on designs, hardware specifications, and links to open-source resources enabling practitioners to replicate the conducted experiments.

A.1. HapRing

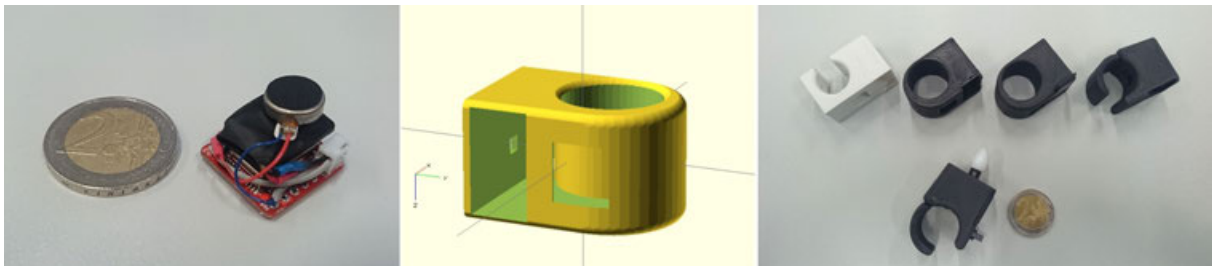


Figure A.1.: Electronics, design and form factor of HapRing.

HapRing is a finger-worn device, avoiding cables by using a low-energy wireless technology. A vibrating element is controlled by embedded software to provide haptic feedback at different intensities according to signals received from the computer. The embedded software running on the HapRing is managed by an RF51822 SoC (System on a Chip) based on a 32-bit ARM Cortex, supporting Bluetooth Smart (2.4 GHz Band) for ultra-low-power wireless applications. All the components are placed on a small development board (18.5 mm \times 21.0 mm) including power connectors (supporting a working voltage from 1.8 V to 3.3 V) and a set of I/O ports used to connect the micro-joystick with command button and the Linear Resonant Actuator (LRA, 5mm diameter \times 3mm thickness) which is a shaft-less vibration motor attached to an active haptic driver (TI DRV2605). As a power source, we used a Lithium Polymer Ion (LyPo) rechargeable battery which outputs a nominal 3.7 V at 40 μ A h. A voltage converter and a micro USB plug were included. An optional IR LED (with 880 nm wavelength for compatibility with a PPT tracking system) is connected to the ring's top for external reference support. Besides, an IMU is integrated, providing 9-DoF data from a 3-axis combo chip (L3GD20H and LSM303D). As we used

symmetrical design, the device works just as well for left-handed users as for right-handed users. The finished prototype is illustrated in Figure A.2, which shows the various components and the size (47 mm height \times 30 mm width \times 22 mm depth). The variant of the device in the figure was 3D-printed with PLA material and has a total weight of 20 grams.

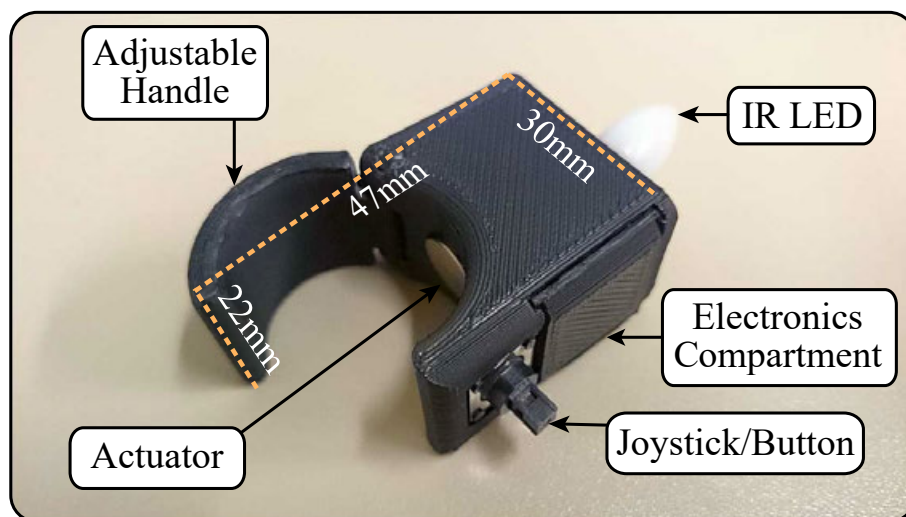


Figure A.2.: Main components of HapRing.

The haptic driver takes advantage of overdriving and active braking to guarantee responsive and clean signals. According to the vibrator characteristics, the frequency range is 20 Hz to 220 Hz. The provided range is sufficient to elicit sensations on the epidermis' tactile corpuscles for haptic feedback related to small displacements, pressure sensations, and small texture patterns. The ring was sketched, modeled, sliced and 3D printed according to the constraints imposed by finger ergonomics and electronics. As such, the final design has beveled edges and a joint that allows users to adjust the size. For the communication with HapRing, the commands can be sent directly through Bluetooth. We developed an alternative interface application that receives and sends commands through a standard UDP port and transmits them to HapRing. This setup is modular and would allow different computers to communicate with HapRing, as often necessary in laboratories. We measured the latency from the collision detection in the 3D environment to the vibration signal triggered on the actuator, which was 23 ms, sending a byte-length message to the device using the UDP-like mechanism to send messages with a "no response flag" provided by the Bluetooth LE Specification. According to perception studies [JGH07], the measured latency is sufficiently small based on average hand velocity for common interactive tasks and vibrotactile related experiments.

Example applications for the HapRing are presented in Figure A.3. The device can be used in multi-touch tablespots to provide vibrotactile sensation according to materials displayed with different textures. Different sensations can also be provided in VR, from enriched textures to tactile effects for collisions in mini-games supporting hand-tracking, and vibration patterns to notify contact with dangerous objects (i.e., hand getting too close to the fire). This device was utilized to conduct the study on vibrotactile patterns (see Section 4.2). Also, the device is available as an open-source hardware project¹.

¹<https://github.com/tlon-citizen/HapRing>

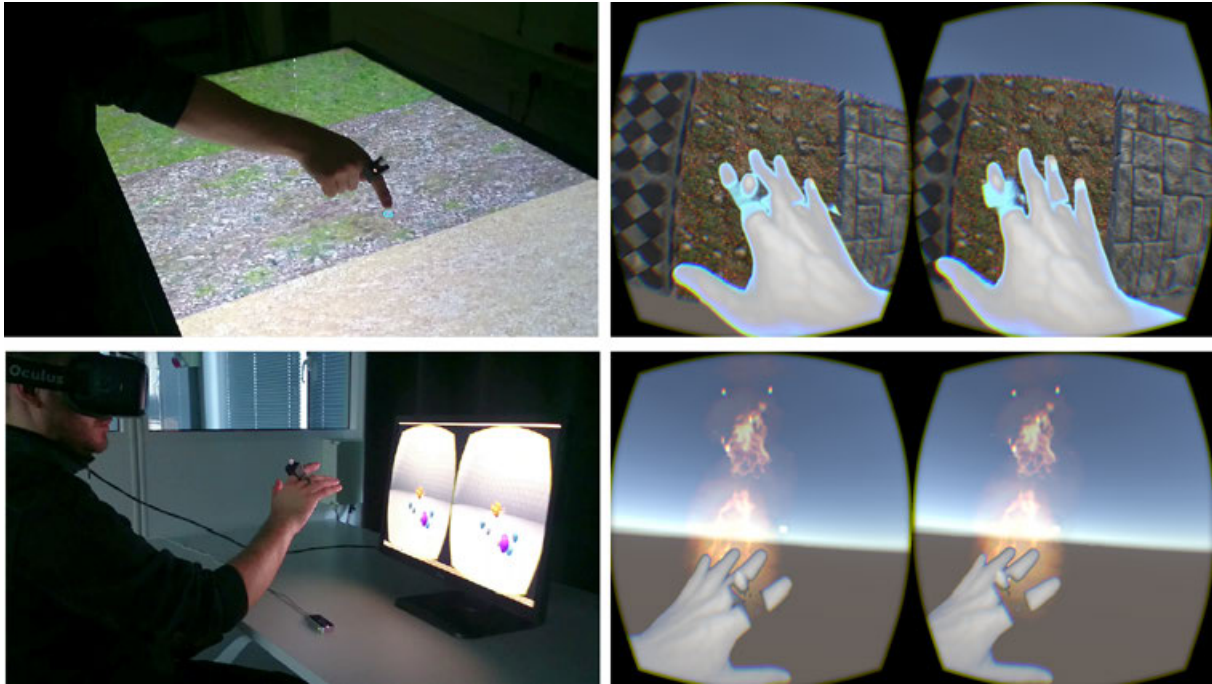


Figure A.3.: HapRing applications.

A.2. HapFinger

HapFinger is a fingertip-worn wireless (Bluetooth 2.4 GHz Band) device to be used in the index finger. A vibrating element is located right at the fingertip and is controlled by embedded software that controls the intensity according to signals received from the computer. The case encloses an RF51822 SoC (System on a Chip) based on a 32-bit ARM Cortex. The device provides feedback with a Linear Resonant Actuator (LRA, 5mm diameter \times 3mm thickness, Precision Microdrives C10-100) spinning at a resonant frequency of 200Hz while varying the intensity from level 0 to 128 and controlled by a dedicated haptic driver (TI DRV2605L) and supporting overdriving and active braking.

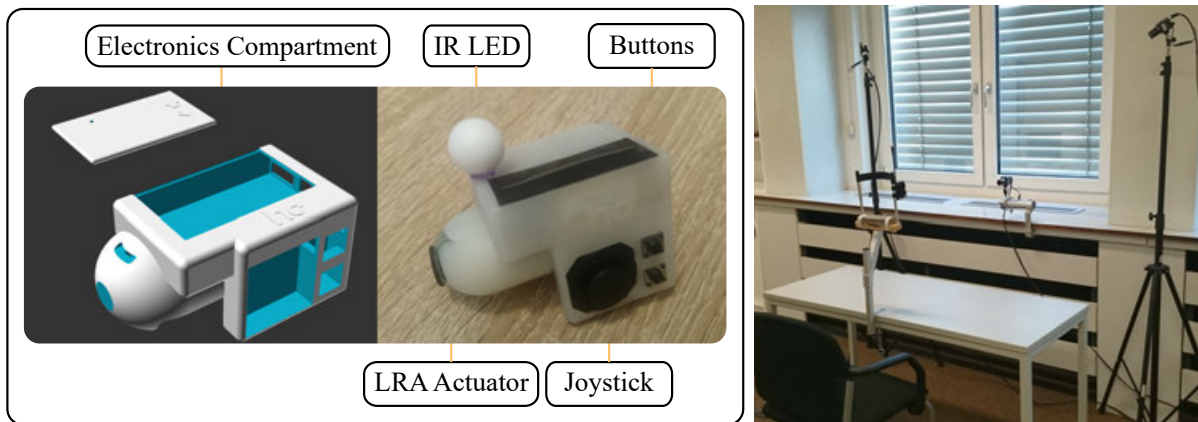


Figure A.4.: HapFinger components and tracking setup.

The device was 3d modeled as a finger contoured electronic enclosure. The device case was 3d-printed with resin material and the total weight, including the battery, is 31 grams. The device can also be configured to provide different vibrotactile patterns according to the task in execution [ALS15]. Additionally, it features input capabilities with an analog 2-DoF joystick and two momentary buttons. These input elements were used in the experiments to confirm selections, pause trials, and answer questions with binary answers. The device is equipped with an infrared LED compatible with active-marker tracking systems. In our case, the device setup uses a PPT system with three cameras (sub-millimeter precision, see Figure A.4 right) that is connected to a VRPN server streaming data to the experiment workstation.

This device was utilized to conduct the study on the ballistic and correction movements for 3D selection (see Section 5.3.2). Also, the device is available as an open-hardware project².

A.3. HapBand

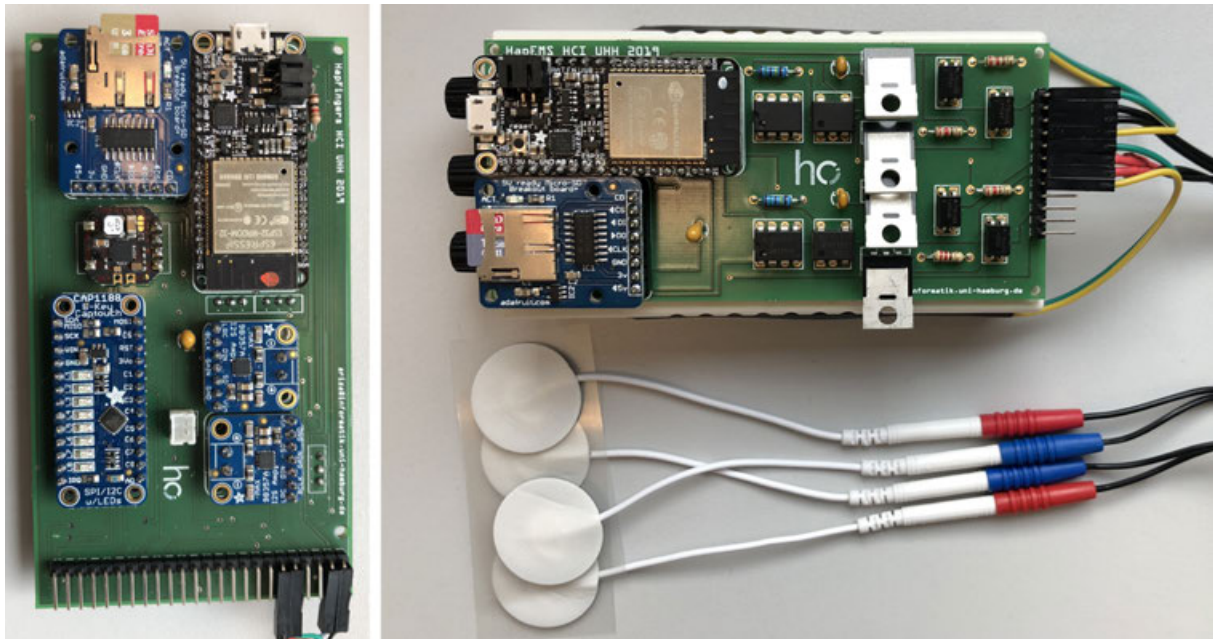


Figure A.5.: HapBand modules.

HapBand is a wearable and wireless device composed of two modules to be worn in the upper arm. The modules are driven by an Espressif ESP32 dual-core microprocessor clocked at 240 Mhz with 520Kb RAM and powered by rechargeable 18650HG2 Li-Ion batteries (3.7V). The modules-to-PC latency is approximately 30 ms. Actuators and electrodes are connected to the modules with thin cables that can be comfortably accommodated along the arm. The tactile module (116mm × 65mm × 15mm, Figure A.5 left) provides tapping and vibration stimuli through a wearable fingertip (64mm × 32mm × 32mm, Figure A.6). This unit provides a tapping sensation that recreates the pressure felt on finger soft touches, stimulating the SA1 receptors for pressure (i.e., Merkel cells). A tactile tap is better than

²<https://github.com/tlon-citizen/HapFinger>

vibrotactile feedback as vibration is sensed by the Pacinian corpuscles deeper in the skin, which does not contribute to pressure sensing [Kur+07].

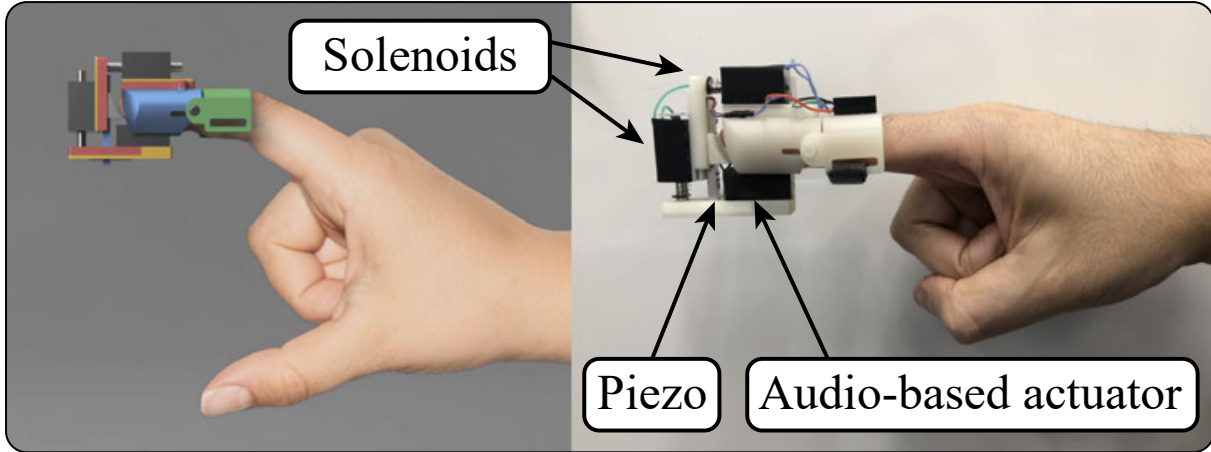


Figure A.6.: HapBand wearable fingertip.

Additionally, there is a TES/EMS module ($116mm \times 52mm \times 25mm$) providing tendon and muscle electrical stimulation (Figure A.5 right). This module uses an off-the-shelf transcutaneous nerve stimulator (Schwa Medico Medizintechnik Art.-Nr. 104099-V08), the PCB and the firmware are based on the openEMSstim project by Pedro Lopes and Max Pfeiffer³⁴. The TES/EMS module supports two channels (i.e., two muscles or tendons can be stimulated independently by two pairs of electrodes connected from the module to the selected arm muscles). For every channel, experiment operators can set the intensity and the duration of the electrical pulse by using a Unity plugin that manages the wireless connection with the module and safely keeps the parameters under the clinical limits established by the analog nerve stimulator.

The device case was 3d-printed with resin material and the total weight is 31 grams. The fingertip wearable (Figure A.6) is composed of a set of pieces. The whole set is presented in Figure A.7, showing how the structure is mechanically connected by electromagnetic solenoids. The top push-pull solenoid provides a tapping sensation on the fingertip and the front solenoid provides soft touches on the finger pulp (not used in the presented studies). The vibration sensations on the fingertip are provided with a piezo actuator measuring $35mm \times 4mm \times 4mm$ (Samsung PHAH353832XX, 120Vpp AC, sine wave @230Hz) which is controlled by a haptic driver (Texas Instruments DRV2667 by the I2C protocol). The piezo element touches the fingertip whenever the top solenoid is closed. Additionally, when the front solenoid is closed, an audio-based actuator ($23mm \times 8mm \times 8mm$, Alps Haptic Reactor⁵) touches the finger to provide tactile sensations on the finger pulp. Such an actuator relies on two resonant frequencies to reproduce compelling vibrotactile feedback. The input signal can be an audio pattern from real-time or pre-recorded sounds. For example, the sound produced by sliding the fingertip on a carpet can be recorded with a microphone, then amplified and reproduced with the Haptic Reactor to resemble the same sensation while a VE user is performing the same finger sliding action over a virtual surface. Our device

³<https://github.com/PedroLopes/openEMSstim/>

⁴<https://bitbucket.org/MaxPfeiffer/letyourbodymove/wiki/Home>

⁵<https://tech.alpsalpine.com/prod/e/html/haptic/>

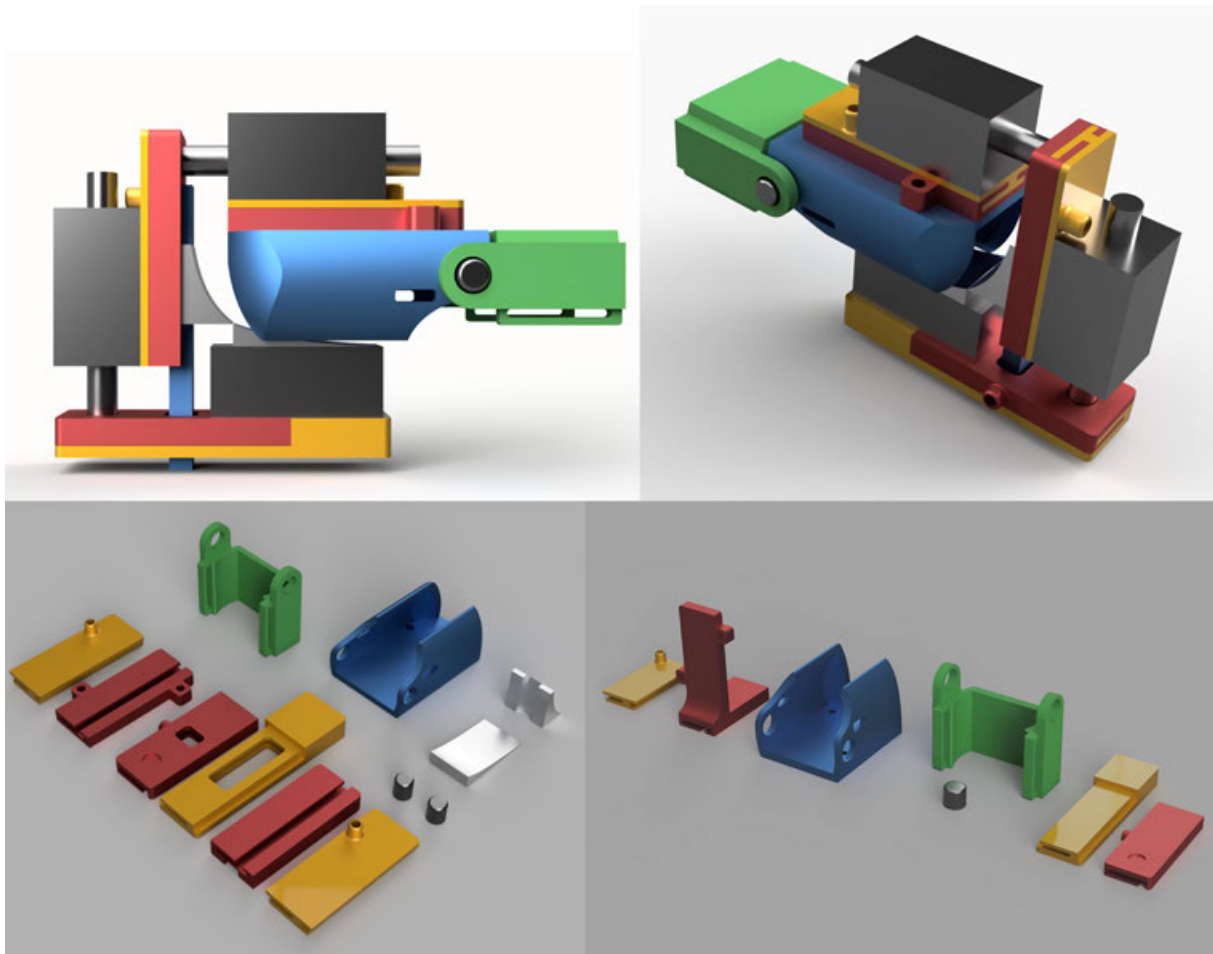


Figure A.7.: 3D-printable parts of the HapBand fingertip.

currently supports pre-recorded patterns and the implementation of real-time streaming is ongoing.

Furthermore, we developed a plugin for Unity to manage and control all the sensors and actuators connected to the HapBand modules (Figure A.8 left). In addition to UI for controlling/enabling sensations, the plugin also presents real-time information regarding the wireless connection, as well as, debugging information from pressure sensors (up to two) and capacitive pins (up to 8, used for input interaction in VEs). For a complete list of all the actuators and sensors available check the list of connection pins for the tactile module (Figure A.8 center) and the TES/EMS module (Figure A.8 right).

This device was utilized to conduct the study combining pseudo-haptics, tactile and kinesthetic feedback (see Section 7.4.2). We published all the required resources for the experiment replicability under an open soft/hardware repository⁶.

⁶<https://github.com/tlon-citizen/HapBand>

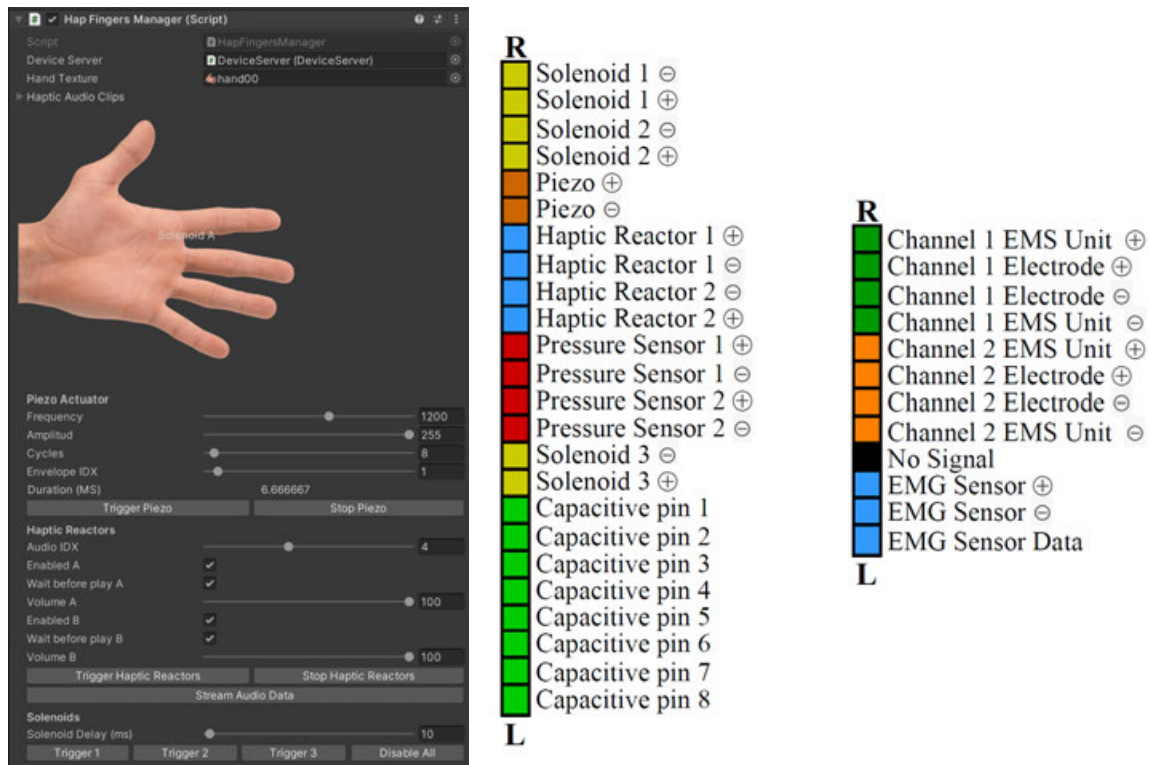


Figure A.8.: HapBand Unity Plugin and pins for actuator/sensor connections.

A.4. HapGloves

The HapGloves are a pair of gloves for VE interaction. They rely on hand tracking (i.e., Leap Motion) to provide vibrotactile feedback on fingers and palm surface. The device contains 14 LRA actuators (PMC10-100⁷) for each hand, driven independently with PWM signals and managed wirelessly from the computer using Bluetooth Low Energy technology (see Figure A.9). All the electronics and power sources are enclosed in a fore-arm band, offering freedom of movement and comfort for common hand-interaction tasks in VR environments.

The actuators are controlled by an Adafruit 16-channel 12-bit pulse width modulation (PWM) driver⁸. A self-made circuit board organizes the connections, provides signal enhancements (including amplifying, basic active breaking, and basic overdriving), and fits directly onto the PWM driver (see Figure A.9a). Each glove is powered by a 3.7V lithium polymer ion (LiPo) rechargeable battery. To mount the circuitry around the arm, all the components are installed in a 3D-printed case, which is attached to a neoprene arm belt. The case is meant to be worn on the forearm, close to the elbow, pointing outside to keep the arms able to rest and interact freely in the personal space. The driver is connected to an ARM Cortex System on a Chip (SoC)⁹ via I2C. In addition, the SoC features Bluetooth Low Energy (BLE), which enables the wireless communication between the computer and the haptic gloves, decoupling the client PC which runs a UDP server sending activation commands to the vibrators according to the user actions.

⁷<http://www.precisionmicrodrives.com/>

⁸<https://www.adafruit.com/product/815>

⁹<https://www.nordicsemi.com/products/nRF51822>

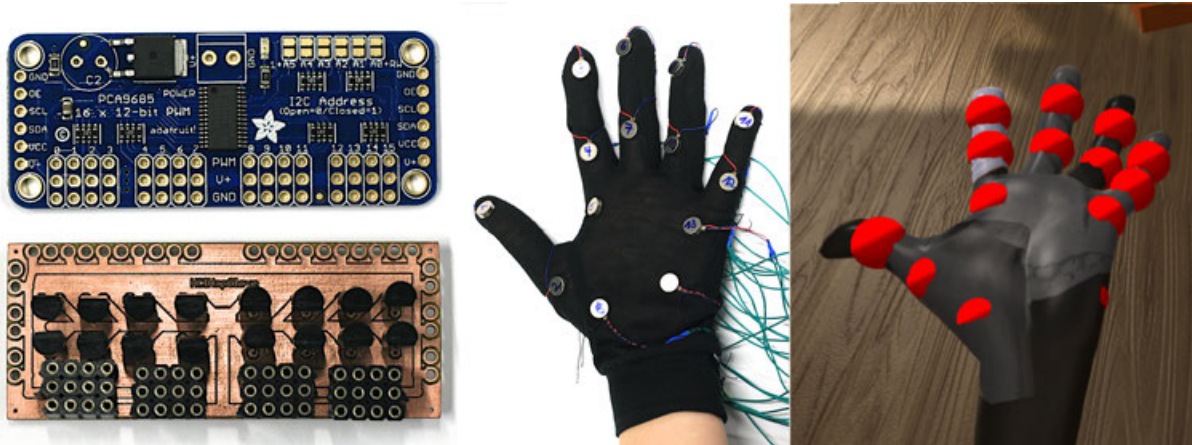


Figure A.9.: Arrangement and components of the vibrotactile display: (a) PWM signal controller for the 14 actuators. (b) Distribution of the vibration actuators on the hand. (c) Corresponding representation of the hand in VR (showing debugging spheres to represent the vibration points).

The case also contains USB battery recharging and its dimensions are 108mm × 80mm × 39mm. The HapGloves computer-to-device latency was measured with a high-speed camera at 240 frames per second. Each frame was analyzed to determine the time the signal was sent and the time the vibration actuators started swinging. The calculated latency is $25\text{ms} \pm 4.166$, which is near the “impact threshold” defined by Jay et al. [JGH07]. This means the user’s performance may decrease slightly, but the user stays unaware of the latency. The user would start noticing the latency when the system’s latency exceeded the “perception threshold” at 50ms. There was no measurable difference in latency between driving one motor and driving all motors at once because of the buffering settings in our embedded code and our multi-threaded approach on the client side. The presented value should be added to the latency between the hand tracking system and the UDP server to get the end-to-end latency, which makes a total of 43ms, which is still compatible with users’ tolerance between sensations corresponding to visual and tactile modalities [Shi+10].

This device was utilized to reproduce the Long-Arm illusion (see Section 6.2). Also, the device is available as an open-hardware project¹⁰.

A.5. HapShoes

HapShoes consist of a pair of anatomic soles. Every sole is connected to a small electronics compartment (i.e., wireless module) that can be comfortably attached to the ankle. Every sole contains an arrangement of pressure sensors (i.e., to detect gait stages and specific stances) and an embedded audio-based tactile actuator (see Figure A.10). Every sole, including the electronics case, weights 52 grams.

Every sole provides audio-based tactile feedback, in the medial plantar area ($9 \times 10 \times 22.6\text{mm}^3$) using a haptic reactor¹¹. An Espressif ESP32 microprocessor controls the haptic reactor through an I2S 3W Class D amplifier and also collects pressure values from an array of six force-sensitive resistors (0.5 inches

¹⁰<https://github.com/tlon-citizen/HapGloves>

¹¹<https://www.alps.com/prod/info/E/HTML/Haptic>

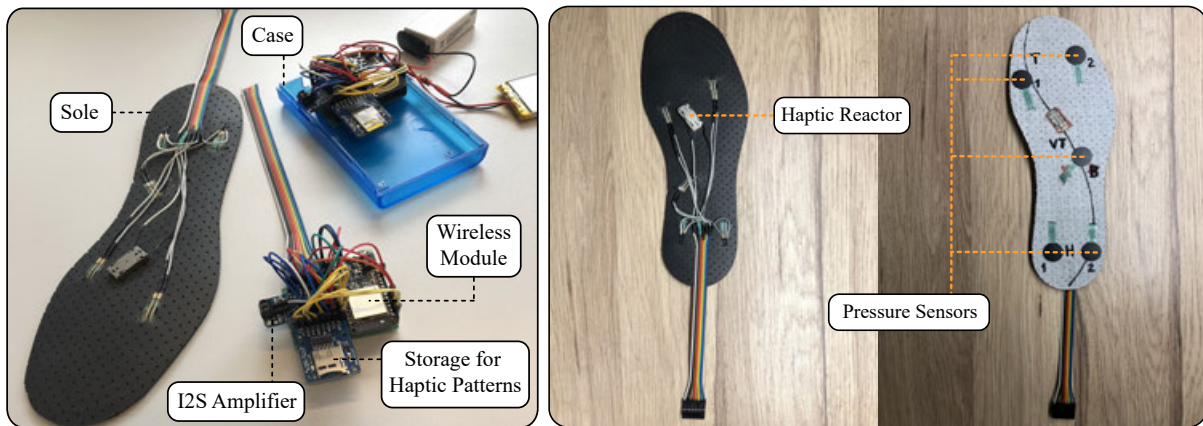


Figure A.10.: HapShoe components.

diameter) distributed ergonomically across the sole, transferring pressure data to the computer at a rate of 50Hz over WiFi. The system features 520Kb RAM and is powered by rechargeable 18650HG2 Li-Ion batteries. The actuator-to-PC latency is approximately 28 ms.

This device was utilized to conduct the study on obstacle detection (see Section 9.2.1).

A.6. HapHandle

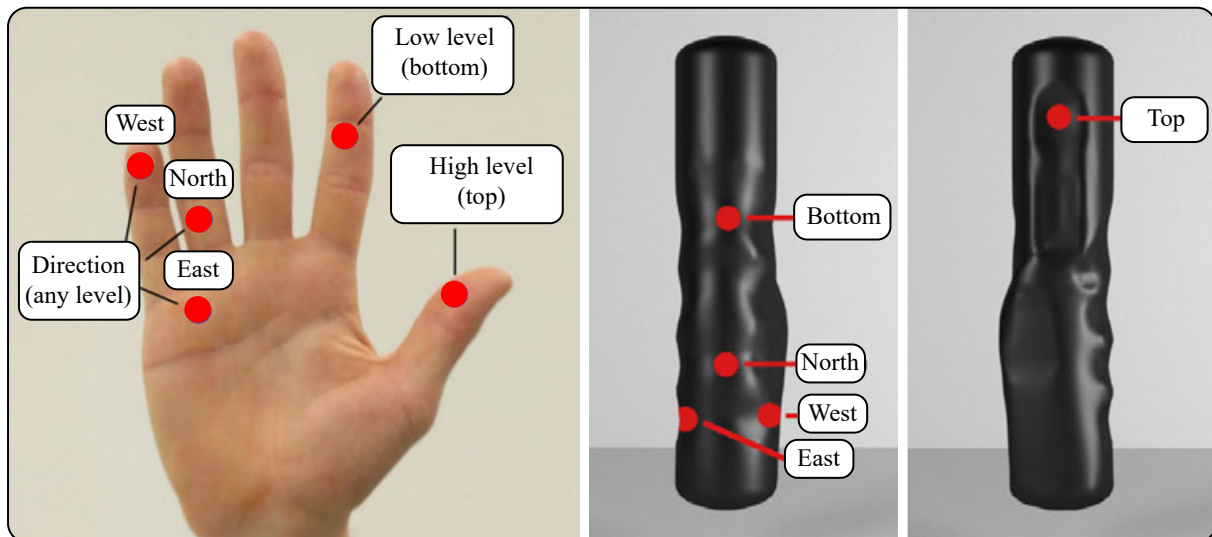


Figure A.11.: Placement of the actuators on the handle and corresponding positions on the hand.

HapHandle is an anatomical and comfortable handle to detect obstacles. It provides vibrotactile feedback according to obstacle distances which are measured by sensors. It also contains five haptic drivers¹² controlling five piezo discs with a 9mm diameter. Every piezo haptic driver integrates a 105-V boost switch, an amplifier, supporting overdriving and active breaking. The tactile signals can be parameter-

¹²<http://www.ti.com/product/DRV2667>

ized by frequency and amplitude simultaneously, as well as signal envelopes at the beginning/end of the signal.

All the piezo elements and drivers are connected to an Arduino-compatible microcontroller¹³ based on an ARM Cortex M0 processor, clocked at 48 MHz at 3.3V, and featuring Bluetooth Low Energy. Distance estimation is supported by two sensors. First, a high-performance optical distance measurement sensor¹⁴, based on an edge-emitting, 905nm (1.3 watts), single-stripe laser transmitter with a 0-40m range and an accuracy of ± 2.5 cm. Second, an ultrasonic distance-sensor¹⁵ with a calibrated beam pattern with a resolution of 1 inch, a 20Hz reading rate, and a range starting from 6 inches to 254 inches.

Additionally, the device includes an IMU with 9-DoF which enables the device to point out at a specific direction, record the distance to the closest obstacle and send the data wirelessly to a processing computer. For a specific position, such processing creates a model of obstacles surrounding the user with the corresponding positions. Once the model is created, the user can perceive vibrotactile notifications for the closer obstacle at different areas of the hand according to the obstacle position and elevation (see Figure A.11).

The HapHandle frequency for vibrotactile stimuli is 240Hz and the handle layout was designed to leave at minimum 11mm space between piezo actuators. This is compatible with studies on two-point discriminability on the palm (~ 10 mm) and pressure sensitivity evoked by vibrotactile stimuli (between 220Hz and 300Hz) [Wei68].

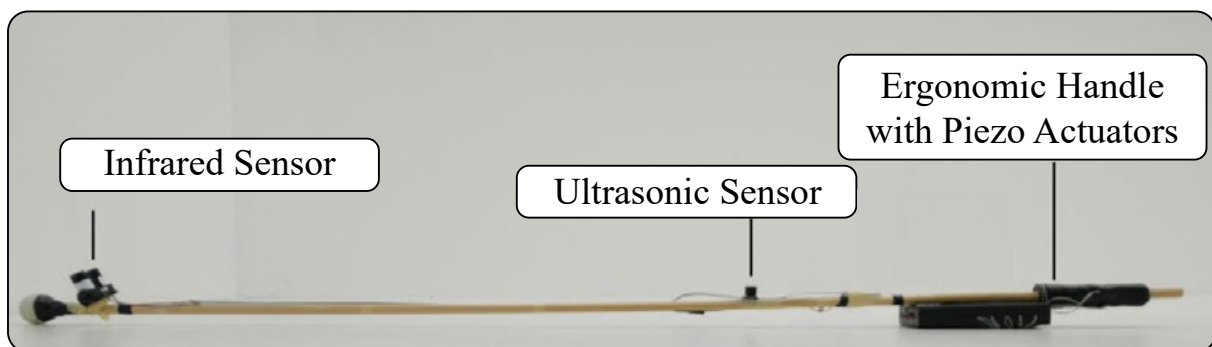


Figure A.12.: HapHandle testing prototype (STIC [Her+19]). The image shows the placement of the sensors, the control board and the HapHandle.

For testing purposes, this device (Figure A.12) was mounted on a typical white cane consisting of a wooden stick with a plastic ball attached to the lower end and a 3D printed plastic ergonomic handle attached to the upper end (151cm long, 477 grams, 1.5cm diameter). To minimize the needed force to balance and sweep the cane horizontally, this case is placed near the handle on the stick's bottom side [Her+19].

This device was utilized to conduct the study on obstacle detection (see Section 10.2.2).

¹³<https://www.adafruit.com/product/2995>

¹⁴<https://www.sparkfun.com/products/14032>

¹⁵https://www.maxbotix.com/Ultrasonic_Sensors/MB1010.htm

A.7. HapModule

HapModule is a minimalistic version of HapRing that can be attached to different parts of the body to provide vibrotactile feedback. It has the shape of a small wearable box and is completely autonomous by using a wireless-enabled microcontroller; the RF51822 SoC (System on a Chip) supporting Bluetooth LE (2.4 GHz Band). All the components are placed on a 3D printed case ($30mm \times 23mm \times 18mm$) including an LRA (PMC10-100) attached to an active haptic driver (TI DRV2605), and a Lithium Polymer Ion (LyPo) rechargeable battery which outputs 3.7V at 150mAh (see Figure A.13).

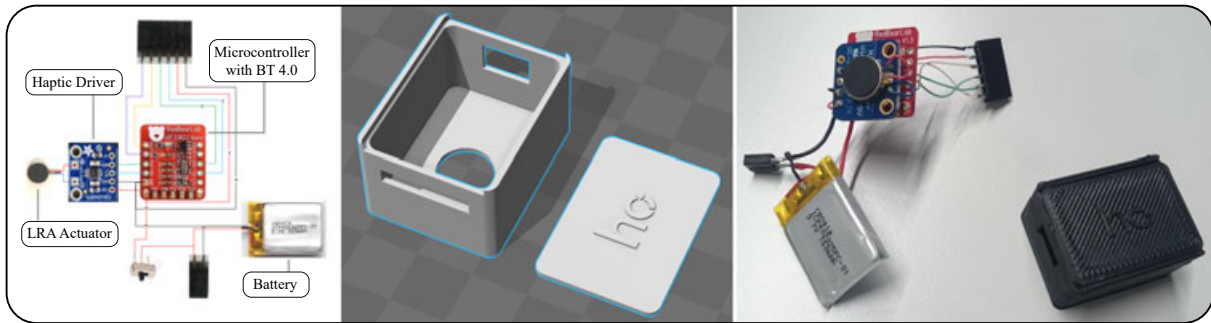


Figure A.13.: Electronic sketch, 3D model of the module case, and picture of the final assembly including the 3D printed case.

This device was utilized to conduct the study on 3D guidance (see Section 8.4).

Bibliography

- [AA13] Argelaguet, F. and Andujar, C. A Survey of 3D Object Selection Techniques for Virtual Environments. In: *Computers & Graphics* 37 (2013), pp. 121–136. DOI: <https://doi.org/10.1016/j.cag.2012.12.003>.
- [AC06] Avanzini, F. and Crosato, P. Haptic-Auditory Rendering and Perception of Contact Stiffness. In: *Haptic and Audio Interaction Design*. Ed. by D. McGookin and S. Brewster. Berlin, Heidelberg: Springer Berlin Heidelberg, 2006, pp. 24–35. ISBN: 978-3-540-37596-8.
- [Ach+14] Achibet, M., Marchal, M., Argelaguet, F., and Lécuyer, A. The Virtual Mitten: A Novel Interaction Paradigm for Visuo-haptic Manipulation of Objects Using Grip Force. In: *2014 IEEE Symposium on 3D User Interfaces (3DUI)*. 2014, pp. 59–66.
- [Ach+15] Achibet, M., Girard, A., Talvas, A., Marchal, M., and Lécuyer, A. Elastic-Arm: Human-scale Passive Haptic Feedback for Augmenting Interaction and Perception in Virtual Environments. In: *2015 IEEE Virtual Reality (VR)*. 2015, pp. 63–68.
- [Ach+17] Achibet, M., Le Gouis, B., Marchal, M., Léziart, P., Argelaguet, F., Girard, A., Lécuyer, A., and Kajimoto, H. FlexiFingers: Multi-finger Interaction in VR Combining Passive Haptics and Pseudo-haptics. In: *2017 IEEE Symposium on 3D User Interfaces (3DUI)*. 2017, pp. 103–106.
- [Ach15] Achibet, M. “Contributions to the design of novel hand-based interaction techniques for virtual environments”. PhD thesis. INSA de Rennes, France, 2015. URL: <https://tel.archives-ouvertes.fr/tel-01312186>.
- [AF18] Abtahi, P. and Follmer, S. Visuo-Haptic Illusions for Improving the Perceived Performance of Shape Displays. In: *Proceedings of the 2018 CHI Conference on Human Factors in Computing Systems*. Association for Computing Machinery, 2018, pp. 1–13. DOI: [10.1145/3173574.3173724](https://doi.org/10.1145/3173574.3173724).
- [ALS15] Ariza, O., Lubos, P., and Steinicke, F. HapRing: A Wearable Haptic Device for 3D Interaction. In: *Mensch Und Computer 2015 - Proceedings*, Stuttgart, Germany, September 6-9, 2015. De Gruyter Oldenbourg, 2015, pp. 421–424. URL: <https://dl.gi.de/20.500.12116/7840>.
- [AMD17] Ahmad, A., Migniot, C., and Dipanda, A. Tracking Hands in Interaction with Objects: A Review. In: *2017 13th International Conference on Signal-Image Technology Internet-Based Systems (SITIS)*. 2017, pp. 360–369. DOI: [10.1109/SITIS.2017.66](https://doi.org/10.1109/SITIS.2017.66).
- [AMH95] Akamatsu, M., MacKenzie, I. S., and Hasbroucq, T. A Comparison of Tactile, Auditory, and Visual Feedback in A Pointing Task Using A Mouse-type Device. In: *Ergonomics* 38 (1995), pp. 816–827. URL: <http://view.ncbi.nlm.nih.gov/pubmed/7729406>.

- [AR03] Armel, K. C. and Ramachandran, V. S. Projecting Sensations to External Objects: Evidence from Skin Conductance Response. In: *Proceedings of the Royal Society of London B: Biological Sciences* 270 (2003), pp. 1499–1506. DOI: [10.1098/rspb.2003.2364](https://doi.org/10.1098/rspb.2003.2364). URL: <http://rspb.royalsocietypublishing.org/content/270/1523/1499>.
- [Ari+15] Ariza, O., Lubos, P., Steinicke, F., and Bruder, G. Ring-shaped Haptic Device with Vibrotactile Feedback Patterns to Support Natural Spatial Interaction. In: *Proceedings of the 25th International Conference on Artificial Reality and Telexistence and 20th Eurographics Symposium on Virtual Environments*. Eurographics Association, 2015, pp. 175–181. DOI: [10.2312/egve.20151326](https://doi.org/10.2312/egve.20151326).
- [Ari+16] Ariza, O., Freiwald, J., Laage, N., Feist, M., Salloum, M., Bruder, G., and Steinicke, F. Inducing Body-Transfer Illusions in VR by Providing Brief Phases of Visual-Tactile Stimulation. In: *Proceedings of the 2016 Symposium on Spatial User Interaction*. Tokyo, Japan: Association for Computing Machinery, 2016, pp. 61–68. DOI: [10.1145/2983310.2985760](https://doi.org/10.1145/2983310.2985760).
- [Ari+17] Ariza, O., Lange, M., Steinicke, F., and Bruder, G. Vibrotactile Assistance for User Guidance Towards Selection Targets in VR and the Cognitive Resources Involved. In: *2017 IEEE Symposium on 3D User Interfaces (3DUI)*. 2017, pp. 92–96. DOI: [10.1109/3DUI.2017.7893323](https://doi.org/10.1109/3DUI.2017.7893323).
- [Ari+18] Ariza, O., Katzakis, N., Bruder, G., and Steinicke, F. Analysis of Proximity-Based Multimodal Feedback for 3D Selection in Immersive Virtual Environments. In: *2018 IEEE Conference on Virtual Reality and 3D User Interfaces (VR)*. 2018, pp. 327–334. DOI: [10.1109/VR.2018.8446317](https://doi.org/10.1109/VR.2018.8446317).
- [ARR02] Avanzini, F., Rath, M., and Rocchesso, D. Physically-based Audio Rendering of Contact. In: *Proceedings. IEEE International Conference on Multimedia and Expo*. Vol. 2. 2002, pp. 445–448. DOI: [10.1109/ICME.2002.1035636](https://doi.org/10.1109/ICME.2002.1035636).
- [AS20] Ariza, O. and Steinicke, F. Conveying Holistic Touch Illusions by Combining Tactile and Proprioceptive Feedback with Pseudo-Haptics in VR (in Submission). In: *INTERACT, International Conference on Human–Computer Interaction*. IFIP, 2020.
- [Azm+16] Azmandian, M., Hancock, M., Benko, H., Ofek, E., and Wilson, A. D. Haptic Retargeting: Dynamic Repurposing of Passive Haptics for Enhanced Virtual Reality Experiences. In: *Proceedings of the 2016 CHI Conference on Human Factors in Computing Systems*. Association for Computing Machinery, 2016, pp. 1968–1979. DOI: [10.1145/2858036.2858226](https://doi.org/10.1145/2858036.2858226).
- [Bad92] Baddeley, A. Working Memory. In: *Science* 255 (1992), pp. 556–559.
- [BAS19] Brauer, C., Ariza, O., and Steinicke, F. An Active Tangible Device for Multitouch-Display Interaction. In: *Proceedings of Mensch Und Computer 2019*. Hamburg, Germany: Association for Computing Machinery, 2019, pp. 439–444. DOI: [10.1145/3340764.3344436](https://doi.org/10.1145/3340764.3344436).
- [Bau+10] Bau, O., Poupyrev, I., Israr, A., and Harrison, C. TeslaTouch: Electro vibration for Touch Surfaces. In: *Proceedings of the 23rd Annual ACM Symposium on User Interface Software and Technology*. Association for Computing Machinery, 2010, pp. 283–292. DOI: [10.1145/1866029.1866074](https://doi.org/10.1145/1866029.1866074).

- [BB91] Bushnell, E. W. and Boudreau, J. P. The Development of Haptic Perception During Infancy. In: *The Psychology of Touch*. Lawrence Erlbaum Associates, Inc., 1991, pp. 139–161.
- [BC03] Burdea, G. C. and Coiffet, P. *Virtual Reality Technology*. Wiley-IEEE Press, 2003.
- [BC19] Buttussi, F. and Chittaro, L. Locomotion in Place in Virtual Reality: A Comparative Evaluation of Joystick, Teleport, and Leaning. In: *IEEE Transactions on Visualization and Computer Graphics* (2019).
- [BC98] Botvinick, M. and Cohen, J. Rubber Hands ‘feel’ Touch That Eyes See. In: *Nature* 391 (1998), p. 756. DOI: [10.1038/35784](https://doi.org/10.1038/35784).
- [BD11] Bullock, I. and Dollar, A. Classifying Human Manipulation Behavior. In: *IEEE International Conference on Rehabilitation Robotics* (2011). DOI: [10.1109/ICORR.2011.5975408](https://doi.org/10.1109/ICORR.2011.5975408).
- [Ber+18] Berger, C., Gonzalez-Franco, M., Ofek, E., and Hinckley, K. The Uncanny Valley of Haptics. In: *Science Robotics* 3 (2018), eaar7010. DOI: [10.1126/scirobotics.aar7010](https://doi.org/10.1126/scirobotics.aar7010).
- [BF05] Bowman, D. A. and Frohlich, B. New Directions in 3D User Interfaces. In: *Proceedings of the 2005 IEEE Conference 2005 on Virtual Reality*. IEEE Computer Society, 2005, p. 312. DOI: [10.1109/VR.2005.58](https://doi.org/10.1109/VR.2005.58).
- [BH17] Bermejo, C. and Hui, P. A Survey on Haptic Technologies for Mobile Augmented Reality. 2017. arXiv: [1709.00698](https://arxiv.org/abs/1709.00698) [[cs](https://arxiv.org/archive/cs).[HC](https://arxiv.org/archive/hc)].
- [BKC01] Biocca, F., Kim, J., and Choi, Y. Visual Touch in Virtual Environments: An Exploratory Study of Presence, Multimodal Interfaces, and Cross-Modal Sensory Illusions. In: *Presence: Teleoper. Virtual Environ* 10 (2001), pp. 247–265. DOI: [10.1162/105474601300343595](https://doi.org/10.1162/105474601300343595).
- [BLS15] Bruder, G., Lubos, P., and Steinicke, F. Cognitive Resource Demands of Redirected Walking. In: *TVCG* (2015).
- [BMK19] Bergström, J., Mottelson, A., and Knibbe, J. Resized Grasping in VR: Estimating Thresholds for Object Discrimination. English. In: *UIST ’19: Proceedings of the 32nd Annual ACM Symposium on User Interface Software and Technology*. null ; Conference date: 20-10-2019 Through 23-10-2019. Association for Computing Machinery, 2019, pp. 1175–1183. DOI: [10.1145/3332165.3347939](https://doi.org/10.1145/3332165.3347939).
- [Bog+06] Bogacz, R., Brown, E., Moehlis, J., Holmes, P., and Cohen, J. The Physics of Optimal Decision Making: A Formal Analysis of Models of Performance in Two-alternative Forced-choice Tasks. In: *Psychological review* 113 (2006), pp. 700–65. DOI: [10.1037/0033-295X.113.4.700](https://doi.org/10.1037/0033-295X.113.4.700).
- [Bow+01] Bowman, D. A., Wingrave, C. A., Campbell, J. M., and Ly, V. Q. Using Pinch Gloves for Both Natural and Abstract Interaction Techniques in Virtual Environments. In: *Proceedings of HCI International*. Vol. 1. 2001, pp. 629–633.
- [Bow+04] Bowman, D. A., Kruijff, E., LaViola Jr, J. J., and Poupyrev, I. *3D User Interfaces: Theory and Practice*. Addison-Wesley, 2004.

- [BR19] Barnaby, G. and Roudaut, A. Mantis: A Scalable, Lightweight and Accessible Architecture to Build Multiform Force Feedback Systems. In: *Proceedings of the 32nd Annual ACM Symposium on User Interface Software and Technology*. Association for Computing Machinery, 2019, pp. 937–948. DOI: [10.1145/3332165.3347909](https://doi.org/10.1145/3332165.3347909).
- [Bro94] Brooks, F. Is There Any Real Virtue in Virtual Reality. In: 1994.
- [BSC07] Bratt, M., Smith, C., and Christensen, H. I. Minimum Jerk Based Prediction of User Actions for A Ball Catching Task. In: *2007 IEEE/RSJ International Conference on Intelligent Robots and Systems*. 2007, pp. 2710–2716.
- [BSS] Bruder, G., Steinicke, F., and Stuerzlinger, W. Touching the Void Revisited: Analyses of Touch Behavior On and Above Tabletop Surfaces. In: *Proceedings of IFIP TC13 Conference on Human-Computer Interaction (INTERACT)*.
- [BSS13a] Bruder, G., Steinicke, F., and Stuerzlinger, W. Effects of Visual Conflicts on 3D Selection Task Performance in Stereoscopic Display Environments. In: *Proceedings of IEEE 3DUI*. 2013, pp. 115–118.
- [BSS13b] Bruder, G., Steinicke, F., and Stuerzlinger, W. Touching the Void Revisited: Analyses of Touch Behavior On and Above Tabletop Surfaces. In: *Lecture Notes in Computer Science: Human-Computer Interaction - INTERACT (2013)*, pp. 278–296.
- [BU18] Ban, Y. and Ujitoko, Y. TactGAN: Vibrotactile Designing Driven by GAN-Based Automatic Generation. In: *SIGGRAPH Asia 2018 Emerging Technologies*. Association for Computing Machinery, 2018. DOI: [10.1145/3275476.3275484](https://doi.org/10.1145/3275476.3275484).
- [Bur+05] Burns, E., Razzaque, S., Panter, A. T., Whitton, M., McCallus, M. R., and Brooks, F. P. The Hand Is Slower Than the Eye: A Quantitative Exploration of Visual Dominance Over Proprioception. In: *IEEE Proceedings of the Virtual Reality (VR)*. IEEE, 2005, pp. 3–10.
- [Bur96] Burdea, G. C. *Force and Touch Feedback for Virtual Reality*. USA: John Wiley & Sons, Inc., 1996. ISBN: 0471021415.
- [Buz+13] Buzzi, M., Buzzi, M., Leporini, B., and Paratore, M. Vibro-Tactile Enrichment Improves Blind User Interaction with Mobile Touchscreens. In: *Lecture Notes in Computer Science: Human-Computer Interaction - INTERACT*. 2013, pp. 641–648.
- [BW11] Böttcher, G. and Wolter, F.-E. *Haptic Interaction with Deformable Objects*. Jan. 2011. ISBN: 978-0-85729-935-2. DOI: [10.1007/978-0-85729-935-2](https://doi.org/10.1007/978-0-85729-935-2).
- [CB04] Chittaro, L. and Burigat, S. 3D Location-pointing As A Navigation Aid in Virtual Environments. In: *AVI*. ACM. 2004.
- [CB05] Cockburn, A. and Brewster, S. Multimodal Feedback for the Acquisition of Small Targets. In: *Ergonomics* 48 (2005), pp. 1129–1150. DOI: [10.1080/00140130500197260](https://doi.org/10.1080/00140130500197260).
- [Cha+10] Chan, L.-W., Kao, H.-S., Chen, M. Y., Lee, M.-S., Hsu, J., and Hung, Y.-P. Touching the Void: Direct-Touch Interaction for Intangible Displays. In: *Proceedings of ACM CHI*. 2010, pp. 2625–2634.

- [Cha+13] Chan, L., Liang, R.-H., Tsai, M.-C., Cheng, K.-Y., Su, C.-H., Chen, M. Y., Cheng, W.-H., and Chen, B.-Y. Fingerpad: Private and Subtle Interaction Using Fingertips. In: *Proceedings of ACM User Interface Software and Technology (UIST)*. 2013, pp. 255–260.
- [Cha+14] Chancey, E. T., Brill, J. C., Sitz, A., Schmuntzsch, U., and Bliss, J. P. Vibrotactile Stimuli Parameters on Detection Reaction Times. In: *Proceedings of the Human Factors and Ergonomics Society Annual Meeting* 58 (2014), pp. 1701–1705. DOI: [10.1177/1541931214581355](https://doi.org/10.1177/1541931214581355). URL: <http://pro.sagepub.com/content/58/1/1701.abstract>.
- [Che+13] Chen, K.-Y., Lyons, K., White, S., and Patel, S. UTrack: 3D Input Using Two Magnetic Sensors. In: *Proceedings of ACM User Interface Software and Technology (UIST)*. 2013, pp. 237–244. DOI: [10.1145/2501988.2502035](https://doi.org/10.1145/2501988.2502035).
- [Che+15] Cheng, L.-P., Roumen, T., Rantzsch, H., Köhler, S., Schmidt, P., Kovacs, R., Jasper, J., Kemper, J., and Baudisch, P. TurkDeck: Physical Virtual Reality Based on People. In: *Proceedings of the 28th Annual ACM Symposium on User Interface Software and Technology*. Association for Computing Machinery, 2015, pp. 417–426. DOI: [10.1145/2807442.2807463](https://doi.org/10.1145/2807442.2807463).
- [Che+17] Cheng, L.-P., Ofek, E., Holz, C., Benko, H., and Wilson, A. D. Sparse Haptic Proxy: Touch Feedback in Virtual Environments Using A General Passive Prop. In: *Proceedings of the 2017 CHI Conference on Human Factors in Computing Systems*. Association for Computing Machinery, 2017, pp. 3718–3728. DOI: [10.1145/3025453.3025753](https://doi.org/10.1145/3025453.3025753).
- [Chi+15] Chinello, F., Malvezzi, M., Pacchierotti, C., and Prattichizzo, D. Design and Development of A 3RRS Wearable Fingertip Cutaneous Device. In: *2015 IEEE International Conference on Advanced Intelligent Mechatronics (AIM)*. 2015, pp. 293–298. DOI: [10.1109/AIM.2015.7222547](https://doi.org/10.1109/AIM.2015.7222547).
- [Cho+17a] Choi, A., Kim, C., Gwak, M., and Sung, M. Y. Haptic Interactions for Probing Real Objects in Remote Places. In: *International Journal of Applied Engineering Research* 12 (2017), pp. 14948–14954.
- [Cho+17b] Choi, I., Culbertson, H., Miller, M. R., Olwal, A., and Follmer, S. Grabity: A Wearable Haptic Interface for Simulating Weight and Grasping in Virtual Reality. In: *Proceedings of the 30th Annual ACM Symposium on User Interface Software and Technology*. Association for Computing Machinery, 2017, pp. 119–130. DOI: [10.1145/3126594.3126599](https://doi.org/10.1145/3126594.3126599).
- [Cho+18] Choi, I., Ofek, E., Benko, H., Sinclair, M., and Holz, C. CLAW: A Multifunctional Handheld Haptic Controller for Grasping, Touching, and Triggering in Virtual Reality. In: *Proceedings of the 2018 CHI Conference on Human Factors in Computing Systems*. Association for Computing Machinery, 2018, pp. 1–13. DOI: [10.1145/3173574.3174228](https://doi.org/10.1145/3173574.3174228).
- [CK13] Choi, S. and Kuchenbecker, K. J. Vibrotactile Display: Perception, Technology, and Applications. In: *Proceedings of the IEEE* 101 (2013), pp. 2093–2104. DOI: [10.1109/JPROC.2012.2221071](https://doi.org/10.1109/JPROC.2012.2221071).

- [CM06] Chatterjee, R. and Matsuno, F. Design of A Touch Sensor Based Single Finger Operated Wearable User-Interface Terminal. In: *Proceedings of SICE-ICASE International Joint Conference*. 2006, pp. 4142–4147. DOI: [10.1109/SICE.2006.314614](https://doi.org/10.1109/SICE.2006.314614).
- [Col96] Collett, T. S. Vision: Simple Stereopsis. In: *Current Biology* 6 (1996), pp. 1392–1395. DOI: [https://doi.org/10.1016/S0960-9822\(96\)00739-7](https://doi.org/10.1016/S0960-9822(96)00739-7).
- [Con+13] Connors, E. C., Yazzolino, L. A., Sánchez, J., and Merabet, L. B. Development of An Audio-based Virtual Gaming Environment to Assist with Navigation Skills in the Blind. In: *JVE* (2013).
- [Cru+92] Cruz-Neira, C., Sandin, D. J., DeFanti, T. A., Kenyon, R. V., and Hart, J. C. The CAVE: Audio Visual Experience Automatic Virtual Environment. In: *Communications of the ACM* 35 (1992), pp. 64–73.
- [CSO18] Culbertson, H., Schorr, S. B., and Okamura, A. M. Haptics: The Present and Future of Artificial Touch Sensation. In: *Annual Review of Control, Robotics, and Autonomous Systems* 1 (2018), pp. 385–409. DOI: [10.1146/annurev-control-060117-105043](https://doi.org/10.1146/annurev-control-060117-105043).
- [Cut89] Cutkosky, M. On Grasp Choice, Grasp Models, and the Design of Hands for Manufacturing Tasks. In: *Robotics and Automation, IEEE Transactions on* 5 (1989), pp. 269–279. DOI: [10.1109/70.34763](https://doi.org/10.1109/70.34763).
- [DB10] Dakopoulos, D. and Bourbakis, N. G. Wearable Obstacle Avoidance Electronic Travel Aids for Blind: A Survey. In: *IEEE Transactions on Systems, Man, and Cybernetics, Part C (Applications and Reviews)* 40 (2010), pp. 25–35.
- [DBS97] DiFranco, D. E., Beauregard, G., and Srinivasan, M. The Effect of Auditory Cues on the Haptic Perception of Stiffness in Virtual Environments. In: 1997.
- [Deb+02] Debus, T., Jang, T.-J., Dupont, P., and Howe, R. Multi-channel Vibrotactile Display for Teleoperated Assembly. In: *Proceedings of the 2002 IEEE International Conference on Robotics and Automation*. 2002, pp. 592–597.
- [Dja98] Djajadiningrat, J. P. “Cubby: what you see is where you act. Interlacing the display and manipulation spaces”. PhD thesis. Industrial Design Engineering, TU Delft, 1998.
- [DKK07] Dvorkin, A. Y., Kenyon, R. V., and Keshner, E. A. Reaching Within A Dynamic Virtual Environment. In: *J. NeuroEng. Rehabil* 4 (2007). DOI: [doi:10.1186/1743-0003-4-23](https://doi.org/10.1186/1743-0003-4-23).
- [DKM99] Douglas, S. A., Kirkpatrick, A. E., and MacKenzie, I. S. Testing Pointing Device Performance and User Assessment with the ISO 9241, Part 9 Standard. In: *Proceedings of the SIGCHI Conference on Human Factors in Computing Systems*. ACM. 1999, pp. 215–222.
- [DM19] Di Luca, M. and Mahnan, A. Perceptual Limits of Visual-Haptic Simultaneity in Virtual Reality Interactions. In: *2019 IEEE World Haptics Conference, WHC 2019, Tokyo, Japan, July 9-12, 2019*. IEEE, 2019, pp. 67–72. DOI: [10.1109/WHC.2019.8816173](https://doi.org/10.1109/WHC.2019.8816173).

- [DPR17] Duen­te, T., Pfeiffer, M., and Rohs, M. Zap++: A 20-Channel Electrical Muscle Stim­ulation System for Fine-Grained Wearable Force Feedback. In: Proceedings of the 19th International Conference on Human-Computer Interaction with Mobile Devices and Ser­vices. Association for Computing Machinery, 2017. DOI: [10.1145/3098279.3098546](https://doi.org/10.1145/3098279.3098546).
- [EB02] Ernst, M. and Banks, M. Humans Integrate Visual and Haptic Information in A Statisti­cally Optimal Fashion. In: *Nature* 415 (2002), pp. 429–433. DOI: [10.1038/415429a](https://doi.org/10.1038/415429a).
- [Ehr12] Ehrsson, H. H. The Concept of Body Ownership and Its Relation to Multisensory Integra­tion. In: *The New Handbook of Multisensory Processes* (Jan. 2012), pp. 775–792.
- [Eri+08] Eriksson, L., Berglund, A., Willen, B., and Svensson, J. On Visual, Vibrotactile and 3D Audio Directional Cues for Dismounted Soldier Waypoint Navigation. In: *The Human Factors and Ergonomics Society 52nd Annual Meeting* (2008), pp. 1282–1286.
- [Ern06] Ernst, M. O. “Human Body Perception From The Inside Out”. In: ed. by G. Knoblich, I. M. Thornton, M. Grosjean, and M. Shiffrar. Oxford University Press, 2006. Chap. A Bayesian View on Multimodal Cue Integration, pp. 105–131.
- [Erp+10] Erp, J. B. F. van, Kyung, K.-U., Kassner, S., Carter, J., Brewster, S., Weber, G., and Andrew, I. Setting the Standards for Haptic and Tactile Interactions: ISO’s Work. In: *Haptics: Generating and Perceiving Tangible Sensations*. Springer Berlin Heidelberg, 2010, pp. 353–358.
- [ES03] ElKoura, G. and Singh, K. Handrix: Animating the Human Hand. In: Proceedings of the 2003 ACM SIGGRAPH/Eurographics Symposium on Computer Animation. Eurographics Association, 2003, pp. 110–119.
- [ESP04] Ehrsson, H. H., Spence, C., and Passingham, R. E. That’s My Hand! Activity in Premotor Cortex Reflects Feeling of Ownership of A Limb. In: *Science* 305 (2004), pp. 875–877. DOI: [10.1126/science.1097011](https://doi.org/10.1126/science.1097011).
- [Fan+16] Fani, S., Ciotti, S., Battaglia, E., Moscatelli, A., and Bianchi, M. W-FYD: A Wearable Fabric-based Display for Haptic Multi-Cue Delivery and Tactile Augmented Reality. In: *IEEE Transactions on Haptics* (2016), pp. 277–283. DOI: [10.1109/TOH.2017.2708717](https://doi.org/10.1109/TOH.2017.2708717).
- [Fan+20] Fang, C., Zhang, Y., Dworman, M., and Harrison, C. Wireality: Enabling Complex Tangi­ble Geometries in Virtual Reality with Worn Multi-String Haptics. In: Proceedings of the 2020 CHI Conference on Human Factors in Computing Systems. Association for Comput­ing Machinery, 2020, pp. 1–10. DOI: [10.1145/3313831.3376470](https://doi.org/10.1145/3313831.3376470).
- [FF19] Franinović, K. and Franzke, L. Shape Changing Surfaces and Structures: Design Tools and Methods for Electroactive Polymers. In: Proceedings of the 2019 CHI Conference on Human Factors in Computing Systems. Association for Computing Machinery, 2019, pp. 1–12. ISBN: 9781450359702. DOI: [10.1145/3290605.3300355](https://doi.org/10.1145/3290605.3300355).
- [FH14] Faeth, A. and Harding, C. Emergent Effects in Multimodal Feedback from Virtual Buttons. In: 21 (2014). DOI: [10.1145/2535923](https://doi.org/10.1145/2535923).

- [FH85] Flash, T. and Hogan, N. The Coordination of Arm Movements: An Experimentally Confirmed Mathematical Model. In: *Journal of Neuroscience* 5 (1985), pp. 1688–1703. DOI: [10.1523/JNEUROSCI.05-07-01688.1985](https://doi.org/10.1523/JNEUROSCI.05-07-01688.1985). URL: <https://www.jneurosci.org/content/5/7/1688>.
- [Fit54] Fitts, P. M. The Information Capacity of the Human Motor System in Controlling the Amplitude of Movement. In: *Journal of Experimental Psychology: General* 47 (1954), pp. 381–391.
- [Fol+12] Follmer, S., Leithinger, D., Olwal, A., Cheng, N., and Ishii, H. Jamming User Interfaces: Programmable Particle Stiffness and Sensing for Malleable and Shape-Changing Devices. In: *Proceedings of the 25th Annual ACM Symposium on User Interface Software and Technology*. Association for Computing Machinery, 2012, pp. 519–528. DOI: [10.1145/2380116.2380181](https://doi.org/10.1145/2380116.2380181).
- [Fre+20] Freiwald, J., Ariza, O., Janeh, O., and Steinicke, F. Walking by Cycling: A Novel In-Place Locomotion User Interface for Seated Virtual Reality Experiences. In: *Proceedings of the 2020 CHI Conference on Human Factors in Computing Systems*. Honolulu, HI, USA: Association for Computing Machinery, 2020, pp. 1–12. DOI: [10.1145/3313831.3376574](https://doi.org/10.1145/3313831.3376574).
- [Gac+16] Gacem, H., Bailly, G., Eagan, J., and Lecolinet, E. Impact of Motorized Projection Guidance on Spatial Memory. In: *SUI*. ACM, 2016.
- [GAF19] Gonzalez, E. J., Abtahi, P., and Follmer, S. Evaluating the Minimum Jerk Motion Model for Redirected Reach in Virtual Reality. In: *The Adjunct Publication of the 32nd Annual ACM Symposium on User Interface Software and Technology*. Association for Computing Machinery, 2019, pp. 4–6. DOI: [10.1145/3332167.3357096](https://doi.org/10.1145/3332167.3357096).
- [Gar08] Garreau, J. Touch Screen Technology, from Iphones to Ovens, Continues to Push Forward. In: (2008). URL: <http://www.washingtonpost.com/wp-dyn/content/article/2008/12/14/AR2008121402455.htm>.
- [GBC07] Gustafson-Pearce, O., Billett, E., and Cecelja, F. Comparison Between Audio and Tactile Systems for Delivering Simple Navigational Information to Visually Impaired Pedestrians. In: *British Journal of Visual Impairment* 25 (2007), pp. 255–265.
- [GC66] Glanzer, M. and Cunitz, A. Two Storage Mechanisms in Free Recall. In: *Journal of Verbal Learning and Verbal Behavior* (1966).
- [GCE08] Geniva, L., Chua, R., and Enns, J. T. Attention for Perception and Action: Task Interference for Action Planning, But Not for Online Control. In: *Experimental Brain Research* (2008), pp. 709–717.
- [Geo14] Georgiou, T. Human Haptic Perception in Virtual Environments: An Investigation of the Interrelationship Between Physical Stiffness and Perceived Roughness. In: 2014.
- [Ges13] Gescheider, G. *Psychophysics: The Fundamentals*. Taylor & Francis, 2013. ISBN: 9781134801299. URL: <https://books.google.de/books?id=fLYWFcuamPwC>.
- [Gib62] Gibson, J. J. Observations on Active Touch. In: *Psychological Review American Psychological Association* 69 (1962), pp. 477–491. DOI: <https://doi.org/10.1037/h0046962>.

- [GJ84] “Neural Mechanisms of Convergence and Accommodation”. In: *Theoretical and Applied Aspects of Eye Movement Research*. Ed. by A. G. Gale and F. Johnson. Vol. 22. Advances in Psychology. North-Holland, 1984, pp. 429–437. DOI: [https://doi.org/10.1016/S0166-4115\(08\)61863-4](https://doi.org/10.1016/S0166-4115(08)61863-4).
- [GL17] Gonzalez-Franco, M. and Lanier, J. Model of Illusions and Virtual Reality. In: *Frontiers in Psychology* 8 (2017), p. 1125. DOI: [10.3389/fpsyg.2017.01125](https://doi.org/10.3389/fpsyg.2017.01125). URL: <https://www.frontiersin.org/article/10.3389/fpsyg.2017.01125>.
- [Gom08] Gomi, H. Implicit Online Corrections of Reaching Movements. In: *Current Opinion in Neurobiology* 18 (2008), pp. 558–564. DOI: <https://doi.org/10.1016/j.conb.2008.11.002>.
- [Gon+19] Goncalves, G., Melo, M., Vasconcelos-Raposo, J., and Bessa, M. Impact of Different Sensory Stimuli on Presence in Credible Virtual Environments. In: *IEEE Transactions on Visualization & Computer Graphics* (2019), p. 1. DOI: [10.1109/TVCG.2019.2926978](https://doi.org/10.1109/TVCG.2019.2926978).
- [GP20] Ghubril, A. C. and Prentice, S. Hype Cycle for HCI. Gartner, <https://www.gartner.com/en/documents/2822817/hype-cycle-for-human-computer-interaction-2020>, Last accessed on 15.02.2019. 2020.
- [GPS12] Giannopoulos, E., Pomés, A., and Slater, M. Touching the Void: Exploring Virtual Objects Through A Vibrotactile Glove. In: *The International Journal of Virtual Reality* 11 (2012), pp. 19–24. URL: <http://hdl.handle.net/2445/53869>.
- [Gra99] Graziano, M. S. A. Where Is My Arm? The Relative Role of Vision and Proprioception in the Neuronal Representation of Limb Position. In: *Proceedings of the National Academy of Sciences of the United States of America* 96 (1999), pp. 10418–10421. URL: <http://www.pnas.org/cgi/content/abstract/96/18/10418>.
- [Gu+16] Gu, X., Zhang, Y., Sun, W., Bian, Y., Zhou, D., and Kristensson, P. O. Dexmo: An Inexpensive and Lightweight Mechanical Exoskeleton for Motion Capture and Force Feedback in VR. In: *Proceedings of the 2016 CHI Conference on Human Factors in Computing Systems*. Association for Computing Machinery, 2016, pp. 1991–1995. DOI: [10.1145/2858036.2858487](https://doi.org/10.1145/2858036.2858487).
- [Gup+13a] Gupta, S., Morris, D., Patel, S., and Tan, D. AirWave: Non-Contact Haptic Feedback Using Air Vortex Rings. In: *Proceedings of ACM Ubicomp*. 2013, pp. 419–428.
- [Gup+13b] Gupta, S., Morris, D., Patel, S. N., and Tan, D. AirWave: Non-Contact Haptic Feedback Using Air Vortex Rings. In: *Proceedings of the 2013 ACM International Joint Conference on Pervasive and Ubiquitous Computing*. Association for Computing Machinery, 2013, pp. 419–428. DOI: [10.1145/2493432.2493463](https://doi.org/10.1145/2493432.2493463).
- [Ham+19] Hamdan, N. A.-h., Wagner, A., Voelker, S., Steimle, J., and Borchers, J. Springlets: Expressive, Flexible and Silent On-Skin Tactile Interfaces. In: *Proceedings of the 2019 CHI Conference on Human Factors in Computing Systems*. Association for Computing Machinery, 2019, pp. 1–14. DOI: [10.1145/3290605.3300718](https://doi.org/10.1145/3290605.3300718).

- [Han+18] Han, T., Anderson, F., Irani, P., and Grossman, T. HydroRing: Supporting Mixed Reality Haptics Using Liquid Flow. In: *Proceedings of the 31st Annual ACM Symposium on User Interface Software and Technology*. Association for Computing Machinery, 2018, pp. 913–925. DOI: [10.1145/3242587.3242667](https://doi.org/10.1145/3242587.3242667).
- [Har+20] Hartfill, J., Gabel, J., Neves-Coelho, D., Vogel, D., Räthel, F., Tiede, S., Ariza, O., and Steinicke, F. Word Saber: An Effective and Fun VR Vocabulary Learning Game. In: *Proceedings of the Conference on Mensch Und Computer*. Magdeburg, Germany: Association for Computing Machinery, 2020, pp. 145–154. DOI: [10.1145/3404983.3405517](https://doi.org/10.1145/3404983.3405517).
- [Hay08] Hayward, V. A Brief Taxonomy of Tactile Illusions and Demonstrations That Can Be Done in A Hardware Store. In: *Brain Research Bulletin* 75 (2008). Special Issue: Robotics and Neuroscience, pp. 742–752. DOI: <https://doi.org/10.1016/j.brainresbull.2008.01.008>.
- [Hay19] Hayward, J. Haptics 2020-2030: Technologies, Markets and Players. IDTechEx, <https://www.idtechex.com/en/research-report/haptics-2020-2030-technologies-markets-and-players/684>, Last accessed on 15.02.2019. 2019.
- [HB07] Hein, A. and Brell, M. ConTACT - A Vibrotactile Display for Computer Aided Surgery. In: *Second Joint EuroHaptics Conference and Symposium on Haptic Interfaces for Virtual Environment and Teleoperator Systems (WHC'07)*. 2007, pp. 531–536. DOI: [10.1109/WHC.2007.33](https://doi.org/10.1109/WHC.2007.33).
- [HE07] Helbig, H. and Ernst, M. Optimal Integration of Shape Information from Vision and Touch. In: *Experimental brain research. Experimentelle Hirnforschung. Expérimentation cérébrale* 179 (2007), pp. 595–606. DOI: [10.1007/s00221-006-0814-y](https://doi.org/10.1007/s00221-006-0814-y).
- [Hee03] Heeter, C. Reflections on Real Presence by A Virtual Person. In: *Presence: Teleoperators and Virtual Environments* 12 (2003), pp. 335–345.
- [Heo+18] Heo, S., Chung, C., Lee, G., and Wigdor, D. Thor's Hammer: An Ungrounded Force Feedback Device Utilizing Propeller-Induced Propulsive Force. In: *Extended Abstracts of the 2018 CHI Conference on Human Factors in Computing Systems*. Association for Computing Machinery, 2018, pp. 1–4. DOI: [10.1145/3170427.3186544](https://doi.org/10.1145/3170427.3186544).
- [Her+19] Hertel, J., Schaare, A., Feuerbach, P., Ariza, O., and Steinicke, F. STIC - Sensory and Tactile Improved Cane. In: *Proceedings of Mensch Und Computer 2019*. Hamburg, Germany: Association for Computing Machinery, 2019, pp. 765–769. DOI: [10.1145/3340764.3344905](https://doi.org/10.1145/3340764.3344905).
- [HG00] Hu, Y. and Goodale, M. A. Grasping After A Delay Shifts Size-Scaling from Absolute to Relative Metrics. In: *Journal of Cognitive Neuroscience* 12 (2000), pp. 856–868. DOI: [10.1162/089892900562462](https://doi.org/10.1162/089892900562462).
- [HI17] Hanamitsu, N. and Israr, A. Haplug: A Haptic Plug for Dynamic VR Interactions. In: *Proceedings of the International AsiaHaptics Conference*. 2017, pp. 479–483. DOI: [10.1007/978-981-10-4157-0_80](https://doi.org/10.1007/978-981-10-4157-0_80).

- [Hin+18] Hinchet, R., Vechev, V., Shea, H., and Hilliges, O. DextrES: Wearable Haptic Feedback for Grasping in VR Via A Thin Form-Factor Electrostatic Brake. In: Proceedings of the 31st Annual ACM Symposium on User Interface Software and Technology. Association for Computing Machinery, 2018, pp. 901–912. DOI: [10.1145/3242587.3242657](https://doi.org/10.1145/3242587.3242657).
- [HLW19] Heo, S., Lee, J., and Wigdor, D. PseudoBend: Producing Haptic Illusions of Stretching, Bending, and Twisting Using Grain Vibrations. In: Proceedings of the 32nd Annual ACM Symposium on User Interface Software and Technology. Association for Computing Machinery, 2019, pp. 803–813. DOI: [10.1145/3332165.3347941](https://doi.org/10.1145/3332165.3347941).
- [Hof+08] Hoffman, D. M., Girshick, A. R., Akeley, K., and Banks, M. Vergence-accommodation Conflicts Hinder Visual Performance and Cause Visual Fatigue. In: *Journal of vision* 8 3 (2008), pp. 1–30.
- [Höl+18] Höll, M., Oberweger, M., Arth, C., and Lepetit, V. Efficient Physics-Based Implementation for Realistic Hand-Object Interaction in Virtual Reality. In: 2018 IEEE Conference on Virtual Reality and 3D User Interfaces (VR). 2018, pp. 175–182. DOI: [10.1109/VR.2018.8448284](https://doi.org/10.1109/VR.2018.8448284).
- [How12] Howard, I. Perceiving in Depth. Volume 3. Other Mechanisms of Depth Perception. 2012. ISBN: 978-0-19-976416-7.
- [Hua+20] Huang, H.-Y., Ning, C.-W., Wang, P.-Y., Cheng, J.-H., and Cheng, L.-P. Haptic-Go-Round: A Surrounding Platform for Encounter-Type Haptics in Virtual Reality Experiences. In: Proceedings of the 2020 CHI Conference on Human Factors in Computing Systems. Association for Computing Machinery, 2020, pp. 1–10. DOI: [10.1145/3313831.3376476](https://doi.org/10.1145/3313831.3376476).
- [Hum+16] Hummel, J., Dodiya, J., Eckardt, L., Wolff, R., Gerndt, A., and Kuhlen, T. A Lightweight Electrotactile Feedback Device to Improve Grasping in Immersive Virtual Environments. In: Proceedings of IEEE Virtual Reality Conference. 2016.
- [Ins01] Insko, B. E. “Passive Haptics Significantly Enhances Virtual Environments”. PhD thesis. 2001. ISBN: 0493172866.
- [IP11] Israr, A. and Poupyrev, I. Tactile Brush: Drawing on Skin with A Tactile Grid Display. In: Proceedings of the SIGCHI Conference on Human Factors in Computing Systems. ACM, 2011, pp. 2019–2028. DOI: [10.1145/1978942.1979235](https://doi.org/10.1145/1978942.1979235). URL: <http://doi.acm.org/10.1145/1978942.1979235>.
- [J O+16] J. Oliveira, V. de, Nedel, L., Maciel, A., and Brayda, L. “Localized Magnification in Vibrotactile HMDs for Accurate Spatial Awareness”. In: *EuroHaptics*. Test, 2016. Chap. Test.
- [Jac+94] Jacob, R. J. K., Sibert, L. E., McFarlane, D. C., and Mullen, M. P. Integrality and Separability of Input Devices. In: 1 (1994), pp. 3–26. DOI: [10.1145/174630.174631](https://doi.org/10.1145/174630.174631).
- [Jah63] Jahnke, J. C. Serial Position Effects in Immediate Serial Recall. In: *Journal of Verbal Learning and Verbal Behavior* 2 (1963), pp. 284–287. DOI: [https://doi.org/10.1016/S0022-5371\(63\)80095-X](https://doi.org/10.1016/S0022-5371(63)80095-X).

- [Jan+17] Jang, S., Stuerzlinger, W., Ambike, S., and Ramani, K. Modeling Cumulative Arm Fatigue in Mid-Air Interaction Based on Perceived Exertion and Kinetics of Arm Motion. In: *Proceedings of the 2017 CHI Conference on Human Factors in Computing Systems*. Association for Computing Machinery, 2017, pp. 3328–3339. DOI: [10.1145/3025453.3025523](https://doi.org/10.1145/3025453.3025523).
- [Je+17] Je, S., Rooney, B., Chan, L., and Bianchi, A. TactoRing: A Skin-Drag Discrete Display. In: *Proceedings of the 2017 CHI Conference on Human Factors in Computing Systems*. Association for Computing Machinery, 2017, pp. 3106–3114. DOI: [10.1145/3025453.3025703](https://doi.org/10.1145/3025453.3025703).
- [JF09] Johansson, R. and Flanagan, J. Coding and Use of Tactile Signals from the Fingertips in Object Manipulation Tasks. In: *Nature reviews. Neuroscience* 10 (May 2009), pp. 345–59. DOI: [10.1038/nrn2621](https://doi.org/10.1038/nrn2621).
- [JGH07] Jay, C., Glencross, M., and Hubbold, R. Modeling the Effects of Delayed Haptic and Visual Feedback in A Collaborative Virtual Environment. In: *ACM Transaction Computer-Human Interaction* 14 (2007), p. 8. DOI: [10.1145/1275511.1275514](https://doi.org/10.1145/1275511.1275514). URL: <http://doi.acm.org/10.1145/1275511.1275514>.
- [Jon+12] Jones, J. A., Suma, E. A., Krum, D. M., and Bolas, M. Comparability of Narrow and Wide Field-Of-View Head-Mounted Displays for Medium-Field Distance Judgments. In: *Proceedings of Symposium on Applied Perception (SAP)*. ACM, 2012, p. 119.
- [Jon18] Jones, L. *Haptics*. The MIT Press, 2018. ISBN: 9780262535809.
- [JYH00] John Lin, Ying Wu, and Huang, T. S. Modeling the Constraints of Human Hand Motion. In: *Proceedings Workshop on Human Motion*. 2000, pp. 121–126. DOI: [10.1109/HUMO.2000.897381](https://doi.org/10.1109/HUMO.2000.897381).
- [Kae+12] Kaercher, S., Fenzlaff, S., Hartmann, D., Nagel, S., and Koenig, P. Sensory Augmentation for the Blind. In: *Frontiers in Human Neuroscience* (2012).
- [KAM14] Katus, T., Andersen, S. K., and Müller, M. M. Common Mechanisms of Spatial Attention in Memory and Perception: A Tactile Dual-Task Study. In: *Cerebral Cortex* (2014).
- [Kat+17] Katzakis, N., Tong, J., Ariza, O., Chen, L., Klinker, G., Röder, B., and Steinicke, F. Stylo and Handifact: Modulating Haptic Perception Through Visualizations for Posture Training in Augmented Reality. In: *Proceedings of the Symposium on Spatial User Interaction (SUI)*. Brighton, United Kingdom: Association for Computing Machinery, 2017, pp. 58–67. DOI: [10.1145/3131277.3132181](https://doi.org/10.1145/3131277.3132181).
- [Kat+18] Kato, G., Kuroda, Y., Kiyokawa, K., and Takemura, H. HapStep: A Novel Method to Sense Footsteps While Remaining Seated Using Longitudinal Friction on the Sole of the Foot. In: *Haptic Interaction*. Springer Singapore, 2018, pp. 105–111. ISBN: 978-981-10-4157-0.
- [KC13] Kim, S. and Cho, K. Usability and Design Guidelines of Smart Canes for Users with Visual Impairments. In: *International Journal of Desig* (2013), pp. 1–7.
- [KEE19] Kilteni, K., Engeler, P., and Ehrsson, H. H. Efference Copy Is Necessary for the Attenuation of Self-generated Touch. In: *bioRxiv* (2019). DOI: [10.1101/823575](https://doi.org/10.1101/823575). URL: <https://www.biorxiv.org/content/early/2019/10/30/823575>.

- [Kel+12] Kellner, F., Bolte, B., Bruder, G., Rautenberg, U., Steinicke, F., Lappe, M., and Koch, R. Geometric Calibration of Head-Mounted Displays and Its Effects on Distance Estimation. In: *IEEE Transactions on Visualization and Computer Graphics (TVCG)* 18 (2012), pp. 589–596.
- [Ken+93] Kennedy, R. S., Lane, N. E., Berbaum, K. S., and Lilienthal, M. G. Simulator Sickness Questionnaire: An Enhanced Method for Quantifying Simulator Sickness. In: *The international journal of aviation psychology* 3 (1993), pp. 203–220.
- [Kha+19] Khamis, M., Schuster, N., George, C., and Pfeiffer, M. ElectroCutsscenes: Realistic Haptic Feedback in Cutsscenes of Virtual Reality Games Using Electric Muscle Stimulation. In: 25th ACM Symposium on Virtual Reality Software and Technology. Association for Computing Machinery, 2019. DOI: [10.1145/3359996.3364250](https://doi.org/10.1145/3359996.3364250).
- [Kil+12] Kilteni, K., Normand, J.-M., Sanchez-Vives, M. V., and Slater, M. Extending Body Space in Immersive Virtual Reality: A Very Long Arm Illusion. In: *PLoS ONE* 7 (2012), pp. 1–15. DOI: [10.1371/journal.pone.0040867](https://doi.org/10.1371/journal.pone.0040867).
- [Kim+13] Kim, S., Son, J., Lee, G., Kim, H., and Lee, W. TapBoard: Making A Touch Screen Keyboard More Touchable. In: Association for Computing Machinery, 2013, pp. 553–562. DOI: [10.1145/2470654.2470733](https://doi.org/10.1145/2470654.2470733).
- [Kir+19] Kirsch, K., Schatzschneider, C., Garber, C., Rosenberger, A., Kirsten, K., Ariza, O., Steinicke, F., and Bruder, G. KiVR Sports: Influencing the Users Physical Activity in VR by Using Audiovisual Stimuli in Exergames. In: Proceedings of Mensch Und Computer 2019. Hamburg, Germany: Association for Computing Machinery, 2019, pp. 777–781. DOI: [10.1145/3340764.3344907](https://doi.org/10.1145/3340764.3344907).
- [KKL16] Kim, H., Kim, M., and Lee, W. HapThimble: A Wearable Haptic Device Towards Usable Virtual Touch Screen. In: Proceedings of the 2016 CHI Conference on Human Factors in Computing Systems. Association for Computing Machinery, 2016, pp. 3694–3705. DOI: [10.1145/2858036.2858196](https://doi.org/10.1145/2858036.2858196).
- [KL13] Kim, S. and Lee, G. Haptic Feedback Design for A Virtual Button Along Force-Displacement Curves. In: Proceedings of the 26th Annual ACM Symposium on User Interface Software and Technology. Association for Computing Machinery, 2013, pp. 91–96. DOI: [10.1145/2501988.2502041](https://doi.org/10.1145/2501988.2502041).
- [KLM85] Klatzky, R., Lederman, S., and Metzger, V. Identifying Objects by Touch: An expert System”. In: *Attention Perception & Psychophysics* 37 (1985), pp. 299–302. DOI: [10.3758/BF03211351](https://doi.org/10.3758/BF03211351).
- [KLO18] Kim, S., Lee, B., and Oulasvirta, A. Impact Activation Improves Rapid Button Pressing. In: Proceedings of the 2018 CHI Conference on Human Factors in Computing Systems. Association for Computing Machinery, 2018, pp. 1–8. DOI: [10.1145/3173574.3174145](https://doi.org/10.1145/3173574.3174145).
- [Koh13] Kohli, L. “Redirected Touching”. PhD thesis. 2013.
- [Kra93] Kramer, J. F. Force Feedback and Textures Simulating Interface Device. 1993. URL: <https://www.google.com/patents/US5184319>.

- [KRM11] Kuchenbecker, K. J., Romano, J., and McMahan, W. Haptography: Capturing and Recreating the Rich Feel of Real Surfaces. In: *Robotics Research*. Springer Berlin Heidelberg, 2011, pp. 245–260.
- [Kru+16] Kruijff, E., Marquardt, A., Trepkowski, C., Lindeman, R. W., Hinkenjann, A., Maiero, J., and Riecke, B. E. On Your Feet!: Enhancing Vection in Leaning-Based Interfaces Through Multisensory Stimuli. In: *Proceedings of the 2016 Symposium on Spatial User Interaction*. SUI '16. Tokyo, Japan: ACM, 2016, pp. 149–158. ISBN: 978-1-4503-4068-7.
- [Kur+07] Kuroki, S., Kajimoto, H., Nii, H., Kawakami, N., and Tachi, S. Proposal for Tactile Sense Presentation That Combines Electrical and Mechanical Stimulus. In: (2007), pp. 121–126.
- [KW14] Kolb, B. and Whishaw, I. Q. *An Introduction to Brain and Behavior*. 4th ed. Worth Publishers, 2014. ISBN: 9781429242288.
- [Lam15] Lamb, T. D. Why Rods and Cones? In: *Eye (London, England)* 30 (2015). DOI: [10.1038/eye.2015.236](https://doi.org/10.1038/eye.2015.236).
- [LaV+17] LaViola, J., Kruijff, E., McMahan, R. P., Bowman, D. A., and Poupyrev, I. *3D User Interfaces: Theory and Practice 2nd Edition*. Addison-Wesley Professional, 2017.
- [LaV00] LaViola Jr., J. J. A Discussion of Cybersickness in Virtual Environments. In: *SIGCHI Bull.* 32.1 (Jan. 2000), pp. 47–56. ISSN: 0736-6906.
- [LB05] Lecuyer, A. and Burkhardt, J.-M. Influence of Color/Display Ratio on the Perception of Mass of Manipulated Objects in Virtual Environments. In: *Proceedings of the 2005 IEEE Conference 2005 on Virtual Reality*. IEEE Computer Society, 2005, pp. 19–25. DOI: [10.1109/VR.2005.49](https://doi.org/10.1109/VR.2005.49).
- [LB13] Lopes, P. and Baudisch, P. Muscle-Propelled Force Feedback: Bringing Force Feedback to Mobile Devices. In: *Proceedings of the SIGCHI Conference on Human Factors in Computing Systems*. Association for Computing Machinery, 2013, pp. 2577–2580. DOI: [10.1145/2470654.2481355](https://doi.org/10.1145/2470654.2481355).
- [LBS14] Lubos, P., Bruder, G., and Steinicke, F. Analysis of Direct Selection in Head-Mounted Display Environments. In: *Proceedings of IEEE Symposium on 3D User Interaction (3DUI)*. 2014, pp. 11–18.
- [LCE08] Liu, G., Chua, R., and Enns, J. T. Attention for Perception and Action: Task Interference for Action Planning, But Not for Online Control. In: *Exp. Brain Res* 185 (2008), pp. 709–717.
- [Lec+00] Lecuyer, A., Coquillart, S., Kheddar, A., Richard, P., and Coiffet, P. Pseudo-haptic Feedback: Can Isometric Input Devices Simulate Force Feedback? In: *Proceedings IEEE Virtual Reality 2000 (Cat. No.00CB37048)*. 2000, pp. 83–90.
- [Léc09] Lécuyer, A. Simulating Haptic Feedback Using Vision: A Survey of Research and Applications of Pseudo-Haptic Feedback. In: *Presence: Teleoper. Virtual Environ* 18 (2009), pp. 39–53. DOI: [10.1162/pres.18.1.39](https://doi.org/10.1162/pres.18.1.39).

- [Lee+12] Lee, J., Kim, Y., Ahn, E., and Kim, G. J. Applying “out of the Body” Funneling and Saltation to Interaction with Virtual and Augmented Objects. In: *Proceedings of IEEE VR Workshop on Perceptual Illusions in Virtual Environments (PIVE)*. 2012, pp. 7–9.
- [Lee+17] Lee, B., Deng, Q., Hoggan, E., and Oulasvirta, A. Boxer: A Multimodal Collision Technique for Virtual Objects. In: *Proceedings of the 19th ACM International Conference on Multimodal Interaction*. Association for Computing Machinery, 2017, pp. 252–260. DOI: [10.1145/3136755.3136761](https://doi.org/10.1145/3136755.3136761).
- [Lee+19] Lee, J., Sinclair, M., Gonzalez-Franco, M., Ofek, E., and Holz, C. TORC: A Virtual Reality Controller for In-Hand High-Dexterity Finger Interaction. In: *Proceedings of the 2019 CHI Conference on Human Factors in Computing Systems*. Association for Computing Machinery, 2019, pp. 1–13. DOI: [10.1145/3290605.3300301](https://doi.org/10.1145/3290605.3300301).
- [Lia+20] Liao, Y.-C., Kim, S., Lee, B., and Oulasvirta, A. Button Simulation and Design Via FDVV Models. In: *Proceedings of the 2020 CHI Conference on Human Factors in Computing Systems*. Association for Computing Machinery, 2020, pp. 1–14. DOI: [10.1145/3313831.3376262](https://doi.org/10.1145/3313831.3376262).
- [LIB15] Lopes, P., Ion, A., and Baudisch, P. Impacto: Simulating Physical Impact by Combining Tactile Stimulation with Electrical Muscle Stimulation. In: *Proceedings of the 28th Annual ACM Symposium on User Interface Software & Technology*. Association for Computing Machinery, 2015, pp. 11–19. DOI: [10.1145/2807442.2807443](https://doi.org/10.1145/2807442.2807443).
- [Lin+02] Lin, J. J.-W., Duh, H. B. L., Abi-Rached, H., Parker, D. E., and Iii, T. A. F. Effects of Field of View on Presence, Enjoyment, Memory, and Simulator Sickness in A Virtual Environment. In: *Proceedings of the IEEE Virtual Reality Conference 2002*. IEEE Computer Society, 2002. ISBN: 0-7695-1492-8.
- [Lin+05] Lindeman, R. W., Sibert, J. L., Mendez-Mendez, E., Patil, S., and Phifer, D. Effectiveness of Directional Vibrotactile Cuing on A Building-clearing Task. In: *SIGCHI-HFCS*. ACM, 2005.
- [Liu+09] Liu, L., Liere, R. van, Nieuwenhuizen, C., and Martens, J. B. Comparing Aimed Movements in the Real World and in Virtual Reality. In: *2009 IEEE Virtual Reality Conference*. 2009, pp. 219–222. DOI: [10.1109/VR.2009.4811026](https://doi.org/10.1109/VR.2009.4811026).
- [Liu11] Liu, L. “Modeling three-dimensional interaction tasks for desktop virtual reality”. PhD dissertation. TU Eindhoven, 2011.
- [LJB15] Lopes, P., Jonell, P., and Baudisch, P. Affordance++: Allowing Objects to Communicate Dynamic Use. In: *Proceedings of the 33rd Annual ACM Conference on Human Factors in Computing Systems*. Association for Computing Machinery, 2015, pp. 2515–2524. DOI: [10.1145/2702123.2702128](https://doi.org/10.1145/2702123.2702128).
- [LJL15] Lee, Y., Jang, I., and Lee, D. Enlarging Just Noticeable Differences of Visual-proprioceptive Conflict in VR Using Haptic Feedback. In: *2015 IEEE World Haptics Conference (WHC)*. IEEE. 2015, pp. 19–24.

- [LKO18] Liao, Y.-C., Kim, S., and Oulasvirta, A. One Button to Rule Them All: Rendering Arbitrary Force-Displacement Curves. In: *The 31st Annual ACM Symposium on User Interface Software and Technology Adjunct Proceedings*. Association for Computing Machinery, 2018, pp. 111–113. DOI: [10.1145/3266037.3266118](https://doi.org/10.1145/3266037.3266118).
- [LL07] Lemmerman, D. K. and LaViola, J. J. Effects of Interaction-Display Offset on User Performance in Surround Screen Virtual Environments. In: *Proceedings of IEEE Virtual Reality*. 2007, pp. 303–304.
- [LL09] Liu, L. and Liere, R. van. Designing 3D Selection Techniques Using Ballistic and Corrective Movements. In: *Proceedings of Joint Virtual Reality Conference of EGVE - ICAT - EuroVR*. 2009, pp. 1–8.
- [Lo+18] Lo, J.-Y., Huang, D.-Y., Sun, C.-K., Hou, C.-E., and Chen, B.-Y. RollingStone: Using Single Slip Taxel for Enhancing Active Finger Exploration with A Virtual Reality Controller. In: *Association for Computing Machinery*, 2018, pp. 839–851. DOI: [10.1145/3242587.3242627](https://doi.org/10.1145/3242587.3242627).
- [Lon+14] Long, B., Seah, S. A., Carter, T., and Subramanian, S. Rendering Volumetric Haptic Shapes in Mid-Air Using Ultrasound. In: *ACM Transactions on Graphics* 33 (2014). DOI: [10.1145/2661229.2661257](https://doi.org/10.1145/2661229.2661257).
- [Lop+17] Lopes, P., You, S., Cheng, L.-P., Marwecki, S., and Baudisch, P. Providing Haptics to Walls & Heavy Objects in Virtual Reality by Means of Electrical Muscle Stimulation. In: *Proceedings of the 2017 CHI Conference on Human Factors in Computing Systems*. CHI '17. Denver, Colorado, USA: Association for Computing Machinery, 2017, pp. 1471–1482. ISBN: 9781450346559. DOI: [10.1145/3025453.3025600](https://doi.org/10.1145/3025453.3025600). URL: <https://doi.org/10.1145/3025453.3025600>.
- [Lop+18] Lopes, P., You, S., Ion, A., and Baudisch, P. Adding Force Feedback to Mixed Reality Experiences and Games Using Electrical Muscle Stimulation. In: *Proceedings of the 2018 CHI Conference on Human Factors in Computing Systems*. Association for Computing Machinery, 2018, pp. 1–13. DOI: [10.1145/3173574.3174020](https://doi.org/10.1145/3173574.3174020).
- [LR05] Lessels, S. and Ruddle, R. A. Movement Around Real and Virtual Cluttered Environments. In: *Presence: Teleoper. Virtual Environ.* 14 (2005), pp. 580–596. DOI: [10.1162/105474605774918778](https://doi.org/10.1162/105474605774918778).
- [Lub+14] Lubos, P., Garber, C., Hoffert, A., Reis, I., and Steinicke, F. The Interactive Spatial Surface - Blended Interaction on A Stereoscopic Multi-Touch Surface. In: *Proceedings of the Mensch Und Computer Workshop on Blended Interaction*. 2014, pp. 343–346. URL: <http://basilic.informatik.uni-hamburg.de/Publications/2014/LGHR14>.
- [Lub+16] Lubos, P., Bruder, G., Ariza, O., and Steinicke, F. Touching the Sphere: Leveraging Joint-Centered Kinespheres for Spatial User Interaction. In: *Proceedings of the 2016 Symposium on Spatial User Interaction*. Tokyo, Japan: Association for Computing Machinery, 2016, pp. 13–22. DOI: [10.1145/2983310.2985753](https://doi.org/10.1145/2983310.2985753).

- [Lub18] Lubos, P. “Supernatural and Comfortable Basic Interactions for 3D User Interfaces”. PhD thesis. Universität Hamburg, 2018.
- [Mac+87] Mackenzie, C. L., Marteniuk, R., Dugas, C., Liske, D., and Eickmeier, B. Three-Dimensional Movement Trajectories in Fitts’ Task: Implications for Control. In: *Quarterly Journal of Experimental Psychology* 39 (1987), pp. 629–647.
- [Mac08] MacLean, K. E. Haptic Interaction Design for Everyday Interfaces. In: *Reviews of Human Factors and Ergonomics* 4 (2008), pp. 149–194. DOI: [10.1518/155723408X342826](https://doi.org/10.1518/155723408X342826).
- [Mac18] MacKenzie, I. S. “Fitts’ Law”. In: *The Wiley Handbook of Human Computer Interaction*. John Wiley & Sons, Ltd, 2018, pp. 347–370. DOI: <https://doi.org/10.1002/9781118976005.ch17>.
- [Mae+17] Maereg, A. T., Nagar, A., Reid, D., and Secco, E. Wearable Vibrotactile Haptic Device for Stiffness Discrimination During Virtual Interactions. In: *Frontiers Robotics AI* 4 (2017), p. 42.
- [Mar+13] Marsh, W. E., Kelly, J. W., Dark, V. J., and Oliver, J. H. Cognitive Demands of Semi-natural Virtual Locomotion. In: *Presence: Teleoperators and Virtual Environments* 22 (2013), pp. 216–234.
- [Mar+16] Martínez, J., García, A., Oliver, M., Molina, J. P., and González, P. Identifying Virtual 3D Geometric Shapes with A Vibrotactile Glove. In: *IEEE Computer Graphics and Applications* 36 (2016), pp. 42–51. DOI: [10.1109/MCG.2014.81](https://doi.org/10.1109/MCG.2014.81).
- [Mar+17] Martinez Cornelio, P. I., De Pirro, S., Vi, C. T., and Subramanian, S. Agency in Mid-Air Interfaces. In: *Proceedings of the 2017 CHI Conference on Human Factors in Computing Systems*. Association for Computing Machinery, 2017, pp. 2426–2439. DOI: [10.1145/3025453.3025457](https://doi.org/10.1145/3025453.3025457).
- [Mar+18] Marquardt, A., Kruijff, E., Trepkowski, C., Maiero, J., Schwandt, A., Hinkenjann, A., Stuerzlinger, W., and Schöning, J. Audio-Tactile Proximity Feedback for Enhancing 3D Manipulation. In: *Proceedings of the 24th ACM Symposium on Virtual Reality Software and Technology*. Association for Computing Machinery, 2018. DOI: [10.1145/3281505.3281525](https://doi.org/10.1145/3281505.3281525).
- [Mas93] Massie, T. Design of A Three Degree of Freedom Force-reflecting Haptic Interface. In: 1993.
- [Mat+12] Mateo, J. C., Simpson, B. D., Gilkey, R. H., Iyer, N., and Brungart, D. S. Spatial Multi-sensory Cueing to Support Visual Target-Acquisition Performance. In: *HFES*. 2012.
- [MD15] Metzger, A. and Drewing, K. Haptically Perceived Softness of Deformable Stimuli Can Be Manipulated by Applying External Forces During the Exploration. In: *2015 IEEE World Haptics Conference (WHC)*. 2015, pp. 75–81.
- [Men+15] Meng, F., Ho, C., Gray, R., and Spence, C. Dynamic Vibrotactile Warning Signals for Frontal Collision Avoidance: Towards the Torso Versus Towards the Head. In: *Ergonomics* 58 (2015), pp. 411–425. DOI: [10.1080/00140139.2014.976278](https://doi.org/10.1080/00140139.2014.976278).

- [MI08] MacKenzie, I. S. and Isokoski, P. Fitts' Throughput and the Speed-accuracy Tradeoff. In: *Proceedings of the SIGCHI Conference on Human Factors in Computing Systems*. ACM, 2008, pp. 1633–1636. DOI: [10.1145/1357054.1357308](https://doi.org/10.1145/1357054.1357308). URL: <http://doi.acm.org/10.1145/1357054.1357308>.
- [Mil+94] Milgram, P., Takemura, H., Utsumi, A., and Kishino, F. Augmented Reality: A Class of Displays on the Reality-virtuality Continuum. In: *Telem manipulator and Telepresence Technologies* 2351 (1994). DOI: [10.1117/12.197321](https://doi.org/10.1117/12.197321).
- [Mil04] Millodot, M. *Dictionary of Optometry and Visual Science*. Butterworth-Heinemann, 2004. ISBN: 9780750688086. URL: <https://books.google.de/books?id=P2ZqAAAAMAAJ>.
- [Miy+15] Miyamoto, N., Aoyama, K., Furukawa, M., Maeda, T., and Ando, H. “Air Tap: The Sensation of Tapping a Rigid Object in Mid-Air”. In: *Haptic Interaction: Perception, Devices and Applications*. Ed. by H. Kajimoto, H. Ando, and K.-U. Kyung. Tokyo: Springer Japan, 2015, pp. 285–291. ISBN: 978-4-431-55690-9. DOI: [10.1007/978-4-431-55690-9_52](https://doi.org/10.1007/978-4-431-55690-9_52). URL: https://doi.org/10.1007/978-4-431-55690-9_52.
- [MJS97] Mine, M. R., Jr, F. B., and Sequin, C. H. Moving Objects in Space: Exploiting Proprioception in Virtual-Environment Interaction. In: *Proceedings of the ACM Annual Conference on Computer Graphics and Interactive Techniques (SIGGRAPH)*. 1997, pp. 19–26.
- [MK10] Myles, K. and Kalb, J. T. Guidelines for Head Tactile Communication (Report ARL-TR-5116). In: *Aberdeen Proving Ground, ARL* (2010).
- [MNT12] Muramatsu, Y., Niitsuma, M., and Thomessen, T. Perception of Tactile Sensation Using Vibrotactile Glove Interface. In: *Cognitive Infocommunications (CogInfoCom), 2012 IEEE 3rd International Conference*. 2012, pp. 621–626. DOI: [10.1109/CogInfoCom.2012.6422054](https://doi.org/10.1109/CogInfoCom.2012.6422054).
- [Mon+14] Monnai, Y., Hasegawa, K., Fujiwara, M., Yoshino, K., Inoue, S., and Shinoda, H. HaptoMime: Mid-air Haptic Interaction with A Floating Virtual Screen. In: *Proceedings of ACM User Interface Software and Technology (UIST)*. 2014, pp. 663–667.
- [Mor89] Moran, C. A. Anatomy of the Hand. In: *Physical Therapy* 69 (1989), pp. 1007–1013. DOI: [10.1093/ptj/69.12.1007](https://doi.org/10.1093/ptj/69.12.1007).
- [Mue+20] Mueller, F. F. et al. Next Steps for Human-Computer Integration. In: *New York, NY, USA: Association for Computing Machinery*, 2020, pp. 1–15. DOI: [10.1145/3313831.3376242](https://doi.org/10.1145/3313831.3376242).
- [MWO14] McGlone, F., Wessberg, J., and Olausson, H. Discriminative and Affective Touch: Sensing and Feeling. In: *Neuron* 82 (2014), pp. 737–755. DOI: <https://doi.org/10.1016/j.neuron.2014.05.001>.
- [Nad+10] Nadkarni, N. K., Zabjek, K., Lee, B., McIlroy, W. E., and Black, S. E. Effect of Working Memory and Spatial Attention Tasks on Gait in Healthy Young and Older Adults. In: *Motor Control* (2010).
- [Nel+14] Nelson, B. C., Kim, Y., Foshee, C., and Slack, K. Visual Signaling in Virtual World-based Assessments: The SAVE Science Project. In: *Information Sciences* (2014).

- [Nor+12] Nordahl, R., Aalborg, D., Nilsson, N., Turchet, L., and Serafin, S. Vertical Illusory Self-motion Through Haptic Stimulation of the Feet. In: *Proceedings of IEEE VR Workshop on Perceptual Illusions in Virtual Environments (PIVE)*. 2012, pp. 21–26.
- [NT93] Napier, J. R. and Tuttle, R. H. *Hands*. Princeton University Press, 1993. URL: <https://books.google.de/books?id=mNQM4jvG7hgC>.
- [Obr+16] Obrist, M., Velasco, C., Vi, C., Ranasinghe, N., Israr, A., Cheok, A., Spence, C., and Gopalakrishnakone, P. Sensing the Future of HCI: Touch, Taste, and Smell User Interfaces. In: *Interactions* 23 (2016), pp. 40–49. DOI: [10.1145/2973568](https://doi.org/10.1145/2973568).
- [Oga18] Ogata, M. Magneto-Haptics: Embedding Magnetic Force Feedback for Physical Interactions. In: *Proceedings of the 31st Annual ACM Symposium on User Interface Software and Technology*. Association for Computing Machinery, 2018, pp. 737–743. DOI: [10.1145/3242587.3242615](https://doi.org/10.1145/3242587.3242615).
- [OH14] Okazaki, R. and Hiroyuki, K. Perceived Distance from Hitting with A Stick Is Altered by Overlapping Vibration to Holding Hand. In: *Proceedings of ACM CHI*. 2014, pp. 1903–1908.
- [OKL18] Oulasvirta, A., Kim, S., and Lee, B. Neuromechanics of A Button Press. In: *Proceedings of the 2018 CHI Conference on Human Factors in Computing Systems*. Association for Computing Machinery, 2018, pp. 1–13. DOI: [10.1145/3173574.3174082](https://doi.org/10.1145/3173574.3174082).
- [Ort+16a] Ortega, F. R., Abyarjoo, F., Barreto, A., Rishe, N., and Adjouadi, M. *Interaction Design for 3D User Interfaces: The World of Modern Input Devices for Research, Applications, and Game Development*. A. K. Peters, Ltd., 2016.
- [Ort+16b] Orts-Escolano, S. et al. Holoportation: Virtual 3D Teleportation in Real-Time. In: *Association for Computing Machinery*, 2016, pp. 741–754. DOI: [10.1145/2984511.2984517](https://doi.org/10.1145/2984511.2984517).
- [Pac+17] Pacchierotti, C., Sinclair, S., Solazzi, M., Frisoli, A., Hayward, V., and Prattichizzo, D. Wearable Haptic Systems for the Fingertip and the Hand: Taxonomy, Review, and Perspectives. In: *IEEE Transactions on Haptics* 10 (2017), pp. 580–600. DOI: [10.1109/TOH.2017.2689006](https://doi.org/10.1109/TOH.2017.2689006).
- [Pal99] Palmer, S. E. *Vision Science: Photons to Phenomenology*. A Bradford Book, 1999.
- [Par15] Parise, C. Crossmodal Correspondences: Standing Issues and Experimental Guidelines. In: *Multisensory research* (2015). DOI: [10.1163/22134808-00002502](https://doi.org/10.1163/22134808-00002502).
- [PE08] Petkova, V. I. and Ehrsson, H. H. If I Were You: Perceptual Illusion of Body Swapping. In: *PLoS ONE* 3 (2008), pp. 1–9. DOI: [10.1371/journal.pone.0003832](https://doi.org/10.1371/journal.pone.0003832).
- [Pez+19] Pezent, E., Israr, A., Samad, M., Robinson, S., Agarwal, P., Benko, H., and Colonnese, N. Tasbi: Multisensory Squeeze and Vibrotactile Wrist Haptics for Augmented and Virtual Reality. In: *2019 IEEE World Haptics Conference (WHC)*. 2019, pp. 1–6.

- [Pfe+14] Pfeiffer, M., Schneegass, S., Alt, F., and Rohs, M. Let Me Grab This: A Comparison of EMS and Vibration for Haptic Feedback in Free-Hand Interaction. In: *Proceedings of the 5th Augmented Human International Conference*. Association for Computing Machinery, 2014. DOI: [10.1145/2582051.2582099](https://doi.org/10.1145/2582051.2582099).
- [PLP09] Phinyomark, A., Limsakul, C., and Phukpattaranont, P. A Novel Feature Extraction for Robust EMG Pattern Recognition. In: *Journal of Computing* 1 (Dec. 2009), pp. 71–80.
- [Pou+98] Poupyrev, I., Ichikawa, T., Weghorst, S., and Billinghamurst, M. Egocentric Object Manipulation in Virtual Environments: Empirical Evaluation of Interaction Techniques. In: *Computer Graphics Forum* 17 (1998), pp. 41–52. DOI: [10.1111/1467-8659.00252](https://doi.org/10.1111/1467-8659.00252).
- [PPB10] Pielot, M., Poppinga, B., and Boll, S. PocketNavigator: Vibro-tactile Waypoint Navigation for Everyday Mobile Devices. In: *MobileHCI*. ACM, 2010.
- [PRI15] Pakov, O., Rantala, J., and Isokoski, P. Sequential and Simultaneous Tactile Stimulation with Multiple Actuators on Head, Neck and Back for Gaze Cuing. In: *IEEE WHC*. 2015.
- [PS15] Pfeiffer, M. and Stuerzlinger, W. 3D Virtual Hand Pointing with EMS and Vibration Feedback. In: *Proceedings of IEEE Symposium on 3D User Interfaces (3DUI)*. 2015, pp. 117–120.
- [Ran+10] Rank, M., Shi, Z., Müller, H., and Hirche, S. Perception of Delay in Haptic Telepresence Systems. In: *Presence* 19 (2010), pp. 389–399. DOI: [10.1162/pres_a_00021](https://doi.org/10.1162/pres_a_00021).
- [Ras09] Rash, C. *Helmet-mounted Displays: Sensation, Perception, and Cognition Issues*. U.S. Army Aeromedical Research Laboratory, 2009. ISBN: 9780615283753.
- [RB04] Riecke, B. E. and Bühlhoff, H. H. Spatial Updating in Real and Virtual Environments: Contribution and Interaction of Visual and Vestibular Cues. In: *Proceedings of the 1st Symposium on Applied Perception in Graphics and Visualization*. Association for Computing Machinery, 2004, pp. 9–17. DOI: [10.1145/1012551.1012553](https://doi.org/10.1145/1012551.1012553).
- [RH93] Reynier, F. and Hayward, V. Summary of the Kinesthetic and Tactile Function of the Human Upper Extremity. In: *McGill Center for Intelligent Machines Technical Report CIM-93-4* (1993).
- [Ric+19] Richards, K., Mahalanobis, N., Kim, K., Schubert, R., Lee, M., Daher, S., Norouzi, N., Hochreiter, J., Bruder, G., and Welch, G. Analysis of Peripheral Vision and Vibrotactile Feedback During Proximal Search Tasks with Dynamic Virtual Entities in Augmented Reality. In: *Symposium on Spatial User Interaction*. Association for Computing Machinery, 2019. DOI: [10.1145/3357251.3357585](https://doi.org/10.1145/3357251.3357585).
- [Rie+18] Rietzler, M., Geiselhart, F., Gugenheimer, J., and Rukzio, E. Breaking the Tracking: Enabling Weight Perception Using Perceivable Tracking Offsets. In: *Proceedings of the 2018 CHI Conference on Human Factors in Computing Systems*. Association for Computing Machinery, 2018, pp. 1–12. DOI: [10.1145/3173574.3173702](https://doi.org/10.1145/3173574.3173702).
- [RKW01] Razzaque, S., Kohn, Z., and Whitton, M. Redirected Walking. In: *Proceedings of Eurographics*. ACM, 2001, pp. 289–294.

- [RL09] Ruddle, R. A. and Lessels, S. The Benefits of Using A Walking Interface to Navigate Virtual Environments. In: *ACM Transactions on Computer-Human Interaction (TOCHI)* 16 (2009), p. 5.
- [RV64] Rock, I. and Victor, J. Vision and Touch: An Experimentally Created Conflict Between the Two Senses. In: *Science* 143 (1964), pp. 594–596. DOI: [10.1126/science.143.3606.594](https://doi.org/10.1126/science.143.3606.594). URL: <https://science.sciencemag.org/content/143/3606/594>.
- [RVB11] Ruddle, R. A., Volkova, E., and Bühlhoff, H. H. Walking Improves Your Cognitive Map in Environments That Are Large-scale and Large in Extent. In: *ACM Transactions on Computer-Human Interaction (TOCHI)* 18 (2011), p. 10.
- [Ryu+20] Ryu, N., Lee, W., Kim, M. J., and Bianchi, A. ElaStick: A Handheld Variable Stiffness Display for Rendering Dynamic Haptic Response of Flexible Object. In: Proceedings of the 33rd Annual ACM Symposium on User Interface Software and Technology. Association for Computing Machinery, 2020, pp. 1035–1045. DOI: [10.1145/3379337.3415862](https://doi.org/10.1145/3379337.3415862).
- [RZ18] Reed, C. and Ziat, M. “Haptic Perception: From the Skin to the Brain”. In: 2018. DOI: [10.1016/B978-0-12-809324-5.03182-5](https://doi.org/10.1016/B978-0-12-809324-5.03182-5).
- [Sag+19] Sagheb, S., Liu, F. W., Bahremand, A., Kidane, A., and LiKamWa, R. SWISH: A Shifting-Weight Interface of Simulated Hydrodynamics for Haptic Perception of Virtual Fluid Vessels. In: Proceedings of the 32nd Annual ACM Symposium on User Interface Software and Technology. Association for Computing Machinery, 2019, pp. 751–761. DOI: [10.1145/3332165.3347870](https://doi.org/10.1145/3332165.3347870).
- [Sam+19] Samad, M., Gatti, E., Hermes, A., Benko, H., and Parise, C. Pseudo-Haptic Weight: Changing the Perceived Weight of Virtual Objects By Manipulating Control-Display Ratio. In: Proceedings of the 2019 CHI Conference on Human Factors in Computing Systems. Association for Computing Machinery, 2019, pp. 1–13. DOI: [10.1145/3290605.3300550](https://doi.org/10.1145/3290605.3300550).
- [SAS19] Schlünsen, R., Ariza, O., and Steinicke, F. A VR Study on Freehand Vs. Widgets for 3D Manipulation Tasks. In: Proceedings of Mensch Und Computer 2019. Hamburg, Germany: Association for Computing Machinery, 2019, pp. 223–233. DOI: [10.1145/3340764.3340791](https://doi.org/10.1145/3340764.3340791).
- [Sch+10] Schätzle, S., Ende, T., Wüsthoff, T., and Preusche, C. VibroTac: An Ergonomic and Versatile Usable Vibrotactile Feedback Device. In: Proceedings of IEEE RO-MAN. 2010, pp. 670–675.
- [Sch+17] Schneider, O., MacLean, K., Swindells, C., and Booth, K. Haptic Experience Design: What Hapticians Do and Where They Need Help. In: *International Journal of Human-Computer Studies* 107 (2017). Multisensory Human-Computer Interaction, pp. 5–21. ISSN: 1071-5819. DOI: <https://doi.org/10.1016/j.ijhcs.2017.04.004>.
- [Sch+19] Schneider, D., Otte, A., Gesslein, T., Gagel, P., Kuth, B., Damlakhi, M. S., Dietz, O., Ofek, E., Pahud, M., Kristensson, P. O., Müller, J., and Grubert, J. ReconViguration: Reconfiguring Physical Keyboards in Virtual Reality. In: *IEEE Transactions on Visualization and Computer Graphics* 25 (2019), pp. 3190–3201.

- [SCL17] Sarupuri, B., Chipana, M., and Lindeman, R. Trigger Walking: A Low-fatigue Travel Technique for Immersive Virtual Reality. In: Jan. 2017, pp. 227–228.
- [Ser+18] Serino, A., Noel, J.-P., Mange, R., Canzoneri, E., Pellencin, E., Ruiz, J. B., Bernasconi, F., Blanke, O., and Herbelin, B. Peripersonal Space: An Index of Multisensory Body–Environment Interactions in Real, Virtual, and Mixed Realities. In: *Frontiers in ICT* 4 (2018). DOI: [10.3389/fict.2017.00031](https://doi.org/10.3389/fict.2017.00031).
- [SFB10] Solazzi, M., Frisoli, A., and Bergamasco, M. Design of A Novel Finger Haptic Interface for Contact and Orientation Display. In: IEEE Haptics Symposium. 2010, pp. 129–132. DOI: [10.1109/HAPTIC.2010.5444667](https://doi.org/10.1109/HAPTIC.2010.5444667).
- [SFR01] Schubert, T., Friedmann, F., and Regenbrecht, H. The Experience of Presence: Factor Analytic Insights. In: *Presence: Teleoperators & Virtual Environments* 10.3 (2001), pp. 266–281.
- [SG08] Scott, J. J. and Gray, R. A Comparison of Tactile, Visual, and Auditory Warnings for Rear-End Collision Prevention in Simulated Driving. In: *Human Factors: The Journal of the Human Factors and Ergonomics Society* 50 (2008), pp. 264–275. DOI: [10.1518/001872008X250674](https://doi.org/10.1518/001872008X250674).
- [SH84] Somers, W. W. and Hamilton, M. J. Estimation of the Stereoscopic Threshold Utilizing Perceived Depth. In: *Ophthalmic and Physiological Optics* 4 (1984), pp. 245–250. DOI: [10.1111/j.1475-1313.1984.tb00362.x](https://doi.org/10.1111/j.1475-1313.1984.tb00362.x).
- [Shi+10] Shi, Z., Zou, H., Rank, M., Chen, L., Hirche, S., and Muller, H. J. Effects of Packet Loss and Latency on the Temporal Discrimination of Visual-Haptic Events. In: *IEEE Transactions on Haptics* (2010), pp. 28–36.
- [Shi+14] Shilkrot, R., Huber, J., Liu, C., Maes, P., and Nanayakkara, S. FingerReader: A Wearable Device to Support Text Reading on the Go. In: Proceedings of ACM CHI. 2014, pp. 2359–2364.
- [Shi+18] Shigeyama, J., Hashimoto, T., Yoshida, S., Aoki, T., Narumi, T., Tanikawa, T., and Hirose, M. Transcalibur: Weight Moving VR Controller for Dynamic Rendering of 2D Shape Using Haptic Shape Illusion. In: Association for Computing Machinery, 2018. DOI: [10.1145/3214907.3214923](https://doi.org/10.1145/3214907.3214923).
- [Shn97] Shneiderman, B. Direct Manipulation for Comprehensible, Predictable and Controllable User Interfaces. In: Intelligent User Interfaces. 1997, pp. 33–39.
- [Sin+19] Sinclair, M., Ofek, E., Gonzalez-Franco, M., and Holz, C. CapstanCrunch: A Haptic VR Controller with User-Supplied Force Feedback. In: Proceedings of the 32nd Annual ACM Symposium on User Interface Software and Technology. Association for Computing Machinery, 2019, pp. 815–829. DOI: [10.1145/3332165.3347891](https://doi.org/10.1145/3332165.3347891).

- [Siu+18] Siu, A. F., Gonzalez, E. J., Yuan, S., Ginsberg, J. B., and Follmer, S. “ShapeShift: 2D Spatial Manipulation and Self-Actuation of Tabletop Shape Displays for Tangible and Haptic Interaction”. In: *Proceedings of the 2018 CHI Conference on Human Factors in Computing Systems*. Association for Computing Machinery, 2018, pp. 1–13. URL: <https://doi.org/10.1145/3173574.3173865>.
- [SK83] Sankoff, D. and Kruskal, J. Time Warps, String Edits, and Macromolecules: the Theory and Practice of Sequence Comparison. In: *Addison-Wesley Publication* (1983).
- [Sla+98] Slater, M., Steed, A., McCarthy, J., and Maringelli, F. The Influence of Body Movement on Subjective Presence in Virtual Environments. In: *Human Factors and Ergonomics Society* 40 (1998), pp. 469–477. URL: <http://www.ingentaconnect.com/content/hfes/hf/1998/00000040/00000003/art00011>.
- [Sno+85] Snodgrass, J., Levy-Berger, G., Haydon, M., Haydon, A., and Berger, I. Human Experimental Psychology. Oxford University Press, 1985. ISBN: 9780195035742. URL: <https://books.google.de/books?id=J-XGQgAACAAJ>.
- [SO15] Stanley, A. and Okamura, A. M. Controllable Surface Haptics Via Particle Jamming and Pneumatics. In: *IEEE Transactions on Haptics* 8 (2015), pp. 20–30. DOI: [10.1109/TOH.2015.2391093](https://doi.org/10.1109/TOH.2015.2391093).
- [SO17] Schorr, S. B. and Okamura, A. M. Fingertip Tactile Devices for Virtual Object Manipulation and Exploration. In: *Proceedings of the 2017 CHI Conference on Human Factors in Computing Systems*. Association for Computing Machinery, 2017, pp. 3115–3119. DOI: [10.1145/3025453.3025744](https://doi.org/10.1145/3025453.3025744).
- [Sod+13] Sodhi, R., Poupyrev, I., Glisson, M., and Israr, A. AIREAL: Interactive Tactile Experiences in Free Air. In: *ACM Transactions on Graphics* 32 (2013). DOI: [10.1145/2461912.2462007](https://doi.org/10.1145/2461912.2462007).
- [Spa+14] Spanlang, B., Normand, J.-M., Borland, D., Kilteni, K., Giannopoulos, E., Pomés, A., González-Franco, M., Pérez-Marcos, D., Arroyo-Palacios, J., Muncunill, X. N., and Slater, M. How to Build An Embodiment Lab: Achieving Body Representation Illusions in Virtual Reality. In: *Frontiers in Robotics and AI* 1 (2014). DOI: [10.3389/frobt.2014.00009](https://doi.org/10.3389/frobt.2014.00009).
- [Spe+09] Spelmezan, D., Jacobs, M., Hilgers, A., and Borchers, J. Tactile Motion Instructions for Physical Activities. In: *Proceedings of the SIGCHI Conference on Human Factors in Computing Systems*. Association for Computing Machinery, 2009, pp. 2243–2252. DOI: [10.1145/1518701.1519044](https://doi.org/10.1145/1518701.1519044).
- [Spe08] Spearman, C. The Method of ‘right and Wrong Cases’ (‘constant Stimuli’) Without Gauss’s Formulae. In: *British Journal of Psychology* 2 (1908), pp. 227–242.
- [SS00] Slater, M. and Steed, A. A Virtual Presence Counter. In: *Presence: Teleoperators and Virtual Environments* 9 (2000), pp. 413–434. DOI: [10.1162/105474600566925](https://doi.org/10.1162/105474600566925).
- [ST14] Stuerzlinger, W. and Teather, R. J. Considerations for Targets in 3D Pointing Experiments. In: *Proceedings of HCI Korea*. Hanbit Media, Inc, 2014, pp. 162–168. URL: <http://dl.acm.org/citation.cfm?id=2729485.2729510>.

- [Sta+98] Stark, B., Carlstedt, T., Hallin, R. G., and Risling, M. Distribution of Human Pacinian Corpuscles in the Hand: A Cadaver Study. In: *Journal of Hand Surgery (British and European Volume)* 23 (1998), pp. 370–372. DOI: [10.1016/S0266-7681\(98\)80060-0](https://doi.org/10.1016/S0266-7681(98)80060-0). URL: <http://jhs.sagepub.com/content/23/3/370.abstract>.
- [Sta00] Standardization, I. O. for. *ISO/DIS 9241-9 Ergonomic requirements for office work with visual display terminals (VDTs) - Part 9: Requirements for non-keyboard input devices*. 2000.
- [Ste+09] Steinicke, F., Bruder, G., Hinrichs, K., Lappe, M., Ries, B., and Interrante, V. Transitional Environments Enhance Distance Perception in Immersive Virtual Reality Systems. In: *Proceedings of the 6th Symposium on Applied Perception in Graphics and Visualization*. Association for Computing Machinery, 2009, pp. 19–26. DOI: [10.1145/1620993.1620998](https://doi.org/10.1145/1620993.1620998).
- [Ste+10] Steinicke, F., Bruder, G., Jerald, J., Fenz, H., and Lappe, M. Estimation of Detection Thresholds for Redirected Walking Techniques. In: *IEEE Transactions on Visualization and Computer Graphics (TVCG)* 16 (2010), pp. 17–27. DOI: [10.1109/TVCG.2009.62](https://doi.org/10.1109/TVCG.2009.62).
- [Ste+13] Steinicke, F., Visell, Y., Campos, J., and Lécuyer, A. *Human Walking in Virtual Environments*. Springer, 2013.
- [Ste16] Steinicke, F. *Being Really Virtual - Immersive Natives and the Future of Virtual Reality*. Springer, 2016.
- [Ste58] Stevens, S. Problems and Methods of Psychophysics. In: *Psychological bulletin* 55 (1958), pp. 177–96.
- [Str+18] Strasnick, E., Holz, C., Ofek, E., Sinclair, M., and Benko, H. Haptic Links: Bimanual Haptics for Virtual Reality Using Variable Stiffness Actuation. In: *Proceedings of the 2018 CHI Conference on Human Factors in Computing Systems*. Association for Computing Machinery, 2018, pp. 1–12. DOI: [10.1145/3173574.3174218](https://doi.org/10.1145/3173574.3174218).
- [Sun+19] Sun, Y., Yoshida, S., Narumi, T., and Hirose, M. PaCaPa: A Handheld VR Device for Rendering Size, Shape, and Stiffness of Virtual Objects in Tool-Based Interactions. In: *New York, NY, USA: Association for Computing Machinery*, 2019, pp. 1–12. DOI: [10.1145/3290605.3300682](https://doi.org/10.1145/3290605.3300682).
- [Sut65] Sutherland, I. E. The Ultimate Display. In: *Proceedings of IFIP Congress 2*. 1965, pp. 506–509.
- [Suz+20] Suzuki, R., Hedayati, H., Zheng, C., Bohn, J. L., Szafr, D., Do, E. Y.-L., Gross, M. D., and Leithinger, D. RoomShift: Room-Scale Dynamic Haptics for VR with Furniture-Moving Swarm Robots. In: *Proceedings of the 2020 CHI Conference on Human Factors in Computing Systems*. Association for Computing Machinery, 2020, pp. 1–11. DOI: [10.1145/3313831.3376523](https://doi.org/10.1145/3313831.3376523).
- [SVG15] Simeone, A. L., Velloso, E., and Gellersen, H. Substitutional Reality: Using the Physical Environment to Design Virtual Reality Experiences. In: *Proceedings of the 33rd Annual ACM Conference on Human Factors in Computing Systems*. Association for Computing Machinery, 2015, pp. 3307–3316. DOI: [10.1145/2702123.2702389](https://doi.org/10.1145/2702123.2702389).

- [Tak+09] Takafumi, A., Hironori, M., Shoichi, H., and Makoto, S. Haptic Ring: Touching Virtual Creatures in Mixed Reality Environments. In: *Proceedings of ACM SIGGRAPH*. 2009, p. 100.
- [TH05] Tsakiris, M. and Haggard, P. The Rubber Hand Illusion Revisited: Visuotactile Integration and Self-attribution. In: *Journal of experimental psychology. Human perception and performance* 31 (2005), pp. 80–91. DOI: [10.1037/0096-1523.31.1.80](https://doi.org/10.1037/0096-1523.31.1.80).
- [THC20] Tanaka, Y., Horie, A., and Chen, X. '. DualVib: Simulating Haptic Sensation of Dynamic Mass by Combining Pseudo-Force and Texture Feedback. In: *26th ACM Symposium on Virtual Reality Software and Technology*. Association for Computing Machinery, 2020, pp. 1–10. DOI: [10.1145/3385956.3418964](https://doi.org/10.1145/3385956.3418964).
- [TMR11] Tamaki, E., Miyaki, T., and Rekimoto, J. PossessedHand: Techniques for Controlling Human Hands Using Electrical Muscles Stimuli. In: *Proceedings of the SIGCHI Conference on Human Factors in Computing Systems*. Association for Computing Machinery, 2011, pp. 543–552. DOI: [10.1145/1978942.1979018](https://doi.org/10.1145/1978942.1979018).
- [TS11] Teather, R. J. and Stuerzlinger, W. Pointing at 3D Targets in A Stereo Head-tracked Virtual Environment. In: *Proceedings of IEEE 3DUI*. 2011, pp. 87–94.
- [TS13] Teather, R. J. and Stuerzlinger, W. Pointing at 3D Target Projections with One-eyed and Stereo Cursors. In: *Proceedings of the SIGCHI Conference on Human Factors in Computing Systems*. ACM, 2013, pp. 159–168. DOI: [10.1145/2470654.2470677](https://doi.org/10.1145/2470654.2470677). URL: <http://doi.acm.org/10.1145/2470654.2470677>.
- [TS55] Taylor, C. and Schwarz, R. J. The Anatomy and Mechanics of the Human Hand. In: *Artificial limbs* 2 (1955), pp. 22–35.
- [TTK18] Takahashi, A., Tanabe, K., and Kajimoto, H. Relationship Between Force Sensation and Stimulation Parameters in Tendon Electrical Stimulation. In: *Haptic Interaction*. Ed. by S. Hasegawa, M. Konyo, K.-U. Kyung, T. Nojima, and H. Kajimoto. Springer Singapore, 2018, pp. 233–238.
- [TTK19] Takahashi, A., Tanabe, K., and Kajimoto, H. Haptic Interface Using Tendon Electrical Stimulation with Consideration of Multimodal Presentation. In: *Virtual Reality & Intelligent Hardware* (2019), pp. 163–175. DOI: <https://doi.org/10.3724/SP.J.2096-5796.2019.0011>.
- [TWC19] Tseng, W.-J., Wang, L.-Y., and Chan, L. FaceWidgets: Exploring Tangible Interaction on Face with Head-Mounted Displays. In: *Proceedings of the 32nd Annual ACM Symposium on User Interface Software and Technology*. Association for Computing Machinery, 2019, pp. 417–427. DOI: [10.1145/3332165.3347946](https://doi.org/10.1145/3332165.3347946).
- [Uso+00] Usoh, M., Catena, E., Arman, S., and Slater, M. Using Presence Questionnaires in Reality. In: *Presence: Teleoperation Virtual Environments* (2000), pp. 497–503.
- [Val+11] Valkov, D., Steinicke, F., Bruder, G., and Hinrichs, K. H. 2d Touching of 3d Stereoscopic Objects. In: *Proceedings of the 2011 Annual Conference on Human Factors in Computing Systems*. ACM, 2011, pp. 1353–1362. DOI: [10.1145/1978942.1979142](https://doi.org/10.1145/1978942.1979142).

- [Van02] Van Erp, J. B. F. Guidelines for the Use of Vibro-tactile Displays in Human Computer Interaction. In: *Proceedings of Eurohaptics*. TNO Technische Menskunde. 2002, pp. 18–22.
- [VCO20] Verschoor, M., Casas, D., and Otaduy, M. A. Tactile Rendering Based on Skin Stress Optimization. In: *ACM Transactions on Graphics (Proceedings of ACM SIGGRAPH)* 39 (2020).
- [Vec+19] Vechev, V., Zarate, J., Lindlbauer, D., Hinchet, R., Shea, H., and Hilliges, O. TacTiles: Dual-Mode Low-Power Electromagnetic Actuators for Rendering Continuous Contact and Spatial Haptic Patterns in VR. In: *2019 IEEE Conference on Virtual Reality and 3D User Interfaces (VR)*. 2019, pp. 312–320. DOI: [10.1109/VR.2019.8797921](https://doi.org/10.1109/VR.2019.8797921).
- [Via+04] Viau, A., Feldman, A. G., McFadyen, B. J., and Levin, M. F. Reaching in Reality and Virtual Reality: A Comparison of Movement Kinematics in Healthy Subjects and in Adults with Hemiparesis. In: *Journal of NeuroEngineering and Rehabilitation*. J. NeuroEng. Rehabil, 2004.
- [VJ84] Vallbo, A. and Johansson, R. Properties of Cutaneous Mechanoreceptors in the Human Hand Related to Touch Sensation. In: *Human neurobiology* 3 (1984), pp. 3–14.
- [VRC06] Vanacken, L., Raymaekers, C., and Coninx, K. Evaluating the Influence of Multimodal Feedback on Egocentric Selection Metaphors in Virtual Environments. In: *Lecture Notes in Computer Science*. 2006. DOI: [10.1007/11821731_2](https://doi.org/10.1007/11821731_2).
- [Wal+02] Wall, S., Paynter, K., Shillito, M., Wright, M., and Scali, S. The Effect of Haptic Feedback and Stereo Graphics in A 3d Target Acquisition Task. In: *Proceedings of Eurohaptics 2002* (2002).
- [WB05] Wingrave, C. and Bowman, D. Baseline Factors for Raycasting Selection. In: *Proceedings of HCI International*. 2005.
- [Web+96] Weber, E., Ross, H., Murray, D., and Society, E. P. E.H. Weber on the Tactile Senses. Erlbaum (UK) Taylor & Francis, 1996. ISBN: 9780863774218. URL: <https://books.google.de/books?id=xEd8JglYzFwC>.
- [Wei+11] Weiss, M., Wacharamanotham, C., Voelker, S., and Borchers, J. FingerFlux: Near-surface Haptic Feedback on Tabletops. In: *Proceedings of ACM User Interface Software and Technology (UIST)*. 2011, pp. 615–620.
- [Wei68] Weinstein, S. Intensive and Extensive Aspects of Tactile Sensitivity As A Function of Body Part, Sex and Laterality. In: *The First Int’l symp. on the Skin Senses* (1968), pp. 199–222. URL: <https://ci.nii.ac.jp/naid/10017541995/en/>.
- [WGS18] Withana, A., Groeger, D., and Steimle, J. Tacttoo: A Thin and Feel-Through Tattoo for On-Skin Tactile Output. In: *Proceedings of the 31st Annual ACM Symposium on User Interface Software and Technology*. Association for Computing Machinery, 2018, pp. 365–378. DOI: [10.1145/3242587.3242645](https://doi.org/10.1145/3242587.3242645).

- [Whi+18] Whitmire, E., Benko, H., Holz, C., Ofek, E., and Sinclair, M. Haptic Revolver: Touch, Shear, Texture, and Shape Rendering on A Reconfigurable Virtual Reality Controller. In: *Proceedings of the 2018 CHI Conference on Human Factors in Computing Systems*. Association for Computing Machinery, 2018, pp. 1–12. DOI: [10.1145/3173574.3173660](https://doi.org/10.1145/3173574.3173660).
- [Wil+08] Willemsen, P., Gooch, A. A., Thompson, W. B., and Creem-Regehr, S. H. Effects of Stereo Viewing Conditions on Distance Perception in Virtual Environments. In: *Presence: Teleoperators & Virtual Environments* 17 (2008), pp. 91–101.
- [WL05] Walker, B. N. and Lindsay, J. Navigation Performance in A Virtual Environment with Bonephones. In: Georgia Institute of Technology. 2005.
- [WM99] Wang, Y. and MacKenzie, C. L. Effects of Orientation Disparity Between Haptic and Graphic Displays of Objects in Virtual Environments. In: *Lecture Notes in Computer Science: Human-Computer Interaction - INTERACT*. 1999, pp. 391–398.
- [Woe+09] Woeldecke, B., Vierjahn, T., Flasko, M., Herder, J., and Geiger, C. Steering Actors Through A Virtual Set Employing Vibro-tactile Feedback. In: *ITEL*. ACM. 2009.
- [WRM95] Wann, J. P., Rushton, S., and Mon-Williams, M. Natural Problems for Stereoscopic Depth Perception in Virtual Environments. In: *Vision Research* 35 (1995), pp. 2731–2736. DOI: [https://doi.org/10.1016/0042-6989\(95\)00018-U](https://doi.org/10.1016/0042-6989(95)00018-U).
- [WW11] Wigdor, D. and Wixon, D. *Brave NUI World: Designing Natural User Interfaces for Touch and Gesture*. Morgan Kaufmann Publishers Inc, 2011.
- [WWG03] Whitney, D., Westwood, D. A., and Goodale, M. A. The Influence of Visualmotion on Fast Reaching Movements to Astationary Object. In: *Letters to Nature* (2003), pp. 869–873.
- [Yan+18] Yang, J., Horii, H., Thayer, A., and Ballagas, R. VR Grabbers: Ungrounded Haptic Retargeting for Precision Grabbing Tools. In: *Proceedings of the 31st Annual ACM Symposium on User Interface Software and Technology*. Association for Computing Machinery, 2018, pp. 889–899. DOI: [10.1145/3242587.3242643](https://doi.org/10.1145/3242587.3242643).
- [YB20] Yu, R. and Bowman, D. A. Pseudo-Haptic Display of Mass and Mass Distribution During Object Rotation in Virtual Reality. In: *IEEE Transactions on Visualization and Computer Graphics* 26 (2020), pp. 2094–2103.
- [Yem+18] Yem, V., Vu, K., Kon, Y., and Kajimoto, H. Effect of Electrical Stimulation Haptic Feedback on Perceptions of Softness-Hardness and Stickiness While Touching A Virtual Object. In: *2018 IEEE Conference on Virtual Reality and 3D User Interfaces (VR)*. 2018, pp. 89–96.
- [Yix+20] Yixian, Y., Takashima, K., Tang, A., Tanno, T., Fujita, K., and Kitamura, Y. ZoomWalls: Dynamic Walls That Simulate Haptic Infrastructure for Room-Scale VR World. In: *Proceedings of the 33rd Annual ACM Symposium on User Interface Software and Technology*. Association for Computing Machinery, 2020, pp. 223–235. DOI: [10.1145/3379337.3415859](https://doi.org/10.1145/3379337.3415859).


- [Yoo+19] Yoon, S. H., Ma, S., Lee, W. S., Thakurdesai, S., Sun, D., Ribeiro, F. P., and Holbery, J. D. HapSense: A Soft Haptic I/O Device with Uninterrupted Dual Functionalities of Force Sensing and Vibrotactile Actuation. In: *Proceedings of the 32nd Annual ACM Symposium on User Interface Software and Technology*. Association for Computing Machinery, 2019, pp. 949–961. ISBN: 9781450368162. DOI: [10.1145/3332165.3347888](https://doi.org/10.1145/3332165.3347888).
- [YS10] Yuan, Y. and Steed, A. Is the Rubber Hand Illusion Induced by Immersive Virtual Reality? In: *Proceedings of the 2010 IEEE Virtual Reality Conference*. IEEE Computer Society, 2010, pp. 95–102. DOI: [10.1109/VR.2010.5444807](https://doi.org/10.1109/VR.2010.5444807).
- [YSK20] Yoshida, S., Sun, Y., and Kuzuoka, H. PoCoPo: Handheld Pin-Based Shape Display for Haptic Rendering in Virtual Reality. In: *Proceedings of the 2020 CHI Conference on Human Factors in Computing Systems*. Association for Computing Machinery, 2020, pp. 1–13. DOI: [10.1145/3313831.3376358](https://doi.org/10.1145/3313831.3376358).
- [Zan+14] Zanotto, D., Turchet, L., Boggs, E. M., and Agrawal, S. K. SoleSound: Towards A Novel Portable System for Audio-tactile Underfoot Feedback. In: *5th IEEE RAS/EMBS International Conference on Biomedical Robotics and Biomechatronics*. 2014, pp. 193–198. DOI: [10.1109/BIOROB.2014.6913775](https://doi.org/10.1109/BIOROB.2014.6913775).
- [Zha+19] Zhang, Y., Kienzle, W., Ma, Y., Ng, S. S., Benko, H., and Harrison, C. ActiTouch: Robust Touch Detection for On-Skin AR/VR Interfaces. In: *Proceedings of the 32nd Annual ACM Symposium on User Interface Software and Technology*. Association for Computing Machinery, 2019, pp. 1151–1159. DOI: [10.1145/3332165.3347869](https://doi.org/10.1145/3332165.3347869).
- [Zho+20] Zhou, Q., Sykes, S., Fels, S., and Kin, K. Gripmarks: Using Hand Grips to Transform In-Hand Objects into Mixed Reality Input. In: *Proceedings of the 2020 CHI Conference on Human Factors in Computing Systems*. Association for Computing Machinery, 2020, pp. 1–11. DOI: [10.1145/3313831.3376313](https://doi.org/10.1145/3313831.3376313).
- [ZK17] Zenner, A. and Kruger, A. Shifty: A Weight-Shifting Dynamic Passive Haptic Proxy to Enhance Object Perception in Virtual Reality. In: *IEEE Transactions on Visualization and Computer Graphics* 23 (2017), pp. 1285–1294. DOI: [10.1109/TVCG.2017.2656978](https://doi.org/10.1109/TVCG.2017.2656978).
- [ZK19a] Zenner, A. and Krüger, A. Estimating Detection Thresholds for Desktop-Scale Hand Redirection in Virtual Reality. In: *2019 IEEE Conference on Virtual Reality and 3D User Interfaces (VR)*. 2019, pp. 47–55.
- [ZK19b] Zenner, A. and Krüger, A. Drag:On: A Virtual Reality Controller Providing Haptic Feedback Based on Drag and Weight Shift. In: *Proceedings of the 2019 CHI Conference on Human Factors in Computing Systems*. Association for Computing Machinery, 2019, pp. 1–12. DOI: [10.1145/3290605.3300441](https://doi.org/10.1145/3290605.3300441).
- [ZS95] Zilles, C. B. and Salisbury, J. K. A Constraint-based God-object Method for Haptic Display. In: *Proceedings 1995 IEEE/RSJ International Conference on Intelligent Robots and Systems. Human Robot Interaction and Cooperative Robots*. Vol. 3. 1995, pp. 146–151.

Eidesstattliche Versicherung

Hiermit erkläre ich an Eides statt, dass ich die vorliegende Dissertationsschrift selbst verfasst und keine anderen als die angegebenen Quellen und Hilfsmittel benutzt habe.

Hamburg, 28.12.2020

Ort, Datum



Unterschrift

